DISSERTATION

SNOW PERSISTENCE AND HYDROLOGIC RESPONSE ACROSS THE INTERMITTENT-PERSISTENT SNOW TRANSITION

Submitted by

John Christopher Hammond

Department of Geosciences

In partial fulfillment of the requirements

For the Degree of Doctor of Philosophy

Colorado State University

Fort Collins, Colorado

Fall 2018

Doctoral Committee:

Advisor: Stephanie Kampf

Tim Covino
Scott Denning
Steven Fassnacht

ABSTRACT

SNOW PERSISTENCE AND HYDROLOGIC RESPONSE ACROSS THE INTERMITTENT-PERSISTENT SNOW TRANSITION

In mountainous regions and high latitudes, seasonal snow is a critical component of the surface energy balance and hydrologic cycle. Snowpacks have been declining in many mountain regions, but the hydrologic responses to snow loss have varied due to interactions of climatic, vegetative, topographic and edaphic factors. With continued climatic change, it remains uncertain whether the southwestern U.S. and other subtropical and mid-latitude dry areas may experience significant reductions in water yield. In this dissertation snow persistence and trends are mapped globally; relationships between snow persistence and annual water yield are examined in different climates, and snowmelt and rain partitioning in the critical zone are modelled to examine potential effects of snow loss on hydrologic response.

Chapter 2 involves mapping the distribution of snow persistence (SP), the fraction of time that snow is present on the ground for a specific period, using MODIS snow cover data, classifying similar areas into snow zones, assessing how snow persistence relates to climatic variables and elevation, and testing for trends in annual SP. SP is most variable from year to year near the snow line, which has a relatively consistent decrease in elevation with increasing latitude across all continents. At lower elevations, SP is typically best correlated with temperature, whereas precipitation has greater relative importance for SP at high elevations. The largest areas of declining SP are in the seasonal snow zones of the Northern Hemisphere. Trend patterns vary within individual regions, with elevation, and on windward-leeward sides of

mountain ranges. This analysis provides a framework for comparing snow between regions, highlights areas with snow changes, and can facilitate analyses of why snow changes vary within and between regions.

In Chapter 3, SP is used to evaluate how water yield relates to snow patterns at the annual time scale across the western U.S. in different climates. I first compare snow cover variables derived from MODIS to more commonly utilized metrics (snow fraction and peak snow water equivalent (SWE)). I then evaluate how SP and SWE relate to annual streamflow (Q) for 119 USGS reference watersheds and examine whether these relationships vary for wet/warm (precipitation surplus) and dry/cold (precipitation deficit) watersheds. Results show high correlations between all snow variables, but the slopes of these relationships differ between climates. In dry/cold watersheds, both SP and SNODAS SWE correlate with Q spatially across all watersheds and over time within individual watersheds. I conclude that SP can be used to map spatial patterns of annual streamflow generation in dry/cold parts of the study region.

In Chapter 4 of the dissertation, I use a series of one-dimensional simulations to study how snow loss may impact hydrologic response in mountain areas at event to annual time scales. I use Hydrus 1-D simulations with historical inputs from fifteen SNOTEL snow monitoring sites to investigate how inter-annual variability of water input type (snowmelt, rainfall) and timing affect soil saturation and deep drainage in different soil types and depths. Greater input rate and antecedent moisture are observed for snowmelt compared to rain events, resulting in greater runoff efficiencies. At the annual scale runoff efficiencies increase with snowmelt fraction and decrease when all input is rainfall. In contrast, deep drainage has no clear correlation to snowmelt fraction. Input that is concentrated in time leads to greater surface runoff and deep

drainage. Soil texture and depth modify partitioning, but these effects are small compared to those caused by variability in climate.

This dissertation's findings have direct implications for climate change impacts in cold dry areas globally. Through the synthesis of the chapters described above I highlight areas where hydrologic response to snow loss may be most sensitive, provide methods for comparing regional snow patterns, demonstrate how snow persistence can help estimate annual streamflow generation, and improve process-based knowledge of hydrologic response to rainfall and snowmelt in the western U.S. Collectively these findings indicate that annual water yield is not directly sensitive to whether input is snowmelt vs. rainfall; instead it is more dependent on the effect that snowpack accumulation has on input timing and rate. Loss of concentrated melt from persistent snowpacks may lead to lower streamflow and compromise deep drainage, and thus aquifer recharge, in semi-arid cold regions. The consequences of streamflow and groundwater recharge loss could be severe in regions already water-stressed, and this needs to be addressed in long-term water supply planning.

ACKNOWLEDGEMENTS

Great thanks to my advisor, Stephanie Kampf, for her superhuman organizational and time management abilities, for keeping me focused and reining in my data mining research ideas, for keeping me involved in projects outside my dissertation to broaden my skillset and knowledge base, for maintaining a collaborative research group, and for her patience in working through many drafts of my slowly improving writing. The articles that we have published and will publish together, as well as this dissertation, are so much better because of this. I am grateful to the National Science Foundation Division of Earth Sciences for the funding I was supported by to conduct this research under grant number EAR-1446870. Thanks to Adrian Harpold for his involvement from a distance and for being receptive to my research ideas from the start. Tim Covino, thank you for introducing me to another train of thought in hydrology and piquing my interest in biogeochemistry, and Scott Denning for asking comprehensive exam questions that linked old and new research interests, sparking ideas for new projects. Steven Fassnacht has provided valuable critique and support of my research ideas, training in snow measurements, and mentorship on what it means to be a scientist. Michelle, thank you for your continued support in pursuit of my passions, your patience in our long-distance relationship, and for helping me to prioritize and make time for what I enjoy in life. Thank you to my parents, John and Rose, for their motivation and guidance and for sparking scientific interest from a young age. Freddy, without your help to get the ball rolling on our remote sensing analyses, this would all have been so much more painful and time consuming. Abby, Kira, Tristan, Alex, Allie and Alyssa, it's been so much fun to nerd out with you all the past few years. Finally, thanks to Kristine and Gregg Kampf and Gigi Richard for their hospitality and generosity on visits to western Colorado.

TABLE OF CONTENTS

Chapter 1. Introduction

1.1.The importance of snow to the hydrologic cycle in mountain areas

In mountainous regions and high latitudes, seasonal snow is a critical component of the surface energy balance and hydrologic cycle. The timing of snow onset and melt and duration of the snow season affect both hydrological and ecological processes such as vegetation phenology and biogeochemical cycling. This research uses snow persistence, the fraction of time snow is present for a defined period, to explore how snow affects hydrologic response. These hydrologic responses include soil moisture dynamics, streamflow generation and groundwater recharge.

Mountain areas generally produce a greater proportion of streamflow than low lying areas (Christensen et al., 2004; Viviroli et al., 2007; Hunsaker at al., 2012), so hydrologic changes in mountains have great implications for downstream areas. Snowpacks in mountain regions have been declining across the western U.S. over the past several decades (Clow, 2010; Fritze et al., 2011; Harpold et al., 2012; Regonda et al., 2005; Stewart et al., 2005), with empirical and modeling studies indicating that snow loss may lead to lower streamflow generation (Regonda et al., 2005; Stewart et al. 2004, 2005; Clow, 2010; Jefferson, 2011; Furey et al., 2012; Berghuijs et al., 2014; Barnhart et al., 2016). Yet hydrologic responses to snow loss are heterogeneous; in some areas loss of snow causes declines in streamflow, but this does not occur everywhere (McCabe et al., 2018). The reasons for variability in hydrologic response to snow loss between regions are often unknown. Hydrologic responses to snow loss likely vary because they are affected by the interactions of climatic, vegetative, topographic and edaphic factors. The relative importance of each factor may change between climatic zones as well as along elevation gradients within a single climatic zone.

1.2. Snowmelt's societal importance

Several of humanity's first civilizations, including those along the Nile, Indus, and Euphrates, thrived in semi-arid areas where the spring and summer snowmelt freshet from upstream mountain areas flooded river valleys with water and sediment, developing some of the most fertile farmland in the world. This reliable, annual melt pulse allowed for the development of complex societies in otherwise inhospitable surroundings. Reliance on the snowmelt freshet continues today, with the western U.S., among many other regions, dependent on spring streamflow that supplies agricultural water use. More than half of global mountainous areas play a substantial role in the hydrology of downstream regions, with heightened importance in arid and semiarid regions (Viviroli et al., 2007). Mountain areas serve as essential water towers, in the following regions: Ethiopian Highlands (Nile River), Taurus and Zagros Mountains (Euphrates and Tigris rivers), Pamir and Tien Shan (Amu-Darya and Syr- Darya rivers), southwest Himalayas (Indus River), High-lands of Lesotho (Orange River), and parts of the southern Rocky Mountains (Colorado River and Rio Grande) (Viviroli et al., 2007). In total, about 2 billion people face reduced water supply due to snow loss this century (Barnett et al., 2005; Mankin et al., 2015). With changes to the duration of snow cover and timing and magnitude of snowmelt, livelihoods of those in Arctic (Callaghan et al., 2011), European (Dodgshon et al., 2007), Himalayan (Xu et al., 2009; Merry et al., 2018) and Andean communities (Valdivia et al., 2010) pertaining to agriculture, hunting, and raising livestock are at risk of being lost.

1.3. Global warming and the changing hydrologic cycle

Under a business as usual scenario of climatic change with 3.7 °C warming by 2100 (representative concentration pathway, RCP 8.5), ice and snow will melt more rapidly and occupy lesser extents. Global precipitation and evaporation are likely to increase overall, though potentially diverging regionally, and water yield at high latitudes is likely to increase whereas decreases are expected in some arid and semi-arid regions (Collins et al., 2013). In the future warmer climate, snow will likely begin accumulating later and melt earlier, with different magnitudes of change by elevation and geographic region (Fassnacht et al., 2018). Spring snow covered extent in the Northern Hemisphere is projected to decrease by 10 to 30% by 2100 (Collins et al., 2013). Despite global losses, regional increases in snowfall and snow accumulation are predicted for high latitudes. Warmer temperatures can allow increased precipitation at high latitudes leading to increases in net snowfall and accumulation (Collins et al., 2013). The southwestern U.S., along with other subtropical and mid-latitude dry areas, is expected to have similar or slightly lower precipitation and higher potential evaporation, leading to a greater moisture deficit (precipitation – evaporation) than in the past (Chou and Neelin, 2004; Held and Soden, 2006; Chou et al., 2009; Seager et al., 2010; Bony et al., 2013). Lower precipitation and higher evaporation may translate into reduced water yield in these regions (Christensen and Lettenmaier, 2007; McCabe and Wolock, 2007; Barnett and Pierce, 2008).

1.4. Snow loss and water management systems

Water management systems are comprised of many interacting components and institutions, fulfilling multiple objectives at hourly to seasonal scales including flood control, hydropower, irrigation, recreation, and water supply. Snow losses have coincided with trends in

the timing and magnitude of reservoir inflows over the past several decades (Stewart et al. 2004; Regonda et al., 2005; Lins and Slack, 2005; Clow, 2010; Hatcher and Jones, 2013), and this has consequences expected for water management systems designed under assumptions of stationarity.

Climate change undermines the assumption of stationarity that has been used in the management of water resources (Milly et al., 2008). In addition to the existing interannual climatic variability, as well as human and natural disturbances, water management must also factor climatic trends into water supply forecasts and rule curves. Where reservoir capacity cannot accommodate winter increases in flow, streamflow may immediately be lost downstream, and in the absence of additional downstream reservoir storage, lost to the oceans (Barnett et al., 2005). Anticipatory adaptive measures in response to these hydrologic changes will be needed to minimize impacts on water users and maximize system performance even when the system is degraded (Middelkoop et al., 2001).

In the Colorado River Basin, a modeling comparison between historical and future climate effects on reservoir system management revealed degraded system performance with reduced total basin storage, reduced hydropower output, and releases from the upper basin to the lower basin mandated by the Colorado River Compact only met some years (Christensen et al., 2004). Climate change in mountain areas generally may also increase flood risk during winter while reducing low flows during summer months, with consequences for irrigation, industrial, and domestic supplies. Tradeoffs between hydroelectric generation, biological flows, irrigation, and recreational releases may be required. Current water demands in certain areas will not be met under future climate conditions, with the demands of a larger future population far from guaranteed (Barnett et al., 2005).

1.5 Key knowledge gaps

While remotely sensed methods for snow research have been around for decades, most prior research has not focused on comparing snow patterns between different geographical areas. Station measurements have been used for this purpose (Serreze et al., 1999; Trujillo and Molotch, 2014), but the station network does not cover all snow-affected areas. Analyses of snow-covered extent have revealed areal losses in snow through time at the continental scale (Brown and Robinson, 2011; Rupp et al. 2013; Estilow et al. 2015; Kim et al. 2015; Kunkel at al. 2016; Hori et al. 2017), whereas analyses of snow measurement stations have been conducted at finer scales (Mote et al. 2005; Regonda et al., 2005; Lopez-Moreno and Vicente-Serrano 2007; Stewart 2009; Jain et al. 2010; Masiokas et al. 2010; Valt and Cianfarra 2010; Harpold et al., 2012; Ma and Qin, 2012; Marty and Meister 2012; Kunkel et al. 2016). We have lacked methods for examining snow changes at intermediate scales along climatic and elevation gradients within continents.

Next, although snow loss is apparent at a variety of scales, the lack of understanding about variable hydrologic responses to snow loss makes it difficult to predict future hydrologic conditions. There are many studies that examine hydrologic responses to snow changes in large river basins or even globally (e.g. Vicuna et al., 2007; Adam et al. 2009; Painter et al., 2010; Anghileri et al., 2016). Others explore potential effects within small watersheds (Nayak et al., 2010; Hunsaker et al., 2012; Godsey et al., 2014). We lack information at intermediate scales that could highlight which parts of large river basins are most sensitive to snow changes and help relate small watershed findings to a broader geographic area. In this dissertation I primarily focus on annual water yield, just one metric for assessing hydrologic response. Other metrics of hydrologic response in snowmelt-dominated areas include the onset of snowmelt and the timing

of peak flow (Clow, 2010) as well as the timing of the center of mass of the snowmelt hydrograph (Stewart et al., 2004).

Another knowledge gap relates to the processes that would create differences in hydrologic response to snow loss. We know that precipitation in some areas is shifting from snow to rain (Huntington et al., 2004; Knowles et al., 2006; Klos et al., 2014), but how exactly this will impact surface runoff, soil storage, deep drainage, vegetation water use and groundwater recharge remains uncertain.

1.6 Research goal and questions

The goal of this research is to examine how and why changes in snow have variable effects on hydrologic response. I use snow persistence to examine snow patterns and trends globally in Chapter 2, which addresses the following questions: (1) where are snow zones located across the globe, and how does this distribution relate to latitude, elevation, temperature, precipitation, and climate indices? (2) how has snow persistence changed since the beginning of the MODIS record?

Chapter 3 then focuses in on the western United States, which contains seasonally snow covered areas in both wet maritime and dry continental climates. This chapter examines how snow persistence relates to streamflow across these different climates and addresses the questions: (1) how do globally available spatial snow cover variables compare with other snow variables more commonly used in streamflow prediction models?,(2) are snow variables useful for estimating streamflow in watersheds that span a wide range of snow persistence and climate conditions? and (3) can snow cover be used to reconstruct streamflow patterns in ungauged watersheds, both spatially and temporally?

Finally, Chapter 4 examines the mechanisms that determine how snow changes affect hydrologic response. This portion of the research uses a physically-based model to simulate hydrologic responses in soil columns under a wide range of climate conditions. The chapter addresses the questions: (1) are snowmelt and rain partitioned differently between surface runoff (Q), deep drainage (D, and evapotranspiration (ET)? and (2) how is this partitioning of rain and snowmelt affected by climate, soil type, and soil depth?

Chapter 2. Global Snow Zone Maps and Trends in Snow Persistence 2001–2016[1]

2.1 Introduction and background

2.1.1 The importance of snow to the surface energy balance and hydrologic cycle

Seasonal snow is a critical component of the surface energy balance and hydrologic cycle, particularly at high elevations and high latitudes. Seasonal inputs of snow support and maintain glaciers and ice sheets, insulate permafrost, and influence sea ice onset and breakup. The physical properties of snow, mainly high albedo and low thermal conductivity, exert strong controls on the surface energy balance, especially in the Northern Hemisphere where large areas are seasonally covered by snow (Barry and Gan 2011). Snow cover affects soil temperature, freeze and thaw, and permafrost stability, all of which moderate land-atmosphere carbon exchange (Zhang 2005, Edwards et al. 2007). Water stored in snow contributes to the timing and magnitude of streamflow, affecting water resource availability (Barnett et al. 2005, Beniston and Stoffel 2014). Climate model simulations indicate that the fraction of meltwater produced at high snowmelt rates is greatly reduced in a warmer climate due to shortening of the snowmelt season and melt occurring during periods of lower available energy (Musselman et al. 2017). This loss of high snowmelt rate may lead to corresponding losses in streamflow generation (Barnhart et al. 2016). Anticipated warming will greatly impact the hydrology of alpine and high latitude areas, with repercussions for biogeochemical cycling, aquatic communities, and anthropogenic water use extending far downstream (Huss et al., 2017).

[1] Hammond, J. C., Saavedra, F. A., & Kampf, S. K. (2018). Global snow zone maps and trends in snow persistence 2001–2016. International Journal of Climatology, https://doi.org/10.1002/joc.5674.

2.1.2 Temporal and spatial snow patterns

Surface station measurements for the past several decades from around the world show varying rates and directions of temporal snow changes in recent decades (Stewart 2009, Kunkel et al. 2016). Snow occurrence has decreased in much of the Northern Hemisphere, especially during spring in locations where air temperature is near freezing (Brown and Mote 2009). Trend analyses in North America have documented declining April 1 snow water equivalent (SWE) (Mote et al. 2005), with the strongest declines in maritime mountain ranges (Regonda et al. 2005) and fewer consistent trends in the continental interior (Harpold et al. 2012). South American studies have had few surface stations to analyze but have documented little significant change in snow water equivalent (SWE) (Masiokas et al. 2010), with snow patterns strongly linked to climatic oscillations (Masiokas et al. 2012). Studies in the European Alps (Valt and Cianfarra 2010, Marty and Meister 2012) and Pyrenees (Lopez-Moreno and Vicente-Serrano 2007) display declines in spring snow depth and snow cover duration. In Asia, Himalayan surface stations demonstrate significant changes in the distribution of snowmelt timing with more snowmelt occurring earlier in the year (Jain et al. 2010). China as a whole has experienced negative trends in snow depth and SWE over the past several decades (Ma and Qin 2012).

Spatial patterns of snow can be monitored with remote sensing, which has the advantage of large spatial extent, providing worldwide utility in data-dense and data-sparse areas. Satellite remote sensing of snow allows studying inter-annual variability in snow cover extent, snow cover duration, and snowline elevation across large areas where sensor networks may not be feasible (Kulkarni et al. 2010, Li et al. 2017). Remote sensing studies have shown declining snow cover extent, snow cover duration, and snow depth across the northern hemisphere over the past several decades (Estilow et al. 2015, Kim et al. 2015, Kunkel at al. 2016, Hori et al. 2017),

with spring snowmelt onset occurring earlier while the onset of snow cover has not significantly changed (Choi et al. 2010). Northern hemisphere spring snow cover extent over the period from 1922–2010 showed accelerated reductions over the past four decades (Brown and Robinson 2011, Rupp et al. 2013), with trends switching direction from positive to negative in some areas of Asia from the early to late 2000's. Seasonal snow cover in South America shows strong inter-annual variability linked to atmospheric circulation patterns and El Niño Southern Oscillation (ENSO) activity for both snow cover and snow mass over the period 1979-2006 (Foster et al. 2009). In recent years (2000-2014), snow persistence in the Central Andes displayed statistically significant declines, with fewer trends in the tropical Andes (Saavedra et al. 2017).

2.1.3 Climate connections to snow patterns

Both surface station and remote sensing studies report widespread decreasing snow trends, with areas at lower elevation or with higher average temperatures displaying the greatest decreases (Vaughan et al. 2013). Multiple studies attribute these changes to increases in temperature (Brown and Mote 2009; Kunkel et al. 2016; Regonda et al. 2005; Harpold et al. 2012), but temperature alone does not fully explain the snow patterns. Precipitation also affects snow, and globally, there has been an increase in the variance of annual precipitation, with increased precipitation at high latitudes in the Northern Hemisphere and decreased precipitation in China and Australia (Dore 2005). Concurrent increases in temperature and precipitation have led to increases in high latitude snow cover duration in North America and Eurasia (Cohen et al. 2012) and decreases in SWE in the Pacific Northwest USA (Mote 2003).

Snow patterns are also linked to climate teleconnections. For example, large snow-covered areas in the Northern Hemisphere influence the onset and strength of climate

teleconnections (Ye and Bao 2001; Wu et al 2012), while teleconnections in turn influence snow accumulation and ablation through their effects on precipitation and temperature (Bednorz 2004; Shaman and Tziperman 2005; Ge and Gong 2009). Snow anomalies in North America and Northern Europe correlate with the North Atlantic Oscillation (NAO) and ENSO (Seager et al. 2010). NAO is a dominant control on precipitation and temperature in the Mediterranean Region, strongest in the Western Mediterranean, with dry and warm periods leading to lower snow accumulation and snow-covered extent (López-Moreno et al. 2011). In South America, El Niño conditions relate to low precipitation and warm air temperatures at low latitudes and high precipitation and warmer temperatures at higher latitudes (Garreaud et al., 2009), and these ENSO cycles in turn affect snow persistence (Saavedra et al. 2018). The Southern Annular Mode (SAM) affects South American climate (Vera and Silvestri, 2009; Fogt et al., 2010), and it correlates with snow persistence south of 35 degrees South (Saavedra et al. 2018). Despite the great distance of separation, SAM exerts a strong influence on Eurasian temperature and precipitation (Wu et al. 2009), an area also showing a strong relationship between snow depth and the NAO (Ye 2001).

2.1.4 Snow persistence

Despite the widespread application of remotely sensed methods for snow research, comparing snow patterns between regions remains challenging because the timing of snow accumulation and melt varies substantially with latitude and elevation. Snow persistence (SP), defined as the fraction of time that snow is present on the ground, offers a path forward for regional comparisons. This metric has been used in both North and South America to define snow zones in a wide range of climates (Richer et al. 2013, Moore et al. 2015, Saavedra et al.

2017). Snow zones are areas that display similar snow patterns: permanent snow zones retain their snow year-round; seasonal snow zones have snow that persists through the winter, and intermittent snow zones do not consistently have snow that last through the winter. Snow persistence is also useful for identifying transitions between rainfall and snowmelt peak streamflow source regimes (Kampf and Lefsky 2016) and for predicting water yield (Saavedra et al. 2017, Hammond et al., 2018).

In this study, snow persistence and snow zones are mapped globally and then used to address the following questions:

1. Where are snow zones located across the globe, and how does this distribution relate to latitude, elevation, temperature, precipitation, and climate indices?
2. How has snow persistence changed since the beginning of the MODIS record?

2.2 Methods

2.2.1 Global snow persistence (SP)

To calculate snow persistence we used Moderate Resolution Imaging Spectroradiometer (MODIS) Terra Snow Cover 8-Day L3 Global 500m Grid (MOD10A2), Collection 6 obtained from the National Snow and Ice Data Center (NSIDC) (NSIDC, Hall and Riggs, 2016). MOD10A2 snow cover is derived from the Normalized Difference Snow Index (NDSI), which is based on the snow reflectance properties, where snow has high reflectance in visible bands and low reflectance in the shortwave infrared. We use MOD10A2 maximum snow cover extent, which is generated from 500 m resolution daily MOD10A1 tiles; maximum snow cover extent is reported for each cell during 8-day time periods. Cloud is only reported if the cell was obscured for all eight days in the period.

We computed the 1 January – 31 December SP and no data index (NDI) for each year as the percent of 8-day MODIS images with snow present where:

$$SP = \frac{S}{n-ND} x100 \quad \text{eq 1.}$$

$$NDI = \frac{ND}{n} x100 \quad \text{eq 2.}$$

Where S is the number of 8-day time intervals classified as snow; n is the total number of 8-day time periods per year, and ND is the number of days classified as having no data (cloud, sensor saturation, missing data). Values for SP and NDI are computed for each MODIS 500 m cell for years 2001-2016. NDI was used to mask SP prior to any subsequent analyses; we excluded all pixels with NDI>30%.

For the resulting SP and NDI grids, we masked polar regions (above the Arctic circle and below the Antarctic Circle), areas classified as water by MODIS/Combined MCD12Q1, and areas with SP < 7%, a threshold that Saavedra et al. (2017) found would represent areas with little to no snow. Using this low SP threshold, we identified the average snowline elevation for latitudes less than 43.5 degrees; this latitude limit was selected because of cloud impairment in coastal areas at higher latitudes. Elevations were derived from ASTER GDEM v2 (NASA LP DAAC, 2015) aggregated to the 500m grid of MODIS SP. We found that coastal fog or persistent clouds in the tropics resulted in a few instances of snow classification errors (Saavedra et al. 2017), so we fit an equation to the snowline elevation vs latitude data to develop a mask for excluding areas where snowfall is unlikely:

Elevation lower limit for mask = 8488 m - 0.001756097 x Abs(latitude in degrees) eq 3.

This mask reduced problems with false snow detections in warm regions.

Using the annual SP grids masked to exclude areas with high cloud cover (NDI), high latitudes, and low elevations in warm regions, we then computed mean annual SP and the

coefficient of variation in annual SP for each grid cell. We used the mean annual SP to map snow zones following the SP thresholds identified by Saavedra et al. (2017): Little or no snow (0-7%), Intermittent snow (7-30%), Seasonal snow (30-90%), Permanent snow (90-100%). We then computed the percent of each continent's surface area in each snow zone. To aid in data display, mean SP was also calculated for each 100-meter elevation bands separated by 0.5 degree latitude increments.

Prior research illustrates that MODIS snow products may under-estimate snow cover in forested areas, with the greatest errors of omission in forest densities greater than 50% (Rittger et al., 2013). Therefore, to estimate where dense forest vegetation obscured snow observations, we mapped areas with dense forest (>50% tree cover) using 2010 MODIS Vegetation Continuous Fields (MOD44B) Collection 5 Percent Tree Cover. 2010 is the most recent year with global coverage.

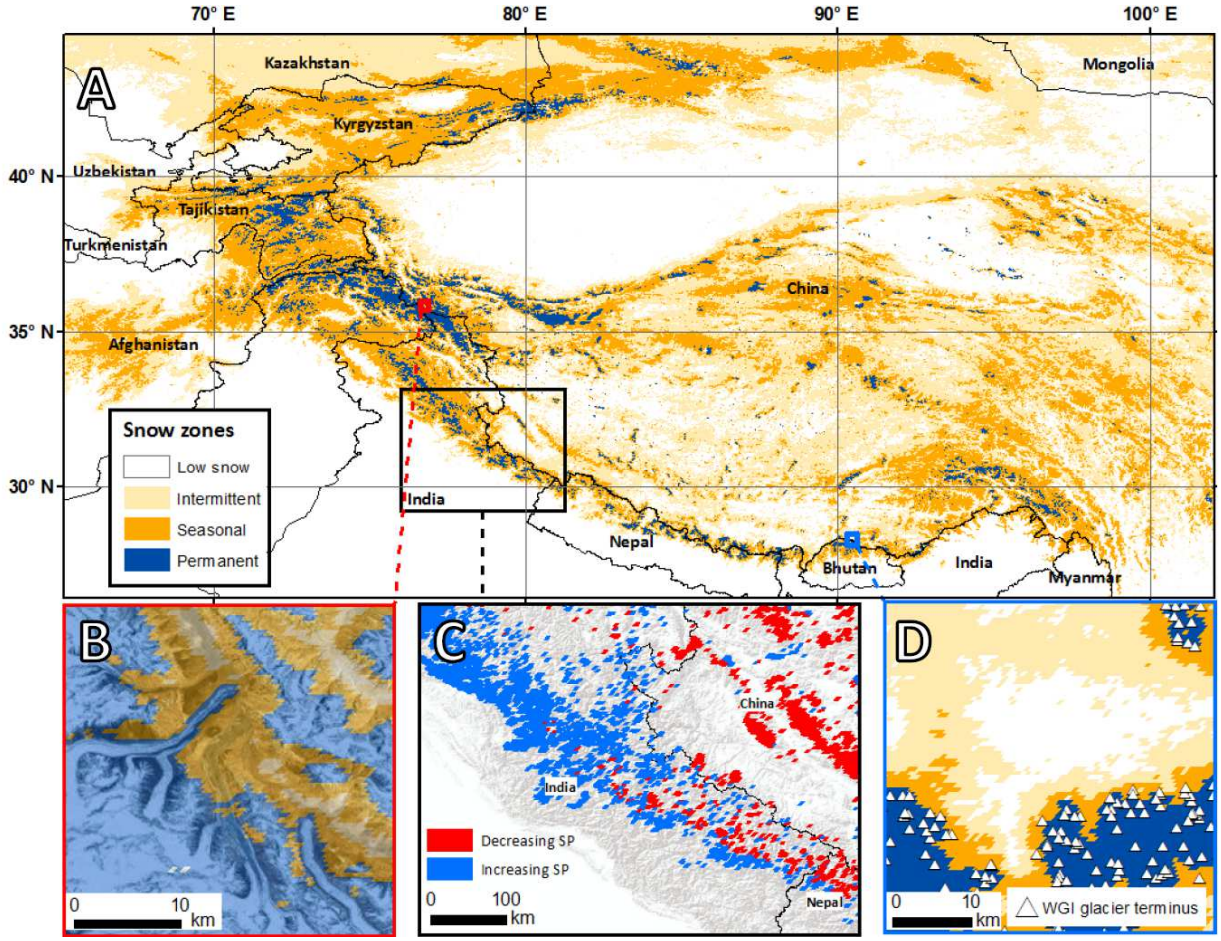

Figure 2.1. Snow zones determined from snow persistence values displayed across the Hindu-Kush Himalaya (A). Little or no snow (0-7%), Intermittent SP (7-30%), Seasonal (30-90%), Permanent (90-100%). Snow zones shown transparently on alpine imagery in Pakistan and China (B). Snow persistence trends (C). World Glacier Inventory (WGI) glacier termini displayed on snow zones exhibiting similar alignment between glacial extent and the boundary of mapped permanent snow (D).

2.2.2 Climate connections to SP

To evaluate how annual precipitation and temperature relate to annual SP, we calculated the relative importance using the Lindeman, Merenda and Gold (lmg) approach included in the relative importance for linear regression "relaimpo" R package (Grömping and Matthias, 2013). This method estimates the individual contribution of each regressor to the full r squared of the combined model (Grömping, 2006). For precipitation and temperature data we utilized TerraClimate 4 km monthly gridded precipitation and mean temperature (Abatzoglou et al.,

2018). Precipitation was totaled and temperature was averaged on a pixel by pixel basis for each year of analysis. For the northern hemisphere, where the snow season straddles the change in calendar year, we used the water year (Oct-Sep), whereas we used the calendar year for southern hemisphere analyses. For the relative importance analysis we aggregated annual SP grids to the 4 km resolution of the precipitation and temperature data.

Finally, we evaluated the linear correlation (r) between SP and four climatic teleconnection indices: North Atlantic Oscillation (NAO), Oceanic Niño Index (ONI), Pacific Decadal Oscillation (PDO), and Southern Annular Mode (SAM). Data for each teleconnection index was obtained from the National Weather Service Climate Prediction Center (http://www.cpc.ncep.noaa.gov/data/teledoc) and consisted of a rolling 3 month mean of the teleconnection index. For each index value, we computed the correlations with annual SP, then found the sum of the absolute values of r for all pixels with significant correlations ($p \leq 0.05$) in half degree latitude and longitude cells. A greater value of this sum indicates stronger correlations between the teleconnection index and SP. Using these sums, for each half degree cell we then identified the index and month of that index that best correlates with SP.

2.2.3. Global SP trends

We used the Mann-Kendall non-parametric trend test (Khaled and Ramachandra 1998) to evaluate trends in annual SP for each MODIS pixel using data for calendar years 2001 to 2016 (Kendall R package, McLeod 2011). If a significant trend ($p \leq 0.05$) was identified, we then applied the Thiel-Sen regression (Thiel 1950; Sen 1968) to determine rate of trend (zyp R package, Bronaugh and Werner 2013). To explore the spatial pattern of trends further, we separated windward and leeward components of several mountain ranges using mountain crests

identified from the Waterbase global watersheds (http,//www.waterbase.org/download_data.html). For each continent and side of mountain range, we computed the area experiencing statistically significant positive and negative annual SP trends. Finally, for the Sierra Nevada mountains of North America, we calculated the mean trend rate in bands of 10% SP (eg. 0-10%, 10-20%, ...) across the mountain range. All statistical methods for these calculations are fully documented in an R package developed by the authors (MODISnow, Saavedra and Hammond, in review CRAN). The package utilizes parallel computing on multiple cores to process raster calculations efficiently given the large size of files involved in these analyses.

2.3. Results

2.3.1. Elevational and latitudinal patterns in snow persistence and snow zones

Latitude, elevation, and climate interact to control snow persistence across the global land surface. Continental and global maps of snow zones and SP coefficient of variation are shown in the supplementary material figures 2.8 to 2.19. An example map of snow persistence for the Hindu-Kush Himalaya (Figure 2.1) illustrates how areas of low snow coincide with low elevations or areas with low precipitation such as the Gobi Desert (Figure 2.1a). Snow persistence increases with elevation, with intermittent and seasonal snow zones found at middle-high elevations of the Himalaya. Areas with the highest snow persistence (permanent snow zone) correspond well with visual glacial features (Figure 2.1b) and with satellite-derived glacial boundaries (Figure 2.1d).

Globally, most of the continental area in the northern hemisphere (63%) has intermittent, seasonal, or permanent snow zones, whereas only 1% of the continental area in the southern

hemisphere has these snow zones due to less land mass at high latitudes. In the northern hemisphere, North America and Asia's snow-covered areas are dominated by the seasonal snow zone (48 and 39% of total land area), whereas Europe has nearly an even split between the intermittent and seasonal snow zones (43%, 42%). In the southern hemisphere (Africa, Oceania, and South America) most of the snow-covered areas are in the intermittent snow zone (0.04-2% of total land area) (Table 2.1).

Table 2.1. Percent area of each continent / region between the Arctic and Antarctic circles in each snow zone based on mean annual SP.

Continent	Low	Intermittent	Seasonal	Permanent
Africa	99.95%	0.04%	0.01%	0.00%
Asia	45.95%	14.39%	39.13%	0.53%
Oceania	98.41%	1.17%	0.41%	0.02%
Europe	15.21%	42.91%	41.63%	0.26%
North America	28.94%	20.71%	48.07%	2.29%
South America	96.32%	2.25%	1.20%	0.24%

Average snow persistence generally increases with both elevation and latitude (Figure 2.2), although some variability in snow persistence is masked by the latitude-elevation averaging in Figure 2.2. Seasonal snow is present near sea level at high latitudes (>60°), but it is only present above 5,000 m in the tropics. Only a few areas have elevations high enough for snow to occur within the tropics (ex. Africa: Mount Kilimanjaro, Ethiopian Highlands, Mount Kenya. North, Central and South America: volcanic peaks of Mexico and Ecuador including Pico De Orizaba, Chimborazo and Cotopaxi, the Cordillera Blanca, Colombian Andes. Asia: Puncak Jaya).

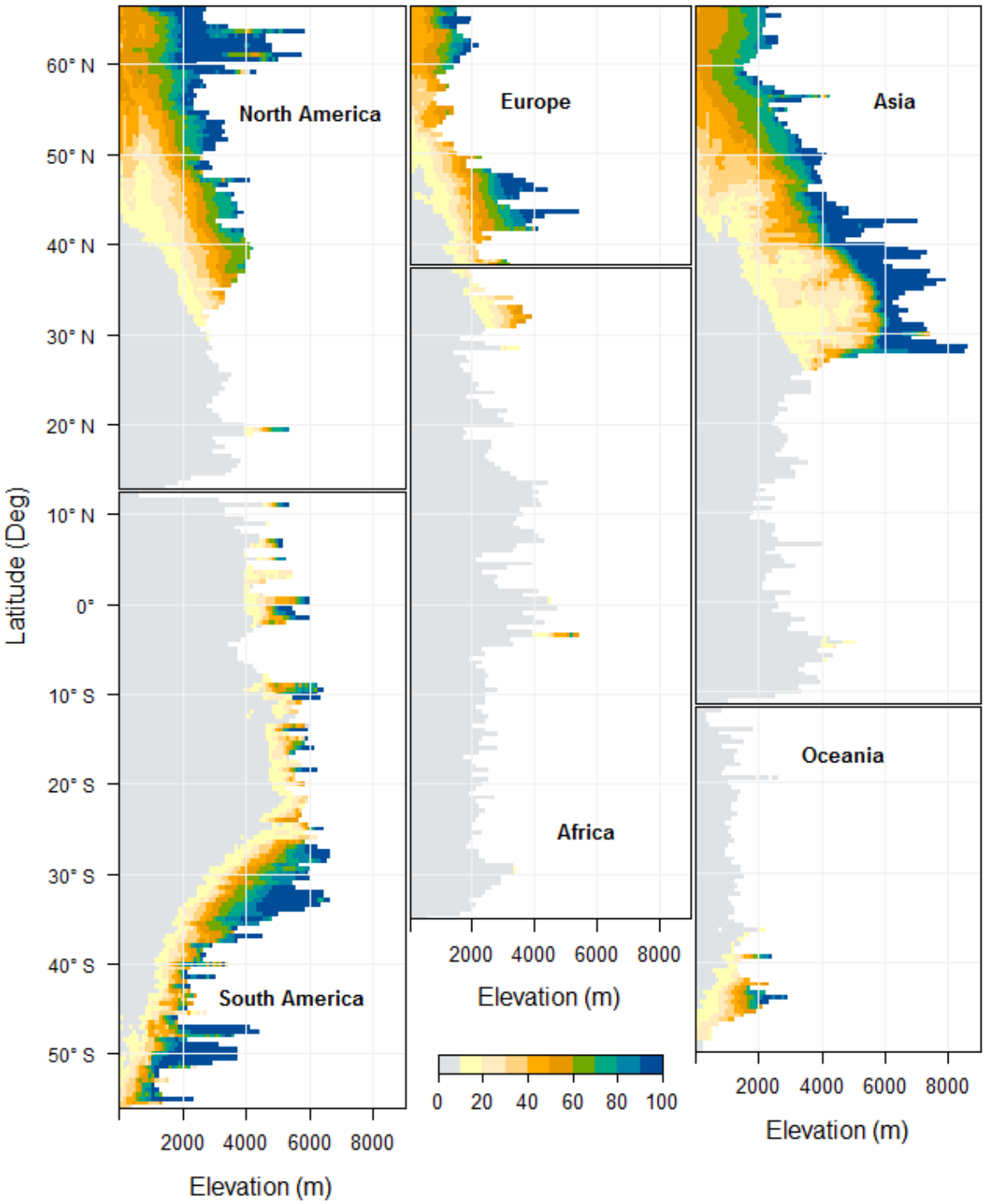

Figure 2.2. Average 2001-2016 snow persistence (%) by latitude and elevation for North America, South America, Africa, Asia, Europe and Oceania.

The average elevation at which snow occurs regularly, hereafter referred to as the snowline, is consistent by latitude between continents for latitudes less than around 35-40° N or

S (Figure 2.3). The snow line elevations diverge for latitudes greater than 40 degrees, where average snow lines are less than 1,500 m elevation (Figure 2.3). The lowest elevation average snow lines are in Asia and North America, which have the largest high latitude land masses. The highest elevation average snow lines are in South America, which has a relatively narrow land mass at high latitude, and in Europe, where much of the land at high latitude is near the coast. The northern hemisphere generally displays higher SP at lower elevation than the southern hemisphere at the same latitude, and within the southern hemisphere Oceania has a lower snow line elevation than South America.

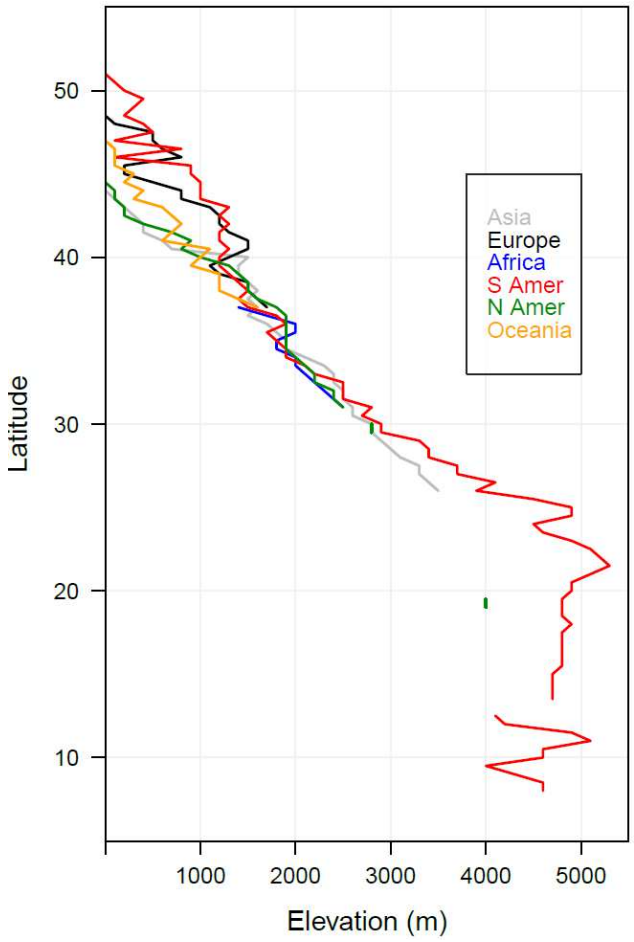

Figure 2.3. Continental average snow line elevations, as defined by the elevation where mean annual snow persistence = 7% from 2001-2016. Latitudes on the y-axis are absolute values.

Interannual variability in SP is greatest at the lower elevation ranges of snow covered area in each region studied (Figure 2.4), generally becoming less variable at higher elevations (Figures 2.9,2.11,2.13,2.15,2.19,2.21). Coefficients of variation (CV) in annual SP are also high in the tropical Andes (Figure 2.4), in much of Europe (Figure 2.19), and in the foothills and plains east of the Rocky Mountains in North America (Figure 2.11). The quality of snow cover data for computing SP is also regionally variable. Southern South America has the greatest overall data loss due to clouds (Figure 2.30), with 20.1% of the snow covered area in South America having missing data (Table 2.5). Oceania (New Zealand) has the largest fraction of area with dense forest (45.5%), which may lead to errors in snow cover and SP values (Figure 2.31). Portions of northern Asia (12.1%), Europe (25%), and North America (17.5%) also have potential errors in SP from dense forest (Table 2.5).

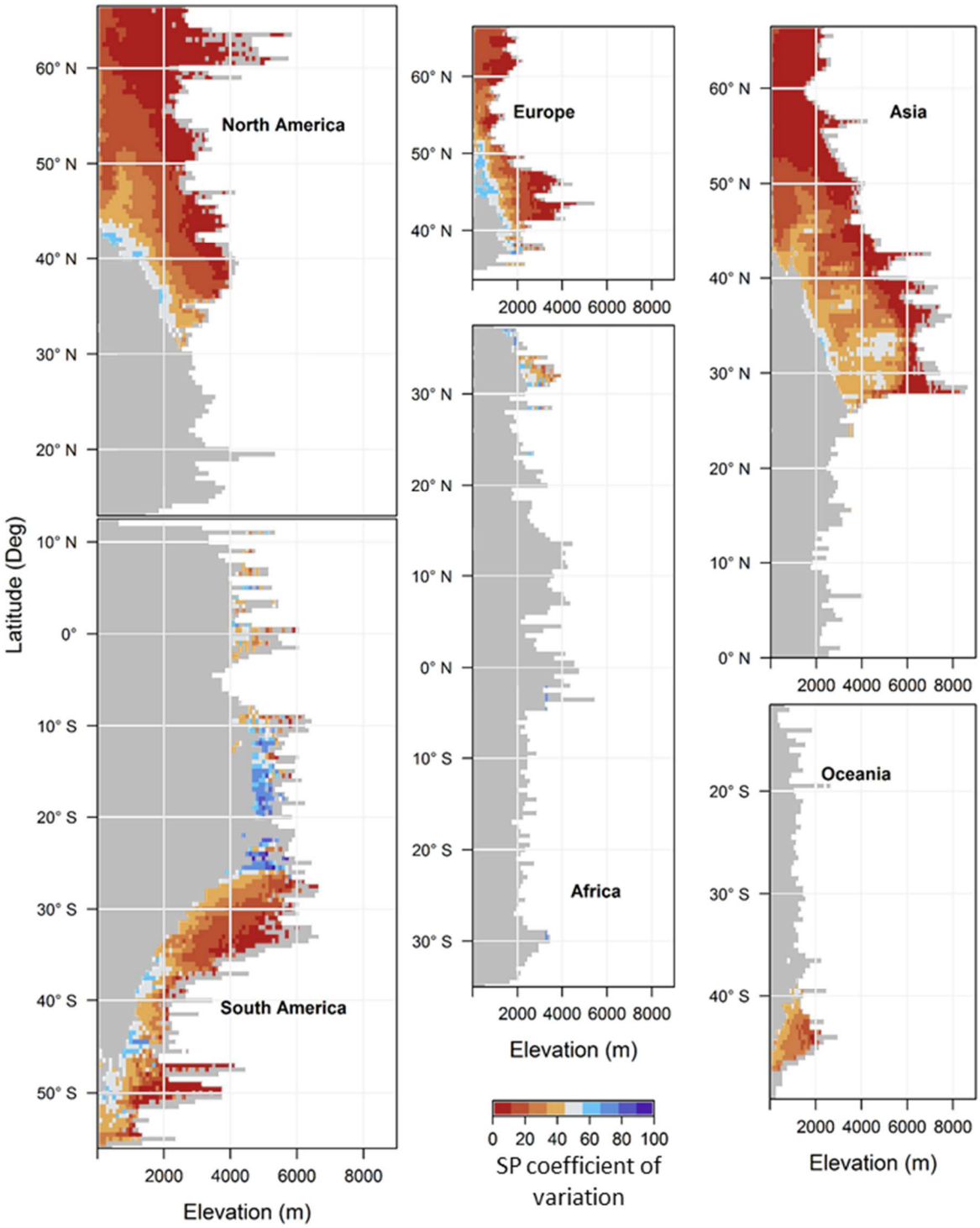

Figure 2.4. Coefficient of variation for annual 2001-2016 snow persistence (%) by latitude and elevation for North America, South America, Africa, Asia, Europe and Oceania.

2.3.2. Climate connections to SP

We computed the relative importance of P and T (Figures 2.32,2.33) in explaining interannual SP variability in an effort to examine how climate influences on SP vary around the world. In general, for lower elevation areas temperature has greater relative importance, whereas high elevation areas are dominated by precipitation importance, with mid elevations displaying a mix of P and T importance (Figure 2.5). Temperature relative importance is greatest overall in low elevations in Europe (from 45-52ºN). In South America from 12-37 degrees south, precipitation dominates in relative importance for SP variability at all elevations (Figure 2.5).

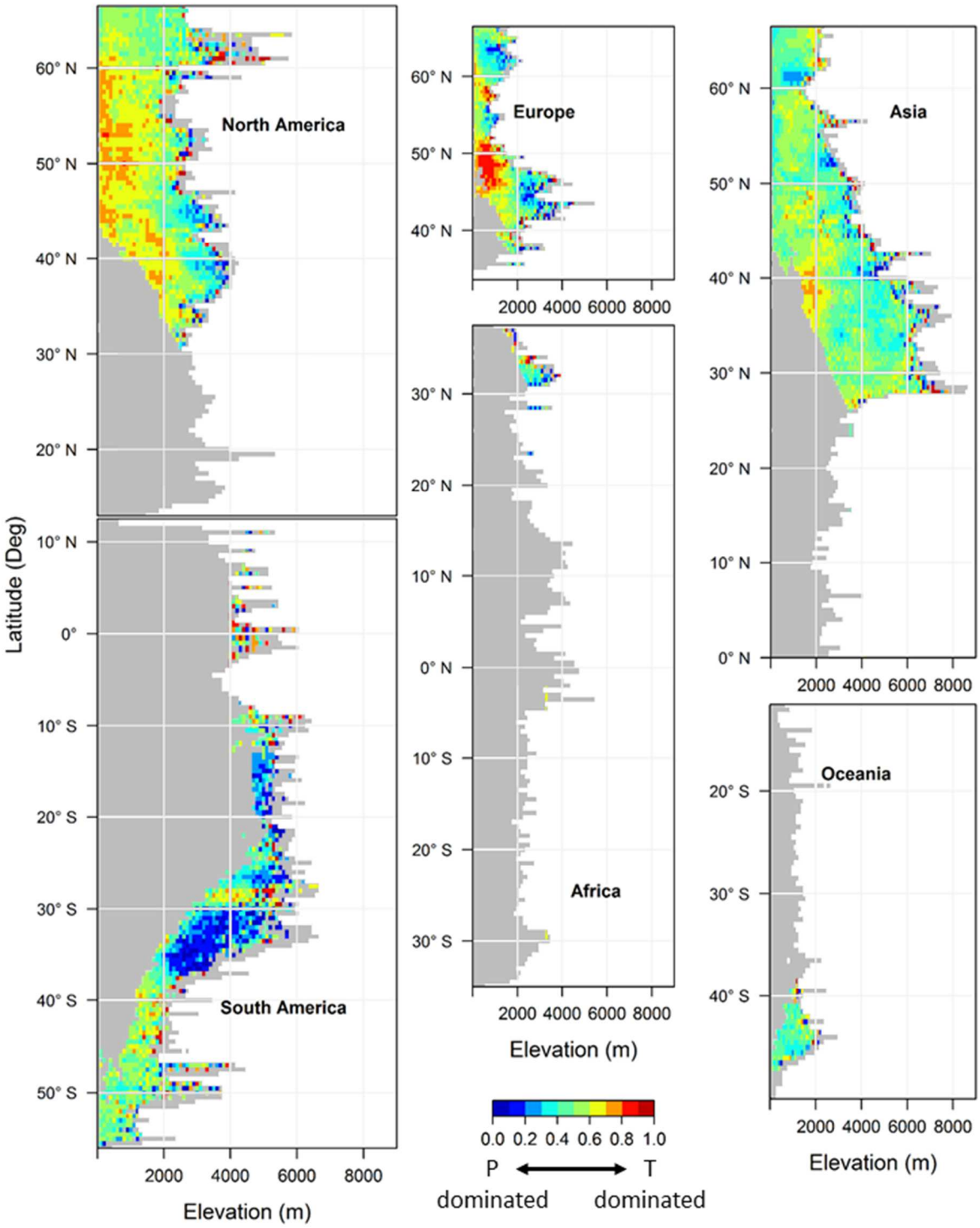

Figure 2.5. Significant results of relative importance analysis of precipitation and temperature in explaining inter-annual snow persistence variability by latitude and elevation for North America, South America, Africa, Asia, Europe and Oceania.

Correlations between SP and climate indices are regionally variable. In South America, SAM is best correlated with SP (Table 2.2, Figure 2.36). In North America, PDO is best correlated with SP along most of the west coast and some parts of the continental interior, whereas ONI has stronger correlations throughout the northern Rockies in the continental interior. East of the Rocky Mountains, SAM is best correlated with SP (Figure 2.35). SAM is also correlated with SP in much of Europe, with NAO, PDO and ONI all having strong correlations in some areas (Figure 2.37). In Asia, climatic teleconnection correlations are quite variable irrespective of latitude and proximity to water, though NAO and SAM dominate correlations by area (Figure 2.38, Table 2.2). Northern Africa displays ONI correlation dominance, without significant teleconnection correlations across the rest of the snow-covered areas of the continent (Figure 2.37). Finally, in Oceania NAO has the strongest correlation with SP, except in the south where ONI has a stronger correlation (Figure 2.39)

Table 2.2. Percent of each continent / region between the Arctic and Antarctic circles within snow-covered areas (SCA, intermittent, seasonal, and permanent snow zones) experiencing significant correlations to climatic teleconnection indices (North Atlantic Oscillation, NAO, Oceanic Nino Index, ONI, Pacific Decadal Oscillation, PDO, Southern Annular Mode, SAM), and the percent of significant correlations where each index has the highest cumulative correlation.

Continent	% SCA with significant correlation to a teleconnection	% correlations where NAO dominant	% correlations where ONI dominant	% correlations where PDO dominant	% correlations where SAM dominant
Africa	52	18	45	9	27
Asia	79	44	13	12	31
Oceania	66	60	24	5	11
Europe	86	53	11	12	25
North America	85	40	17	21	21
South America	66	35	13	7	45

2.3.3. Trends in SP

Trends in SP from 2001-2016 were dominated by declines at most elevations and latitudes (Figure 2.6). Only Africa and Oceania have greater areas with positive trends in SP than with negative trends, but the trend magnitudes are small in these regions (<0.1% yr^{-1}). Overall, 6% of land areas, corresponding to nearly 2.7 million km^2, have exhibited declines in SP while 1%, 0.5 million km^2, have shown increases (Table 2.3). Of the area experiencing decreasing SP, about half is in Asia, followed by Europe and North America. Asia also contains most of the area experiencing increasing SP trends, followed by North America and Europe.

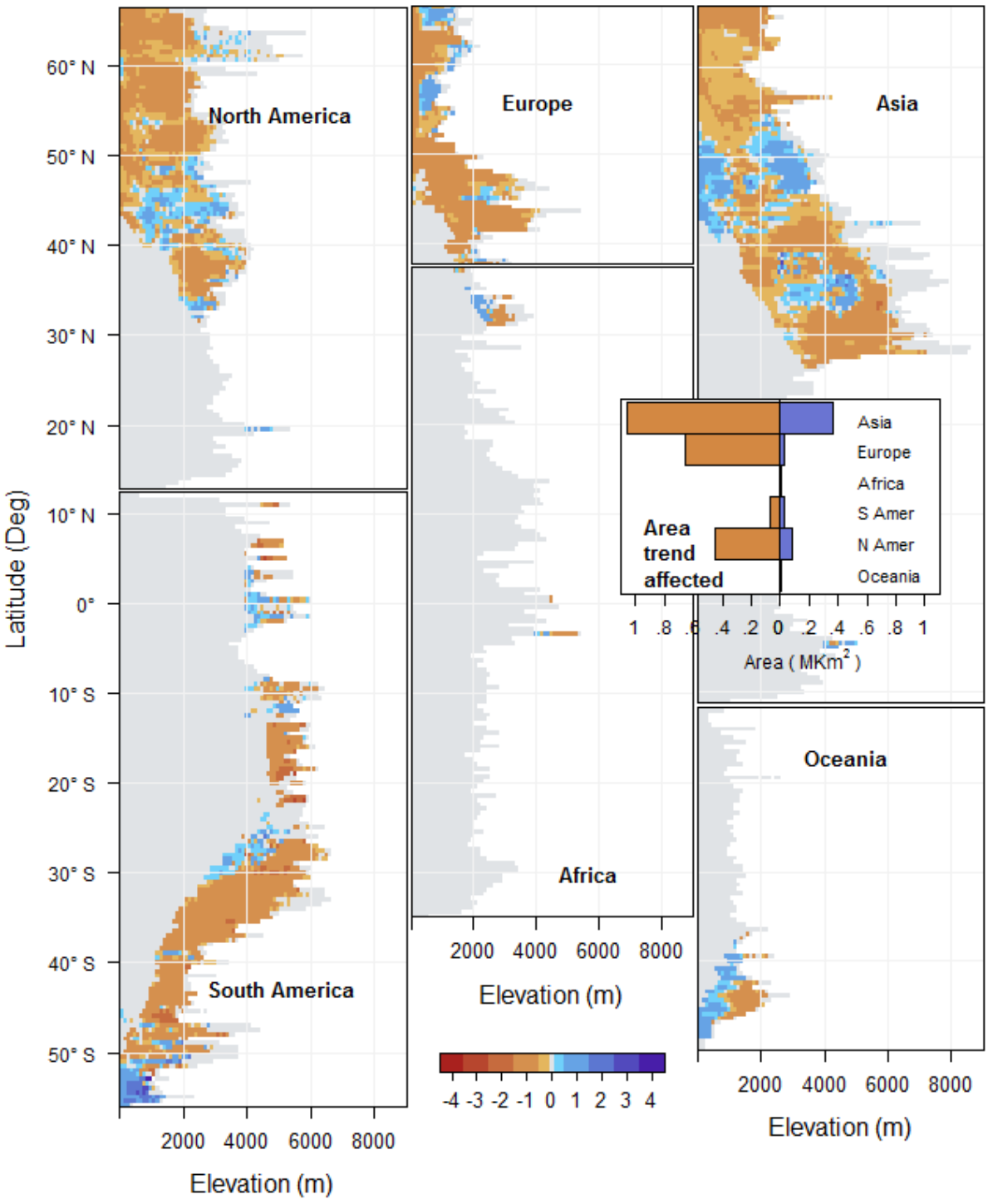

Figure 2.6. Average global trends in annual snow persistence from 2001-2016 by latitude and elevation. Inset displays the total area with a significant trend (orange=decreasing, blue=increasing) by continent.

Table 2.3. Total area (km^2) and percent of each continent / region shown in parentheses, between the Arctic and Antarctic circles experiencing significant trends in SP excluding areas in the low snow zone. The total percent of each continental area experiencing trends and the total percent of each continent within snow-covered areas (SCA, intermittent, seasonal, and permanent snow zones) are displayed in the last two columns.

Continent	Trend	Intermittent	Seasonal	Permanent	Total area	Total %	Total % in SCA
Africa	+	63 (0)	2 (0)	0 (0)	65	0.00	0.43
	-	22 (0)	16 (1)	0 (0)	38	0.00	0.25
Asia	+	85,761 (1)	254,025 (2)	2,808 (1)	342,594	0.81	1.51
	-	180,037 (3)	1,164,189 (7)	2,967 (1)	1,347,192	3.18	5.93
Oceania	+	6,296 (7)	427 (1)	2 (0)	6,724	0.08	5.19
	-	479 (1)	815 (2)	57 (3)	1,350	0.02	1.04
Europe	+	17,574 (0)	13,143 (0)	490 (2)	31,207	0.33	0.40
	-	200,566 (5)	449,258 (12)	386 (2)	650,210	6.90	8.29
North America	+	44,382 (1)	30,877 (0)	243 (0)	75,501	0.37	0.52
	-	69,937 (2)	544,212 (6)	2,344 (1)	616,493	3.04	4.26
South America	+	10,013 (3)	4,441 (2)	265 (1)	14,719	0.08	2.25
	-	17,231 (4)	29,953 (14)	2,668 (6)	49,851	0.28	7.64
Global	+	164,089 (1)	302,913 (1)	3,807 (1)	470,809	0.37	1.03
	-	468,272 (3)	2,188,442 (7)	8,421 (1)	2,665,135	2.08	5.82

In some cases, trends differed for windward and leeward sides of mountain ranges. For example, in the Himalaya (Figure 2.1c, 2.42), the windward side of the mountain range has less total snow-covered area. 3% of this area has significant declining SP, and 3% has significant increasing SP (Table 2.4). In contrast, on the leeward side of the mountains, more of the snow-covered area has declining SP (5%) compared to increasing SP (1%). In the Cascades, increasing SP trends dominate on the windward side (7% of snow-covered area), whereas the leeward side has both increasing and decreasing trends for 2% of snow-covered area (Figure 2.41). In the Alps and the Sierra Nevada, decreasing SP trends dominate on both windward and leeward sides of the mountains, reaching up to 17% on the windward side of the Sierra (Figures 2.43 and 2.44).

Table 2.4. Total snow-covered area (km^2) and percent of the snow-covered area displaying positive or negative trends in SP on each side of the mountain crest divide.

Range	Position	Area (km^2)		Total % in SCA		Net % in SCA
		+	-	+	-	
Alps	windward	329	2417	0.1	9.6	-9.5
	leeward	79	9250	0.2	1.5	-1.3
Cascades	windward	11255	640	7.2	0.4	+6.8
	leeward	3024	4129	1.7	2.4	-0.7
Himalaya	windward	6186	6238	3.1	3.1	0
	leeward	13462	54533	1.2	4.7	-3.5
Sierra	windward	2	4971	<0.01	16.9	-16.9
	leeward	101	6217	0.2	12.4	-12.2

Trends in SP also vary by elevation. In mountain regions, snow persistence increases with elevation, and this pattern varies between years. For example, during the drought in the Sierra Nevada mountains, the lower boundary of seasonal snow (SP=30%) was 700 m higher in elevation than it was during a high snow year (Figure 2.7a). The greatest difference in snow

persistence between years was at mid elevations, near the seasonal-intermittent snow zone boundary (SP=30%, Figure 2.7a). Across the entire Sierra Nevada, low snow, intermittent, and seasonal snow zones below SP ~60% were dominated by negative trends from 2001-2016 (Figure 2.7b).

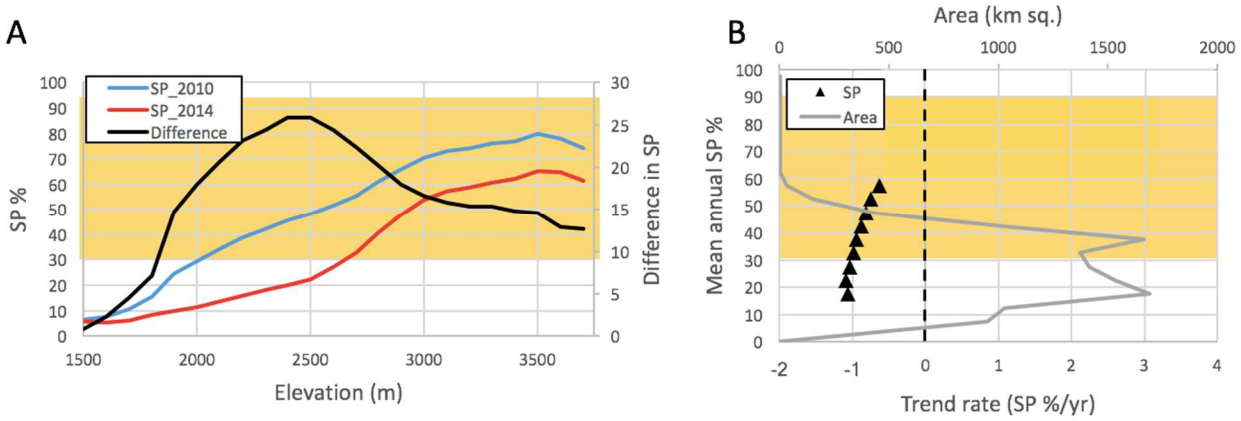

Figure 2.7. A, Annual snow persistence (SP) vs. elevation for the East Walker watershed in the Eastern Sierra Nevada Mountains showing the greatest difference in snow persistence at mid-elevations between a high snow year (2010) and low snow year (2014). B, Mean annual SP vs. 2001-2016 trend in annual SP for the East Walker watershed in 0.5% SP bands; secondary x-axis displays the total area with a significant trend in each SP band. Orange background indicates the seasonal snow zone. Vertical dashed line in B indicates SP trend = 0. SP categories with total area less than 10 km^2 are omitted from this figure because of limited snow cover data; these are the highest elevation, highest SP bands.

2.4. Discussion

2.4.1. Global snow zones and snow persistence

By percent of the global land surface, intermittent, seasonal, and permanent snow zones are located primarily in the northern hemisphere because of the large land mass at high latitude. For the few isolated areas in the tropics that are high enough in elevation to support snow occurrence and accumulation, the snow is in isolated alpine refugia. Although processes of snow accumulation and ablation are locally complex, our analysis highlights the key role of global temperature in snow climatology. Similar snow line elevations between continents in the northern and southern hemisphere demonstrate how latitude and elevation effects on temperature are strongly linked to snow presence. This relationship is not as consistent at high latitudes, where the large continents with inland mountain ranges (Asia, North America) have lower average snow elevations than those with mountain ranges closer to coasts (South America, Europe). This is likely because of cooler temperature for similar latitudes in large continental interiors, but it may be influenced by other processes such as snow redistribution from Siberian winds (Hirashima et al., 2004).

2.4.2. Climate connections to SP

Relative importance results are consistent with the inference that temperature controls snow line. Prior research has identified linear patterns in the correlations between snowpack and temperature/precipitation, with elevations below a threshold experiencing temperature control and elevations above the threshold controlled by variability in precipitation (Morán-Tejeda et al. 2013). Our relative importance results (Figure 2.5) similarly show elevational and regional dependence in precipitation vs temperature controls on SP. These results can be used to estimate

the elevation threshold at which precipitation becomes a more dominant influence on SP in each region. However, our findings also illustrate substantial regional variability in patterns of relative importance of temperature and precipitation. The shift from temperature to precipitation with elevation is strongest in Europe, followed by North America and Asia. In contrast South American and Oceania have a mix of temperature and precipitation relative importance, with precipitation dominating at mid-latitudes of South America (Figure 2.5).Generally the strength of the relative importance fits is not very strong, although it is significant in many locations (Figure 2.34); locations with the strongest relative importance fit ($r^2>0.5$) are also those with greater relative importance of precipitation. This may be because the precipitation total can better represent climate conditions throughout the snow season, whereas averaged temperature may smooth out important variability in temperature that affects snow accumulation and melt.

Correlation analyses with climate indices illustrate how teleconnection patterns can affect snow persistence globally. The findings are consistent with previous studies highlighting the importance of different teleconnection patterns in different regions (Ge and Gong 2009; Seager et al. 2010; Saavedra et al. 2018), but they also illustrate how interconnected and spatially variable these influences can be (Figures 2.35-2.39). More of the snow covered areas in Northern Hemisphere significantly correlated with the teleconnections tested (Table 2.2).

2.4.3. Trends

Most land areas that receive snow (93%) did not experience significant trends in snow persistence from 2001-2016, partially because of the small time-frame analyzed (16 years), only half the span of a typical climatology study. However, the dominance of negative over positive trends globally is consistent with concomitant rising global air temperatures (Hansen et al. 2010),

and the short-term trends documented here can have severe consequences for the areas affected, including lower annual water yield (Hammond et al., 2018a) and changes in the timing of water supplied from snowy areas. For example, the drought and associated low snow in the Sierra Nevada of North America caused a $2.7 billion agricultural impact and over 10,000 direct job losses in 2015 alone (Howitt et al., 2015). Similarly in Europe, multi-billion dollar impacts are expected from snow losses in the ski industry (Elsasser and Messerli 2001, Moen and Fredman 2007). The lack of significant trends detected in other areas relates to the time scales at which climatic processes and atmospheric-oceanic oscillations operate (Mote et al. 2005, Dyer and Mote 2006), with ENSO periodicity from 2-7 years and PDO from 8-12 years. When interpreting the global SP trends presented here, long term climate cycles, the start date and end date for the period of analysis, and land cover change all need to be examined to determine the causes of trends (Jones 2011).

However, although the time period analyzed is relatively short for a trend analysis, it does provide insight into which areas may be most sensitive to changing climate. Previous research has indicated that mid-elevation snowpacks are likely to be the most sensitive to climate warming (Nolin and Daly 2006, Sproles et al. 2013), whereas high-elevation regions that remain well below freezing during winter months have not exhibited these changes (Stewart 2009). This implies a connection between snow trends and temperatures, where snowpack sensitivity to temperature is greatest in places that are already relatively warm, such as those in temperate climates and low elevations, with warm snowpacks in wet regions most likely to experience the greatest snow loss (Luce et al. 2014). Recent modeling suggests that snow at low and mid-elevations may completely disappear by 2100 (Beniston 2012). Compared to these prior findings, our results suggest that the highest elevation snowpacks are not entirely stable; we found

declining trends over 1-6% of each continent's permanent snow zone. Declining snow persistence affected 7% of the seasonal snow zone globally, which was the greatest total area ($>2x10^6$ km^2) with declining trends in snow persistence. Declining trends in snow persistence affected less of the intermittent snow zone (3%), which is not fully consistent with predictions that the lowest elevations of snow are most sensitive to changes in climate conditions. This may be because of the combined effects of precipitation and temperature on snow persistence; short-term trends can be particularly affected by precipitation patterns in areas where precipitation has high relative importance for SP (Figure 2.5). Even though temperature relative importance is typically greatest in the low elevation intermittent snow zone, the smaller area affected by trends in this zone may reflect the importance of weather patterns during each individual year in this zone. The intermittent snow zone is sensitive to whether time periods of precipitation coincide with low enough temperature for snow. Seasonal snow, in contrast, develops only if temperatures in the winter stay consistently cold enough for snow to remain on the ground all season.

Differences in snow persistence trends across snow zones highlight the importance of using snow zones or some other snow climatology metric as a context for interpreting trends. Different regions will have varying susceptibility to "dry snow droughts", which are low snow years when the low snowpack is caused by lack of precipitation, vs. "warm snow droughts," which are low snow years when warm temperatures prevent precipitation from accumulating on the landscape as a snowpack (Harpold et al. 2017). Windward-leeward sides of mountain ranges also have hydroclimatic shifts that affect their snow persistence trends, and it is clear that snow changes are not consistent even within single mountain ranges. The windward-leeward patterns across mountain ranges (Table 2.4) could be examined in greater detail in future research.

2.4.4. Uncertainties

MODIS snow products have been widely used in snow research and have compared favorably to field snow measurements in multiple studies (Krajci et al. 2014, Marchane et al. 2015). The snow persistence grids generated in this study shows general agreement by visual comparison with other gridded snow and ice products (NH SCE Robinson et al. 2012, MODICE, Painter et al. 2012). Qualitative evaluations suggest that SP works well for identifying permanent snow and ice compared to glacial inventories (e.g. Figure 2.1) and to minimum annual exposed snow and ice from MODICE. The intermittent snow zone boundary from the present study displays a similar overall spatial distribution as maximum annual northern hemisphere snow cover extent (NH SCE).

However, there are some identified shortcomings in the MODIS snow product related to vegetation, thin snow, and clouds (Hall and Riggs 2007). For finer spatial and temporal resolution analysis, a fractional snow product and/or a daily snow product may be more appropriate to use than the 8-day binary product (snow/no snow) we used here (Rittger et al. 2013). Tests of these finer resolution products in the western U.S. and South America have shown that application of the daily fractional product is greatly limited because of gaps in data due to clouds (Hammond, Saavedra unpublished data). Using the 8-day product limits the temporal precision of snow persistence, which will have some unknown effect on the trend analyses. As highlighted in our masking methods, the MODIS snow cover product also has some errors such as mapping snow in very cloudy areas known to have no snow or over white salt flats (Saavedra et al. 2017). Cloud and other forms of missing data were most prevalent in South America (20%) (Tables 2.5). Errors in snow cover retrieval from vegetation are likely greatest in in Oceania (45%) and Europe (25%) (Table 2.5), as highlighted in the maps of forest cover

>50% (Figures 2.8-2.19). Simple vegetative thresholds for binary snow identification are included in current MODIS snow cover products (MOD10A1, MOD10A2), but more detailed adjustment methods may be needed for dense forested areas. Several studies have proposed vegetation adjustment methods for MODIS fractional snow products (Nolin 2010, Raleigh et al. 2012), and further research could address how to adjust for vegetation in the binary snow products used in this study. Finally, we established the thresholds for separating snow zones based on the work of Saavedra et al. (2017) in the Andes, but further research in different regions should evaluate whether these boundaries are appropriate for other regions.

2.4.5. Implications and potential uses of the SP product

Snow remote sensing techniques are advancing rapidly, allowing detailed snow mapping in areas with the resources for field and airborne monitoring (Painter et al. 2016). While these advances are taking place, there is still an important role for MODIS snow products because they allow comparison of snow zones across the globe and provide particularly valuable snow information in places that lack in situ or airborne measurements. The need for hydroclimatic trend detection and attribution studies is ongoing (Stewart 2009), as this information helps water and land managers plan for future conditions. At the global or regional scale we still lack detailed knowledge of the annual and mean annual first and last snow occurrence, snow season length, and snow intermittence (the number of times snow melts to expose bare ground during the snow season). Assessing how snow persistence and these other snow cover-based metrics change through time will highlight areas most sensitive to future snow loss and hydrologic change. Snow persistence shows promise for aiding streamflow forecasting (Saavedra 2017, Hammond et al. 2018a), and in the near future, global SP may be combined with global soil

moisture storage and response metrics (McColl et al. 2017) to aid in coarse scale flow estimation. At finer timesteps useful for prediction, NASA's Land Data Assimilation Systems (LDAS), which is under continuous development, utilizes station, satellite, and radar precipitation measurements to forecast hydrological response, and shows increased accuracy when snow covered area is included to better constrain predictions (Liu et al., 2015). Snow persistence maps can also be useful in other applications such as identifying habitat ranges for snow-dependent species, planning grazing rotations, selecting crop type and timing, or planning closures for remote mountain roads.

2.5. Conclusions

Snow cover affects 36% of the global land surface area between the Arctic and Antarctic circles, with most (98%) of that area in the northern hemisphere. The accumulation of snow starts at similar elevations for the same latitude across the globe, but coastal proximity and windward-leeward effects can alter this relationship. Snow persistence is correlated with both temperature and precipitation, with greater relative importance of temperature at low elevations of the northern hemisphere and greater relative importance of precipitation at high elevations of the northern hemisphere and in South America. Annual patterns in snow persistence are most strongly correlated with the North Atlantic Oscillation, but multiple climate indices correlate with snow persistence throughout global snow covered areas. Of the areas with snow cover, 6% have had declining snow persistence since 2001, while 1% have had increasing snow persistence. The greatest areas with declining snow persistence were in Asia, North America, and Europe. Declining trends covered the greatest extent of areas with winter seasonal snow cover (7%), whereas only 1% of areas with permanent snow cover have experienced declining trends from

2001-2016. The global snow persistence datasets and associated trend analysis presented here can be used for land management decision making (e.g. transportation, wildlife habitat, horticulture and grazing) and to identify areas sensitive to future climatic change. Ongoing collection of MODIS data will allow continual updating of this analysis to track snow changes into the future.

Chapter 3. How Does Snow Persistence Relate to Annual Streamflow in Mountain Watersheds of the Western U.S. with Wet Maritime and Dry Continental Climates?[2]

3.1. Introduction

Spatiotemporal changes in the mountain snowpack of the western U.S. are well documented (Regonda et al., 2005; Stewart et al., 2005; Clow, 2010; Fritze et al., 2011; Harpold et al., 2012), with both data-based and modeling studies suggesting that streamflow generation is sensitive to loss of snow on multiple time scales (Regonda et al., 2005; Stewart et al. 2004, 2005; Clow, 2010; Jefferson, 2011; Furey et al., 2012; Berghuijs et al., 2014; Barnhart et al., 2016). Areas conducive to snowfall are forecast to shrink considerably (Klos et al., 2014, Luce et al., 2014), and recent analyses across catchments in the U.S. suggest that a shift in precipitation (P) from snow to rain will lead to a decrease in annual streamflow across all climate types (Berghuijs et al., 2014). However, streamflow responses to changes in snow are regionally variable (Stewart, 2009), and the reasons for this variability are not clear. Berghuijs et al. (2014) found that watersheds differ in their streamflow sensitivity to snow fraction changes, but they did not examine which physical factors led to differences in these sensitivities. Additionally, Berghuijs et al. (2014) relied on the MOPEX network of watersheds, which are mainly located in the humid eastern U.S. Few of the MOPEX watersheds are in the western U.S., a region that includes areas with both greater snow accumulation and greater aridity than represented in the MOPEX dataset.

[2] Hammond, J. C., Saavedra, F. A., & Kampf, S. K. (2018). How does snow persistence relate to annual streamflow in mountain watersheds of the Western U.S. with wet maritime and dry continental climates? Water Resources Research, 54, 2605–2623. https://doi.org/10.1002/2017WR021899

The western U.S. includes both wet coastal climates and dry continental interior climates with elevations ranging from sea level to over 4,000m. Recent simulation studies (e.g. Mankin and Diffenbaugh, 2015; Naz et al. 2016) have highlighted how decreased snowmelt contributions to streamflow across the region could create water supply problems. In wet basins, water demand can be met by rainfall runoff, whereas in dry basins snow loss poses a greater risk to water supply (Mankin and Diffenbaugh, 2015). These simulation studies were conducted for large river basins (>5,000 km^2) that span a range of climates and elevations. The large basin scale of analysis has been widely applied in the region (Vicuna et al., 2007; Painter et al., 2010; Anghileri et al., 2016). Similarly, detailed studies of individual small watersheds (<500 km^2) (Nayak et al., 2010; Hunsaker et al., 2012; Godsey et al., 2014) have advanced process understanding at specific sites, but progress in scaling new process-based knowledge to the watershed scale and beyond has been limited (Sivapalan, 2005). Both large basin and small watershed scales of study provide important insights, but they do not capture all elements of streamflow sensitivity to snow. Large basin scale analysis can obscure information about which parts of the basin are most sensitive to snow loss, and individual watershed analyses lack a regional context to determine whether or not the sites are representative of trends elsewhere. The western U.S. lacks a systematic study comparing multiple small watershed streamflow responses to snow changes.

This research fills a key knowledge gap by comparing small watershed responses to changes in snow across a large number of watersheds in the western U.S. The motivations for the study are both the need to understand how loss of snow may affect streamflow in the study region and the need for simple methods to predict streamflow in other data-sparse regions with snowmelt-dominated streamflow. This paper examines (1) how globally available spatial snow cover variables compare with other snow variables more commonly used in streamflow

prediction models, (2) whether snow variables are useful for estimating streamflow in watersheds that span a wide range of snow persistence and climate conditions, and (3) whether snow cover could be useful for reconstructing streamflow patterns in ungauged watersheds, both spatially and temporally.

3.2. Background

Mechanisms of streamflow response to changes in snow are embedded in process hydrologic models (Huntington et al., 2012; Mahanama et al., 2012; Vano et al., 2012; Barnhart et al., 2016), so few studies examine these connections directly with empirical data. This may be because models enable researchers to experiment with how individual climate variables affect streamflow. While model-based research has merit, advances in understanding often require both models and empirical analysis (Sivapalan, 2003; Sivapalan et al., 2003; McDonnell et al., 2007). Empirical analyses have recently become more prominent in hydrology because of the need to predict streamflow in ungauged areas where input data to support complex hydrologic models are lacking. For example, several empirical snow studies demonstrate that the importance of temperature and precipitation for snowpack varies along elevational and regional gradients (Kapnick and Hall, 2012; Morán-Tejeda et al., 2013) and that precipitation may be more important for snow changes in dry areas relative to wet areas (Mankin and Diffenbaugh, 2015). Several recent hydrologic empirical studies have used the Budyko framework to relate streamflow to climate (Wang and Hejazi, 2011; Jones et al., 2012; Berghuijs et al., 2014; Liang et al., 2015), but this framework has limitations for studying snow-dominated areas because it does not account for the phase of precipitation (rain, snow) or the accumulation of snow on a watershed. Studies that do apply the Budyko framework to examine streamflow connections to

snow have used some form of hydrologic modeling to reconstruct portions of the water balance (Berghuijs et al. 2014; Barnhart et al. 2016).

Empirically examining streamflow responses to snow requires information on spatial patterns of snow across watersheds. Researchers have characterized changes in snow using the fraction of precipitation falling as snow (Klos et al., 2014), the snow water equivalent (SWE) either at maximum accumulation, or at a fixed date each year (Mote, 2003; Barnett et al., 2008; Skaugen et al., 2012); the snow-covered area (Wang et al., 2005; Déry and Brown, 2007; Rupp et al., 2013; Marchane et al., 2015); and the snow cover duration (Hantel et al., 2000; Bulygina et al., 2009). Each of these variables has strengths and weaknesses in characterizing the snow across watersheds. Separating rain and snow components from daily precipitation records is difficult because of the dependence of snowfall on temperature and humidity during a short time period (Dai, 2008; Marks et al., 2013; Froidurot et al., 2014).

Methods for mapping SWE spatially have improved, but these often rely on ground SWE measurements, which are typically not extensive enough to map SWE patterns over large areas (Dozier et al., 2008; Guan et al., 2013; Jörg-Hess et al., 2013). Areas near the transition between seasonal and intermittent winter snow may be particularly sensitive to snow loss (Regonda et al. 2005; Christensen and Lettenmaier, 2007; Adam et al., 2009; Sproles et al. 2013), but there is limited in situ snow monitoring in these locations.

Of the 790 SNOTEL stations in the conterminous western US, only 8% (63) fall within the intermittent or low snow zones, where snow is not consistently present throughout the winter, and the remaining 92% are within the winter seasonal snow zone, where snow persists throughout the winter (Moore et al., 2015). While this configuration of stations is useful for its intended purpose of monitoring locations that consistently have snow, the station network under-

samples both areas of dynamic change within the intermittent-persistent snow transition and less accessible high alpine areas.

Unlike SWE, snow cover can be more easily derived globally from remotely sensed snow covered area, particularly in regions with limited cloud cover (Hall and Riggs, 2007). While snow cover does not directly indicate the quantity of water contained in a snowpack, it is useful for studying snowmelt hydrology because it can be mapped continuously over space, thus reducing gaps in information between point monitoring locations. Prior studies have used snow cover extent or snow cover duration to map changes in snow patterns over time (Déry and Brown, 2007; Derksen and Brown, 2012). A related metric, snow persistence (SP), is the fraction of time that snow is present on the ground, and this metric has been useful for defining boundaries between intermittent and seasonal snow zones in a wide range of climates (Richer et al. 2013; Moore et al. 2015; Saavedra et al. 2017) and for identifying where peak streamflow source regimes shift from rainfall to snowmelt (Kampf and Lefsky, 2016).

Snow covered area products have been incorporated into streamflow forecasting models in Europe (Gomez-Landesa et al., 2001, Kolberg et al., 2006), Asia (Immerzeel et al., 2009; Jain et al., 2010; Duethmann et al., 2014; Uysal et al., 2016), and North America (Rodell and Houser, 2004; Andreadis and Lettenmaier, 2006; Roy et al., 2010; Su et al., 2010; Tang and Lettenmaier, 2010; De Lannoy et al. 2012, Sproles et al., 2016). Currently, a major focus of the use of remotely sensed snow metrics for hydrologic forecasting is determining the most effective means of assimilating the remotely sensed observations into hydrologic models for operational use (Andreadis and Lettenmaier, 2006; Bender et al., 2014; Xu et al., 2014). Moving forward, methods integrating multiple snow data products (SWE and SCA estimates) will likely improve the accuracy of hydrologic forecasting in snow-dominated areas.

3.3 Study area

Our study area is the mountainous regions of the western United States (Figure 3.1), which cover a wide variety of climate types including warm temperate fully humid (Cfb) in the Cascades of the northwest, warm temperate with dry summers climate (Csb) in the Sierras further south, and cold arid steppe (BSk) climate in the Basin and Range (Kottek et al., 2006). For the watersheds sampled, mean annual precipitation (P) is between 900 and 3,500 mm/y in the western Cascades, which exceeds the mean annual potential evapotranspiration (PET) by a factor of 1.5 or more (Figure 3.1a). P in the Basin and Range is only 300 to 1,000 mm/y, with P/PET closer to 0.5. In the Northern and Southern Rockies, P exceeds PET only at the higher elevations, whereas at lower elevations P≤PET.

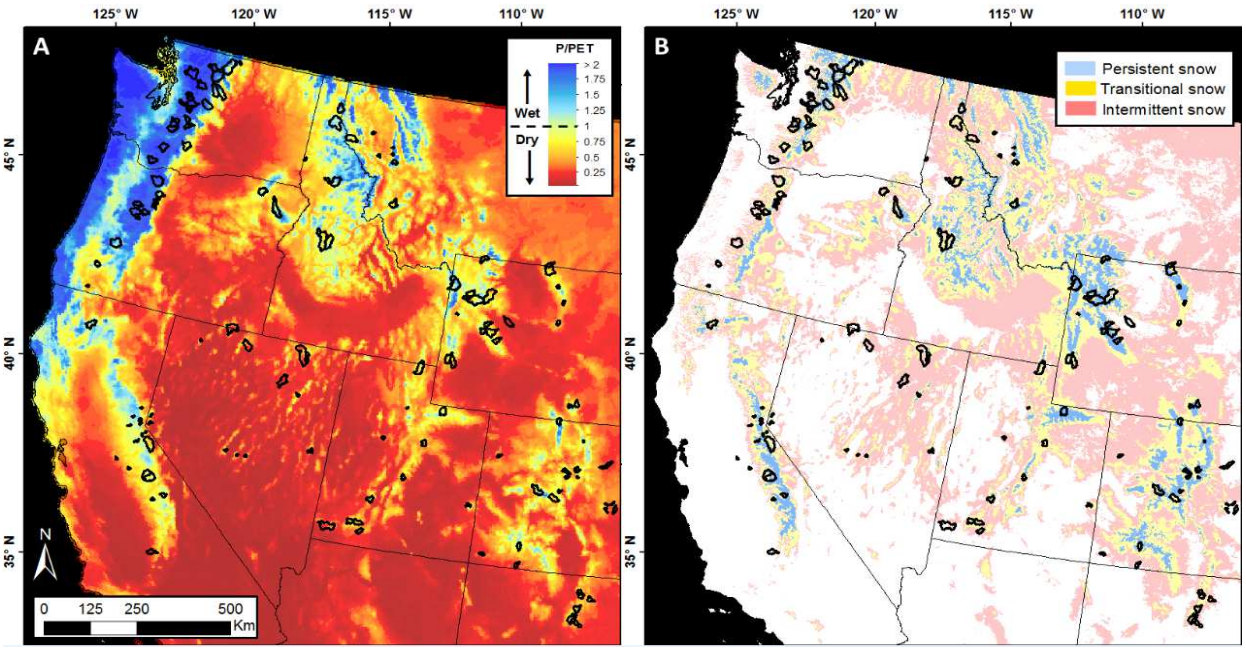

Figure 3.1. USGS reference watersheds (Falcone, 2011) displayed in black across the western U.S. plotted on top of (A) mean annual P/PET and (B) snow zones (Moore et al., 2015). Mean annual P/PET in A for water years 2001-2015 from PRISM (Daly, 2013) and gridMET (Abatzoglou, 2012) datasets. Intermittent snow zones have mean annual 1 Jan – 3 Jul 25%<SP<50%, transitional snow zones have mean annual 1 Jan – 3 Jul 50%<SP<75%, and persistent snow zones have mean annual 1 Jan – 3 Jul SP>75%. The transitional and persistent zones combined represent the areas with seasonal snow that is present throughout the winter.

Small watersheds used in this study range in snow persistence from intermittent to persistent, with intermittent snow tending to occur at low elevations and persistent snow at high elevations. Moore et al. (2015) defined intermittent snow as areas with mean 1 January – 3 July SP between 25-50%, transitional snow with SP between 50-75%, and persistent snow where SP is greater than 75% of the 1 January – 3 July time period. All areas with SP>50% are considered the seasonal snow zone, which is a combination of the persistent and transitional snow zones. Moore et al. (2015) used these SP thresholds to map snow zones across the western US using MODIS snow cover data (Figure 3.1b). Elevation extents of the intermittent, transitional, and persistent snow zones defined in Figure 3.1b differ substantially across the region, with higher elevation snow zone boundaries at high latitudes and in the continental interior. The elevation extents of snow zones change from year to year, most notably with intermittent and transitional snow zone boundaries increasing in elevation during periods of extended or severe drought.

Table 3.1. Climate, snow, and streamflow variables examined, data sources, and spatial resolutions

Type	Variable	Data source	Resolution
Climate			
	Precipitation (P)	PRISM, Daly (2013)	4-km
	Temperature (T)	TOPOWX, Oyler et al. (2014)	800-m
	Potential evapotranspiration (PET)	gridMET, Abatzoglou (2013)	4-km
Snow			
	Snow persistence (SP)	Hammond et al. (2017a)	500-m
	Snow season length (SS)	Hammond et al. (2017b)	500-m
	Fraction of precipitation falling as snow (SF)	Klos et al. (2014)	4-km
	Peak snow water equivalent (SWE)	SNODAS, NOHRSC (2004)	1-km
Streamflow	Discharge (Q)	USGS	Daily

3.4 Methods

We examined how snow and climate variables relate to annual and mean annual streamflow for small watersheds across the western U.S. from 2001-2015 (Table 3.1). This time period was selected to coincide with the availability of MODIS snow cover products for the analyses. For snow and climate variables, we used both point values from ground stations and gridded data products.

3.4.1 Climate variables

The climate variables we analyzed were precipitation (P), temperature (T), potential evapotranspiration (PET), and aridity (P/PET). For P, we used AN81m monthly precipitation (P) data from the PRISM data archive (Daly, 2013) at 2.5 min resolution. For temperature, we used the monthly 800 meter resolution TopoWX gridded mean (T), minimum (Tmin) and maximum (Tmax) air temperatures from the Montana Climate Office (Oyler et al., 2015). For PET, we used reference evapotranspiration from the 4 kilometer resolution University of Idaho data product (Abatzoglou, 2013). To rectify the difference in spatial resolution of the multiple gridded datasets used we used nearest neighbor interpolation to the 500 m resolution of MODIS data, with interpolated grids snapped to the MODIS layers for agreement between grid boundaries. Unless otherwise specified, climate variables were computed as water year total (P, PET) or average (T) values. We use water year precipitation in this analysis because of our goal to explain variability in water year flow. We used a mean annual P/PET threshold of 1 to separate watersheds into wet (precipitation surplus) and dry (precipitation deficit) climates.

3.4.2. Snow variables

We analyzed four different snow variables: snow persistence (SP), snow season length (SS), fraction of precipitation falling as snow (SF), and peak snow water equivalent (SWE). For SP and SS we used MODIS/Terra Snow Cover 8-Day L3 Global 500m Grid, Collection 5 obtained from the National Snow and Ice Data Center (NSIDC) (NSIDC, Hall et al., 2006). We computed the 1 January – 3 July SP for each year as the fraction of 8-day MODIS images with snow present. The selected period brackets the temporal extent of peak snow accumulation to complete snow ablation in most parts of the western United States (Moore et al., 2015); we used this partial year SP rather than water year SP because initial tests revealed stronger relationships between partial year SP and streamflow. The 3 July date was used as the last MODIS image date each year because the 8-day MODIS image does not fall on the first of the month in this case. For comparison, we computed SP from ground-based SNOTEL station data for the same time period and compared these values to MODIS-derived SP, and we examined correlations between SNOTEL peak SWE and SP. SNOTEL SP was calculated as the percent of days with SWE > 0 for 1 January to 3 July. To evaluate whether dense forest vegetation obscured snow cover in parts of the study area, we also calculated the fraction of each watershed with dense forest (>50% tree cover) using 2010 MODIS Vegetation Continuous Fields (MOD44B) Collection 5 Percent Tree Cover. 2010 is the most recent year with full coverage for the study region.

We computed snow season length (SS) for each water year as the length of time from the first occurrence of snow to the last occurrence of snow for each pixel. For each of the study watersheds, we calculated watershed average SP and SS by averaging all pixels in the watershed contributing area.

The mean-annual monthly fraction of precipitation falling as snow (SF) was obtained for the 1979 – 2012 period (Klos et al, 2014) and then averaged for months January through June to match the SP calculation. Klos et al. (2014) combined observed temperature and precipitation data with an empirical probabilistic precipitation phase model (Dai, 2008) to estimate and map the fraction of precipitation falling as snow. We chose not to compute snow fractions for each year of the study and instead focused on readily available SWE and MODIS variables representing snow presence on the ground (SP, SS) for comparison with streamflow.

For peak SWE, we used both point and gridded data. For point data, we compiled peak SWE for each water year at 790 SNOTEL stations within our study area boundary for water years 2001 to 2015 from the National Water and Climate Center (NWCC) Report Generator 2.0 (NWCC, 2016). For gridded data, we compiled daily SNODAS SWE from NSIDC (National Operational Hydrologic Remote Sensing Center, 2004). The Snow Data Assimilation (SNODAS) program provides spatial SWE estimates daily at 1 km^2 resolution across the entire contiguous USA. This product incorporates remotely-sensed and ground-based snow observations to run the National Operational Hydrologic Remote Sensing Center (NOHRSC) Snow Model (NSM) with the objective of producing the closest approximation of daily snow conditions. SNODAS values are available from 1 October, 2003 to present. For each study watershed, we calculated a daily average SWE value by averaging all SNODAS grid cells within the watershed boundary and computed SNODAS peak SWE as the maximum watershed average SWE value for each water year.

3.4.3. Streamflow variables

For annual streamflow volume (Q), we identified USGS reference watersheds in the western U.S. using the GAGES II dataset (Falcone, 2011), with records of discharge from 2001 to 2015. Since the purpose of our study was to examine how snow relates to streamflow in watersheds with different climate characteristics, we needed relatively small watersheds without large ranges of variability in snow. Therefore, we selected only watersheds with drainage areas <500 km^2, which restricts the study primarily to smaller watersheds while allowing a large enough sample size to address the study objectives. To the extent possible, we chose watersheds that drain only one snow zone, have minimal flow alteration, and have experienced limited land use change over the study time period. We excluded watersheds with limited snow (mean annual SP<30%) because of our study emphasis on snow-streamflow relationships. Substantially glaciated watersheds were excluded in all regions except for the North Cascades, where all small watersheds in the persistent snow zone contain glaciers. The final sample set included 119 watersheds spread throughout the mountain ranges of the study area on either side of the regional mountain crests and capturing the full range of snow zones in each region (Figure 3.1b). We compiled daily discharge records for the full study period at each gauge and calculated annual and mean annual unit area Q values. Water year total precipitation was used to compute the annual and mean annual runoff ratio (Q/P) for each watershed. Ten watersheds with mean annual Q/P>1.1 were removed from the sample, assuming that these high runoff ratios reflected either errors associated with precipitation estimation, impoundments within the watershed, glacial and multiyear snow storage and melt, and/or groundwater discharge.

3.4.4. Analysis

Our study objectives were to compare snow variables, address the utility of using remotely sensed snow covered area data as a predictive measure of streamflow, and to examine how snow relates to streamflow response in different climates. To evaluate how the snow variables relate to one another at watershed scale, we computed cross-correlations between watershed average values of SP, SS, SF, and peak SWE from SNODAS. We also examined how climate variables (P, T, P/PET) relate to two of the snow variables (SP, peak SWE) at watershed scale. For these analyses, we computed total P and average T for months October to June to overlap with the period used for SP calculation and capture patterns in P and T active during much of the period of snow accumulation and ablation.

To examine how snow and climate variables relate to annual streamflow volumes, we computed univariate watershed-scale correlations between watershed average snow variables (SP, peak SWE) and streamflow variables (Q, Q/P). For these analyses, we used water year total P and PET and water year average T. We also determined the relationship between Q/P and SP and Q/P and SWE for each watershed independently using linear regressions on annual data, and we calculated the slope and significance of these relationships at each watershed.

Finally, to illustrate how SP can be used to examine spatial patterns of streamflow generation, we applied the relationship between SP and Q to map mean annual streamflow patterns in the Upper Colorado River Basin. We fit a second order polynomial to the Q vs. SP relationship ($R^2 = 0.81$). We then applied this equation to the mean annual SP grid to obtain modeled Q at the 500 m scale across the basin, with areas below SP 30% masked because our initial sample of reference watersheds excluded watersheds with SP<30%. We also tested this relationship using streamflow data from watersheds of Canada and Argentina obtained from the

Global Runoff Data Centre (GRDC, German Federal Institute of Hydrology, Koblenz, Germany).

3.5. Results

3.5.1. Climate

The study watersheds were classified as wet or dry based on a P/PET threshold of 1 to separate areas of precipitation surplus and deficit. 48 watersheds were classified as wet, with 31 in the Cascades, 12 in the Northern Rockies, two in the Southern Rockies, and three in the Sierra Nevada. 71 watersheds fit the dry classification, with 20 located in the Basin and Range, 20 in the Northern Rockies, 21 in the Southern Rockies, and 10 in the Sierra Nevada. Wet and dry watershed groups have similar ranges of Tmax, but differ significantly in Tmean and Tmin, with dry watersheds overall colder than wet (Figure 3.2; dry Tmean median 4.8 ^{0}C, wet Tmean median 6.1 ^{0}C; dry Tmin median -0.7 ^{0}C, wet Tmin median 1.6 ^{0}C). Thus, throughout the rest of the paper we refer to wet watersheds as wet/warm, and dry watersheds as dry/cold. The range of peak SWE was similar in both dry/cold and wet/warm watersheds, but the median is lower in the dry/cold group (dry/cold peak SWE median 331 mm, wet/warm peak SWE median 600 mm). The SP ranges and median values are similar for both wet/warm and dry/cold groups, and Q is substantially higher in wet/warm watersheds than in dry/cold (dry/cold Q median 270 mm/y, wet/warm Q median 1,110 mm/y; Table 3.2, Figure 3.2).

Table 3.2. Mean annual hydroclimatic properties of watersheds used in this study, mean (range). Dry/cold (P/PET <1), Wet/warm (P/PET ≥1).

	Tmean (C)	**P (mm/y)**	**Q (mm/y)**	**Q/P**	**SWE (mm)**	**SP (%)**
Wet/warm	5.8 (-0.2 – 10.0)	1825 (1027-3425)	1395 (298-3102)	0.71 (0.26-1.1)	541 (43-1012)	60 (22-83)
Dry/cold	4.4 (-0.2- 11.2)	723 (300-1300)	303 (6-730)	0.37 (0.01-0.88)	330 (39-785)	61 (31-86)

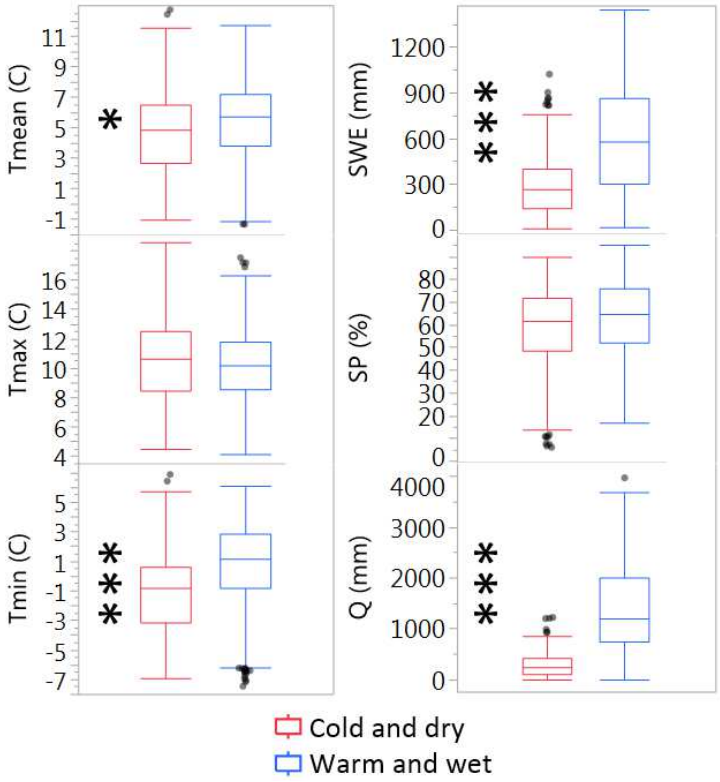

Figure 3.2. Boxplots displaying annual mean (Tmean), maximum (Tmax), and minimum temperature (Tmin), peak snow water equivalent (SWE), snow persistence (SP), and streamflow (Q) ranges for wet/warm (blue) and dry/cold (red) watersheds. Asterisks denote significant differences between wet/warm and dry/cold watershed groups: *p<0.05; **p<0.01; ***p<0.001, no asterisk = not significant at p<0.05.

3.5.2. Snow variables

To evaluate whether snow cover could be useful for reconstructing streamflow patterns in ungauged watersheds, both spatially and temporally, we first compared snow cover variables (SP and SS) to snow fall fraction (SF) and peak snow water equivalent (SWE). This helps identify what snow cover information may indicate hydrologically compared to these other variables. At the mean annual time scale, all snow variables (SP, SS, SF, peak SWE) display strong positive relationships with each other, with the strongest relationships between SP and SF ($r \geq 0.76$), and SP and SS season ($r \geq 0.77$) (Figure 3.3, Table 3.3). The snow cover variables, SP and SS, have steeper slopes for the dry/cold watersheds than for the wet/warm when plotted against

precipitation. For low SP (<50%), dry/cold watersheds have shorter snow season lengths than warm and wet watersheds. The correlations between SP, SS and SF are also different for wet/warm and dry/cold watersheds. At low snow persistence (<50%) and low snow season duration (<225 days), wet/warm watersheds have lower SF than dry/cold watersheds. The relationships between SP and peak SWE have considerable scatter and also differ for the wet/warm and dry/cold watershed subsets. These differences are largest for high SP (>50%), where wet/warm watersheds have higher peak SWE for the same SP than do dry/cold watersheds.

Table 3.3. Correlation coefficients for mean annual snow and climate variables. Dry/cold (P/PET <1), Wet/warm (P/PET ≥1). *p<0.05; **p<0.01; ***p<0.001, no asterisk = not significant at p<0.05

Variables	All	Wet/warm	Dry/cold
SP vs T	-0.75***	-0.85***	-0.77***
SS vs T	-0.62***	-0.64***	-0.78***
SF vs T	-0.91***	-0.94***	-0.89***
SWE vs T	-0.21**	-0.60***	-0.40***
SP vs P	-0.09	-0.38*	0.42***
SS vs P	0.15	0.01	0.27***
SF vs P	-0.59***	-0.58***	0.05
SWE vs P	0.42***	-0.15	0.72***
SP vs SS	0.85***	0.77***	0.93***
SP vs SF	0.76***	0.90***	0.80***
SP vs SWE	0.63***	0.77***	0.72***
SWE vs SF	0.26**	0.75***	0.41***

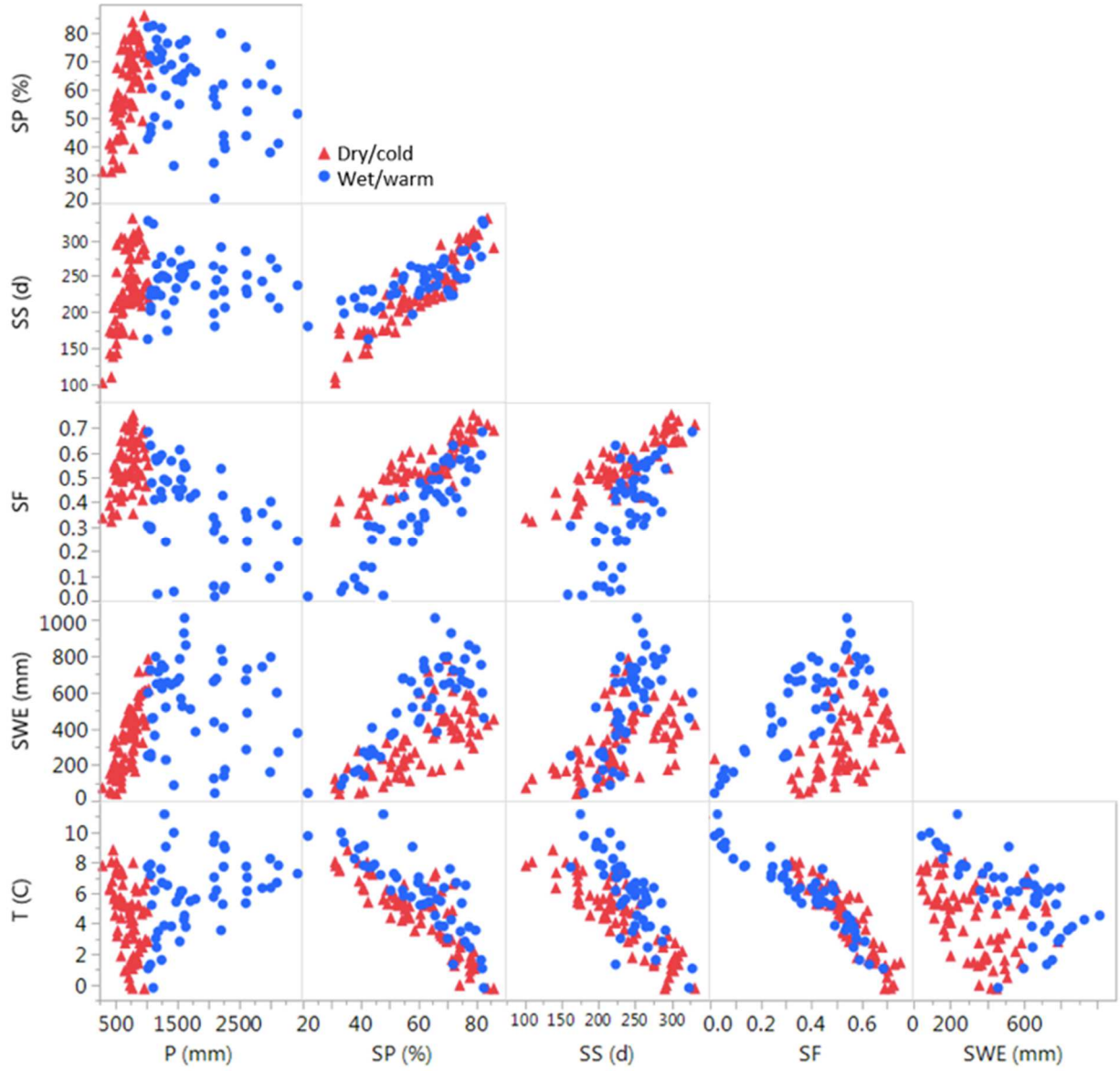

Figure 3.3. Mean annual snow variable (snow persistence SP, snow season SS, snow fraction SF, peak snow water equivalent SWE) and climate variable (mean air temperature T, water year precipitation P) cross correlation chart at the watershed scale. Correlation coefficient values for each tile are in Table 3.3. Red triangles dry/cold (P/PET <1), blue circles wet/warm (P/PET ≥1).

To assess how satellite snow cover data (SP and SS) compare to ground-based values we examined how MODIS SP compares to SNOTEL station values of SP. This analysis showed that MODIS-derived SP is lower than at SNOTEL sites (Figure 3.4). On average, mean annual values

of SP from SNOTEL are 9.5% higher than SP from MODIS at SNOTEL sites. This difference between MODIS and SNOTEL SP is greater for wet/warm sites (mean = 11.2%, coefficient of variation = 0.70) than for dry/cold sites (mean = 7.8%, coefficient of variation = 0.85). Though watershed scale SP is low relative to site scale SP, SP and peak SWE are strongly correlated at both SNOTEL site and watershed scales (Table 3.4).

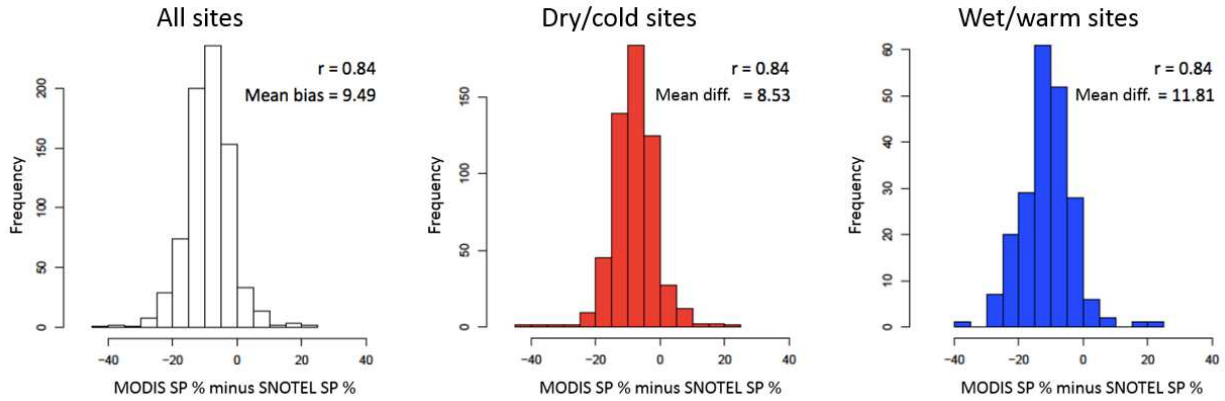

Figure 3.4. Histograms of annual MODIS snow persistence minus SNOTEL site snow persistence derived from daily SWE data at the point scale. Pearson correlation coefficients and mean difference for each group of SNOTEL sites are displayed in the top right corner of each sub-plot. Dry/cold (P/PET <1), Wet/warm (P/PET ≥1).

Table 3.4. Annual correlation coefficients between SP and peak SWE at point scale (SNOTEL sites) and at watershed scale (SNODAS average over watershed). All correlations significant with p<0.001. Dry/cold (P/PET <1), Wet/warm (P/PET ≥1).

Variable	All	Wet/warm	Dry/cold
Point (SNOTEL) SWE and SP	0.57	0.58	0.60
Watershed (SNODAS) SWE and SP	0.62	0.69	0.67

3.5.3. Streamflow relationships to snow and climate

Analyses of how snow variables relate to streamflow use only SP and SWE. We chose to use SP rather than SS because these two variables are similar, and SP has stronger relationships to streamflow (Table 3.6). At both mean annual (Figure 3.5, Table 3.5) and annual (Figures 3.6, 3.7, Table 3.5) time scales, both Q and Q/P tend to increase with SP and peak SWE in dry/cold watersheds, but the relationships between snow and streamflow variables are much weaker in wet/warm watersheds. Individual watersheds also display inter-annual patterns reflecting the overall Q/P SP relationship (Figure 3.7a,3.b). Figure 3.7c displays the slope of the relationship between annual Q/P and SP by watershed. The relationship between Q/P and SP is positive in nearly all (68/71) dry/cold watersheds, indicating more streamflow export with higher snow persistence, and significant in most of them (43/71). In contrast, few of the relationships between Q/P and SP were significant in wet/warm watersheds (11/48).

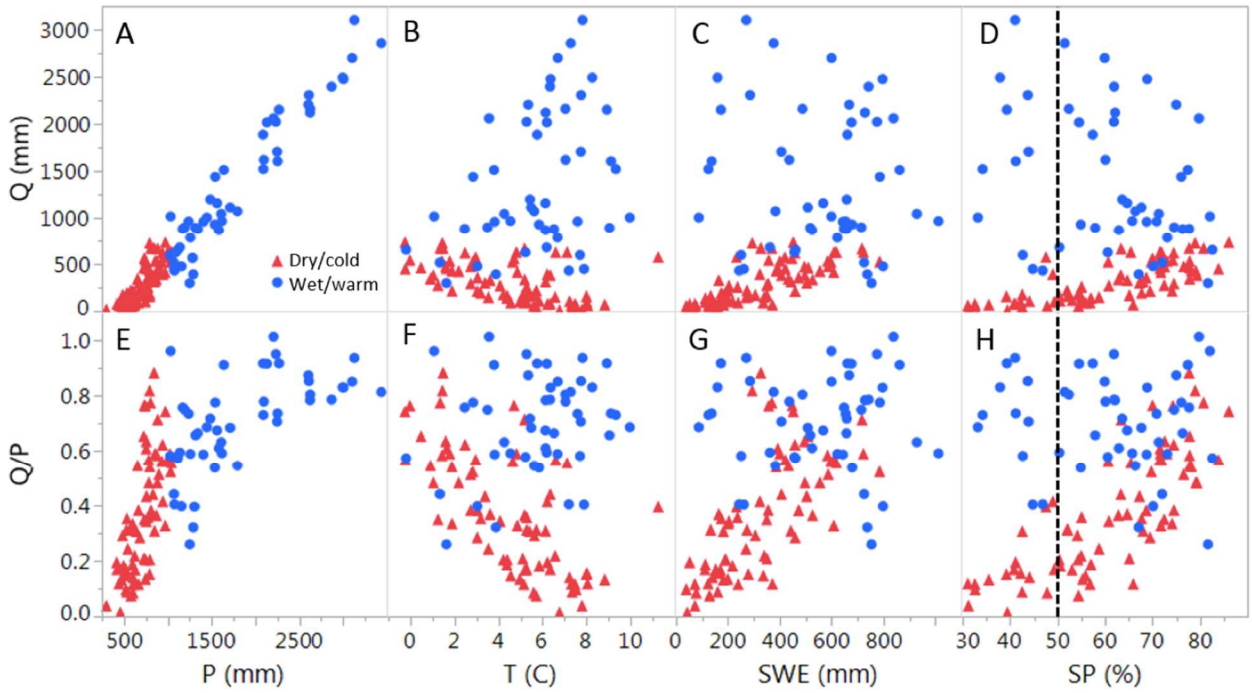

Figure 3.5. Mean annual water year streamflow (Q) and runoff ratio (Q/P) vs. precipitation (P; A,E), mean temperature (T; B,F), peak snow water equivalent (SWE; C,G) and snow persistence (SP; D,H) for 2001 to 2015 (P,T, SP) and for 2004-2015 (SWE) at USGS reference watersheds. Dry/cold (P/PET <1), Wet/warm (P/PET ≥1). Vertical lines in (D,H) mark the transition between intermittent and seasonal snow zones (SP=50%).

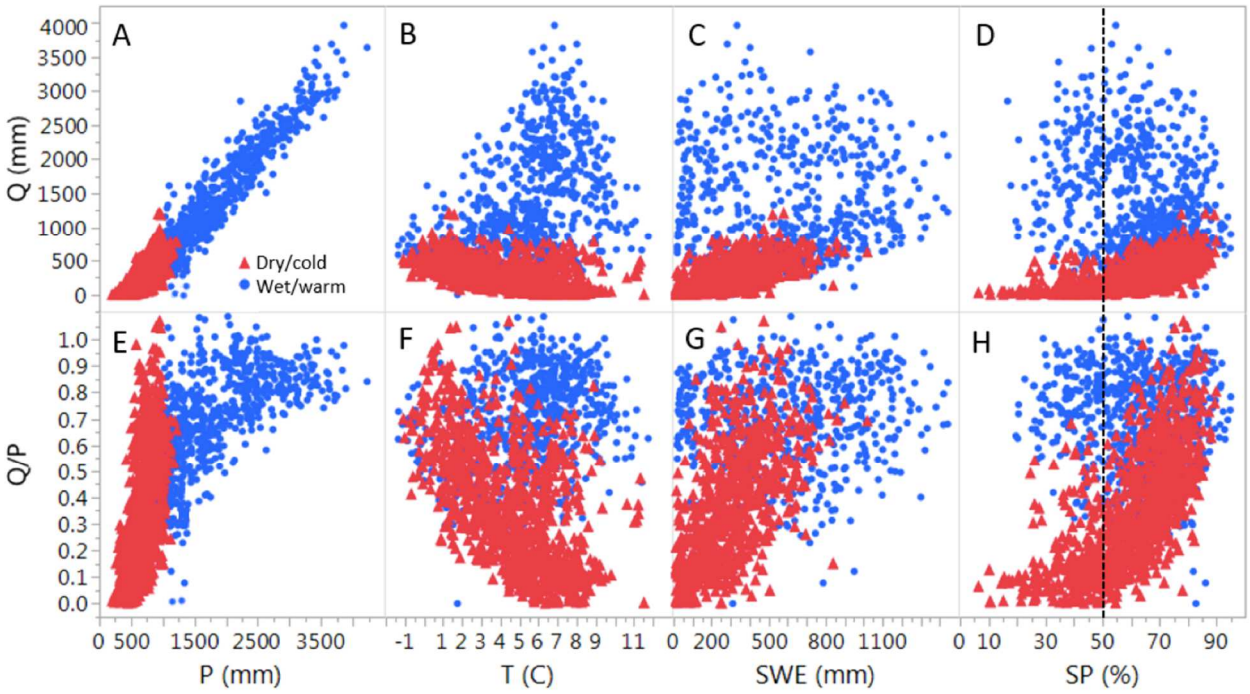

Figure 3.6. Water year streamflow (Q) and runoff ratio (Q/P) vs. precipitation (P; A,E), mean temperature (T; B,F), peak snow water equivalent (SWE; C,G) and snow persistence (SP; D,H) for 2001 to 2015 (P,T, SP) and for 2004-2015 (SWE) at USGS reference watersheds. Dry/cold (P/PET <1), Wet/warm (P/PET ≥1). Vertical lines in (D,H) mark the transition between intermittent and seasonal snow zones.

Table 3.5. Watershed-scale correlation coefficients between independent variables (P, SP, peak SWE) and response variables (Q, Q/P) for dry/cold (P/PET <1) and wet/warm (P/PET ≥1) watersheds at annual time steps and as mean annual values (2001-2015). *p<0.05; **p<0.01; ***p<0.001, no asterisk = not significant at p<0.05. Values in parentheses are for the truncated period of record for water years (2004-2015) that matches the SNODAS period of record for peak SWE.

Variables	Time Scale	All watersheds	Wet/warm	Dry/cold
P and Q	annual	0.96***	0.95***	0.80***
	mean annual	0.97***	0.96***	0.78***
SP and Q	annual	(0.06*) 0.08**	(-0.16***) -0.16***	(0.68***) 0.67***
	mean annual	(0.002) 0.02	(-0.35*) -0.32*	(0.73***) 0.73***
SWE and Q	annual	0.38***	0.06	0.76***
	mean annual	0.39***	-0.14	0.75***
P and Q/P	annual	0.69***	0.52***	0.54***
	mean annual	0.71***	0.58***	0.57***
SP and Q/P	annual	(0.37***) 0.38***	(0.02) 0.04	(0.74***) 0.74***
	mean annual	(0.38***) 0.39***	(-0.13) -0.08	(0.79***) 0.79***
SWE and Q/P	annual	0.48***	0.08	0.63***
	mean annual	0.55***	-0.07	0.68***

3.6. Discussion

3.6.1. Snow variables

Many conventions have been applied to characterize snow patterns across watersheds, including changes in the fraction of precipitation falling as snow, snow water equivalent, snow-covered area, and snow cover duration. Our results demonstrate that these types of metrics are highly correlated with one another, but they each convey different information about the snowpack. The fraction of precipitation falling as snow must usually be reconstructed retrospectively and will include uncertainties depending on the accuracy and time scale of available source data (Nolin and Daly, 2006; Dai, 2008). We chose not to focus on this variable, although future research could expand into analyses of the likelihood that snow fall will persist on the ground.

SWE has been the standard variable used for hydrologic prediction through statistical forecast models and process models (Christensen and Lettenmaier, 2007; Franz et al., 2008; Koster et al., 2010; Restrepo et al., 2012), and extensive research has been and continues to be dedicated to obtaining spatial patterns of SWE to improve streamflow prediction (Fassnacht et al., 2003; Bavera et al., 2014; Kahl et al., 2014; Painter et al., 2016). Even though the SNODAS SWE product is sometimes not as accurate as desirable for areas without ground SWE measurements (Clow, 2012; Hedrick et al., 2015), our results show that it is highly correlated with Q in dry/cold watersheds (Figures 3.5,3.6). This indicates that it does have utility for hydrologic prediction in dry/cold climates.

Snow cover products also have utility for understanding hydrologic response, although they too have uncertainties. We found that MODIS SP derived from the 8-day binary snow cover product tends to be lower than SP measured at SNOTEL sites. MODIS-derived SP likely differs

from station SP due to the difference in measurement scale and mix of land covers sampled. SNOTEL sites are typically located in relatively flat forest clearings, which may not be representative of the areas surrounding the stations (Dressler et al, 2006; Meromy et al., 2013), and a single MODIS pixel with 500 meter sides may contain snow in both forested and clearing areas. Additionally, SNOTEL sites become less reflective of their surrounding areas as the melt season progresses (Meromy et al., 2013). Comparing the 8-day remotely sensed MODIS SP to SNOTEL SP calculated from daily SWE measurements also introduces temporal discrepancies because the MODIS product is the maximum snow presence condition of the 8-day period, whereas SNOTEL SP contains 8 values for the same period. In an intermittent to transitional snowpack, this effect could lower SNOTEL SP because of the potential for SNOTEL SWE to melt fully and accumulate within an 8 day period. Additionally, prior research has shown through comparison with higher resolution Landsat imagery that MODIS snow products may under-estimate snow cover in forested areas (Rittger et al., 2013). Daily and 8-day products may identify snow cover one day when snow is present on the canopy in snow covered areas and report no snow the next time period when snow is on the ground beneath the trees, but the canopy is snow free. I conducted additional analyses to investigate the utility of MOD10A1 (daily binary snow cover product), MOD10A1F (daily fractional snow covered area), MODSCAG (daily fractional snow covered area) for calculating snow persistence in the western U.S. This revealed that daily binary and fractional products had greater areas of restricted data due to senor saturation and cloud cover issues, and in areas without problematic cloud cover, produced similar correlations to annual water yield to those from the 8-day maximum product. Even with the discrepancies in spatial scale between SNOTEL sites and MODIS pixels, however, the MODIS SP values are highly correlated with SNOTEL SP and peak SWE, and SP

is almost as well correlated with Q as is peak SWE. Therefore, an important finding of our research here is that a remotely sensed snow metric derived solely from snow cover data (SP) correlates both Q and Q/P nearly as well as SNODAS peak SWE in dry/cold watersheds (Table 3.5). Snow persistence is not widely used in hydrologic analyses, but it has the advantage of spatial continuity and global availability. It is a useful alternative to spatial SWE in areas where SWE measurements are sparse, and creating a gridded SWE product like SNODAS is not feasible (Saavedra et al., 2017). In the western U.S., SP can also be mapped at finer resolution (500 m) than the SNODAS product (1 km^2). Finer resolution snow information is often beneficial for estimating water yield in small watersheds with spatially variable snow conditions (Molotch and Bales, 2005; DeBeer and Pomeroy, 2010; Rice and Bales, 2010) because mountainous watersheds have high topographic variability, with a large fraction of streamflow coming from small areas.

3.6.2. Climatic differences in the hydrologic role of snow

Climatic differences in how streamflow relates to snow variables stem from the relative importance of precipitation and temperature in snow accumulation (Figure 3.3, Table 3.3). Precipitation is the dominant control on streamflow volume across the region as a whole (Figures 3.5,3.6, Table 3.5), which is consistent with previous research (Kim et al., 2000; Fu et al., 2007). Consequently, snow variable correlations with Q are strongest where P most influences snow accumulation. Precipitation totaled over periods shorter than the water year displays a weaker relationship with annual flow (Figure 3.11,3.12). However, when comparing correlations between water year flow and mean temperature averaged for different time periods, correlations improve when using Dec-Feb mean temperature period for wet/warm watersheds, but decline for

dry/cold watersheds when any period less than the water year is used (Figures 3.13,3.14). Peak SWE in the wet/warm watersheds is more strongly linked to temperature than to precipitation, whereas peak SWE in the dry/cold watersheds has a stronger connection to precipitation (Figure 3.3) because winter precipitation in these areas is more likely to fall as snow. As a result, snow variables (peak SWE, SP) are better correlated with streamflow in dry/cold regions, where snow variables are good proxies for precipitation, than in wet/warm regions, where temperature is a key control on whether precipitation falls as rain or snow. These relationships in dry/cold watersheds are present both spatially, comparing multiple watersheds (Figure 3.5,3.6), and temporally, comparing different years in individual watersheds (Figure 3.7).

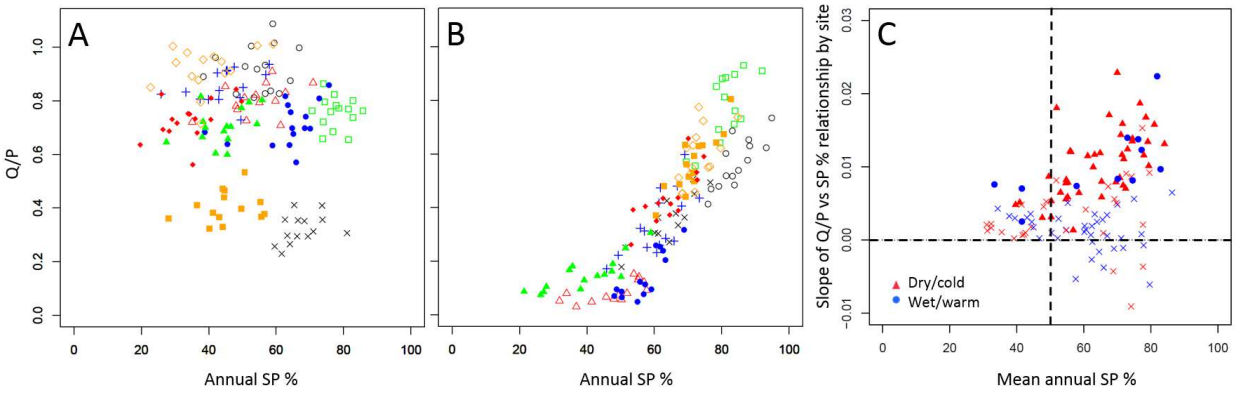

Figure 3.7. Annual water year runoff ratio (Q/P) vs SP for 2001 to 2015 at ten individual wet/warm (A) and dry/cold (B) watersheds shown by different symbols. C, Slope of the relationship between annual Q/P and SP by watershed. Dry (P/PET <1), Wet (P/PET ≥1). Significant results in C are shown by filled symbols; x's indicate regressions that are not significant (p>0.05). 43/71 regressions were significant for dry/cold watersheds. 11/48 regressions were significant for wet watersheds. Red (blue) symbols denote dry/cold (wet/warm) watersheds. Dry/cold (P/PET <1), Wet/warm (P/PET ≥1).

Relationships between P, T and SWE may be obscured when analyzing data at the water year or Oct-June time scale because this time range would include warm periods with rain instead of snow. To assess the effects of the time period chosen for correlation analysis of climate and snow variables we compared the relationships between SP and SWE with P total and

T average for four different periods: the water year, October to June, January to June, and December to February. For both SWE and SP, T averaged for the January – June period shows the strongest correlations amongst the temporal periods we tested, with limited differences in correlation strength between time periods (Figures 3.15,3.16). The correlations between P and both SP and SWE generally decline when using P from truncated periods as compared to the water year for dry/cold watersheds, and for wet/warm watersheds, the relationship remains weak for all periods of analysis. Therefore, we conclude that the poor relationship between P and snow variables in wet/warm watersheds is not an artifact of the time scale of analysis.

3.6.3. Applications using SP to predict streamflow

Relationships between snow persistence and streamflow generation in dry/cold watersheds highlight the key role of high elevation mountains in producing streamflow for lowlands of the interior west. As an example application of this finding, we used an equation fit to the mean annual Q vs. SP relationship for dry/cold watersheds to map mean annual Q across the Upper Colorado River Basin (UCRB). Here we directly use remotely sensed snow information to estimate streamflow, which differs from previous studies in which remotely sensed data was used as input to hydrologic models to forecast streamflow (Andreadis and Lettenmaier, 2006; Jain et al., 2010; Roy et al., 2010). This map clearly illustrates how most of the streamflow generated in the basin is from high elevation areas (Figure 3.8), with 50% of the UCRB flow predicted by this method coming from above 3,000 masl. The map shows finer resolution patterns and even higher Q in the headwaters of the UCRB than currently available from the latest Colorado River Basin Technical Report (U.S. Bureau of Reclamation, 2012). The streamflow pattern is consistent with prior analysis of contributions to streamflow by elevation

(Fassnacht, 2006) and with results of recent hydrological model simulations that show that over half of the total water yield in the western U.S. originates as snowmelt even though only 37% percent of precipitation falls as snow (Li et al., 2017). Similar disproportionate streamflow contributions from snow-dominated regions have been observed worldwide (Viviroli et al., 2003). While prior studies have focused on the importance of the high elevation snowpack for streamflow, an important contribution here is that lower elevations with more intermittent snow are still important for streamflow generation, contributing the remaining 50% of flow to the Colorado River Basin, or possibly more since we excluded areas with SP<30%. Snow measurements are sparse in areas with intermittent snow, and we recommend that future snow monitoring expand into these areas that also contribute substantial streamflow to the river.

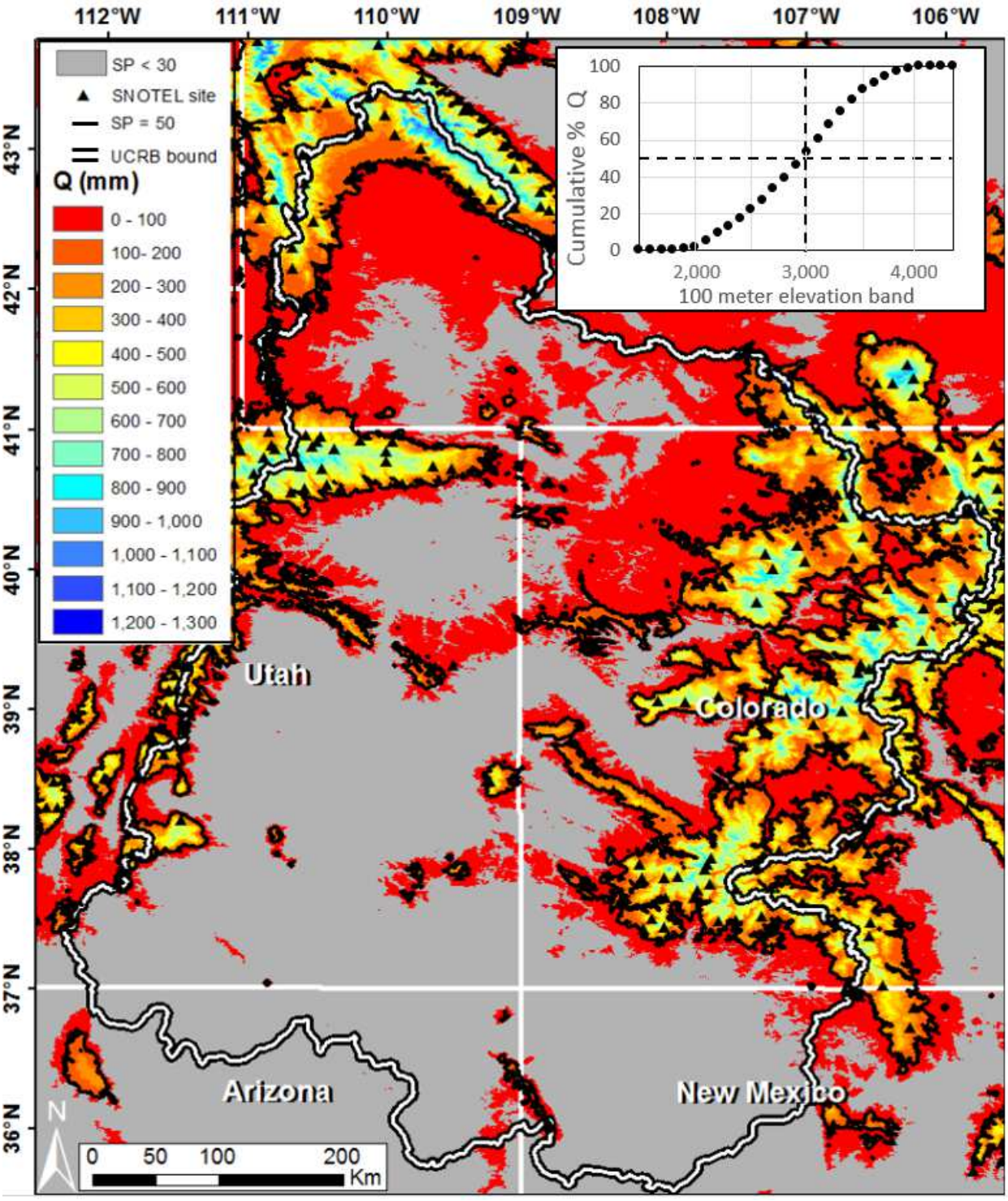

Figure 3.8. Mean annual streamflow (Q) for the Upper Colorado River Basin modeled from the relationship between mean annual SP and mean annual Q (Figure 3.5d), with an inset graph displaying the curve of cumulative Q with elevation. SP 50 is the boundary between intermittent and seasonal snow cover.

If the relationships identified between SP and Q in the western U.S. are similar in other dry/cold parts of the world, SP could be useful for first order estimates of annual streamflow volume. Preliminary analysis of the relationship between annual Q and SP in dry/cold watersheds of Canada and Argentina using data from the Global Runoff Data Centre (GRDC, German Federal Institute of Hydrology, Koblenz, Germany) shows a similar relationship as observed in dry/cold watersheds of the western U.S. (Figure 3.9). In the future, we hope to test this relationship in dry/cold watersheds of South America and Asia in places without significant glacial influence. This would be most useful in locations that have sparse or inaccurate precipitation data. Water year P is still the strongest predictor of water year Q in the western U.S., where relatively high quality and high resolution gridded P data are available. Global gridded P products are typically much coarser than those available in North America and Europe and coarser than the MODIS-derived SP. These products are modeled and interpolated from station, radar and satellite data and can have considerable uncertainties (Fekete et al., 2004; Bosilovich et al., 2008; Kidd et al., 2012; Schamm et al., 2014; Levy et al., 2017) with heightened uncertainty of over 100% in high latitude and topographically complex areas including the Rocky Mountains, Tibetan Plateau, and Andes (Tian and Peters-Lidard, 2010; Saavedra et al., 2018).

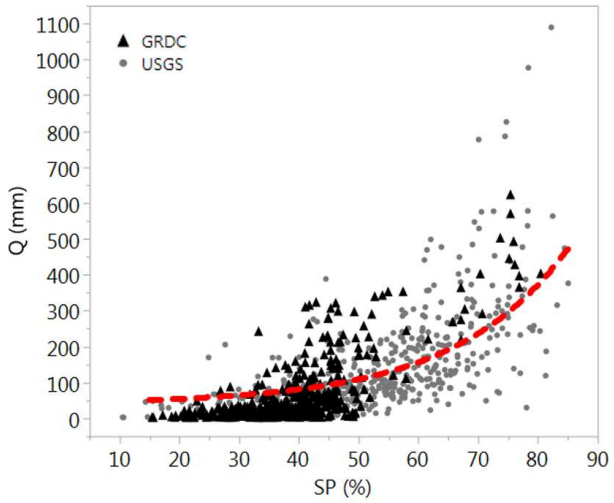

Figure 3.9. Annual streamflow (Q) vs Oct 1 - Sept 30 snow persistence (SP) for semi-arid and arid (P/PET < 1) watersheds from USGS watersheds in the western U.S. and GRDC watersheds in Canada and Argentina. The Global Runoff Data Centre, 56068 Koblenz, Germany. Red line shows best fit with USGS watersheds used in the present study in the western U.S. Fit properties: $R^2 = 0.45$, equation = $Q = 6.7091e^{0.0498*SP}$.

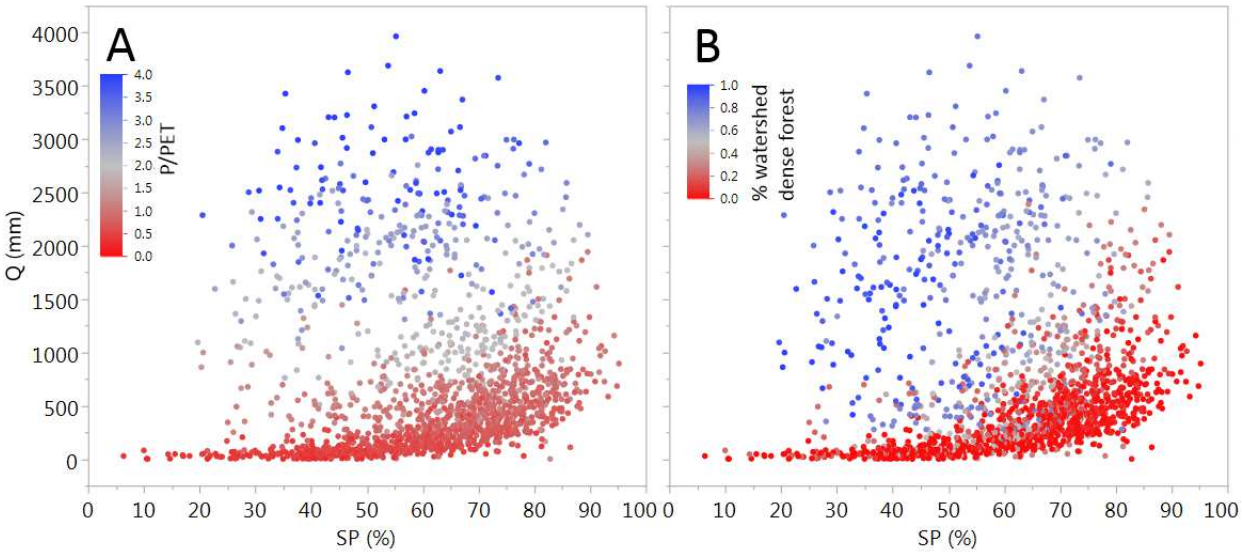

Figure 3.10. Water year streamflow vs snow persistence colored by aridity (P/PET, A) and the percent of watershed area affected by dense forest cover (B).

3.6.4. Uncertainties

The processes linking snow to streamflow are complex, and a wide range of factors besides climate and snow persistence could affect the trajectory of hydrologic responses to changes in snow. When more of the P is rain instead of the snow, more exposure of the ground surface to the atmosphere can lead to greater ET if soil moisture is not limiting. However, both soil moisture limitations and winter dormancy of vegetation can vary the response of ET to snow loss (Goulden et al., 2012). Wildfires and insect infestations across the western U.S. lead to complex snow accumulation and melt responses that vary over time as forest stands progress from their disturbed state (Burles and Boon, 2011; Winkler, 2011; Pugh and Small, 2012; Gleason et al., 2013; Harpold et al., 2014). Wildfire events are expected to burn more total area in coming years (Westerling et al., 2011; Moritz et al. 2012), and forest recovery from wildfire and insect infestations can last decades (Vanderhoof and Williams, 2015). Where large areas of forested land are affected by these disturbances, snow accumulation and melt could experience significant alterations in addition to those directly from climate. These kinds of effects would contribute variability in the streamflow response to snow (Figures 3.5,3.6), although we expect that they would not alter the dominant tendencies identified here unless they are particularly severe. An example of such a severe change is high severity wildfire, which may shift streamflow generation to surface overland flow during summer, enhancing the importance of rainfall for streamflow generation. Research comparing watersheds with a wide range of snow, climate, and vegetation conditions (e.g. Maurer and Bowling, 2014; Harpold and Molotch, 2015; Biederman et al., 2015) is needed to help understand these mechanisms and the combined influences of climate and land changes on streamflow generation in dynamic landscapes.

All of the data sources we used for this analysis also have uncertainties. We addressed uncertainties in snow products by using multiple data sources (SNOTEL, SNODAS, MODIS).

To ensure that our findings about climate differences in streamflow response to snow are not artifacts of data product selection, we also conducted the same analyses using alternate climate data products. We found that the differences in streamflow sensitivity to snow by climate were similar using different precipitation products (Table 3.7a,b) (Daly, 2013; Livneh et al., 2013) and different reference potential evapotranspiration (Abatzoglou, 2013; Cristea et al., 2013; Table 3.7b,c). This increases confidence that the findings are not an artifact of the data uncertainties or processing approach. Additionally, the gridded data sources utilized in this study had different spatial resolutions, introducing error into correlation tests between gridded variables. Resampling to the resolution of MODIS data without interpolation minimizes the introduced error, but spatial patterns captured by SP are not as well captured in the coarser gridded products (gridMET PET, PRISM P, SNODAS SWE).

Previous research has identified shortcomings in MODIS snow products related to vegetation (Hall and Riggs 2007). Methods have been developed for adjusting MODIS fractional snow products in areas with dense vegetation (Nolin 2010, Raleigh et al. 2012, Rittger et al., 2013), and simple vegetative thresholds for binary snow identification are included in current MODIS snow cover products. Rittger et al. (2013) demonstrated that most errors occur in areas where tree cover fraction is >50%. To evaluate the potential scope of vegetation errors in our study, we computed the percent area of each watershed with tree cover fraction > 50 %, plotting water year flow vs snow persistence (Figure 3.10). Many of the watersheds with dense forest, and thus expected errors in remotely sensed snow cover, coincide with areas with high P/PET. These watersheds also tend to fall outside the range of observed Q vs SP relationship in dry/cold watersheds. If the SP for these watersheds is biased low, then correction of SP would shift the densely forested points in Figure 3.9b further to the right. Such a correction would likely not

affect the dry/cold Q vs. SP relationship much, but it would alter the wet/warm relationship. Further study of the relationship between snow accumulation and streamflow generation using refined vegetation corrections could address these uncertainties in greater detail.

Finally, our study faced some sampling challenges, which may have contributed uncertainties. With the climatic range across the western U.S., it is challenging to separate out the effects of P and T on snow and streamflow through empirical analysis alone because dry watersheds are in the continental interior and tend to have colder ranges of temperatures than the wet maritime watersheds. Future studies could use proxy variables that capture P and T effects (e.g. Kormos et al., 2016) to examine the relative importance of P and T from a different perspective. While we were able to obtain a reasonable sample size of unmodified watersheds across the western U.S. as a whole, individual sub-regions do not all have discharge measurements in all snow zones. For example, in the high relief terrain of the Cascade and Sierra mountain ranges, current gauge locations tend to integrate multiple snow zones, rather than exclusively sampling a single snow zone. Current stream gauge networks were primarily designed for water supply and flood forecasting, meaning they tend to be at lower elevations in larger rivers. Few of the existing gauges in these mountain areas sample watersheds that cover only the lower elevation intermittent snow zone. Increased monitoring of discharge in watersheds near the transition between intermittent and seasonal snow would help improve understanding of how streamflow changes is affected by snow changes (Figure 3.8).

3.7. Conclusions

Both snow persistence derived from remotely sensed snow cover data and modeled peak snow water equivalent are strongly correlated with annual and mean annual streamflow in

dry/cold (precipitation deficit) but not in wet/warm (precipitation surplus) watersheds of the western U.S. Climate type affects correlations between snow and streamflow because of the relative importance of precipitation for total snow accumulation. In dry/cold watersheds, snow variables predict streamflow almost as well as precipitation alone because peak snow accumulation is strongly correlated with precipitation. For these areas, the snow variable derived from snow cover data, snow persistence, has nearly as strong a correlation with annual streamflow as a spatial snow water equivalent product. SNODAS SWE, despite having been shown to be inaccurate at the pixel scale in mountainous terrain nevertheless demonstrates utility in predicting Q in dry/cold watersheds. Because snow cover data are available globally at 500 m resolution, these findings about how snow persistence relates to annual streamflow allow detailed spatial mapping of streamflow across snowmelt-dominated dry regions. For example, we used the Q vs. SP relationship to map mean annual streamflow across the Upper Colorado River Basin and estimated that 50% of the basin streamflow comes from >3000 m elevation. Similar approaches could be used to map streamflow patterns and potentially forecast streamflow for dry/cold watersheds in parts of the world with limited streamflow monitoring. The ability to estimate streamflow using snow persistence expands our ability to track hydrologic change in snow-dominated regions across the globe.

Chapter 4. Snowmelt and Rainfall Partitioning Through the Critical Zone Varies by Climate Type and Soil Properties in Snowmelt Dominated Locations

4.1 Introduction

Snowmelt is the dominant source of streamflow generation and groundwater recharge in many high elevation and high latitude locations (Regonda et al. 2005; Stewart et al. 2005; Earman et al., 2006; Clow, 2010; Jefferson, 2011; Furey et al., 2012). Soils modulate the partitioning of rainfall and snowmelt input into subsurface storage, deep drainage, evaporative losses and surface runoff. Partitioning of snowmelt into these different outputs is likely to change as global temperatures continue to rise (Harpold et al., 2015; Harpold et al., 2017). Snow persistence shows declines around the globe, and these snow losses may lead to changes in input magnitude and timing (Chapter 2). As areas of "at risk snow" become more apparent (Nolin and Daly, 2006), there is an urgent need for mechanistic studies that quantify the partitioning of snowmelt through the critical zone (Brooks et al., 2015; Meixner et al., 2016), and this has become an active field of research in mountain regions (Harpold and Molotch, 2015; Kampf et al., 2015; Tetzlaff et al., 2015; Webb et al., 2015).

Snowmelt has been shown to yield both more streamflow and more groundwater recharge per unit of precipitation than rain (Earman et al., 2006; Berghuijs et al., 2014; Li et al., 2017). However, soil properties will also affect how changes in inputs affect partitioning. Both streamflow and deep drainage are affected by soil texture, soil depth, and rooting depth (Cho and Olivera, 2009; Seyfried et al., 2005). Given the considerable heterogeneity in climate, soils, topography, and vegetation, different locations may not all respond in the same way to loss of snow. Despite the fact that snowmelt is highly important to hydrologic responses in high

elevation and high latitude areas, much remains unknown regarding how these factors interact to determine partitioning into components of the soil water balance.

The goal of this study is to improve our understanding of how changes in precipitation phase from snow to rain affect input partitioning in a changing climate. Hydrologic partitioning of input, P, in the critical zone can be tracked using the water balance (equation 1), where partitioning components include fluxes for surface runoff, Q; evaporation, E; transpiration, T; deep drainage below the root zone, D; and storage within the soil root zone, ΔS.

$$P = Q + E + T + D + \Delta S \quad \text{eq. 1}$$

A modeling approach is used to examine partitioning across a wide range of climate and soil conditions. Specific questions guiding the research are: (1) Are snowmelt and rain partitioned differently between Q, ET, and D? and (2) How is this partitioning of rain and snowmelt affected by climate, soil type, and soil depth? I hypothesize that reducing the fraction of precipitation falling as snow leads to lower surface runoff and deep drainage because it reduces the concentration of input during snowmelt (Figure 4.1). I define input concentration as the mean length of input events for a given period (i.e. water year) divided by the total number of input events during that period. This metric is thus used to evaluate whether input is more continuous or discrete in nature. Concentrated input from snowmelt leads to greater soil saturation, which causes saturation excess runoff and deep drainage below the root zone. I also hypothesize that the elevated runoff and deep drainage caused by snowmelt will be greatest in dry climates, where soil saturation is less frequent, compared to wet climates

and shallow soils, which can saturate with lower water input. Figure 4.1 shows the conceptual understanding of climatic effects on critical zone partitioning where input concentration and climate type interact to control hydrologic response.

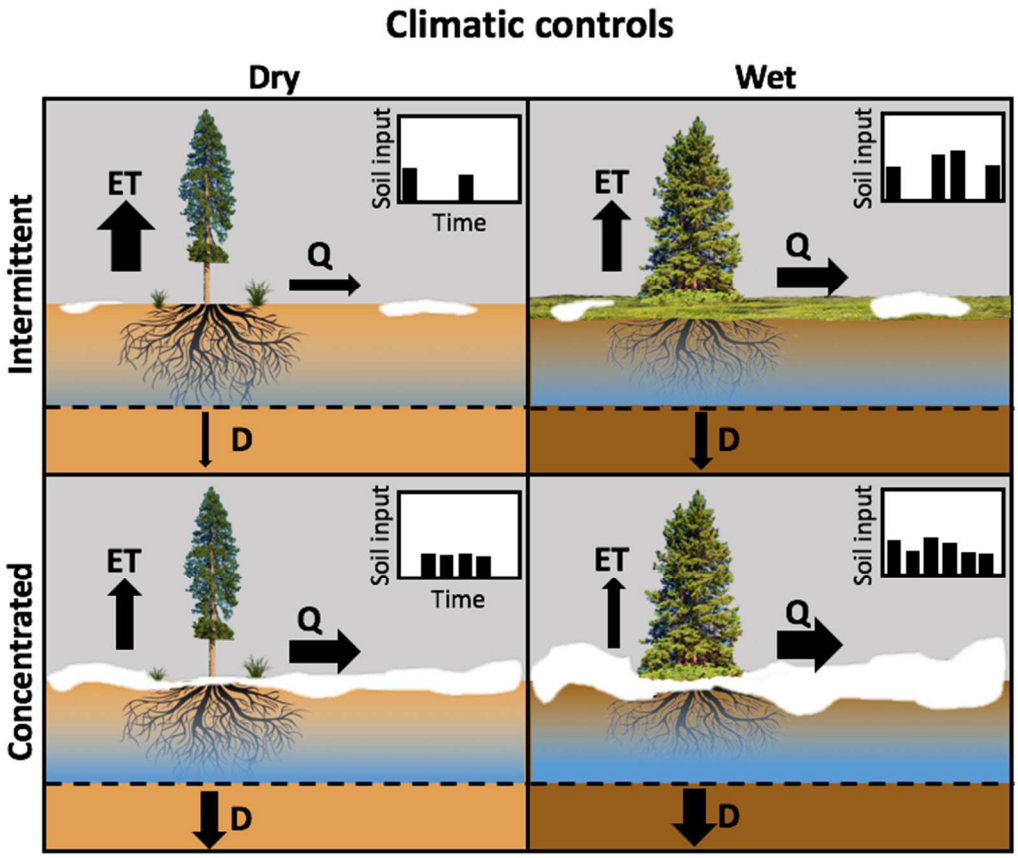

Figure 4.1. Conceptual illustration of the hypothesis about importance of concentrated snowmelt input to generating streamflow in dry climates. The wet climate generates more surface runoff (Q) and deep drainage (D) and less evapotranspiration (ET) compared to the dry climate. In both climates, input that is concentrated in time can increase both Q and D because it is more likely to allow soil saturation than intermittent input, which allows ET during periods of drying.

4.2 Background

Climate-dependent factors, including snow persistence, precipitation timing, and seasonal patterns in evaporative demand, affect soil moisture response to rainfall and snowmelt inputs. Prior research has demonstrated strong links between snowmelt and soil moisture dynamics at multiple scales (Loik et al. 2004; Williams et al. 2009; Blankinship et al. 2014; Kormos et al., 2014; Harpold and Molotch, 2015; Webb et al. 2015; Kampf et al. 2015). Concentrated melt from a winter snowpack can enhance downslope connectivity through the soil in valley bottoms, near streams, or in concave hollows, providing a mechanism for streamflow generation and deep

drainage that is not active in the same areas during drier seasons (McNamara et al. 2005; Hinckley at al., 2014). Consequently streamflow can be insensitive to inputs when soil moisture storage is below a certain value, yet streamflow is generated rapidly once a threshold storage value is exceeded (McNamara et al., 2005; Liu et al., 2008; Seyfried et al., 2009). McNamara et al. (2005) hypothesized that when dry-soil barriers are breached, there is sudden connection to upslope soils, leading to delivery of water to areas that were previously disconnected. Such breaching of dry-soil barriers was only observed for periods of concentrated and sustained input.

Near-surface soil moisture response is closely related to snow disappearance (Harpold and Molotch, 2014; Webb et al., 2015; Harpold et al., 2015). Kampf et al. (2015) observed that earlier snowmelt timing led to lower average soil moisture conditions not as conducive to streamflow generation as later snowmelt, suggesting a relationship between the persistence of a snowpack, soil moisture state, and streamflow generation. The effects of earlier snowmelt on soil moisture dynamics may also vary with precipitation conditions after snowmelt. Late-spring precipitation can overwrite the signal of earlier snowmelt timing on spring and summer soil moisture (Liator et al., 2008, Conner et al., 2016), whereas if this late spring precipitation does not fall, the effects of earlier snowmelt on soil moisture can persist longer (Blankenship et al, 2014). If input comes during wetter winter periods with low evaporative demand, it may be more likely to saturate soil and create streamflow or deep drainage than fall, spring and summer inputs that are more likely to be at least partially partitioned to ET because … (Molotch et al., 2009). Earlier snow disappearance can lead to diverging patterns in growing season length, where earlier snowmelt can lead to a longer growing season, if energy hinders vegetation growth, or a shorter growing season where soil water stress limits plant activity (Harpold et al., 2015; Harpold, 2016).

Soil moisture patterns are also affected by soil and topographic properties, which generally remain stable through timespans of hydrologic analysis. These more static properties can produce temporally stable spatial patterns of soil moisture (Williams et al., 2009). Soils with greater storage capacity may show less moisture limitation on ET during the late spring and summer (Jepsen et al., 2016). With similar magnitude of input on north- and south-facing slopes, north facing slopes have higher sustained moisture content, and especially when combined with deeper profiles and more deeply weathered rock, north-facing slopes can be more conducive to deep drainage (Langston et al., 2015). Where soils are shallow, winter precipitation may be in excess compared to the soil storage capacity, with input contributing to surface runoff and deep drainage (Smith et al., 2011). While deeper soil profiles can buffer changes in volume and timing of runoff, the preservation of surface runoff with snow loss can be at the expense of subsurface storage and groundwater recharge (Markovich et al., 2016).

This chapter presents a combined analysis of climatic and edaphic effects on how water input is partitioned between soil storage, streamflow, ET, and deep drainage. This combined analysis can help improve understanding of critical zone partitioning in mountain areas and highlight areas most sensitive to snow loss.

4.3 Methods

To evaluate soil moisture response to rainfall and snowmelt over a wide range of climate and soil conditions I use HYDRUS-1D (Šimůnek et al. 1998), a physically-based finite element model for simulating one-dimensional water movement in variably saturated, multi-layer, porous media.

4.3.1 Study design, site selection, and data sources

I utilize daily input data from five SNOTEL sites in each of three regions: the Cascades, Sierra, and Uinta for a total of 15 sites. Daily rather than hourly data was chosen to limit the effects of missing and incorrect values on the analyses. The three regions chosen represent dominant climate types in the western U.S., and within each region, sites were selected to span an intermittent to persistent snow gradient and represent snow input variability. Snow persistence is defined as the fraction of time that an area is snow covered, where areas with intermittent snow are characterized by shallow snowpacks with multiple mid-winter melt events and those with persistent snow accumulate deeper snowpacks throughout the fall, winter and spring with a concentrated melt pulse during spring and early summer months (Moore et al. 2015). With these climate scenarios I simulated soil moisture response to variable climatic conditions for ~35 years at each site (Figure 4.2, Table 4.1).

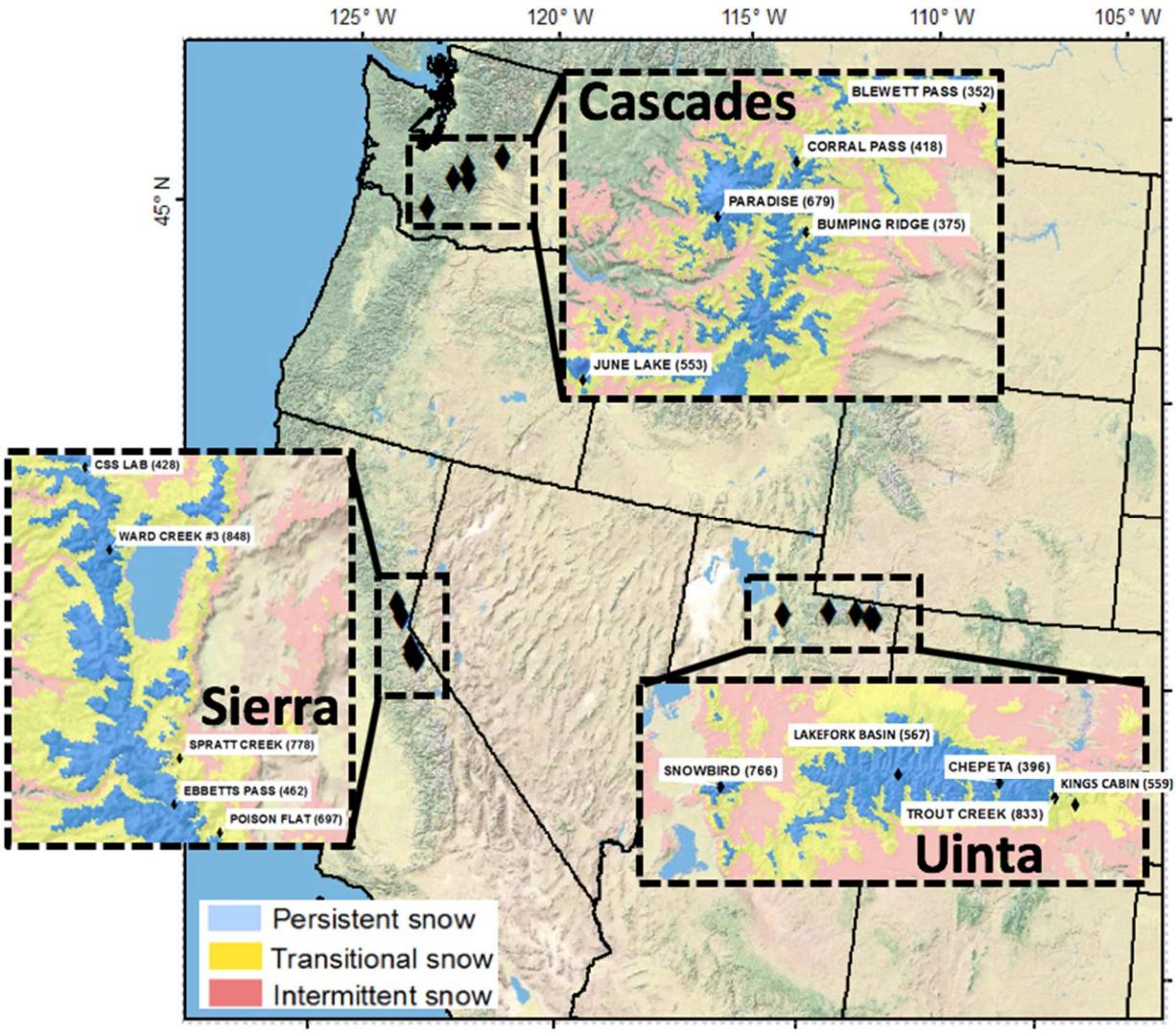

Figure 4.2. SNOTEL sites utilized in this study with insets displaying snow zones classified by mean annual snow persistence (Moore et al., 2015).

Daily precipitation (P), snow water equivalent (SWE), and volumetric water content (VWC) at 5, 20, and 50 cm were obtained for each SNOTEL site using the Natural Resource Conservation Service (NRCS) National Weather and Climate Center (NWCC, 2016) Report Generator (Table 4.1). The records were quality controlled to ensure reasonable precipitation, SWE and VWC values as in Harpold and Molotch (2015). Unrealistic values were removed (i.e. negative SWE, VWC below zero or above unity); all daily VWC outside of three standard deviations from the mean were removed, and a manual screening was performed on VWC data

to identify shifts and other artifacts not captured by the first two automated procedures. Daily potential evapotranspiration (PET) was extracted from daily gridMET (Abatzoglou, 2013) rasters for the 4 km pixel containing each SNOTEL site over the time period matching the available SNOTEL record. This product uses the ASCE Penman-Monteith method to compute PET.

While 365 of the 747 SNOTEL sites in the western U.S. have soil moisture sensors, only a fraction of these sites have detailed soil profile data. The sites with soil profile data have information obtained from soil samples taken at moisture probe installations and processed in the lab for texture, water retention properties, and hydraulic conductivity. Dr. Harpold obtained detailed soil profile data, in the form of pedon primary characterization files from the NRCS, and I selected three profiles greater than 100 cm in depth (Figure 4.3, Table 4.2) to represent the ranges of available soil textures and hydraulic conductivity.

4.3.2 Model setup and simulations

In HYDRUS-1D, I simulated water flow and root water uptake for a vertical domain 10 m deep. The domain was discretized into 500 nodes with higher node density near the surface (~0.15 cm for top 5 cm vs ~5 cm for the bottom of the profile). For the surface boundary, I used time variable atmospheric boundary conditions with daily input from snowmelt and rain, PET and surface runoff generation allowed. For the lower boundary, I allowed free drainage from the bottom of the soil profile. Soil water input was calculated by totaling snowmelt and rainfall input at the daily time step from SNOTEL precipitation and SWE values. Melt was computed for any day when SWE decreased; if SWE decreased, and the precipitation was greater than 0, total soil water input was assumed to be melt plus precipitation. Within HYDRUS, I assigned a constant leaf area index (LAI) of three, as this value generally fits mixed conifer forests (Jensen et al.,

2011) where SNOTEL sites are installed. I assumed a radiative extinction coefficient of 0.39, which is the default assigned. LAI and the radiation extinction coefficient are used in the estimation and separation of potential evaporation and transpiration as part of the root water uptake sub-routine. Through calibration these models were not sensitive to changes in the extinction coefficient, and it was left as the default. Root water uptake in the model was estimated using Feddes parameters for a conifer forest (Lv, 2014), with roots uniformly distributed from the soil surface to the interface with a lower hydraulic conductivity layer representing regolith or bedrock.

I created soil layers with depths and textures taken from the NRCS soil pedon measurements. From this information I applied the neural network capability of HYDRUS-1D, which draws from the USDA ROSETTA pedotransfer function model (Schaap et al., 2001), to determine soil hydraulic parameters from the NRCS pedon primary characterizations. I used percent sand, silt and clay, bulk density, wilting point, and field capacity in the neural network function. Below the depth of the soil pedon measurements, I configured the simulations to have a deep layer with lower hydraulic conductivity but the same water retention parameters as the layer above. The initial hydraulic conductivity of this lower layer was set at one half that of the layer above; values were modified during calibration. A low conductivity "bedrock" layer was added to the profile setup to allow simulation of deep drainage from the root zone to lower layers while aiding in calibration so that lower root zone layers retained water similar to their behavior in situ as compared to a freely draining soil profile with an atmospheric boundary condition below. The initial water content for all layers in each simulation was 0.2 VWC.

4.3.3 Calibration

For model calibration, I used three SNOTEL sites (432 Currant Creek, 698 Pole Creek R.S., 979 Van Wyck) that had detailed NRCS pedon primary characterizations to depths greater than 100 cm and >15 years of daily soil moisture records at 5, 20 and 50 cm. I used the daily records of precipitation, SWE, and PET from these sites to simulate soil water movement for the period of record at each site. I calibrated to observed VWC at 5, 20 and 50 cm depths (ex. Figure 4.13, Table 4.4). Simulations used two sequences of historical climate inputs, the first as a spin up period, and the second for calibration. Calibration was conducted by adjusting the hydraulic conductivity of the bottom layer to match observed VWC. Rather than force-fitting the models, my goal was to get simulations that behaved similarly to the observed soil moisture, so I could use a reasonable parameterization for model experiments. I also aimed to use similar parameters for all sites (i.e. identical root uptake parameters, 1/10 Ks of bottom root zone layer for low K layer). This calibration approach is consistent with other studies using HYDRUS – 1D, which also applied similar manual calibration starting with basic soils data and application of the ROSETTA pedotransfer function (Scott et al., 2000). Previous research that has applied a similar type of model to simulate soil moisture responses to snowmelt also calibrated to observed water content measurements by adjusting permeability of the "bedrock" layer (Flint et al., 2008).

I evaluated performance using mean bias and the Nash Sutcliffe model coefficient of efficiency (NSCE). Calibrations of VWC generally improved with depth, with poor NSCE (-0.82 to 0.15, Table 4.4) between observed and modeled 5 cm VWC where moisture is highly variable in time, and improved values at 20 cm (0.17 to 0.45) and 50 cm (0.14 to 0.58). I faced difficulty in obtaining close fits between modeled soil moisture and reported values from SNOTEL sensors. The chosen root uptake parameters for conifer forest (h1 0 cm, h2 0 cm, h3h -5,100 cm,

h3l -12,800 cm, h4 -21,500 cm, T_{Plow} 0.5 cm/d, T_{Phigh} 0.1 cm/d) more effectively lowered root zone water contents during dry periods as compared to deciduous values included in the HYDRUS-1D library, but still did not produce water contents resembling the low observed values. Soil moisture sensors can be affected by unexplained drifts and shifts in magnitude of reported values through time, which may have also affected calibrations. While I could have applied inverse modeling to calibrate more parameters and achieve a better fit (Sutanto et al., 2012), I elected to preserve the soil profile parameters determined from soil texture and only modify the lower layer hydraulic conductivity, for which there were no prior measurements. During calibration I tried to match the timing of response first, followed by magnitude, consistent with the approaches applied in other HYDRUS applications (Sutanto et al., 2012). Further details on model calibration can be found in the supplementary materials (Figure 4.13 and Table 4.4).

4.3.4 Simulation scenarios

I applied each of the 15 climate scenarios (Table 4.1) to each of the soil profiles developed during calibration. To address the question of whether snowmelt and rainfall are partitioned differently, I conducted additional simulations that treated all precipitation as rain and compared those to the simulations with the original climate data. To examine how soil depth affects partitioning I altered the depth of rooting zones to 1.5x and 2x their original depth. The layer above bedrock was extended to match this new rooting zone depth. I altered the depth of one soil profile (1056, loam, historical inputs) by fine scale 20 cm increments to study the effect of profile depth in more detail. Finally, to examine how input timing affects partitioning, I artificially produced intermittent (four five-day periods of low magnitude) and concentrated

input (one twenty-day period of high magnitude) of the same annual total to study the effects of input concentration for one wet (559) and one dry (375) site using the loam profile (1056) for all years of data.

4.3.5 Analysis

Using the simulation results, I examined how rain and snowmelt were partitioned into surface runoff (Q), evapotranspiration (ET), soil storage (S), and deep drainage (D). Daily soil storage is reported as the total soil water within the rooting zone only, and D is any water passing below the rooting zone (106-127 cm depending on the soil profile). In this study I assess partition components in units of length (cm) as well as their ratio to total input (unitless, e.g. Q/P). Analysis of model outputs is performed at both event and annual time scales.

To separate out the responses to rain and snowmelt, I defined rainfall events as days with precipitation while SWE equaled zero and snowmelt events for days with declining SWE and no simultaneous precipitation. Multi-day events occurred as long as the conditions were continuously satisfied; total rain and snowmelt were computed for each defined event. For response variables (Q, ET, S, D) a one-day lag after the last day of input was also included for computing event totals. Only events with a day of zero input following the classification of snowmelt or rain input were used in the reported results. Other events represented a mix of both rain and snow inputs and were not used in the event analysis. Antecedent S for each event was determined by taking the root zone storage from the day prior to the first event input.

At the annual scale, mean saturation (Sat) at each observed depth was calculated as the average annual VWC divided by soil porosity. Soil water input and partitioning components (rain, snowmelt, Q, ET, D) were totaled for each year, and the change in water year storage

determined by subtracting the values of S at the end of the year from the value at the beginning of the year. At the annual scale I also report the maximum SWE for the water year and computed input concentration as the mean length of all soil water input events divided by the total number of events per year. The average rate of snowmelt was calculated as the mean rate of SWE decline throughout the entire year.

Using both the event and annual results, I examined (1) whether partitioning of rainfall input differed from that of snowmelt input, and (2) how partitioning was affected by climate, soil texture, and soil depth. I identified quasi-discrete rainfall and snowmelt events by selecting continuous periods of input followed by at least five days of no input. I totaled input for all days of the event and totaled response variables for these days as well as one day following the end of input. Only events with entirely rainfall or entirely snowmelt input were considered, with events consisting of rainfall and snowmelt as well as rain on snow excluded.

To determine how climate and soil properties affected partitioning, Pearson correlation tests were conducted between explanatory variables (P, PET, P/PET, peak SWE, SP, average melt rate) and dependent variables (Q,D,E,T, mean saturation at 100 cm). To evaluate whether there were differences in partitioning by climate, watersheds were classified as dry (precipitation deficit, PET>P) and wet (precipitation surplus, PET<P). I performed ANOVA tests on event and annual analysis groupings to determine whether there were significant differences in hydrologic response between groups. For question 1, I tested for differences in event partitioning between input type (rain or snowmelt) and differences in annual partitioning between historical and all rain scenarios. For question 2, I tested for differences in annual partitioning between climate (wet, dry) and soil depth groupings. Additionally for question 2, I tested the pairwise difference in linear regression slopes using indicator-variable regression with interaction in JMP (SAS-

based statistical software) to determine whether the rate of change between explanatory and response variable differed by climate or soil depth grouping.

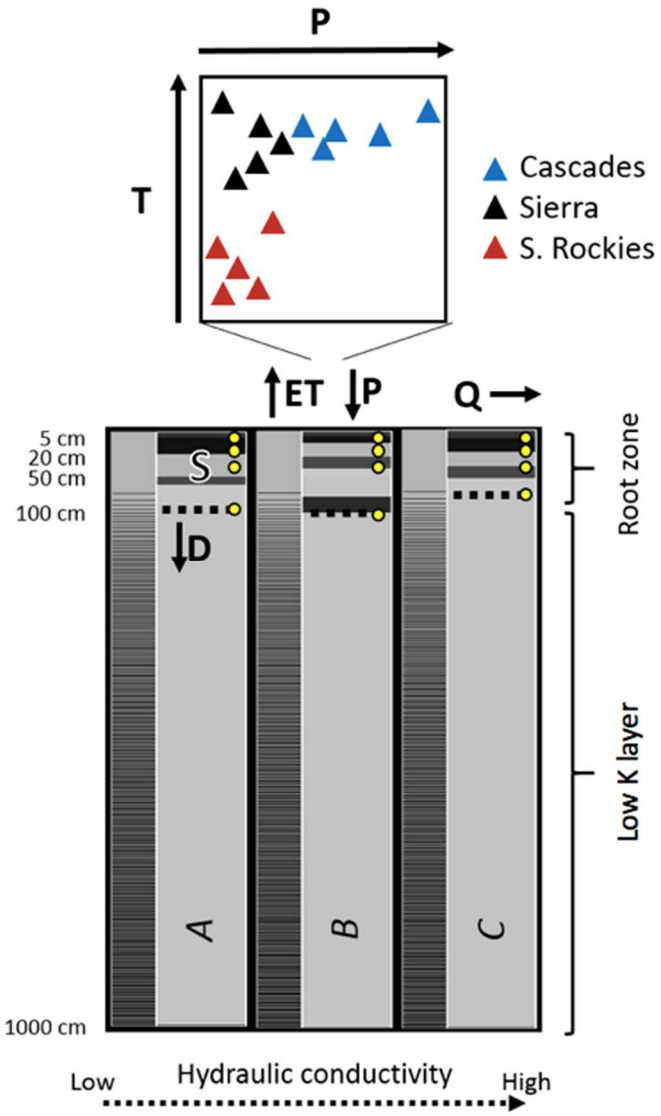

Figure 4.3. Modeling domain layout. Symbols in the graph above represent the range of climate scenarios used plotted by mean annual precipitation (P) and mean annual temperature (T), and the three soil profiles below represent the soil parameter sets labeled with italicized capital letters (A) loam (B) sandy clay loam (C) sandy loam. Different layers in each soil profile are represented as shades of gray.

Table 4.1. SNOTEL station properties including the start and end of data records and the elevation of the site and mean annual climatic characteristics: mean annual precipitation (MAP), mean annual temperature (MAT), mean annual snow persistence (MASP, %), snow zone, and mean annual aridity index (P/PET).

SNOTEL ID	Region	State	Start	End	Elevation (m)	MAP (cm)	MAT (C)	MASP	Snow zone	Aridity
352	Cascades	WA	1981	2015	1292	90	6.3	54	transitional	0.8
553	Cascades	WA	1982	2015	1049	433	6.9	65	transitional	4.4
375	Cascades	WA	1978	2015	1405	146	4.9	69	transitional	1.8
679	Cascades	WA	1980	2015	1564	263	4.8	77	persistent	4.9
418	Cascades	WA	1981	2015	1768	158	3.6	83	persistent	1.9
778	Sierra	CA	1980	2015	1864	69	8.0	53	transitional	0.7
697	Sierra	CA	1980	2015	2358	98	3.8	63	transitional	0.6
428	Sierra	CA	1981	2015	2089	180	6.0	72	transitional	1.3
848	Sierra	CA	1978	2015	2028	197	5.9	74	transitional	1.3
462	Sierra	CA	1978	2015	2672	142	4.0	78	persistent	1
559	Uinta	UT	1979	2015	2659	74	1.4	60	transitional	0.6
833	Uinta	UT	1979	2015	2901	70	1.5	69	transitional	0.7
396	Uinta	UT	1981	2015	3228	81	-0.1	76	persistent	0.9
567	Uinta	UT	1980	2015	3342	98	0.0	86	persistent	0.9
766	Uinta	UT	1989	2015	2938	157	3.2	87	persistent	1.3

Table 4.2. Soil profile properties derived from NRCS pedon reports, ROSETTA (Ros.) neural network. Columns are SNOTEL site, soil profile horizon, depth range of horizon, rock percent of sample volume, organic carbon percent of sample volume, sand percent of sample weight, silt percent of sample weight, clay percent of sample weight, Db_{33} bulk density of soil sample desorbed to 33kPa, Θ_{33} water content at field capacity, Θ_{1500} water content at wilting point, soil texture, residual water content Θ_r, saturated water content Θ_s, pore size distribution parameter α, and Ks saturated hydraulic conductivity. The lowest horizon Ks value is the result of calibration. Soil textures abbreviated as follows: sandy loam (SL), sand (S), loamy sand (LS), sandy clay loam (SCL), loam (L). SNOTEL 515, Harts Pass, WA, SNOTEL 1049, Forestdale Creek, CA, SNOTEL 1056, Lightning Ridge, UT.

Site	Hor.	Depth (cm)	rock % vol	organic C % vol	sand % wt	silt % wt	clay % wt	Db_{33} g cm^{-3}	Θ_{33}	Θ_{1500}	Text.	Ros. Θ_r	Ros. Θ_s	Ros. α (1/cm)	Ros. Ks (cm/d)
515	A1	0-15	9	9	53.5	35.6	10.9	0.63	0.41	0.14	SL	0.06	0.62	0.009	17.4
515	A2	13-38	8	8	57.6	35.3	7.1	0.64	0.47	0.14	SL	0.05	0.60	0.011	20.5
515	2Bw1	38-61	27	3	73.1	22.1	4.8	0.86	0.3	0.08	SL	0.04	0.55	0.032	15.1
515	2Bw2	61-81	55	1	81	11	8	1.46	0.16	0.09	LS	0.05	0.40	0.036	5.49
515	Cd	81-106	7	1	91.3	4.1	4.6	1.52	0.14	0.05	S	0.05	0.38	0.033	17.4
515	Cd	106-1000	7	1	91.3	4.1	4.6	1.52	0.14	0.05	S	0.05	0.38	0.033	1.74
1049	A	0-9	10	7	52.6	25.2	22.2	0.94	0.40	0.14	SCL	0.08	0.55	0.014	5.17
1049	Bt1	9-20	14	2	48.6	25.4	26	1.13	0.30	0.14	SCL	0.08	0.50	0.014	2.13
1049	Bt2	20-43	14	1	52.9	23.8	23.3	1.24	0.32	0.12	SCL	0.07	0.47	0.016	1.74
1049	Bt3	43-63	21	1	53.4	24	22.6	1.19	0.33	0.13	SCL	0.07	0.48	0.015	2.18
1049	Bt4	63-77	19	1	55.5	25.9	18.6	1.39	0.32	0.12	SL	0.06	0.42	0.017	1.22
1049	Bt5	77-110	11	0	52.4	30.2	17.4	1.21	0.39	0.13	SL	0.06	0.45	0.013	2.22
1049	Bt5	110-1000	11	0	52.4	30.2	17.4	1.21	0.39	0.13	SL	0.06	0.45	0.013	0.22
1056	A	0-10	11	3	36.1	48.8	15.1	1.17	0.30	0.12	L	0.06	0.44	0.010	2.41
1056	A	10-38	7	2	35.3	49.5	15.2	1.27	0.28	0.11	L	0.06	0.41	0.006	1.47
1056	Bt1	38-76	6	2	36	48.6	15.4	1.25	0.30	0.10	L	0.06	0.42	0.006	1.59
1056	Bt2	76-89	16	1	39.3	46	14.7	1.26	0.34	0.09	L	0.06	0.41	0.007	1.54
1056	2B	89-127	6	2	36.3	48.2	15.5	1.18	0.24	0.09	L	0.06	0.44	0.006	2.23
1056	2B	127-1000	6	2	36.3	48.2	15.5	1.18	0.24	0.09	L	0.06	0.44	0.006	0.22

4.4. Results

Study sites exhibited substantial variability at the annual scale in both precipitation input as well as surface runoff and deep drainage output (Figure 4.4). Patterns in Q and D follow patterns in P at most sites, with the greatest P for sites in the Cascades region and the lowest P in the Uinta. The wide range of climate conditions simulated provide a good opportunity for testing how climate, soil type, and soil depth affect input partitioning into Q, ET, D, and storage (S). The first section of the results focuses on comparing snowmelt and rainfall partitioning, as well as climatic influences, using only the loam profile to keep soil properties constant while varying input. The following section then assesses edaphic influences on partitioning with soil texture and soil profile depth chosen as explanatory variables.

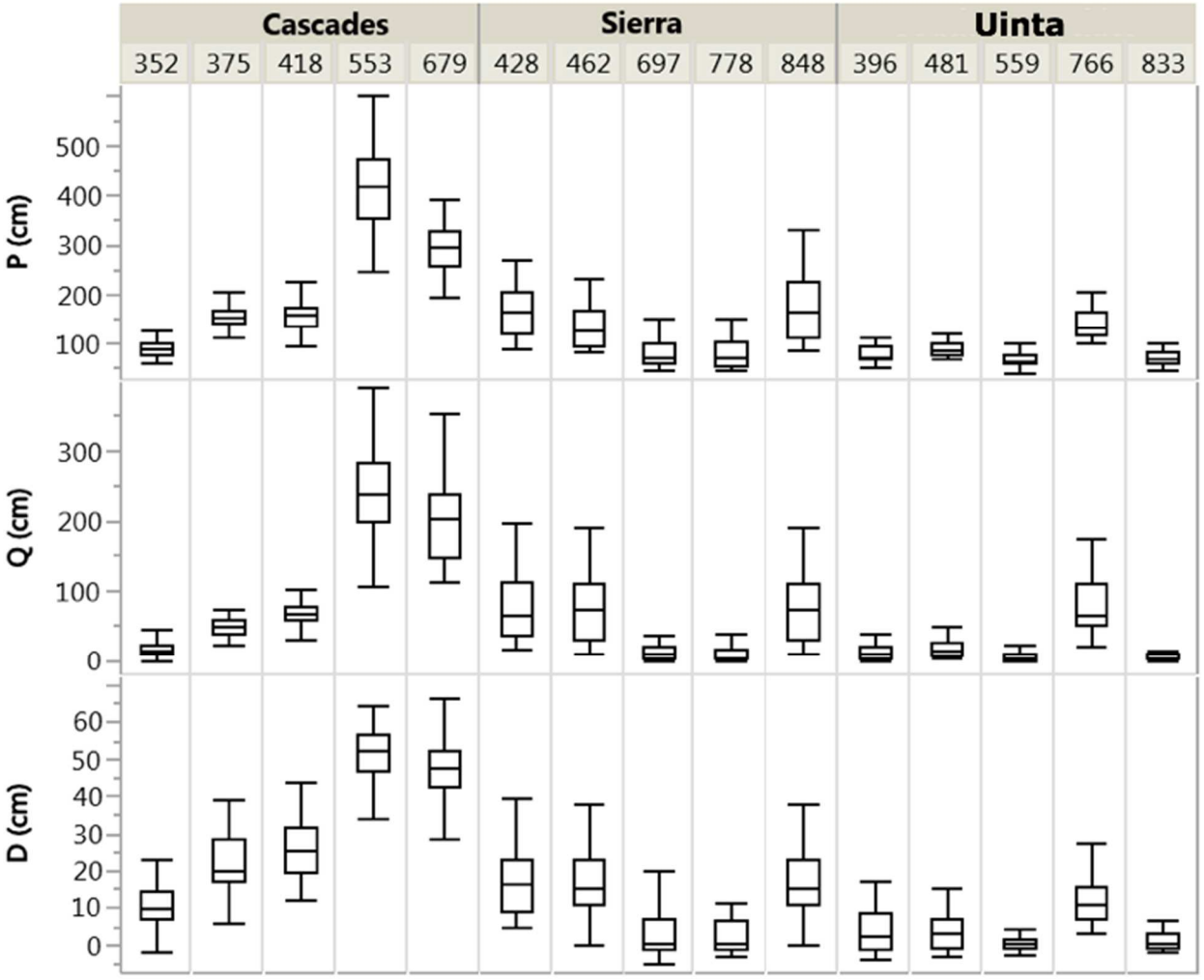

Figure 4.4. Ranges of annual precipitation (P), surface runoff (Q), and deep drainage (D) for each SNOTEL site climate scenario used in this analysis for soil profile 1056, loam.

4.4.1 Snowmelt vs rainfall and climatic influences on partitioning

At the event scale input rates were significantly greater on average for snowmelt as compared to rainfall in each of the three regions and on the whole (ANOVA $p<0.0001$, mean snowmelt for all regions = 1.14 cm/d, mean rainfall for all regions = 0.87 cm/d, Figure 4.5), though rainfall events had a higher maximum input rate (maximum snowmelt for all regions = 8.04 cm/d, maximum rainfall for all regions = 14.73 cm/d). Snowmelt events tended to occur on wetter soils, as estimated by antecedent soil moisture storage for the rooting zone (ANOVA

p<0.0001, mean S for snowmelt for all regions = 56.6 cm, mean S for rainfall for all regions = 48.2 cm). Average runoff ratios (Q/P) were higher for snowmelt as compared to rainfall (ANOVA p<0.0001, mean Q/P snowmelt for all regions = 0.20, mean Q/P rainfall for all regions = 0.03), with lower ET/P for snowmelt as compared to rainfall (mean snowmelt for all regions = 0.24, mean rainfall for all regions = 0.40).

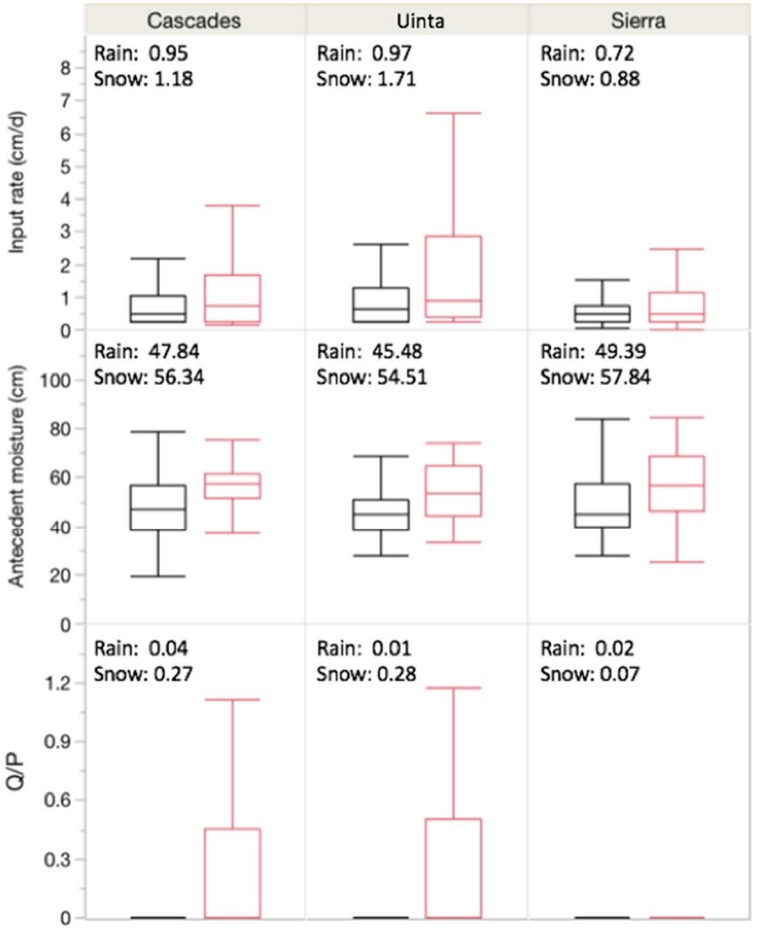

Metric	All regions	Cascades	Uinta	Sierra
Mean input rate (cm/d)	0.0001	0.0001	0.0001	0.0001
Antecedent moisture (cm)	0.0001	0.0001	0.0001	0.0001
Q/P	0.0001	0.0001	0.0001	0.0001

Figure 4.5. Boxplots of event input rate (cm/d) (top), antecedent soil moisture storage (S, cm) (middle) and event runoff ratio (Q/P, bottom) by region and event type (rain black, snowmelt red). Text in each subplot gives mean values. Table below displays ANOVA p-values for rain vs snow overall, as well as for specific regions. Results from the simulations with climate types in Figure 4.6, loam soil type.

At the annual scale, I investigated the relationships between water balance components by first computing correlations (Table 4.3). Annual precipitation (P) is positively correlated with surface runoff (Q, r=0.97), deep drainage (D, r=0.92), and mean saturation (Sat, r=0.73) at 100 cm depth (Figure 4.6). The relationship is linear for Q but nonlinear for D and Sat. Peak SWE is also highly correlated with Q, D, and Sat (r=0.70-0.83) because it is highly correlated with P (r=0.74). The other snow variables, SP and melt rate, do have significant correlations with Q, D, and Sat, but their correlation coefficients are substantially lower (r=0.44-0.63). Evaporation (E) and transpiration (T) have the weakest correlations with P (r=-0.07-0.13) of all partitioned components, but they are significantly correlated with SP (r=0.15-0.23).

Table 4.3. Correlations between annual values of climatic and water balance terms for historical input scenarios. Variables included are precipitation (P), potential evapotranspiration (PET), peak snow water equivalent (peak SWE), snow persistence (SP), average melt rate over the year (melt rate), mean saturation at 100 cm depth (Sat 100cm), surface runoff (Q), deep drainage (D), transpiration (T), evaporation (E), and aridity index (P/PET). P-value of correlation, *<0.5, **<0.01, ***<0.001.

	P	PET	peakSWE	SP	Melt rate	Sat 100	Q	D	T	E
PET	-0.43***									
peakSWE	0.74***	-0.46***								
SP	0.35***	-0.74***	0.65***							
Melt rate	0.54***	-0.36***	0.80***	0.62***						
Sat 100	0.73***	-0.55***	0.70***	0.49***	0.50***					
Q	0.97***	-0.42***	0.83***	0.39***	0.63***	0.73***				
D	0.92***	-0.55***	0.78***	0.44***	0.53***	0.86***	0.91***			
T	0.13**	0.09*	0.08	0.15***	0.20***	0.30***	0.09*	0.06		
E	-0.07	-0.07	-0.10*	0.23***	0.11*	-0.22***	-0.08	-0.18***	0.41***	
P/PET	0.98***	-0.55***	0.76***	0.43***	0.54***	0.74***	0.96***	0.93***	0.03	-0.07

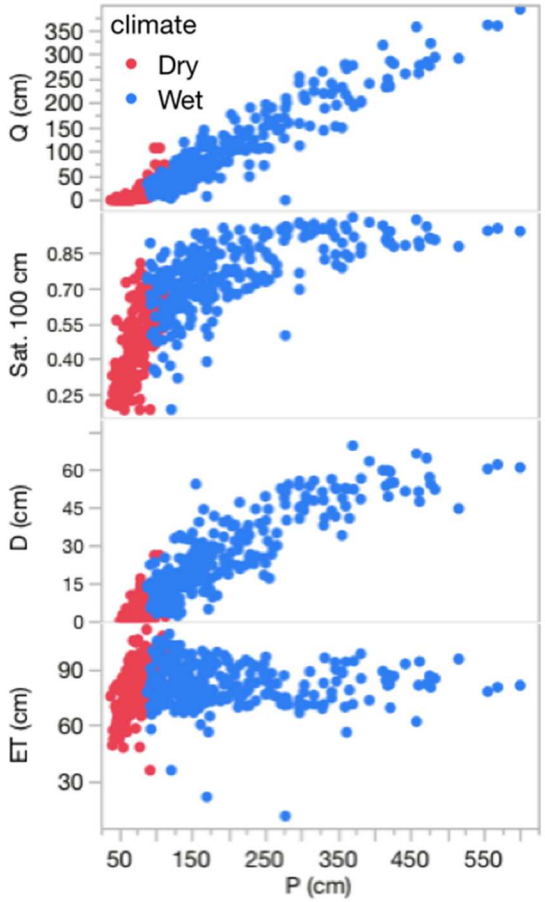

Figure 4.6. Annual surface runoff (Q), mean saturation at 100 cm depth, deep drainage (D) and evapotranspiration (ET) vs annual precipitation and classified by climate type. Dry P/PET <1=, Wet P/PET >1.

Precipitation is the primary driver of differences in partitioning (Figure 4.6), so normalizing Q, D, and ET by P can help in examining partitioning patterns. Comparing the hypothetical scenarios where I treated all precipitation as rain to historical scenarios at the annual scale indicated that all rain led to significantly lower Q/P ($p<0.0001$, mean 0.17 vs 0.31) and ET/P (only for dry catchments, $p<0.0001$, mean 0.72 vs 0.78) but slightly higher D/P ($p<0.0001$, mean 0.10 vs 0.09) (Figure 4.7). Ranges of S/P were weakly different ($p = 0.04$) between all rain and historical scenarios for dry site years but not for wet site years.

Another effect of loss of snow can be a decrease in input rate, as melt of a seasonal snowpack concentrates input in a short period of time. To examine the effect of input

concentration I also generated my own experimental intermittent and concentrated inputs for a wet site (375) and a dry site (559) while keeping P constant. Increasing input concentration led to significantly greater Q/P in the dry site ($p<0.05$, Figure 4.8) but no significant difference in the wet site. In contrast, D/P was significantly greater ($p<0.0001$) for the concentrated input scenarios for both dry and wet sites, as no deep drainage was produced with intermittent input. ET/P was significantly lower in concentrated scenarios, with a greater difference in dry climates ($p=0.004$, mean 0.80 vs. 0.66) than in wet climates ($p=0.013$, mean 0.34 vs. 0.28).

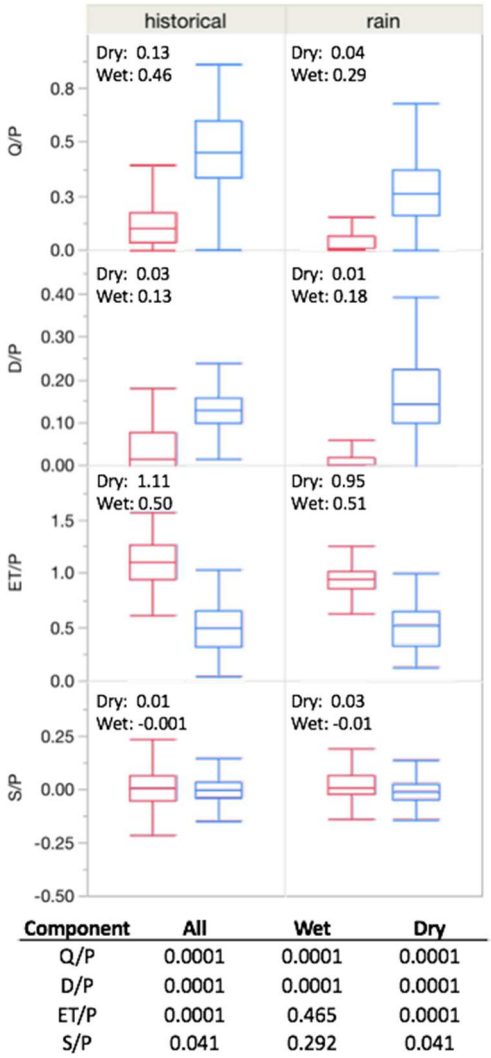

Component	All	Wet	Dry
Q/P	0.0001	0.0001	0.0001
D/P	0.0001	0.0001	0.0001
ET/P	0.0001	0.465	0.0001
S/P	0.041	0.292	0.041

Figure 4.7. Boxplots of annual Q/P, D/P, ET/P and change in S/P by input scenario; historical or all rain using all sites and years. Table below displays ANOVA p-values for historical vs all rain scenarios overall, as well as for different climates. Text in boxes indicates mean values. Dry P/PET <1=, Wet P/PET >1.

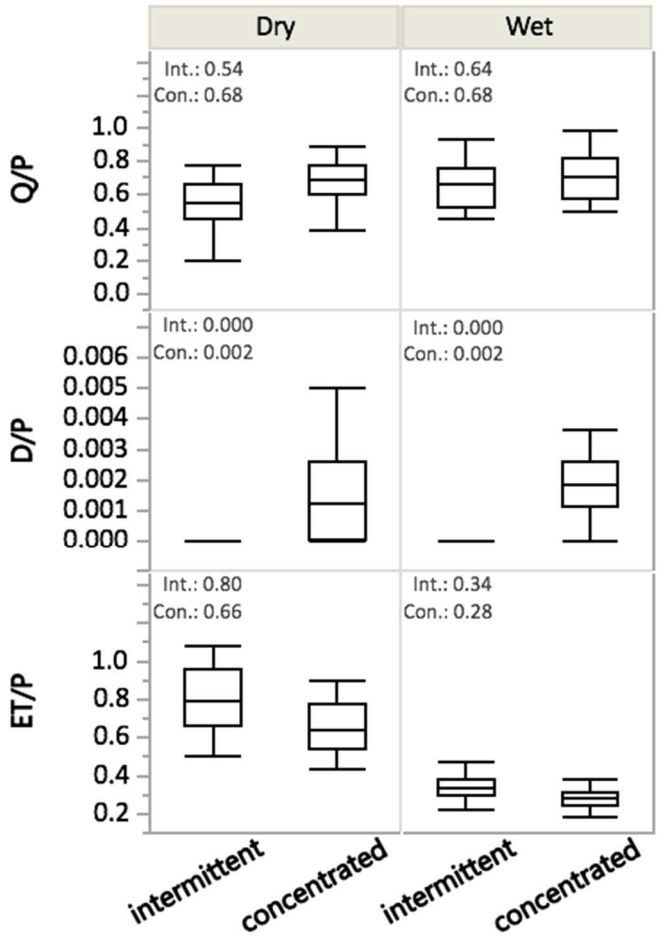

Component	All	Wet	Dry
Q/P	0.027	0.464	0.011
D/P	0.0001	0.0001	0.0001
ET/P	0.034	0.013	0.004

Figure 4.8. Boxplots of annual Q/P, D/P, and ET/P for experimental scenarios for a dry site (375) and a wet site (559) altering input to be concentrated or intermittent. I artificially produced intermittent (four five-day periods of low magnitude) and concentrated input (one twenty-day period of high magnitude) of the same annual total and simulated these inputs on the loam profile (1056). Table below displays ANOVA p-values for intermittent vs concentrated scenarios overall, as well as for different climates. Dry P/PET <1=, Wet P/PET >1.

I also examined the effect of snow and input concentration at the annual time scale by evaluating how the snowmelt as a fraction of total input and the input concentration (mean length of events divided by number of events) related to unitless response variables Q/P, D/P, ET/P (Figure 4.9, Table 4.5). Q/P increases with snowmelt fraction where snowmelt fraction is >0.5 and increases with input concentration where input concentration <0.07 (Figure 4.9). The ranges

of Q/P are higher in wet than in dry climates, with wet climates showing greater sensitivity to increasing snowmelt fraction and input concentration. D/P and ET/P are not clearly related to snowmelt fraction, but they do have some correlation with input concentration. D/P shows slight increases with input concentration <0.07, and ET/P decreases with input concentration <0.07. D/P ranges are higher in wet than in dry climates, with many dry years not generating D. ET/P ranges are lower for wet climates, where greater input is portioned to Q and D.

In summary, at the annual scale Q/P and D/P generally increase with increases in snowmelt fraction (Table 4.5, Q/P r = 0.41, D/P r = 0.20) and input concentration (Q/P r = 0.57, D/P r = 0.37), whereas ET/P is not related to snowmelt fraction and generally declines with input concentration (r = -0.60).

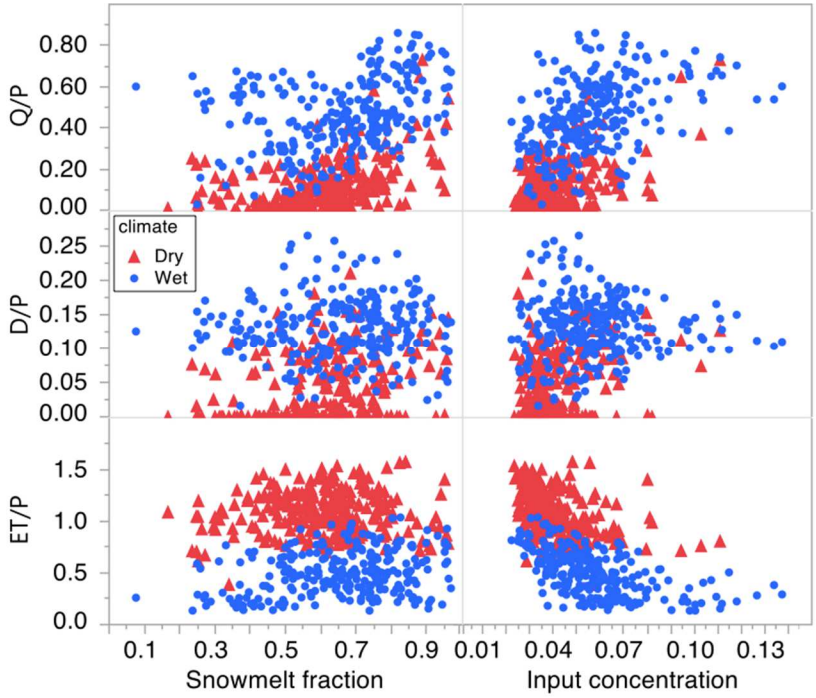

Figure 4.9. Ratio of runoff (Q), deep drainage (D) and evapotranspiration (ET) to input (P) snowmelt fraction of input and input concentration. Dry P/PET <1=, Wet P/PET >1.

4.4.2 Soil controls on partitioning

To compare the effects of climate to those of soil type on partitioning, I first examine how partitioned components relate to soil saturation. P is strongly correlated with mean saturation at 100 cm depth ($r = 0.73$, Table 4.3, Figure 4.6), which is a necessary precursor to deep drainage (Figure 4.14). Figure 4.10 displays the relationships between Q, D and ET vs mean saturation at 100 cm depth as separated by climate type and soil texture. Soil storage, which correlates with mean saturation at depth, mediates the conversion of input to output; mean saturation at 100 cm illustrates how storage is highly correlated with all three outputs. Mean saturation at 100 cm depth displayed strong relationships with Q, D, and ET for all, wet, and dry site years (Figure 4.10, Table 4.7). Q is generally low (<50 mm) until saturation is greater than >0.5, and it has a nonlinear increase at higher saturations. D in the simulations also has a nonlinear increase with mean annual saturation, but its magnitudes are substantially lower than when saturation goes above 0.6, with most values <50 mm. ET increases with saturation for saturation values <0.5, indicating that greater water availability in the soil zone increases ET. Above saturations of around 0.75, ET decreases, which may be because of less evaporative demand in the wet climates that produce the highest levels of soil saturation (also see Figure 4.15).

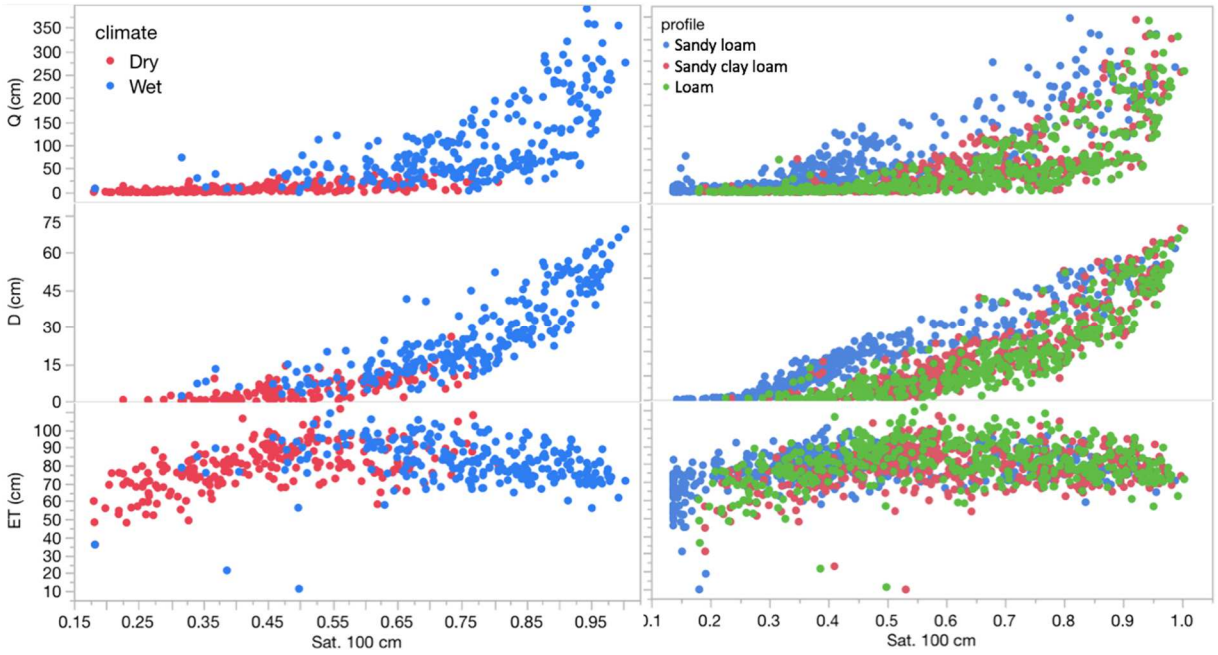

Figure 4.10. Annual surface runoff (Q), deep drainage (D) and evapotranspiration (ET) vs annual mean saturation at 100 cm depth (Sat. 100 cm) and classified by climate type (left) and soil texture (right). Dry P/PET <1=, Wet P/PET >1.

To evaluate the influence of soil type on partitioning, I plotted the same relationships shown in Figure 4.9 with soil texture separations rather than wet/dry climate separations (Figure 4.16). The response patterns are similar between soil types except for the sandy loam profile, which displays higher Q and D per unit saturation as compared to the loam and sandy clay loam profiles. The sandy clay loam also has slightly higher Q and D for the same levels of saturation as the loam profile. Example time series of daily 50 and 100 cm VWC, Q, D, E and T are shown in Figure 4.11. Here, with non-normalized values, small differences in Q,D,E and T are apparent between the different soil types, but these differences in response are muted at the annual scale.

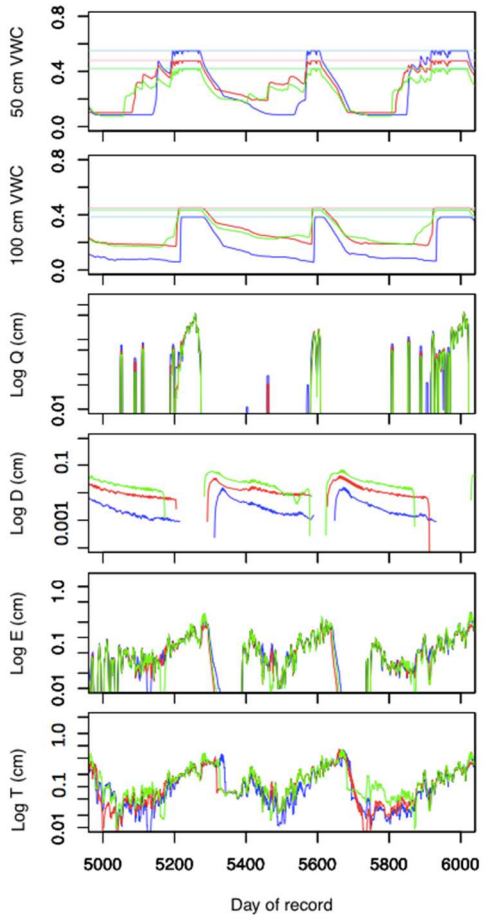

Figure 4.11. Time series of 50 cm VWC, 100 cm VWC, surface runoff (Q), deep drainage (D), evaporation (E) and transpiration (T) for SNOTEL site 698 input on SNOTEL site 515 (blue), 1049 (red) and 1056 (green) profile.

To assess the influence of our poorly constrained soil profile depths on partitioning, I altered the soil profile to be 1.5x and 2x its original depth (Figure 4.12). For the historical input scenarios Q/P declines significantly with deeper soils for wet sites ($p=0.005$) but not for dry sites. D/P increases ($p<0.01$) with deeper soils for wet sites ($p=0.0001$) but not for dry sites. Changes in ET/P and S/P with soil depth are not significant via ANOVA tests. To investigate changes in partitioning with depth further, I chose one site (396) and altered the soil profile depth by 20 cm increments. Changes in mean Q/P, and D/P were most pronounced within the first 1.5x of profile depth, while ET/P changes were of lower magnitude throughout the depths studied (Figure 4.17). Q/P median values are similar between soil depths; values initially decline from

the shallowest profile (0.13 at 100 cm depth to 0.11 at 300 cm), then generally increases with profile depth (0.14 at 280 cm depth). Median D/P decreases with profile depth for a greater extent of the depths studied (0.06 at 100 cm depth to 0.00 220 cm depth), then increases slightly for the deepest profiles (0.01 at 300 cm depth). D/P is negative at times reflecting movement of water upward across the root zone boundary rather than downward. Median ET/P increases with profile depth due to the downward extension of the root zone with increasing profile depth (1.2 at 100 cm depth to 1.3 at 300 cm depth). Overall, I observe mixed patterns in Q, D, and ET with profile depth.

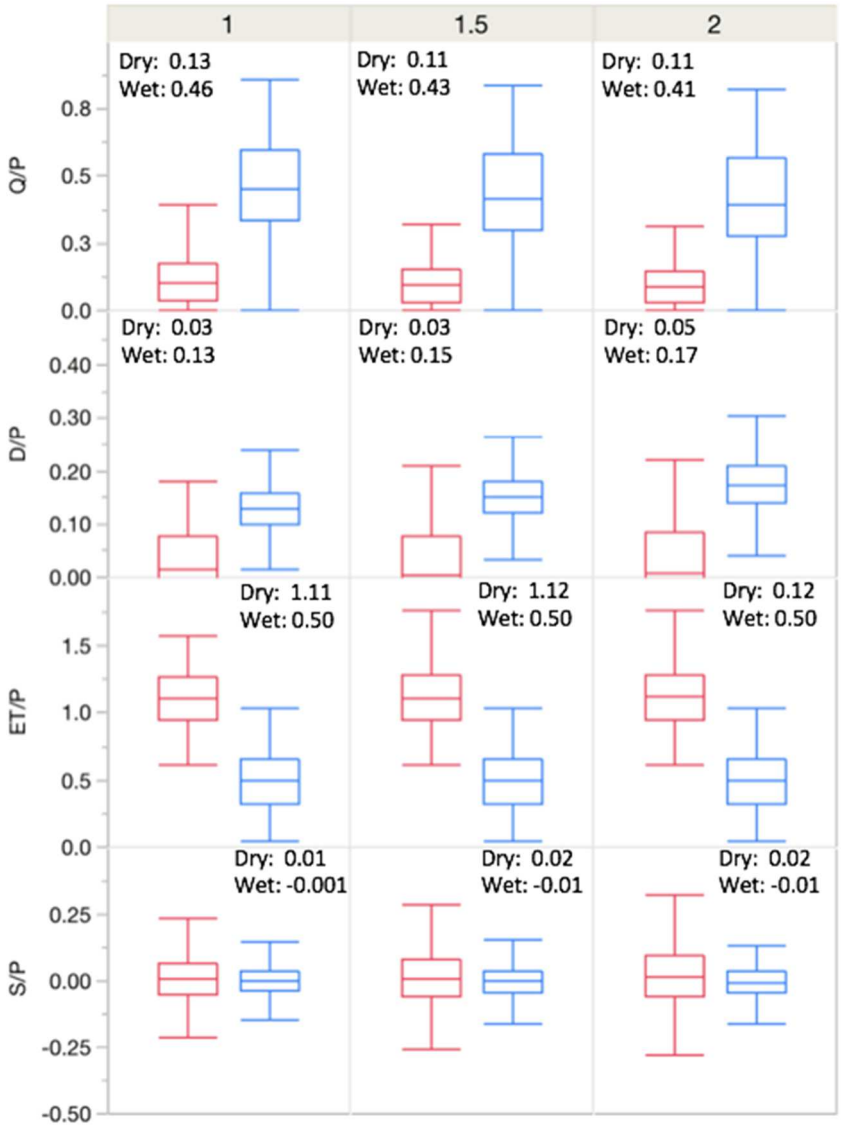

Component	All	Wet	Dry
Q/P	0.040	0.005	0.313
D/P	0.0001	0.0001	0.057
ET/P	0.967	0.984	0.786
S/P	0.956	0.236	0.328

Figure 4.12. Boxplots of annual Q/P, D/P, ET/P and change in S/P by profile depth at 1x, 1.5x and 2x the original depth. Table below displays ANOVA p-values for comparisons of each component between the three depths. Text in each subplot gives mean values. Dry P/PET <1=, Wet P/PET >1.

4.5 Discussion

4.5.1 Snowmelt vs rainfall and climatic controls on partitioning

Event analysis demonstrate significant differences in input partitioning for snowmelt and rainfall at event scales. The combination of greater average input rate and wetter antecedent conditions for snowmelt leads to a greater fraction of input being exported as surface runoff (Q) (Figure 4.5). This stands in agreement with previous studies showing that snowfall and subsequent melt tend to occur when soils are at elevated moisture contents due to lower ET (Liu et al., 2008; Williams et al., 2009; Bales, 2011).

At the annual time scale the correlation between snowmelt fraction and response variables was weak-moderate (Figure 4.9). This indicates that over longer periods of time, the type of input (snowmelt or rainfall) is not as strong of an influence on hydrologic response. The differences apparent at the event time scale had to do with seasonality of input, where input during the winter or spring on wetter soils would be more likely to produce soil saturation and runoff. These seasonal effects become more muted at the annual time scale. However, when input scenarios were forced into the extreme case of all rain, they showed a lower Q/P (Dry: 0.13 vs. 0.04; Wet: 0.46 vs. 0.29), corroborating the event results that indicated snowmelt elevates runoff (Figure 4.7).

Multiple hydrologic processes change when precipitation shifts from snow to rain: (1) input concentration changes; (2) timing of input changes, and (3) ET responses change. Experiments with changing input concentration (Figure 4.8) illustrated how D/P increased significantly with more concentrated input in all climates, whereas the change in Q/P with input concentration was only significant in dry climates. In this study, concentrated input leads to both saturation excess runoff (similar to Hunsaker et al., 2012; Barnhart et al., 2016; Li et al., 2017;

Hammond et al., 2018), and deep drainage (similar to Langston et al., 2015). Wet climates can have sufficient near-surface saturation to generate runoff without concentrated input (Figures 4.7,4.9), whereas the concentrated input can be more important for producing the conditions that generate runoff in dry climates. Concentrated input from melt of a deep snowpack can also help create the conditions that saturate the soil at depth, allowing groundwater recharge. The same input spread out over time, depending on storage conditions, will allow more opportunity for water loss through ET and therefore lower likelihood of deep drainage and groundwater recharge. Input during the wet winter period, whether rainfall or snowmelt, likely leads to deep drainage or surface runoff, whereas fall, spring or summer input is more likely to contribute to soil storage and be at least partially partitioned to ET.

The effects of snow loss on D were not as consistent across our simulations as the effects on Q. In general, far greater Q/P was generated than D/P, so Q was more sensitive to changes in input: Q was higher for snowmelt than rainfall events; Q/P decreased in all rain simulations, increased in concentrated input simulations, and increased with both snowmelt fraction and input concentration at the annual time scale. In contrast D/P increased for all rain simulations in wet climates but decreased in dry, increased in concentrated input simulations, and was not affected by snowmelt fraction, differing from the hypothesis that concentrated input would increase D in all climates (Figure 4.1). This variability in D/P across the simulation experiments is likely because S mediates the connection between input and D. Q is affected only by near-surface storage and can therefore more rapidly respond to input rate and concentration, partially explaining why there is an effect of snowmelt fraction on Q but not D. Input concentration was an important driver of D in hypothetical scenarios (Figure 4.8) but not a strong control in

historical climate where concentrations in time were more similar than the experimental separations (Figure 4.9).

With continued warming and a greater fraction of precipitation falling as rain than snow in some areas, earlier and slower snowmelt is expected (Trujillo and Molotch, 2014; Musselman et al., 2017), especially in more arid areas where sublimation and longwave radiation cool the snowpack (Harpold and Brooks, 2018). Earlier snowmelt during periods of lower ET may generate higher flow, but if this melt occurs at an overall slower input rate, more of it could contribute to soil storage in the root zone and be subsequently used by vegetation. Previous research showed that loss of snow can lead to higher ET until soil moisture becomes limiting (Tague and Peng, 2013), and our simulations show some evidence for this. T is lower for low values of saturation in dry climates, and the lowest T occurs for the lowest snowmelt fractions (Figure 4.15). This moisture limitation has some support when looking at T alone, but not when ET are combined as a fraction of input. Overall, lower magnitude and intermittent input from rain leads to less drainage to the lower root zone (Figures 4.7,4.9), with E and T losses higher near the surface. The timing of soil water input events relative to vegetation phenology may limit the effect of precipitation phase, and in the case of snow, storage. Mid-winter rain and melt events may still be conducive to generating surface runoff and deep drainage if antecedent moisture conditions are high, though not able to produce output at the same efficiency as concentrated input from a deep snowpack. The countervailing effects of (1) earlier snowmelt during periods of lower ET, and (2) slower melting leading to less concentrated input, are likely dependent on the relative magnitudes of input and other site dependent factors and should be considered for further research.

4.5.2 Soil controls on partitioning

Soil texture and depth generally did not change partitioning at the annual time scale as much as the varying climate scenarios. Precipitation is a strong driver of partitioning in our scenarios, with precipitation highly correlated with annual mean saturation and mean saturation strongly correlated with partitioned components. We evaluated soil profiles deeper than the originals , but may have seen enhanced deep drainage if we also evaluated shallower profiles. The three soil textures evaluated did not differ in their responses to annual snowmelt fraction and input concentration (Figure 4.16), but did show differences at the daily scale (Figure 4.10). Altering soil profile depth and the associated root zone to 1.5x and 2x the original depth led to decreases in Q/P and increases in D/P at wet but not dry sites, where differences were insignificant (Figure 4.12). Overall, the nature of the soil profile might be expected to affect the sensitivity of the hydrologic response to climate, but my results do not reflect this at the annual scale.

The concentrated input effect of snowmelt has been shown to be more prominent in shallow soils (<0.5 m); for example, Williams et al. (2009) showed that soil water input from snowmelt events more often exceeded field capacity than summer rains in shallow soils. Where soils are shallow, winter precipitation may be in excess compared to the soil storage capacity, with rain or snowmelt additions contributing to surface runoff and deep drainage (Smith et al., 2011). Deeper rooting depths can allow more water to remain in storage and be lost to ET before contributing to surface runoff and deep drainage (Smith et al., 2011), but our simulations do not reflect this phenomena. Soil and vegetation properties, as well as regional weather patterns, could conceivably override the effects of earlier snowmelt on critical zone partitioning. For

example, input from only rain increased deep drainage from historical conditions at wet sites (Figure 4.7).

4.5.3 Uncertainties of this study

Given the complex nature of soil water movement in heterogeneous mountain topography, this study makes several assumptions and simplifications in order to test the hypotheses. The simulations do not include the intricacies of vegetation water use, and the routine chosen assumes a static leaf area index (LAI) with root uptake controlled only by PET and soil moisture conditions. Additionally, I faced difficulties during calibration that rendered simulations wetter than measured water contents; therefore, the representation of partitioning shown here displays relative response between climates and soil profiles rather than absolute quantification of these partitioned components. The water balance in hydrologic models can be highly sensitive to the method chosen to represent root uptake and plant water use (Gerten et al., 2004), and hydrologic models generally poorly capture or replicate the interactions between soil, vegetation and atmospheric properties that combine to control plant water use (Gómez-Plaza et al., 2001; Gerten et al., 2004; Zeng et al., 2005). Further, forest canopy can have a greater impact on soil moisture than snowmelt timing (Maurer and Bowling, 2014; Webb et al., 2015). Dense forests can prolong the length of the snowmelt season, resulting in snow that lingers longer and melts slower due to shading, ultimately leading to higher forest water uptake than under a sparse canopy (Molotch et al., 2009). With these points as cautions, coupled models of plant physiology, soil physics and hydrology could assess deep drainage dynamics at greater spatial scales following the results of this study.

The simulations used here only allow for matrix flow, excluding macropore flow, for a simplified representation of soil water movement. Preferential flow though the profile could have enhanced deep drainage relative to surface runoff, which may explain why rates of deep drainage were so low in the simulations as compared to studies where preferential flow is included in modeling deep drainage and aquifer recharge and constitutes 60-80% volumetric contribution to aquifer recharge (Wood et al., 1997; Jaynes et al., 2001; Sukhija et al., 2003). However, the simulated Q/P vs snowmelt fraction plots from HYDRUS simulations follow the same general pattern as Q/P vs SP in Chapter 3. This lends confidence to the HYDRUS simulations, as their simulated values are in the same range as observed streamflow. The physically-based modeling approach has proven well-suited to represent soil water flow in a wide variety of natural soils (Scott et al., 2000; Chen et al., 2014; Hicnkley et al., 2014, Wyatt et al., 2017). The use of this 1-d model ignores lateral subsurface flow; while simulating only vertical flow is reasonable for SNOTEL sites located in relatively flat forest openings, some lateral surface and subsurface flow likely affected the measurements used to calibrate the models. Partitioning of the water balance components reported here would be greatly altered in sloping terrain. In addition, I did not allow for frozen soils in my simulations, but this can be a strong influence on soil input partitioning in high elevation or high latitude areas (Bayard et al., 2005; Niu and Yang, 2006)

4.5.4 Implications and opportunities for further research

The results from this one dimensional modeling study have direct implications relating to the reductions in snow persistence shown in Chapter 2, and the relationship between snow persistence and peak snow water equivalent with annual water yield and runoff efficiency in Chapter 3. In the context of streamflow, results from this chapter show that concentrated input

regardless of type (rain or snowmelt) leads to greater surface runoff, partially analogous to quickflow at the watershed scale, though the 1D model does not allow for subsurface lateral stormflow that also contributes to event response in multidimensional space. The fact that concentrated snowmelt input at dry sites in this study leads to greater surface runoff supports the hypothesized mechanism of greater streamflow generation with higher snow persistence presented in Chapter 3. With further declines in seasonal snow and the loss of persistent snow cover in Chapter 2, large areas of cold, semi-arid regions could experience substantial reductions to annual water yield and runoff efficiency.

Concentrated input also leads to greater deep drainage than that from intermittent input, with deep drainage not activated in dry climates with intermittent inputs. Aquifer recharge requires deep drainage, though deep drainage is not itself aquifer recharge in all situations. With reductions or absence of deep drainage in dry climates, groundwater levels likely lower and groundwater storage may remain constant or decline depending on the groundwater flow rate, and rate of withdrawals. An analysis of the effects of climate change on groundwater recharge across the western United States revealed that mountain aquifer recharge is expected to decline due to decreased snowpack (Meixner et al., 2016), due to snowmelt more efficiently infiltrating to the root zone (Earman et al., 2006), and because a high magnitude of water is released from snowpack when ET is low. These results support those reported in this study indicating likely declines in aquifer recharge and groundwater storage in semi-arid cold regions where snowpacks are declining.

Strong correlations between mean saturation at depth and deep drainage suggest that soil moisture measurements as shallow as 50 cm could provide estimates of deep drainage (Table 4.7), and inform annual estimates of aquifer recharge in mountain areas. This use of deep

saturation for deep drainage estimation is supported by other recent research (Xie et al., 2018), which used soil moisture data along with actual evapotranspiration estimates to approximate deep drainage spatially. In addition, the date of saturation onset at 100 cm strongly correlates with the date of drainage onset (r=0.82, Figure 4.14), so estimating the timing and duration of deep drainage at sites across the mountainous U.S. using this method could be feasible. I was unable to look at deep drainage at the event scale because of its lagged response that leads to an inability to separate event response from one period of input from another.

While physically based hydrologic models are useful for analyzing hydrologic partitioning within the critical zone, empirical hydrometric and experimental tracer studies are needed to constrain the outputs of these models due to the complexity of soil moisture dynamics. Few studies combine hydrometric data, geochemical tracers, and isotopic tracers to analyze hydrologic response to snowmelt (Cowie et al., 2017), but this combination of information provides multiple lines of evidence for examining hydrologic partitioning through the critical zone. Further advances in hydrologic partitioning at larger scales could also utilize remotely observable processes including vegetation response (Hwang et al., 2012), and intermittent stream response (Spence and Mengistu, 2016).

4.6 Conclusions

The initial hypotheses for this study were that runoff and deep drainage would be greater from snowmelt than rainfall and that this effect would be greatest in dry climates, where soil saturation is less frequent, compared to wet climates and shallow soils, which can saturate with lower water input. Results confirmed the greater runoff generation from snowmelt, which tends to be greater in input concentration, and occurs on wetter soils than rainfall, resulting in higher

runoff response at the event time scale. Whether input is snowmelt or rainfall becomes less important at longer time scales where seasonality is muted. The effects of snowmelt vs. rainfall on deep drainage are not as clear. Hypothetical scenarios with concentrated input, analogous to melt of a deep snowpack, do enhance deep drainage over intermittent input. However, in wet climates, input that is exclusively rain may lead to higher deep drainage than mixed rain and snowmelt input. Deep drainage does increase with input concentration in dry climates, consistent with the initial hypothesis; snowmelt in these areas is most likely to provide the concentrated input needed to activate deep drainage. The three soil textures included here show similar partitioning between Q, ET, and D when compared between climate scenarios; while the textures produce differences at short timescales, these aggregate to small effects at the annual scale. With deeper profiles, I observed weak patterns in partitioning opposing our hypothesis that the shallowest soils would generate the greatest deep drainage, but I also did not simulate the depths of profiles where this effect has been shown to occur prior. Deep drainage requires saturation low in the root zone, so soil moisture measurements here may be useful in estimation of deep drainage and aquifer recharge. Processes affecting the duration of saturation below the root zone could compromise deep drainage especially in dry climates, including changes in snowmelt rate and duration. With continued snow loss in mountain and high latitude areas, surface runoff and deep drainage could face substantial reductions due to the loss of concentrated snowmelt input.

Chapter 5. Conclusions

This dissertation presented a global snow persistence classification and trend analysis, investigated the effects of snow persistence on annual water yield at the watershed scale in different climate types, and analyzed the mechanisms driving snowmelt and rainfall partitioning in mountain soil profiles at event and annual time scales.

5.1 Key findings and implications

In Chapter 2, findings can be organized around three main points: a global snow climatology, snow persistence in relation to climatic variables, and global trends in snow persistence. The snow climatology reveals similar snowline elevations by latitude and elevation around the globe that are regionally modified by coastal proximity and windward-leeward location. In relation to climate variables, snow persistence is influenced more by temperature at low elevations and precipitation at high elevations, with climatic indices changing dominance by region. Trends in snow persistence are predominantly negative, occurring mostly in seasonal snow areas at high latitude. The methods and products generated in this chapter provide one way to compare snow characteristics and snow loss between different regions globally via remote sensing, addressing a key gap in the understanding of regional snow loss. These products can also be used for further climatological analysis of how snow persistence changes along climatic and vegetative gradients. The relative importance of precipitation and temperature in controlling snow persistence by elevation and latitude may help to identify areas most sensitive to future snow loss, with areas in dry climates and at elevations where temperature is the dominant control on snow persistence likely being more vulnerable.

In Chapter 3, I demonstrated that snow persistence is a useful metric for annual water yield estimation, both spatially and temporally. Snow persistence and modeled peak SWE are strongly correlated with annual and mean annual streamflow in dry/cold (precipitation deficit) but not in wet/warm (precipitation surplus) watersheds of the western U.S. Climate type affects correlations between snow and streamflow because of the relative importance of precipitation for total snow accumulation. In dry/cold watersheds, snow variables predict streamflow almost as well as precipitation alone because peak snow accumulation is strongly correlated with precipitation. The result that hydrologic response of dry/cold watersheds is more sensitive to snow loss than wet/warm watersheds contributes to understanding of how snow loss will impact water resources in different climate types. However, research at sub-annual time scales is needed to determine the importance of precipitation phase and timing on response. This chapter also fills a gap in the understanding of snow's influence on hydrologic response at different scales by focusing on watersheds rather than the more commonly studied basin scale or plot scales. A method is also presented for mapping streamflow generation though space and estimate annual water yield in other snow-dominated cold and dry watersheds across the globe without significant glacial influence. The ability to estimate streamflow using snow persistence expands the ability to track hydrologic change in semi-arid, snow-dominated regions across the globe.

In Chapter 4, I evaluate the influence of input type, climate, soil texture and depth on the partitioning of inputs into surface runoff, deep drainage and evapotranspiration at sites across the western U.S. Snowmelt exerts strong controls on partitioning at the event scale with greater runoff generated due to higher input rate and wetter antecedent conditions, but it is of lesser influence on runoff generation and deep drainage at the annual scale where average soil wetness dominates. Simulations illustrate that the connection between input type and deep drainage is

inconsistent, and this is probably because the two are separated by the full soil zone. Storage dynamics at depth as well as ET throughout the profile interact with input to affect D. While soil texture impacts the partitioning of input at sub-annual scales, the profiles used in this study show similar response at the annual scale. This implies that study of the broad effects of input change may be possible without needing to consider soil type heterogeneity as a primary controlling factor. Lower surface runoff is evident with deeper soil profiles, yet deep drainage is relatively constant due to simultaneous decreases in surface runoff and increases in evapotranspiration that reduce storage. The simulation results indicate that the occurrence of deep drainage may be estimated using soil moisture sensors at sufficient depth. This provides one way forward in estimating deep drainage and groundwater recharge at many locations using established sensor networks. Taken together, the combined results and broader implications from each chapter of this dissertation are presented in Figure 5.1 below.

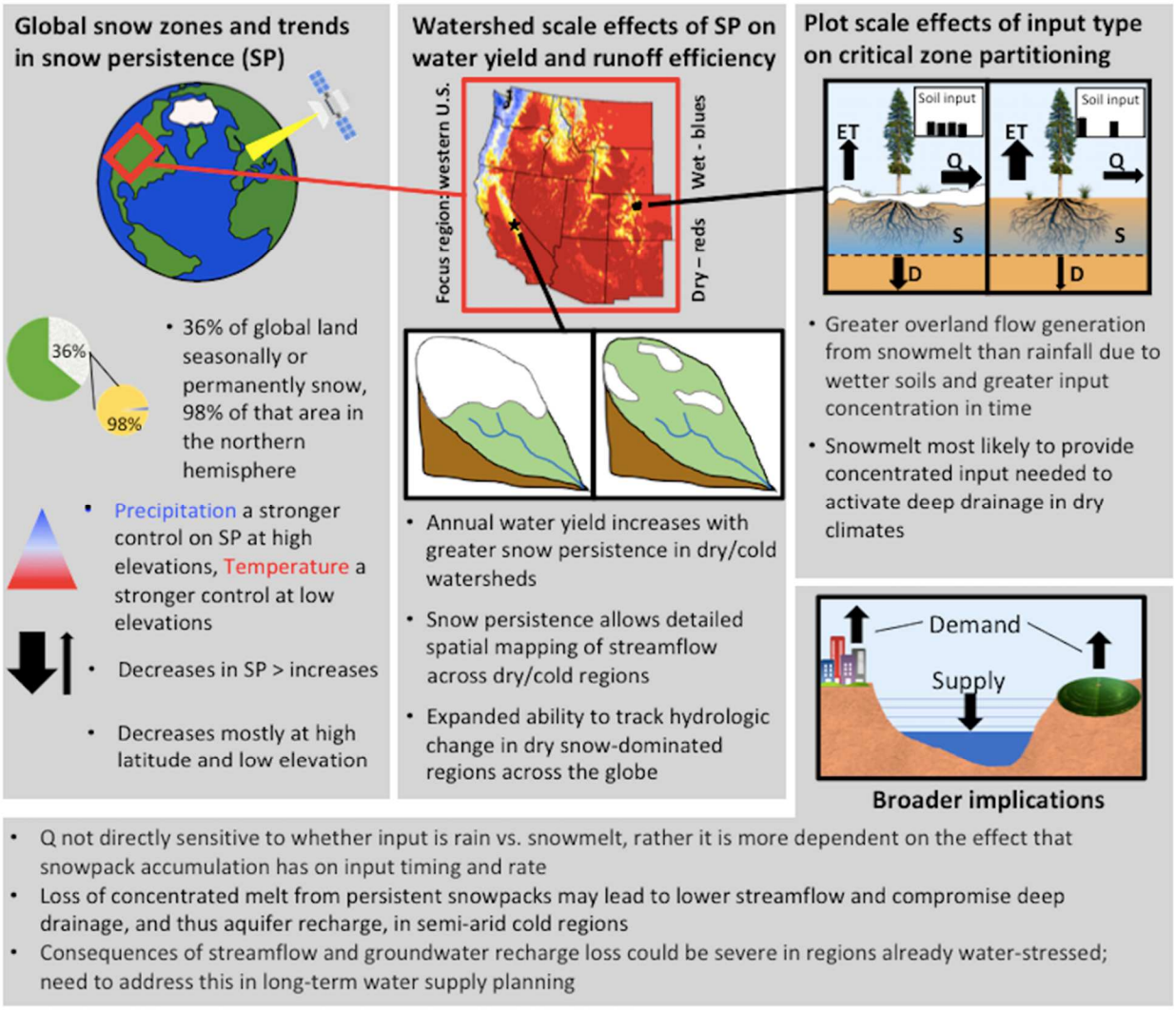

Figure 5.1. Combined results and broader hydrologic implications from this dissertation.

5.2 Global warming and the changing hydrologic cycle

Findings in this study have direct implications for climate change impacts in cold dry areas globally. If empirical results are indicators of future snow-streamflow relationships, snow persistence exponentially increases water yield, so its loss could lead to large streamflow declines, particularly where snow persistence is currently high. The consequences could also be severe in dry regions if the phrase "wet wetter, dry drier" applies to future climate, as commonly

described in simplified climate predictions. Recent research suggests this adage is not as simple as once thought, as aridity changes over land have not followed a simple intensification of existing patterns (Greve et al., 2014). Whether these patterns will emerge in subsequent decades is uncertain and further complicated by higher intensity precipitation events expected in many areas, with longer periods between events (Collins et al., 2013).

Snow persistence in dry/cold regions at mid-latitudes, (i.e. the western U.S.) is closely related to winter and annual precipitation, but with continued warming, this may shift to more temperature dependence. This may reduce the utility of snow persistence for annual water yield prediction in these areas. The relationship between Q and Q/P with SP may also change in the future, given an increase in vapor pressure deficit (VPD) (Abatzoglou and Williams, 2016), in cold dry areas. Increased VPD could drive increased sublimation from the snowpack (Hood et al., 1999; Jackson and Prowse, 2009; Zhou et al., 2012) simultaneously increasing cold content, and lessening snow water equivalent. This combination could lead to snow that persists the same amount of time or longer under warming scenarios, yet contains less input resulting in lower Q/P. In contrast, at high latitudes where increased precipitation is expected (Emori and Brown, 2005; Seager et al., 2010), and snow accumulation may increase (Collins et al., 2013), the relationship between SP with Q and Q/P may change so that snow persists for a similar amount of time given a reduction in snow during the shoulder seasons, but produces greater flow due to greater melt resulting from increased peak accumulation.

With model simulations predicting higher potential evapotranspiration but both mixed increases and decreases in precipitation in the western U.S. (Collins et al., 2013), predictions of water yield are uncertain. While potential evapotranspiration will increase, increased carbon dioxide in the atmosphere reduces a plant's physiological tendency to transpire partly

counteracting the effect of warming (Swann et al., 2016). Combined with truncated snow accumulation and melt seasons in mid-latitude dry/cold areas, predictions of water yield may become more difficult.

Low flow temperature sensitivity can be double that of annual water yield, with warm winters corresponding to slightly lower water yield and longer, more severe summer low flows. (Dierauer et al., 2018). Further research is needed on the combined effects of greater winter rainfall and streamflow, decreasing summer streamflow, and possibly higher transpiration in the western U.S., especially since current model simulations produce scenarios in which increases in water demand outstrip increases in water supply. Global model simulations in the IPCC AR5 have greater disagreement between individual models in the magnitude and direction of water yield response in the southwestern U.S. than in AR4 (Collins et al., 2013), though multiple regional studies focusing on the Colorado River basin show streamflow declines through a combination of evapotranspiration increases and precipitation decreases (Christensen and Lettenmaier, 2007; McCabe and Wolock, 2007; Barnett and Pierce, 2008).

5.3. Snow loss and water management

In forecasting reservoir inflows and optimizing reservoir storage, managers need to pay attention to water yield at middle elevations with intermittent snow cover, not just high elevations with persistent snow cover and greater station coverage. There is the possibility for dramatic losses in water yield at the intermittent-persistent snow transition, where the Q-SP curve slope is steepest. It remains unclear whether existing water management plans are prepared for this loss. The loss of groundwater is also an important consideration for future water management in the western U.S.. Lag times between mountain groundwater recharge and

emergence of that groundwater as baseflow downstream or as water available in aquifers in lowlands mean that impacts of recharge reductions may not be immediately evident.

For the past several decades, reservoirs have been managed during the conditions of inter-annual climatic variability and climatic trends. Future management faces the challenge and uncertainties of magnified trends, altered climatic variability, and increased demand (Kiparsky et al., 2014). Climate change adds to historical challenges for reservoir management, but in most cases does not introduce entirely new challenges. Instead, climate change is likely to stress water resources that are already at or beyond natural limits (Dettinger et al., 2015). Water managers and society as a whole currently face challenging tasks of repairing decayed water infrastructure and building new water infrastructure (Milly et al., 2008). In the Colorado River Basin, high sensitivity of reservoir system performance to future climate simulations reflects a fragile equilibrium with current system demands slightly less than long-term mean annual inflow. Simulations incorporating future climatic and demographic change produce situations in which reservoir inflows are exceeded by demands year after year (Christensen et al., 2004).

For the operation of existing and potential future infrastructure, statistical models of reservoir inflow and storage based on historical relationships between snow courses and meteorological sites will not be sufficient. Nonstationary probabilistic models of relevant environmental variables (e.g. Soundharajanet al., 2016) could be used to model the optimization of water systems (Milly et al., 2008). Nonstationary hydrologic variables can be forecast stochastically, with evolving probability density functions and accompanying estimates of uncertainty (Milly et al., 2008). Adaptation procedures need to be developed to encompass envelopes of potential inputs and demands with acceptable uncertainty bounds rather than fixed projections of changes in discharge (Kundzewicz et al., 2008).

But do we need to build more dams to increase storage capacity to buffer seasonal changes in hydroclimatology and adapt to nonstationary inputs and demand? Some suggest that the importance of dams in providing water security will increase, as storage can offset the vulnerabilities of water resources systems to future climate scenarios (Ehsani et al., 2017). The trajectory of global planned water infrastructure in headed in this direction, with global dam construction continuing to increase dramatically. 3,700 major hydroelectric dams (>1 MW) are planned or under construction, primarily in countries with emerging economies, totaling to a small fraction of expected future electric demand and reducing the number of remaining free-flowing large rivers by nearly a quarter (Zarfl et al., 2015). Globally, 48% of river volume is already moderately to severely impacted by flow regulation or fragmentation, and assuming completion of all dams planned and under construction, this number would nearly double to 93% (Grill et al., 2015).

Multiple strategies for adaptation to climatic change and increased demand have emerged in the western U.S. These include new dams, desalination, basin imports via pipeline, municipal conservation, permanent transfers from agriculture, water markets, land fallowing, canal lining, retirement of grass lawns by purchase, groundwater banking, reuse, new rate structures, consumer education, municipal conservation, indoor fixture rebates, new landscape design, water loss management from leaky mains, and aquifer storage and recovery (Dettinger et al., 2015). Integrating the above techniques in different combinations depending on existing infrastructure, expected changes to demand, and logistical challenges will likely be required to prepare for uncertain future hydroclimatic changes, Additionally, renegotiation of river compacts and treaties (e.g. Colorado River Compact and Columbia River Treaty) is necessary given that they were first setup and agreed to during the anomalously wet 20th century, with incomplete

information on the quantity and spatial distribution of water yield, and during periods of far lesser demand.

5.4 Opportunities for further research

Snow persistence demonstrates utility in spatial and temporal water yield estimation in the western U.S. If the relationships identified between snow persistence and streamflow in the western U.S. are similar in other dry/cold parts of the world, snow persistence could be useful for first order estimates of annual streamflow volume, especially in places with sparse or inaccurate precipitation data. With increasing record length, snow persistence derived from MODIS snow covered area products will provide greater certainty in climatological trend analyses by filtering out interannual meteorological variability, and allow for further trend mapping at the 500 meter resolution globally. Further, vegetation adjustments and updated cloud removal algorithms could improve SP estimate uncertainty in areas with high density forests and persistent clouds. Multiple techniques for reducing uncertainty due to cloud cover have been employed utilizing spatial and temporal interpolation during periods of cloud cover (Gao et al., 2010; Hall et al., 2010), whereas remote sensing of snow cover in areas with dense forest cover is lacking despite the combination of multiple remotely sensed and modeled products (land skin temperature and others in the MODIS snow detection algorithm). In areas with dense surface stations, interpolating snow depth and SWE may be one way to reduce this uncertainty. Though much of the research presented here focused on the utility of the snow persistence metric, additional insight may be gained by looking at how intermittent snow is throughout the winter season, that is, how many times a snowpack melts entirely before accumulating again. Information on snow

intermittence would provide insight into the spatial distribution and frequency of mid-winter soil moisture inputs.

To bridge the apparent disparity between the annual watershed scale importance of snow persistence for streamflow (Chapter 3) and the more muted correlation between snowmelt fraction and runoff generation (Chapter 4), sub-annual empirical analyses of hydrologic response to snowmelt and rainfall input at the catchment scale are needed. Assessing hydrologic response to snowmelt and rainfall input at the event time scale would help clarify how input type and input timing affect streamflow generation. Combined hydrometric and tracer studies assessing partitioning at plot and catchment scale as well as a synthesis of previous tracer and hydrometric work in various mountain study sites could also narrow this knowledge gap. Additionally, increased monitoring of streamflow and snow in watersheds near the transition between intermittent and seasonal snow would help improve our understanding of how snow loss may affect streamflow at multiple time scales. Finally, additional annual watershed scale analyses could analyze whether other variables of hydrologic response including peak flow timing, centroid timing etc. follow clear patterns with decreases in snow persistence in different climate types.

A major unknown in hydrologic response to snow loss is the impact that past and future changes to reservoir inflows yields on systems of water infrastructure. One of the next steps to connect and extend the research from this dissertation to meaningful information for water supply management is to analyze the empirical response of reservoir storage to the climatic change that has already occurred over the past several decades. Despite numerous studies documenting trends in reservoir inflows, there is a surprising lack of studies using empirical reservoir storage data to quantify the impacts on storage in response to changes in inflow timing

and magnitude. Are climatic signals from headwaters being overwritten by current dam management, or propagated downstream? How does the transmission of climatic signals from headwaters downstream manifest in systems with different storage capacities relative to annual flow and snowpack storage? How do these signals change when moving from headwater reservoirs down network to the mouth of major drainage basins? Connecting trends in snowpack storage to observed streamflow, reservoir inflows and reservoir storage is crucial to adapting water management systems to future non-stationary climatic variability.

Though the research presented here makes advances in understanding of the hydrologic response of snow loss along climatic gradients and at different measurement scales, a great deal remains uncertain regarding the present and future hydrology of mountain areas. With increased demand on water resources due to population growth, the factors controlling streamflow generation and their connection to climatic and land cover change warrant further study.

References

Abatzoglou, J. T. (2013). Development of gridded surface meteorological data for ecological applications and modelling. *International Journal of Climatology*, 33(1), 121–131.

Abatzoglou, J. T., & Williams, A. P. (2016). Impact of anthropogenic climate change on wildfire across western US forests. *Proceedings of the National Academy of Sciences*, *113*(42), 11770-11775.

Abatzoglou, J. T., Dobrowski, S. Z., Parks, S. A., & Hegewisch, K. C. (2018). TerraClimate, a high-resolution global dataset of monthly climate and climatic water balance from 1958–2015. *Scientific data*, *5*, 170191.

Adam JC, Hamlet AF, Lettenmaier DP (2009) Implications of global climate change for snowmelt hydrology in the twenty-first century. *Hydrol Process* 23(2009):962–972.

Andreadis, K. M., & Lettenmaier, D. P. (2006). Assimilating remotely sensed snow observations into a macroscale hydrology model. *Advances in water resources*, *29*(6), 872-886.

Anghileri, D., Voisin, N., Castelletti, A., Pianosi, F., Nijssen, B., & Lettenmaier, D. P. (2016). Value of long-term streamflow forecasts to reservoir operations for water supply in snow-dominated river catchments. *Water Resources Research*, *52*(6), 4209-4225.

Bales, R. C., Hopmans, J. W., O'Geen, A. T., Meadows, M., Hartsough, P. C., Kirchner, P., ... & Beaudette, D. (2011). Soil moisture response to snowmelt and rainfall in a Sierra Nevada mixed-conifer forest. *Vadose Zone Journal*, *10*(3), 786-799.

Bales, R. C., Molotch, N. P., Painter, T. H., Dettinger, M. D., Rice, R., & Dozier, J. (2006). Mountain hydrology of the western United States. *Water Resources Research*, *42*(8). doi:10.1029/2005WR004387.

Barnett, T. P., Adam, J. C., & Lettenmaier, D. P. (2005). Potential impacts of a warming climate on water availability in snow-dominated regions. Nature, 438(7066), 303-309.

Barnett, T., and D. Pierce, 2008: When will Lake Mead go dry? Water Resour. Res., 44, W03201.

Barnett, T. P., Pierce, D. W., Hidalgo, H. G., Bonfils, C., Santer, B. D., Das, T., Bala, G., Wood, A., Nozawa, T., Mirin, A.A., Cayan, D. R., Dettinger, M.D. (2008). Human-induced changes in the hydrology of the western United States. *Science*, *319* (5866), 1080-1083.

Barnhart, T. B., Molotch, N. P., Livneh, B., Harpold, A. A., Knowles, J. F., & Schneider, D. (2016). Snowmelt rate dictates streamflow. Geophysical Research Letters, 43(15), 8006-8016.

Barry, R., & Gan, T. Y. (2011). *The global cryosphere, past, present and future*. Cambridge University Press.

Bartos, M. D., & Chester, M. V. (2015). Impacts of climate change on electric power supply in the Western United States. *Nature Climate Change*, *5*(8), 748.

Bavera, D., Bavay, M., Jonas, T., Lehning, M., & De Michele, C. (2014). A comparison between two statistical and a physically-based model in snow water equivalent mapping. *Advances in Water Resources*, *63*, 167-178.

Bayard, D., Stähli, M., Parriaux, A., & Flühler, H. (2005). The influence of seasonally frozen soil on the snowmelt runoff at two Alpine sites in southern Switzerland. *Journal of Hydrology*, *309*(1-4), 66-84.

Bednorz, E. (2004). Snow cover in eastern Europe in relation to temperature, precipitation and circulation. *International Journal of Climatology*, *24*(5), 591-601.

Bender S., Miller P., Bernard B., and Lhotak J., (2014). Use of snow data from remote sensing in operational streamflow prediction. Proceedings of the Western Snow Conference, 2014, Durango, CO.

Beniston, M. (2012). Is snow in the Alps receding or disappearing? Wiley Interdisciplinary Reviews, Climate Change, 3(4), 349-358.

Beniston, M., & Stoffel, M. (2014). Assessing the impacts of climatic change on mountain water resources. *Science of the Total Environment*, *493*, 1129-1137.

Berghuijs, W., Woods, R., and Hrachowitz, M. (2014). A precipitation shift from snow towards rain leads to a decrease in streamflow, Nature Climate Change, 4, 583-586.

Biederman JA, Somor AJ, Harpold AA, Gutmann ED, Breshears DD, Troch PA, Brooks PD (2015) Recent tree die-off has little effect on streamflow in contrast to expected increases from historical studies. Water Resources Research, 51, 9775-9789.

Bony, S., G. Bellon, D. Klocke, S. Sherwood, S. Fermepin, and S. Denvil, 2013: Robust direct effect of carbon dioxide on tropical circulation and regional precipitation. Nature Geosci., doi:10.1038/ngeo1799.

Bosilovich, M. G., Chen, J., Robertson, F. R., & Adler, R. F. (2008). Evaluation of global precipitation in reanalyses. *Journal of applied meteorology and climatology*, *47*(9), 2279-2299.

Bronaugh, D., & Werner, A. (2013). zyp: Zhang+ Yue-Pilon trends package. *R package version*, 09-1.

Brown, R. D., & Mote, P. W. (2009). The response of Northern Hemisphere snow cover to a changing climate. *Journal of Climate*, *22*(8), 2124-2145.

Brown, R. D., & Robinson, D. A. (2011). Northern Hemisphere spring snow cover variability and change over 1922–2010 including an assessment of uncertainty. *The Cryosphere*, *5*(1), 219-229.

Bulygina, O. N., Razuvaev, V. N., & Korshunova, N. N. (2009). Changes in snow cover over Northern Eurasia in the last few decades. *Environmental Research Letters*, *4*(4), 045026.

Burles, K., & Boon, S. (2011). Snowmelt energy balance in a burned forest plot, Crowsnest Pass, Alberta, Canada. *Hydrological processes*, *25*(19), 3012-3029.

Choi, G., Robinson, D. A., & Kang, S. (2010). Changing northern hemisphere snow seasons. *Journal of Climate*, *23*(19), 5305-5310.

Chou, C., and J. D. Neelin, 2004: Mechanisms of global warming impacts on regional tropical precipitation. J. Clim., 17, 2688–2701.

Chou, C., J. D. Neelin, C. A. Chen, and J. Y. Tu, 2009: Evaluating the "Rich-Get-Richer'' mechanism in tropical precipitation change under global warming. J. Clim., 22, 1982–2005.

Christensen NS, Lettenmaier DP (2007). A multimodel ensemble approach to assessment of climate change impacts on the hydrology and water resources of the Colorado River Basin. *Hydrol Earth Syst Sci* 11:1417–1434.

Christensen, N. S., Wood, A. W., Voisin, N., Lettenmaier, D. P., & Palmer, R. N. (2004). The effects of climate change on the hydrology and water resources of the Colorado River basin. *Climatic change*, *62*(1-3), 337-363.

Clow DW (2010) Changes in the timing of snowmelt and streamflow in Colorado: A response to recent warming. *J Clim* 23(9):2293–2306.

Clow DW, Nanus L, Verdin KL, Schmidt J (2012) Evaluation of SNODAS snow depth and snow water equivalent estimates for the Colorado Rocky Mountains, USA. *Hydrol Process* 26(17):2583–2591.

Cohen, J. L., Furtado, J. C., Barlow, M. A., Alexeev, V. A., & Cherry, J. E. (2012). Arctic warming, increasing snow cover and widespread boreal winter cooling. *Environmental Research Letters*, *7*(1), 014007.

Collins, M., R. Knutti, J. Arblaster, J.-L. Dufresne, T. Fichefet, P. Friedlingstein, X. Gao, W.J. Gutowski, T. Johns, G. Krinner, M. Shongwe, C. Tebaldi, A.J. Weaver and M. Wehner, 2013: Long-term Climate Change: Projections, Com- mitments and Irreversibility. In: *Climate Change 2013: The Physical Science Basis. Contribution of Working Group I to*

the Fifth Assessment Report of the Intergovernmental Panel on Climate Change [Stocker, T.F., D. Qin, G.-K. Plattner, M. Tignor, S.K. Allen, J. Boschung, A. Nauels, Y. Xia, V. Bex and P.M. Midgley (eds.)]. Cambridge University Press, Cambridge, United Kingdom and New York, NY, USA.

Conner, L. G., Gill, R. A., & Belnap, J. (2016). Soil moisture response to experimentally altered snowmelt timing is mediated by soil, vegetation, and regional climate patterns. *Ecohydrology*, *9*(6), 1006-1016.

Cristea NC, Kampf SK, Burges SJ (2013) Revised Coefficients for Priestley-Taylor and Makkink-Hansen Equations for Estimating Daily Reference Evapotranspiration. *J Hydrol Eng* 18(10):1289–1300.

Dai, A. (2008), Temperature and pressure dependence of the rain-snow phase transition over land and ocean, Geophys. Res. Lett., 35, L12802, doi:10.1029/2008GL033295.

Daly, C (2013) Descriptions of PRISM spatial climate datasets for the conterminous United States. PRISM Doc., 14 pp.

Daly, S.F., R. Davis, E. Ochs, and T. Pangburn, 2000. An approach to spatially distributed snow modelling of the Sacramento and San Joaquin basins, California. Hydrological Processes, 14, 3257-3271, [doi:10.1002/1099-1085(20001230)14:18<3257::AID-HYP199>3.0.CO;2-Z].

De Lannoy, G. J., Reichle, R. H., Arsenault, K. R., Houser, P. R., Kumar, S., Verhoest, N. E., & Pauwels, V. (2012). Multiscale assimilation of Advanced Microwave Scanning Radiometer–EOS snow water equivalent and Moderate Resolution Imaging Spectroradiometer snow cover fraction observations in northern Colorado. *Water Resources Research*, *48*(1).

DeBeer, C. M., & Pomeroy, J. W. (2010). Simulation of the snowmelt runoff contributing area in a small alpine basin. *Hydrology and Earth System Sciences*, *14*(7), 1205.

Derksen, C., & Brown, R. (2012). Spring snow cover extent reductions in the 2008–2012 period exceeding climate model projections. *Geophysical Research Letters*, *39*(19).

Dettinger, M., Udall, B., & Georgakakos, A. (2015). Western water and climate change. *Ecological Applications*, *25*(8), 2069-2093.

Déry, S. J., & Brown, R. D. (2007). Recent Northern Hemisphere snow cover extent trends and implications for the snow-albedo feedback. *Geophysical Research Letters*, *34*(22).

Dierauer, J. R., Whitfield, P. H., & Allen, D. M. (2018). Climate Controls on Runoff and Low Flows in Mountain Catchments of Western North America. *Water Resources Research*.

DiMiceli, C.M., M.L. Carroll, R.A. Sohlberg, C. Huang, M.C. Hansen, and J.R.G. Townshend (2011), Annual Global Automated MODIS Vegetation Continuous Fields (MOD44B) at 250 m Spatial Resolution for Data Years Beginning Day 65, 2000 - 2010, Collection 5 Percent Tree Cover, University of Maryland, College Park, MD, USA.

Dore, M. H. (2005). Climate change and changes in global precipitation patterns: what do we know?. *Environment international*, *31*(8), 1167-1181.

Dozier J, Painter TH, Rittger K, Frew JE (2008) Advances in Water Resources Time – space continuity of daily maps of fractional snow cover and albedo from MODIS. *Adv Water Resour* 31(11):1515–1526.

Dressler, K. A., Leavesley, G. H., Bales, R. C., & Fassnacht, S. R. (2006). Evaluation of gridded snow water equivalent and satellite snow cover products for mountain basins in a hydrologic model. *Hydrological Processes: An International Journal*, *20*(4), 673-688.

Duethmann, D., Peters, J., Blume, T., Vorogushyn, S., & Güntner, A. (2014). The value of satellite-derived snow cover images for calibrating a hydrological model in snow-dominated catchments in Central Asia. Water Resources Research, 50(3), 2002-2021.

Dyer, J. L., & Mote, T. L. (2006). Spatial variability and trends in observed snow depth over North America. *Geophysical Research Letters*, *33*(16).

Edwards, A. C., Scalenghe, R., & Freppaz, M. (2007). Changes in the seasonal snow cover of alpine regions and its effect on soil processes, a review. Quaternary international, 162, 172-181.

Ehsani, N., Vörösmarty, C. J., Fekete, B. M., & Stakhiv, E. Z. (2017). Reservoir operations under climate change: storage capacity options to mitigate risk. *Journal of Hydrology*, *555*, 435-446.

Elsasser, H., & Messerli, P. (2001). The vulnerability of the snow industry in the Swiss Alps. *Mountain research and development*, *21*(4), 335-339.

Emori, S., and S. Brown, 2005: Dynamic and thermodynamic changes in mean and extreme precipitation under changed climate. Geophys. Res. Lett., 32, L17706.

Estilow, T. W., Young, A. H., & Robinson, D. A. (2015). A long-term Northern Hemisphere snow cover extent data record for climate studies and monitoring. Earth System Science Data, 7(1), 137-142.

Falcone, JA (2011) GAGES-II: geospatial attributes of gages for evaluating streamflow. Digit. Spat. Data set.

Fassnacht, S. R. (2004). Estimating Alter-shielded gauge snowfall undercatch, snowpack sublimation, and blowing snow transport at six sites in the coterminous USA. *Hydrological Processes*, *18*(18), 3481-3492.

Fassnacht, S. R. (2006). Upper versus lower Colorado River sub-basin streamflow: characteristics, runoff estimation and model simulation. *Hydrological processes*, *20*(10), 2187-2205.

Fassnacht, S. R., Dressler, K. A., & Bales, R. C. (2003). Snow water equivalent interpolation for the Colorado River Basin from snow telemetry (SNOTEL) data. *Water Resources Research*, *39*(8).

Fassnacht, S. R., Venable, N. B., McGrath, D., & Patterson, G. G. (2018). Sub-Seasonal Snowpack Trends in the Rocky Mountain National Park Area, Colorado, USA. *Water*, *10*(5), 562.

Fekete, B. M., Vörösmarty, C. J., Roads, J. O., & Willmott, C. J. (2004). Uncertainties in precipitation and their impacts on runoff estimates. *Journal of Climate*, *17*(2), 294-304.

Flint, A. L., Flint, L. E., & Dettinger, M. D. (2008). Modeling soil moisture processes and recharge under a melting snowpack. *Vadose Zone Journal*, *7*(1), 350-357.

Fogt, R. L., Bromwich, D. H., & Hines, K. M. (2011). Understanding the SAM influence on the South Pacific ENSO teleconnection. *Climate Dynamics*, *36*(7-8), 1555-1576.

Foster, J. L., Hall, D. K., Kelly, R. E. J., & Chiu, L. (2009). Seasonal snow extent and snow mass in South America using SMMR and SSM/I passive microwave data (1979–2006). *Remote Sensing of Environment*, *113*(2), 291-305.

Franz, K. J., Hogue, T. S., & Sorooshian, S. (2008). Operational snow modeling: Addressing the challenges of an energy balance model for National Weather Service forecasts. *Journal of Hydrology*, *360*(1), 48-66.

Fritze H, Stewart IT, Pebesma E (2011) Shifts in Western North American Snowmelt Runoff Regimes for the Recent Warm Decades. *J Hydrometeorol* 12(5):989–1006.

Froidurot, S., I. Zin, B. Hingray, and A. Gautheron (2014). Sensitivity of precipitation phase over the Swiss Alps to different meteorological variables, J. Hydrometeorol., 15(2), 685–696, doi:10.1175/JHM-D-13-073.1.

Fu, G., Charles, S. P., & Chiew, F. H. (2007). A two-parameter climate elasticity of streamflow index to assess climate change effects on annual streamflow. *Water Resources Research*, *43*(11).

Furey PR, Kampf SK, Lanini JS, Dozier AQ (2012). A Stochastic Conceptual Modeling Approach for Examining the Effects of Climate Change on Streamflows in Mountain Basins. *J Hydrometeorol* 13(Xu 1999):837–855.

Gao, Y., Xie, H., Yao, T., & Xue, C. (2010). Integrated assessment on multi-temporal and multi-sensor combinations for reducing cloud obscuration of MODIS snow cover products of the Pacific Northwest USA. *Remote Sensing of Environment*, *114*(8), 1662-1675.

Garreaud, R. D., Vuille, M., Compagnucci, R., & Marengo, J. (2009). Present-day south american climate. *Palaeogeography, Palaeoclimatology, Palaeoecology*, *281*(3-4), 180-195.

Ge, Y., & Gong, G. (2009). North American snow depth and climate teleconnection patterns. *Journal of Climate*, *22*(2), 217-233.

Gerten, D., Schaphoff, S., Haberlandt, U., Lucht, W., & Sitch, S. (2004). Terrestrial vegetation and water balance—hydrological evaluation of a dynamic global vegetation model. *Journal of Hydrology*, 286(1-4), 249-270.

Gleason, K. E., Nolin, A. W., & Roth, T. R. (2013). Charred forests increase snowmelt: Effects of burned woody debris and incoming solar radiation on snow ablation. *Geophysical Research Letters*, *40*(17), 4654-4661.

Godsey, S. E., Kirchner, J. W., & Tague, C. L. (2014). Effects of changes in winter snowpacks on summer low flows: case studies in the Sierra Nevada, California, USA. *Hydrological processes*, *28*(19), 5048-5064.

Gomez-Landesa, E., Rango, A., & Hall, D. K. (2001). Improved snow cover remote sensing for snowmelt runoff forecasting. IAHS PUBLICATION, 61-65.

Gómez-Plaza, A., Martınez-Mena, M., Albaladejo, J., & Castillo, V. M. (2001). Factors regulating spatial distribution of soil water content in small semiarid catchments. *Journal of Hydrology*, *253*(1-4), 211-226.

Goulden ML, et al. (2012). Evapotranspiration along an elevation gradient in California's Sierra Nevada. *J Geophys Res Biogeosciences* 117(3). doi:10.1029/2012JG002027.

Greve, P., Orlowsky, B., Mueller, B., Sheffield, J., Reichstein, M., & Seneviratne, S. I. (2014). Global assessment of trends in wetting and drying over land. *Nature geoscience*, *7*(10), 716.

Grill, G., Lehner, B., Lumsdon, A. E., MacDonald, G. K., Zarfl, C., & Liermann, C. R. (2015). An index-based framework for assessing patterns and trends in river fragmentation and flow regulation by global dams at multiple scales. *Environmental Research Letters*, *10*(1), 015001.

Grömping, U. (2006). Relative importance for linear regression in R: the package relaimpo. Journal of statistical software, 17(1), 1-27.

Groemping, U., Matthias, L. (2013) Relative importance of regressors in linear models, R package version 2.2, 10.1139/gen-2016-0039.

Guan B, et al. (2013). Snow water equivalent in the Sierra Nevada: Blending snow sensor observations with snowmelt model simulations. *Water Resour Res* 49(8):5029–5046.

Hall, DK, & Riggs, GA (2007). Accuracy assessment of the MODIS snow products. *Hydrological Processes*, *21*(12), 1534-1547.

Hall, D. K., Riggs, G. A., Foster, J. L., & Kumar, S. V. (2010). Development and evaluation of a cloud-gap-filled MODIS daily snow-cover product. *Remote sensing of environment*, *114*(3), 496-503.

Hall, D. K. and G. A. Riggs. 2016. *MODIS/Terra Snow Cover 8-Day L3 Global 500m Grid, Version 6*. [2000-01-01:2016-12-31]. Boulder, Colorado USA. NASA National Snow and Ice Data Center Distributed Active Archive Center. doi: https://doi.org/10.5067/MODIS/MOD10A2.006. [12/08/2016].

Hammond, J. C., F. A. Saavedra, S. K. Kampf (2017a). MODIS MOD10A2 derived snow persistence and no data index for the western U.S., HydroShare, http://dx.doi.org/10.4211/hs.1c62269aa802467688d25540caf2467e

Hammond, J. C., F. A. Saavedra, S. K. Kampf (2017b). MODIS MOD10A2 derived snow season for the western U.S., HydroShare, http://www.hydroshare.org/resource/197adcdc76b34591bd78a811bf1df

Hammond, J. C., Saavedra, F. A., & Kampf, S. K. (2018a). How does snow persistence relate to annual streamflow in mountain watersheds of the Western U.S. with wet maritime and dry continental climates? *Water Resources Research*, 54. https://doi.org/10.1002/2017WR021899

Hammond, J. C., Saavedra, F. A., & Kampf, S. K. (2018b). Global snow zone maps and trends in snow persistence 2001–2016. International Journal of Climatology, https://doi.org/10.1002/joc.5674.

Hansen, J., R. Ruedy, M. Sato, and K. Lo, 2010, Global surface temperature change, Rev. Geophys., 48, RG4004, doi,10.1029/2010RG000345.

Hantel, M., Ehrendorfer, M., & Haslinger, A. (2000). Climate sensitivity of snow cover duration in Austria. *International Journal of Climatology*, *20*(6), 615-640.

Harpold AA, Molotch NP (2015) Sensitivity of soil water availability to changing snowmelt timing in the western US. *Geophysical Research Letters*, 42**,** 8011-8020.

Harpold, A. A. (2016). Diverging sensitivity of soil water stress to changing snowmelt timing in the western US. *Advances in Water Resources*, *92*, 116-129.

Harpold, A. A., Biederman, J. A., Condon, K., Merino, M., Korgaonkar, Y., Nan, T., Sloat, L.L., Ross, M., Brooks, P. D. (2014). Changes in snow accumulation and ablation following the Las Conchas Forest Fire, New Mexico, USA. *Ecohydrology*, *7*(2), 440-452.

Harpold, A. A., Molotch, N. P., Musselman, K. N., Bales, R. C., Kirchner, P. B., Litvak, M., & Brooks, P. D. (2015). Soil moisture response to snowmelt timing in mixed-conifer subalpine forests. *Hydrological Processes*, *29*(12), 2782-2798.

Harpold, A., Brooks, P., Rajagopal, S., Heidbuchel, I., Jardine, A., & Stielstra, C. (2012). Changes in snowpack accumulation and ablation in the intermountain west. *Water Resources Research*, *48*(11).

Harpold, A., Dettinger, M., & Rajagopal, S. (2017). Defining snow drought and why it matters. EOS-Earth & Space Science News, 98.

Hatcher, K. L., & Jones, J. A. (2013). Climate and streamflow trends in the Columbia River basin: Evidence for ecological and engineering resilience to climate change. *Atmosphere-Ocean*, *51*(4), 436-455.

Hedrick A, et al. (2015) Independent evaluation of the SNODAS snow depth product using regional-scale lidar-derived measurements. *Cryosphere* 9(1):13–23.

Held, I., and B. Soden, 2006: Robust responses of the hydrological cycle to global warming. J. Clim., 19, 5686–5699.

Hirashima, H., Kodama, Y., Sato, N., Ohata, T., Yabuki, H., & Georgiadi, A. (2004). Nonuniform distribution of tundra snow cover in Eastern Siberia. *Journal of Hydrometeorology*, *5*(3), 373-389.

Hood, E., M. Williams, and D. Cline (1999), Sublimation from a seasonal snowpack at a continental mid-latitude alpine site, Hydrol. Processes, 13, 1781–1797.

Hori, M., Sugiura, K., Kobayashi, K., Aoki, T., Tanikawa, T., Kuchiki, K., ... & Enomoto, H. (2017). A 38-year (1978–2015) Northern Hemisphere daily snow cover extent product derived using consistent objective criteria from satellite-borne optical sensors. *Remote Sensing of Environment*, *191*, 402-418.

Howitt, R., Medellín-Azuara, J., MacEwan, D., Lund, J., & Sumner, D. (2015). Economic analysis of the 2015 drought for California agriculture. UC Davis Center for Watershed Sciences.

Hunsaker, C. T., Whitaker, T. W., & Bales, R. C. (2012). Snowmelt runoff and water yield along elevation and temperature gradients in California's southern Sierra Nevada. *JAWRA Journal of the American Water Resources Association*, *48*(4), 667-678.

Huntington, T. G., Hodgkins, G. A., Keim, B. D., & Dudley, R. W. (2004). Changes in the proportion of precipitation occurring as snow in New England (1949–2000). *Journal of Climate*, *17*(13), 2626-2636.

Huntington, J. L., & Niswonger, R. G. (2012). Role of surface-water and groundwater interactions on projected summertime streamflow in snow dominated regions: An integrated modeling approach. *Water Resources Research*, *48*(11).

Huss, M., Bookhagen, B., Huggel, C., Jacobsen, D., Bradley, R. S., Clague, J. J., ... & Mark, B. G. (2017). Toward mountains without permanent snow and ice. *Earth's Future*, *5*(5), 418-435.

Hwang, T., Band, L. E., Vose, J. M., & Tague, C. (2012). Ecosystem processes at the watershed scale: Hydrologic vegetation gradient as an indicator for lateral hydrologic connectivity of headwater catchments. *Water Resources Research*, *48*(6).

Immerzeel, W. W., Droogers, P., De Jong, S. M., & Bierkens, M. F. P. (2009). Large-scale monitoring of snow cover and runoff simulation in Himalayan river basins using remote sensing. Remote sensing of Environment, 113(1), 40-49.

Jackson, S. I., and T. D. Prowse (2009), Spatial variation of snowmelt and sublimation in a high-elevation semi-desert basin of western Canada, Hydrol. Processes, 28(13), 2611–2627, doi:10.1002/hyp.7320.

Jaeger, W. K., Amos, A., Bigelow, D. P., Chang, H., Conklin, D. R., Haggerty, R., ... & Plantinga, A. J. (2017). Finding water scarcity amid abundance using human–natural system models. *Proceedings of the National Academy of Sciences*, 201706847.

Jain, S. K., Goswami, A., & Saraf, A. K. (2010). Assessment of snowmelt runoff using remote sensing and effect of climate change on runoff. *Water resources management*, *24*(9), 1763-1777.

Jaynes, D. B., Ahmed, S. I., Kung, K. J., & Kanwar, R. S. (2001). Temporal dynamics of preferential flow to a subsurface drain. *Soil Science Society of America Journal*, *65*(5), 1368-1376.

Jefferson AJ (2011) Seasonal versus transient snow and the elevation dependence of climate sensitivity in maritime mountainous regions. *Geophys Res Lett* 38(16). doi:10.1029/2011GL048346.

Jensen, J. L., Humes, K. S., Hudak, A. T., Vierling, L. A., & Delmelle, E. (2011). Evaluation of the MODIS LAI product using independent lidar-derived LAI: A case study in mixed conifer forest. *Remote Sensing of Environment*, *115*(12), 3625-3639.

Jepsen, S. M., Harmon, T. C., Meadows, M. W., & Hunsaker, C. T. (2016). Hydrogeologic influence on changes in snowmelt runoff with climate warming: Numerical experiments

on a mid-elevation catchment in the Sierra Nevada, USA. *Journal of Hydrology*, *533*, 332-342.

Jones, J. A. (2011). Hydrologic responses to climate change, considering geographic context and alternative hypotheses. *Hydrological Processes*, *25*(12), 1996-2000.

Jones, J. A., Creed, I. F., Hatcher, K. L., Warren, R. J., Adams, M. B., Benson, M. H., & Clow, D. W. (2012). Ecosystem processes and human influences regulate streamflow response to climate change at long-term ecological research sites. *BioScience*, *62*(4), 390-404.

Jörg-Hess S, Fundel F, Jonas T, Zappa M (2013). A statistical approach to refining snow water equivalent climatologies in Alpine terrain. *Cryo. Disc.*, 7.

Kahl, A., Winstral, A., Marks, D., & Dozier, J. (2014). Using satellite imagery and the distributed Isnobal energy balance model to derive SWE heterogeneity in mountainous basins. *Putting Prediction in Ungauged Basins into Practice. Ottawa: Canadian Water Resources Association*, 243-253.

Kampf, S. K., & Lefsky, M. A. (2016). Transition of dominant peak flow source from snowmelt to rainfall along the Colorado Front Range, Historical patterns, trends, and lessons from the 2013 Colorado Front Range floods. *Water Resources Research*.

Kampf, S., Markus, J., Heath, J., & Moore, C. (2015). Snowmelt runoff and soil moisture dynamics on steep subalpine hillslopes. *Hydrological Processes*, *29*(5), 712-723.

Kapnick, S., & Hall, A. (2012). Causes of recent changes in western North American snowpack. *Climate Dynamics*, *38*(9), 1885-1899.

Khaled, H. H., and Ramachandra, A. R.: A modified Mann-Kendall trend test for autocorrelated data, Journal of Hydrology, 204, 182–196, 10.1016/S0022-1694(97)00125-X, 1998.

Kidd, C., Bauer, P., Turk, J., Huffman, G. J., Joyce, R., Hsu, K. L., & Braithwaite, D. (2012). Intercomparison of high-resolution precipitation products over northwest Europe. *Journal of Hydrometeorology*, *13*(1), 67-83.

Kim, J., Miller, N. L., Farrara, J. D., & Hong, S. Y. (2000). A seasonal precipitation and stream flow hindcast and prediction study in the western United States during the 1997/98 winter season using a dynamic downscaling system. *Journal of Hydrometeorology*, *1*(4), 311-329.

Kim, Y., Kimball, J. S., Robinson, D. A., & Derksen, C. (2015). New satellite climate data records indicate strong coupling between recent frozen season changes and snow cover over high northern latitudes. Environmental Research Letters, 10(8), 084004.

Kiparsky, M., Joyce, B., Purkey, D., & Young, C. (2014). Potential impacts of climate warming on water supply reliability in the Tuolumne and Merced river basins, California. *PloS one*, *9*(1), e84946.

Klos PZ, Link TE, Abatzoglou JT (2014) Extent of the rain-snow transition zone in the western U.S. under historic and projected climate. *Geophys Res Lett* 41(13):4560–4568.

Knowles, N., Dettinger, M. D., & Cayan, D. R. (2006). Trends in snowfall versus rainfall in the western United States. *Journal of Climate*, *19*(18), 4545-4559.

Kolberg, S., Rue, H., & Gottschalk, L. (2006). A Bayesian spatial assimilation scheme for snow coverage observations in a gridded snow model. *Hydrology and Earth System Sciences Discussions*, *10*(3), 369-381.

Kormos, P. R., Luce, C. H., Wenger, S. J., & Berghuijs, W. R. (2016). Trends and sensitivities of low streamflow extremes to discharge timing and magnitude in Pacific Northwest mountain streams. *Water Resources Research*, *52*(7), 4990-5007.

Koster, R. D., Mahanama, S. P., Livneh, B., Lettenmaier, D. P., & Reichle, R. H. (2010). Skill in streamflow forecasts derived from large-scale estimates of soil moisture and snow. Nature Geoscience, 3(9), 613-616.

Kottek M, Grieser J, Beck C, Rudolf B, Rubel F (2006) World map of the Köppen-Geiger climate classification updated. *Meteorol Zeitschrift* 15(3):259–263.

Krajčí, P., Holko, L., Perdigão, R. A., & Parajka, J. (2014). Estimation of regional snowline elevation (RSLE) from MODIS images for seasonally snow covered mountain basins. Journal of Hydrology, 519, 1769-1778.

Kulkarni, A. V., Rathore, B. P., & Singh, S. K. (2010). Distribution of seasonal snow cover in central and western Himalaya. Annals of Glaciology, 51(54), 123-128.

Kundzewicz, Z. W., Mata, L. J., Arnell, N. W., Döll, P., Jimenez, B., Miller, K., ... & Shiklomanov, I. (2008). The implications of projected climate change for freshwater resources and their management.

Kunkel, K. E., Robinson, D. A., Champion, S., Yin, X., Estilow, T., & Frankson, R. M. (2016). Trends and Extremes in Northern Hemisphere Snow Characteristics. Current Climate Change Reports, 2(2), 65-73.

Langston, A. L., Tucker, G. E., Anderson, R. S., & Anderson, S. P. (2015). Evidence for climatic and hillslope-aspect controls on vadose zone hydrology and implications for saprolite weathering. *Earth Surface Processes and Landforms*, *40*(9), 1254-1269.

Lee, S., Klein, A. G., & Over, T. M. (2005). A comparison of MODIS and NOHRSC snow-cover products for simulating streamflow using the Snowmelt Runoff Model. Hydrological Processes, 19(15), 2951-2972.

Levy, M. C., Cohn, A., Lopes, A. V., & Thompson, S. E. (2017). Addressing rainfall data selection uncertainty using connections between rainfall and streamflow. *Scientific reports*, *7*(1), 219.

Li, D., Wrzesien, M. L., Durand, M., Adam, J., & Lettenmaier, D. P. (2017). How much runoff originates as snow in the western United States, and how will that change in the future?. *Geophysical Research Letters*.

Li, X., Fu, W., Shen, H., Huang, C., & Zhang, L. (2017). Monitoring snow cover variability (2000–2014) in the Hengduan Mountains based on cloud-removed MODIS products with an adaptive spatio-temporal weighted method. *Journal of Hydrology*.

Liang, W., Bai, D., Wang, F., Fu, B., Yan, J., Wang, S., ... & Feng, M. (2015). Quantifying the impacts of climate change and ecological restoration on streamflow changes based on a Budyko hydrological model in China's Loess Plateau. *Water Resources Research*, *51*(8), 6500-6519.

Lins, H. F., & Slack, J. R. (2005). Seasonal and regional characteristics of US streamflow trends in the United States from 1940 to 1999. *Physical Geography*, *26*(6), 489-501.

Litaor, M. I., Williams, M., & Seastedt, T. R. (2008). Topographic controls on snow distribution, soil moisture, and species diversity of herbaceous alpine vegetation, Niwot Ridge, Colorado. *Journal of Geophysical Research: Biogeosciences*, *113*(G2).

Liu, F., Parmenter, R., Brooks, P. D., Conklin, M. H., & Bales, R. C. (2008). Seasonal and interannual variation of streamflow pathways and biogeochemical implications in semi-arid, forested catchments in Valles Caldera, New Mexico. *Ecohydrology: Ecosystems, Land and Water Process Interactions, Ecohydrogeomorphology*, *1*(3), 239-252.

Liu, Y., Peters-Lidard, C. D., Kumar, S. V., Arsenault, K. R., & Mocko, D. M. (2015). Blending satellite-based snow depth products with in situ observations for streamflow predictions in the Upper Colorado River Basin. *Water resources research*, *51*(2), 1182-1202.

Livneh B, et al. (2013) A long-term hydrologically based dataset of land surface fluxes and states for the conterminous United States: Update and extensions. *J Clim* 26(23):9384–9392.

López-Moreno, J. I., & Vicente-Serrano, S. M. (2007). Atmospheric circulation influence on the interannual variability of snow pack in the Spanish Pyrenees during the second half of the 20th century. *Hydrology Research*, *38*(1), 33-44.

López-Moreno, J. I., Vicente-Serrano, S. M., Morán-Tejeda, E., Lorenzo-Lacruz, J., Kenawy, A., & Beniston, M. (2011). Effects of the North Atlantic Oscillation (NAO) on combined

temperature and precipitation winter modes in the Mediterranean mountains: observed relationships and projections for the 21st century. *Global and Planetary Change*, *77*(1-2), 62-76.

Luce, C. H., Lopez-Burgos, V., & Holden, Z. (2014). Sensitivity of snowpack storage to precipitation and temperature using spatial and temporal analog models. *Water Resources Research*, *50*(12), 9447-9462.

Lv, L. (2014). Linking montane soil moisture measurements to evapotranspiration using inverse numerical modeling. Utah State University.

Ma, L. J., & Qin, D. H. (2012). Spatial-Temporal Characteristics of Observed Key Parameters for Snow Cover in China during 1957--2009. *Journal of Glaciology and Geocryology*, *34*(1), 1-11.

Mahanama, S., Livneh, B., Koster, R., Lettenmaier, D., & Reichle, R. (2012). Soil moisture, snow, and seasonal streamflow forecasts in the United States. *Journal of Hydrometeorology*, *13*(1), 189-203.

Mankin, J. S., & Diffenbaugh, N. S. (2015). Influence of temperature and precipitation variability on near-term snow trends. *Climate Dynamics*, *45*(3-4), 1099.

Mankin, J. S., Viviroli, D., Singh, D., Hoekstra, A. Y., & Diffenbaugh, N. S. (2015). The potential for snow to supply human water demand in the present and future. *Environmental research letters*, *10*(11), 114016.

Marchane, A., Jarlan, L., Hanich, L., Boudhar, A., Gascoin, S., Tavernier, A., ... & Berjamy, B. (2015). Assessment of daily MODIS snow cover products to monitor snow cover dynamics over the Moroccan Atlas mountain range. Remote Sensing of Environment, 160, 72-86.

Markovich, K. H., Maxwell, R. M., & Fogg, G. E. (2016). Hydrogeological response to climate change in alpine hillslopes. *Hydrological Processes*, *30*(18), 3126-3138.

Marks, D., Winstral, A., Reba, M., Pomeroy, J., & Kumar, M. (2013). An evaluation of methods for determining during-storm precipitation phase and the rain/snow transition elevation at the surface in a mountain basin. *Advances in Water Resources*, *55*, 98-110.

Marty, C., & Meister, R. (2012). Long-term snow and weather observations at Weissfluhjoch and its relation to other high-altitude observatories in the Alps. *Theoretical and Applied Climatology*, *110*(4), 573-583.

Masiokas, M. H., Villalba, R., Christie, D. A., Betman, E., Luckman, B. H., Le Quesne, C., ... & Mauget, S. (2012). Snowpack variations since AD 1150 in the Andes of Chile and Argentina (30°–37° S) inferred from rainfall, tree-ring and documentary records. *Journal of Geophysical Research, Atmospheres*, *117*(D5).

Masiokas, M. H., Villalba, R., Luckman, B. H., & Mauget, S. (2010). Intra-to multidecadal variations of snowpack and streamflow records in the Andes of Chile and Argentina between 30 and 37 S. *Journal of Hydrometeorology*, *11*(3), 822-831.

Maurer, G. E., & Bowling, D. R. (2014). Seasonal snowpack characteristics influence soil temperature and water content at multiple scales in interior western US mountain ecosystems. *Water Resources Research*, *50*(6), 5216-5234.

McCabe, G., and D. Wolock, 2007: Warming may create substantial water supply shortages in the Colorado River basin. Geophys. Res. Lett., 34, L22708.

McColl, K. A., Alemohammad, S. H., Akbar, R., Konings, A. G., Yueh, S., & Entekhabi, D. (2017). The global distribution and dynamics of surface soil moisture. *Nature Geoscience*, *10*(2), 100-104.

McDonnell, J. J., Sivapalan, M., Vaché, K., Dunn, S., Grant, G., Haggerty, R., ... & Selker, J. (2007). Moving beyond heterogeneity and process complexity: A new vision for watershed hydrology. *Water Resources Research*, *43*(7).

McLeod, A. I.: Kendall-package: Kendall correlation and trend tests: http://www.stats.uwo.ca/faculty/aim, 2011.

McNamara, J. P., Chandler, D., Seyfried, M., & Achet, S. (2005). Soil moisture states, lateral flow, and streamflow generation in a semi-arid, snowmelt-driven catchment. *Hydrological Processes: An International Journal*, *19*(20), 4023-4038.

Meixner, T., Manning, A. H., Stonestrom, D. A., Allen, D. M., Ajami, H., Blasch, K. W., ... & Flint, A. L. (2016). Implications of projected climate change for groundwater recharge in the western United States. *Journal of Hydrology*, *534*, 124-138.

Meromy, L., Molotch, N. P., Link, T. E., Fassnacht, S. R., & Rice, R. (2013). Subgrid variability of snow water equivalent at operational snow stations in the western USA. *Hydrological Processes*, *27*(17), 2383-2400.

Middelkoop, H., Daamen, K., Gellens, D., Grabs, W., Kwadijk, J. C., Lang, H., ... & Wilke, K. (2001). Impact of climate change on hydrological regimes and water resources management in the Rhine basin. *Climatic change*, *49*(1-2), 105-128.

Milly, P. C. D., Betancourt, J., Falkenmark, M., Hirsch, R. M., Kundzewicz, Z. W., Lettenmaier, D. P., & Stouffer, R. J. (2008). Stationarity is dead: Whither water management?. *Science*, *319*(5863), 573-574.

Moen, J., & Fredman, P. (2007). Effects of climate change on alpine skiing in Sweden. *Journal of sustainable tourism*, *15*(4), 418-437.

Molotch, N. P., & Bales, R. C. (2005). Scaling snow observations from the point to the grid element: Implications for observation network design. *Water Resources Research*, *41*(11).

Molotch, N. P., & Bales, R. C. (2006). SNOTEL representativeness in the Rio Grande headwaters on the basis of physiographics and remotely sensed snow cover persistence. *Hydrological Processes*, *20*(4), 723-739.

Molotch, N. P., Brooks, P. D., Burns, S. P., Litvak, M., Monson, R. K., McConnell, J. R., & Musselman, K. (2009). Ecohydrological controls on snowmelt partitioning in mixed-conifer sub-alpine forests. *Ecohydrology: Ecosystems, Land and Water Process Interactions, Ecohydrogeomorphology*, *2*(2), 129-142.

Moore, C., Kampf, S., Stone, B., & Richer, E. (2014). A GIS-based method for defining snow zones: application to the western United States. *Geocarto International*, *30*(1), 62-81.

Morán-Tejeda, E., López-Moreno, J. I., & Beniston, M. (2013). The changing roles of temperature and precipitation on snowpack variability in Switzerland as a function of altitude. *Geophysical Research Letters*, *40*(10), 2131-2136.

Moritz, M. A., Parisien, M. A., Batllori, E., Krawchuk, M. A., Van Dorn, J., Ganz, D. J., & Hayhoe, K. (2012). Climate change and disruptions to global fire activity. *Ecosphere*, *3*(6), 1-22.

Mote, P. W. (2003). Trends in snow water equivalent in the Pacific Northwest and their climatic causes. *Geophysical Research Letters*, *30*(12).

Mote, P. W., Hamlet, A. F., Clark, M. P., & Lettenmaier, D. P. (2005). Declining mountain snowpack in western North America. Bulletin of the American meteorological Society, 86(1), 39-49.

Musselman, K. N., Clark, M. P., Liu, C., Ikeda, K., & Rasmussen, R. (2017). Slower snowmelt in a warmer world. Nature Climate Change, 7(3), 214-219.

NASA LP DAAC, 2015, ASTER Level 1 Precision Terrain Corrected Registered At-Sensor Radiance. Version 3. NASA EOSDIS Land Processes DAAC, USGS Earth Resources Observation and Science (EROS) Center, Sioux Falls, South Dakota (https://lpdaac.usgs.gov), accessed January 1, 2016, at http://dx.doi.org/10.5067/ASTER/AST_L1T.003.

National Operational Hydrologic Remote Sensing Center (2004) Snow Data Assimilation System (SNODAS) Data Products at NSIDC, [10/01/2003-09/30/2015]. Boulder, Colorado USA: National Snow and Ice Data Center.

National Water and Climate Center [NWCC] (2016) Report Generator 2.0, [10/01/2003-09/30/2015]. Portland, Oregon, USA.

Nayak, A., Marks, D., Chandler, D. G., & Seyfried, M. (2010). Long-term snow, climate, and streamflow trends at the Reynolds Creek experimental watershed, Owyhee Mountains, Idaho, United States. *Water Resources Research*, *46*(6).

Naz, B. S., Kao, S. C., Ashfaq, M., Rastogi, D., Mei, R., & Bowling, L. C. (2016). Regional hydrologic response to climate change in the conterminous United States using high-resolution hydroclimate simulations. *Global and Planetary Change*, *143*, 100-117.

Niu, G. Y., & Yang, Z. L. (2006). Effects of frozen soil on snowmelt runoff and soil water storage at a continental scale. *Journal of Hydrometeorology*, *7*(5), 937-952.

Nolin, A. W. (2010). Recent advances in remote sensing of seasonal snow. Journal of Glaciology, 56(200), 1141-1150.

Nolin, A. W., & Daly, C. (2006). Mapping "at risk" snow in the Pacific Northwest. *Journal of Hydrometeorology*, *7*(5), 1164-1171.

Oyler JW, Ballantyne A, Jencso K, Running SW (2014) Creating a topoclimatic daily air temperature dataset for the conterminous United States using homogenized station data and remotely sensed land skin temperature. Inter. J. Clim., 35, 2258-2279.

Painter, T. H., Berisford, D. F., Boardman, J. W., Bormann, K. J., Deems, J. S., Gehrke, F., ... & Mattmann, C. (2016). The Airborne Snow Observatory: Fusion of scanning lidar, imaging spectrometer, and physically-based modeling for mapping snow water equivalent and snow albedo. *Remote Sensing of Environment*, *184*, 139-152.

Painter, T. H., Brodzik, M. J., Racoviteanu, A., & Armstrong, R. (2012). Automated mapping of Earth's annual minimum exposed snow and ice with MODIS. *Geophysical Research Letters*, *39*(20).

Painter, T. H., Deems, J. S., Belnap, J., Hamlet, A. F., Landry, C. C., & Udall, B. (2010). Response of Colorado River runoff to dust radiative forcing in snow. *Proceedings of the National Academy of Sciences*, *107*(40), 17125-17130.

Pugh, E., & Small, E. (2012). The impact of pine beetle infestation on snow accumulation and melt in the headwaters of the Colorado River. *Ecohydrology*, *5*(4), 467-477.

Raleigh, M. S., Rittger, K., Moore, C. E., Henn, B., Lutz, J. A., & Lundquist, J. D. (2013). Ground-based testing of MODIS fractional snow cover in subalpine meadows and forests of the Sierra Nevada. Remote Sensing of Environment, 128, 44-57.

Regonda SK, Rajagopalan B, Clark M, Pitlick J (2005) Seasonal cycle shifts in hydroclimatology over the western United States. *Journal of Climate* 18(2):372–384.

Restrepo, P., Rakovec, O., Noh, S. J., He, M., Clark, M., Hendricks Franssen, H. J., & Van Dijk, A. I. J. M. (2012). Advancing data assimilation in operational hydrologic forecasting:

progresses, challenges, and emerging opportunities. Hydrology and Earth System Sciences, 16 (10), 2012.

Rice, R., & Bales, R. C. (2010). Embedded-sensor network design for snow cover measurements around snow pillow and snow course sites in the Sierra Nevada of California. *Water resources research*, *46*(3).

Richer, E. E., Kampf, S. K., Fassnacht, S. R., & Moore, C. C. (2013). Spatiotemporal index for analyzing controls on snow climatology: application in the Colorado Front Range. *Physical Geography*, *34*(2), 85-107.

Rittger, K., Painter, T. H., & Dozier, J. (2013). Assessment of methods for mapping snow cover from MODIS. *Advances in Water Resources*, 51, 367-380.

Robinson, David A., Estilow, Thomas W., and NOAA CDR Program (2012),NOAA Climate Date Record (CDR) of Northern Hemisphere (NH) Snow Cover Extent (SCE), Version 1.

Rodell, M., & Houser, P. R. (2004). Updating a land surface model with MODIS-derived snow cover. *Journal of Hydrometeorology*, *5*(6), 1064-1075.

Roy, A., Royer, A., & Turcotte, R. (2010). Improvement of springtime streamflow simulations in a boreal environment by incorporating snow-covered area derived from remote sensing data. *Journal of hydrology*, *390*(1), 35-44.

Rupp, D. E., Mote, P. W., Bindoff, N. L., Stott, P. A., & Robinson, D. A. (2013). Detection and attribution of observed changes in Northern Hemisphere spring snow cover. *Journal of Climate*, *26*(18), 6904-6914.

Saavedra, F. A., Kampf, S. K., Fassnacht, S. R., & Sibold, J. S. (2017). A snow climatology of the Andes Mountains from MODIS snow cover data. *International Journal of Climatology*, 37(3), 1526-1539.

Saavedra, F.A., Kampf, S.K., Fassnacht, S.R., Sibold, J.S. (2018). Changes in Andes Mountains snow cover from MODIS data 2000-2016. *The Cryosphere*.

Schaap, M. G., Leij, F. J., & Van Genuchten, M. T. (2001). Rosetta: A computer program for estimating soil hydraulic parameters with hierarchical pedotransfer functions. *Journal of Hydrology*, *251*(3-4), 163-176.

Schamm, K., Ziese, M., Becker, A., Finger, P., Meyer-Christoffer, A., Schneider, U., ... & Stender, P. (2014). Global gridded precipitation over land: a description of the new GPCC First Guess Daily product. *Earth System Science Data*, *6*(1), 49-60.

Scott, R. L., Shuttleworth, W. J., Keefer, T. O., & Warrick, A. W. (2000). Modeling multiyear observations of soil moisture recharge in the semiarid American Southwest. *Water Resources Research*, *36*(8), 2233-2247.

Seager, R., Kushnir, Y., Nakamura, J., Ting, M., & Naik, N. (2010). Northern Hemisphere winter snow anomalies: ENSO, NAO and the winter of 2009/10. *Geophysical research letters*, *37*(14).

Seager, R., N. Naik, and G. A. Vecchi, 2010: Thermodynamic and dynamic mechanisms for large-scale changes in the hydrological cycle in response to global warming. J. Clim., 23, 4651–4668.

Sen, P. K.: Estimates of the Regression Coefficient Based on Kendall's Tau, Journal of the American Statistical Association, 63, 1379-1389, 10.1080/01621459.1968.10480934, 1968.

Serreze, M. C., Clark, M. P., Armstrong, R. L., McGinnis, D. A., & Pulwarty, R. S. (1999). Characteristics of the western United States snowpack from snowpack telemetry (SNOTEL) data. *Water Resources Research*, *35*(7), 2145-2160.

Seyfried, M. S., Grant, L. E., Marks, D., Winstral, A., & McNamara, J. (2009). Simulated soil water storage effects on streamflow generation in a mountainous snowmelt environment, Idaho, USA. *Hydrological Processes: An International Journal*, *23*(6), 858-873.

Seyfried, M. S., Schwinning, S., Walvoord, M. A., Pockman, W. T., Newman, B. D., Jackson, R. B., & Phillips, F. M. (2005). Ecohydrological control of deep drainage in arid and semiarid regions. *Ecology*, *86*(2), 277-287.

Shaman, J., & Tziperman, E. (2005). The effect of ENSO on Tibetan Plateau snow depth: A stationary wave teleconnection mechanism and implications for the South Asian monsoons. *Journal of Climate*, *18*(12), 2067-2079.

Šimůnek, J., M. Šejna, and M. Th. van Genuchten. 1998. The HYDRUS-1D software package for simulating the one-dimensional movement of water, heat, and multiple solutes in variably saturated media. Version 1.0. IGWMC-TPS-70. Golden, Colo.: Colorado School of Mines, International Ground Water Modeling Center.

Sivapalan, M. (2003). Prediction in ungauged basins: a grand challenge for theoretical hydrology. *Hydrological Processes*, *17*(15), 3163-3170.

Sivapalan, M. (2005). Pattern, process and function: elements of a unified theory of hydrology at the catchment scale. *Encyclopedia of hydrological sciences*.

Sivapalan, M., Blöschl, G., Zhang, L., & Vertessy, R. (2003). Downward approach to hydrological prediction. *Hydrological processes*, *17*(11), 2101-2111.

Skaugen, T., Stranden, H. B., & Saloranta, T. (2012). Trends in snow water equivalent in Norway (1931–2009). *Hydrology Research*, *43*(4), 489-499.

Smith, T. J., McNamara, J. P., Flores, A. N., Gribb, M. M., Aishlin, P. S., & Benner, S. G. (2011). Small soil storage capacity limits benefit of winter snowpack to upland vegetation. *Hydrological Processes*, *25*(25), 3858-3865.

Soundharajan, B. S., Adeloye, A. J., & Remesan, R. (2016). Evaluating the variability in surface water reservoir planning characteristics during climate change impacts assessment. *Journal of Hydrology*, *538*, 625-639.

Spence, C., & Mengistu, S. (2016). Deployment of an unmanned aerial system to assist in mapping an intermittent stream. *Hydrological Processes*, *30*(3), 493-500.

Sproles EA, Nolin AW, Rittger K, Painter TH (2013) Climate change impacts on maritime mountain snowpack in the Oregon Cascades. *Hydrol Earth Syst Sci* 17(7):2581–2597.

Sproles, E. A., Orrega, N. C., Kerr, T., and Lopez, A. D. (2016). Developing a snowmelt forecast model in the absence of field data. Water Resource Management. 30: 2581. doi:10.1007/s11269-016-1271-4.

Stewart IT, Cayan DR, Dettinger MD (2005) Changes toward earlier streamflow timing across western North America. *Journal of Climate* 18(8):1136–1155.

Stewart, I. T. (2009). Changes in snowpack and snowmelt runoff for key mountain regions. *Hydrological Processes*, *23*(1), 78-94.

Stewart, I. T., Cayan, D. R., & Dettinger, M. D. (2004). Changes in snowmelt runoff timing in western North America under a business as usual climate change scenario. *Climatic Change*, *62*(1-3), 217-232.

Su, H., Yang, Z. L., Dickinson, R. E., Wilson, C. R., & Niu, G. Y. (2010). Multisensor snow data assimilation at the continental scale: The value of Gravity Recovery and Climate Experiment terrestrial water storage information. *Journal of Geophysical Research: Atmospheres*, *115*(D10).

Sukhija, B. S., Reddy, D. V., Nagabhushanam, P., & Hussain, S. (2003). Recharge processes: piston flow vs preferential flow in semi-arid aquifers of India. *Hydrogeology Journal*, *11*(3), 387-395.

Sutanto, S. J., Wenninger, J., Coenders-Gerrits, A. M. J., & Uhlenbrook, S. (2012). Partitioning of evaporation into transpiration, soil evaporation and interception: a comparison between isotope measurements and a HYDRUS-1D model. *Hydrology and Earth System Sciences*, *16*(8), 2605-2616.

Swann, A. L., Hoffman, F. M., Koven, C. D., & Randerson, J. T. (2016). Plant responses to increasing CO2 reduce estimates of climate impacts on drought severity. *Proceedings of the National Academy of Sciences*, *113*(36), 10019-10024.

Tague, C., & Peng, H. (2013). The sensitivity of forest water use to the timing of precipitation and snowmelt recharge in the California Sierra: Implications for a warming climate. *Journal of Geophysical Research: Biogeosciences*, *118*(2), 875-887.

Tang, Q., & Lettenmaier, D. P. (2010). Use of satellite snow-cover data for streamflow prediction in the Feather River Basin, California. *International Journal of Remote Sensing*, *31*(14), 3745-3762.

Tetzlaff, D., Buttle, J., Carey, S. K., McGuire, K., Laudon, H., & Soulsby, C. (2015). Tracer-based assessment of flow paths, storage and runoff generation in northern catchments: a review. *Hydrological Processes*, 29(16), 3475-3490.

Theil, H.: A rank-invariant method of linear and polynomial regression analysis, Mathematic, 53, 386–392, 1950.

Tian, Y., & Peters-Lidard, C. D. (2010). A global map of uncertainties in satellite-based precipitation measurements. *Geophysical Research Letters*, *37*(24).

Trujillo, E., and N. P. Molotch (2014), Snowpack regimes of the Western United States, *Water Resources Research,* 50(7), 5611–5623, doi:10.1002/2013WR014753.

U.S. Bureau of Reclamation, 2012. Colorado River Basin Water Supply and Demand Study: Technical Report B – Water Supply Assessment. 1-91.

Uysal, G., Şorman, A. A., & Şensoy, A. (2016). Streamflow Forecasting Using Different Neural Network Models with Satellite Data for a Snow Dominated Region in Turkey. Procedia Engineering, 154, 1185-1192.

Valt, M., & Cianfarra, P. (2010). Recent snow cover variability in the Italian Alps. Cold Regions Science and Technology, 64(2), 146-157.

Vanderhoof, M. K., & Williams, C. A. (2015). Persistence of MODIS evapotranspiration impacts from mountain pine beetle outbreaks in lodgepole pine forests, south-central Rocky Mountains. *Agricultural and Forest Meteorology*, *200*, 78-91.

Vano, J. A., Das, T., & Lettenmaier, D. P. (2012). Hydrologic sensitivities of Colorado River runoff to changes in precipitation and temperature. *Journal of Hydrometeorology*, *13*(3), 932-949.

Vaughan, D.G., J.C. Comiso, I. Allison, J. Carrasco, G. Kaser, R. Kwok, P. Mote, T. Murray, F. Paul, J. Ren, E. Rignot, O. Solomina, K. Steffen and T. Zhang, 2013: Observations: Cryosphere. In: Climate Change 2013: The Physical Science Basis. Contribution of Working Group I to the Fifth Assessment Report of the Intergovernmental Panel on Climate Change [Stocker, T.F., D. Qin, G.-K. Plattner, M. Tignor, S.K. Allen, J. Boschung, A. Nauels, Y. Xia, V. Bex and P.M. Midgley (eds.)]. Cambridge University Press, Cambridge, United Kingdom and New York, NY, USA.

Vera, C., & Silvestri, G. (2009). Precipitation interannual variability in South America from the WCRP-CMIP3 multi-model dataset. *Climate dynamics*, *32*(7-8), 1003-1014.

Vicuna, S., Maurer, E. P., Joyce, B., Dracup, J. A., & Purkey, D. (2007). The sensitivity of California water resources to climate change scenarios. *JAWRA Journal of the American Water Resources Association*, *43*(2), 482-498.

Viviroli, D., Weingartner, R., & Messerli, B. (2003). Assessing the hydrological significance of the world's mountains. *Mountain research and Development*, *23*(1), 32-40.

Viviroli, D., Dürr, H. H., Messerli, B., Meybeck, M., & Weingartner, R. (2007). Mountains of the world, water towers for humanity: Typology, mapping, and global significance. *Water resources research*, *43*(7).

Wang, D., & Hejazi, M. (2011). Quantifying the relative contribution of the climate and direct human impacts on mean annual streamflow in the contiguous United States. *Water Resources Research*, *47*(10).

Wang, L., Sharp, M., Brown, R., Derksen, C., & Rivard, B. (2005). Evaluation of spring snow covered area depletion in the Canadian Arctic from NOAA snow charts. *Remote Sensing of Environment*, *95*(4), 453-463.

Webb, R. W., Fassnacht, S. R., & Gooseff, M. N. (2015). Wetting and drying variability of the shallow subsurface beneath a snowpack in California's Southern Sierra Nevada. *Vadose Zone Journal*, *14*(8).

Westerling, A. L., Bryant, B. P., Preisler, H. K., Holmes, T. P., Hidalgo, H. G., Das, T., & Shrestha, S. R. (2011). Climate change and growth scenarios for California wildfire. *Climatic Change*, *109*(1), 445-463.

Williams, C. J., McNamara, J. P., & Chandler, D. G. (2009). Controls on the temporal and spatial variability of soil moisture in a mountainous landscape: the signature of snow and complex terrain. *Hydrology and Earth System Sciences*, *13*(7), 1325-1336.

Winkler, R. D. (2011). Changes in snow accumulation and ablation after a fire in south-central British Columbia. *Streamline Watershed Management Bulletin*, *14*(2), 1-7.

Wood, W. W., Rainwater, K. A., & Thompson, D. B. (1997). Quantifying macropore recharge: Examples from a semi-arid area. *Groundwater*, *35*(6), 1097-1106.

Wu, Z., Li, J., Jiang, Z., & Ma, T. (2012). Modulation of the Tibetan Plateau snow cover on the ENSO teleconnections: From the East Asian summer monsoon perspective. *Journal of Climate*, *25*(7), 2481-2489.

Wu, Z., Li, J., Wang, B., & Liu, X. (2009). Can the Southern Hemisphere annular mode affect China winter monsoon?. *Journal of Geophysical Research: Atmospheres*, *114*(D11).

Wyatt, B. M., Ochsner, T. E., Fiebrich, C. A., Neel, C. R., & Wallace, D. S. (2017). Useful Drainage Estimates Obtained from a Large-Scale Soil Moisture Monitoring Network by Applying the Unit-Gradient Assumption. *Vadose Zone Journal*, *16*(6).

Xie, Y., Crosbie, R., Yang, J., Wu, J., & Wang, W. (2018). Usefulness of Soil Moisture and Actual Evapotranspiration Data for Constraining Potential Groundwater Recharge in Semiarid Regions. *Water Resources Research*.

Xu, X., Li, J., & Tolson, B. A. (2014). Progress in integrating remote sensing data and hydrologic modeling. Progress in Physical Geography, 38(4), 464-498.

Ye, H. (2001). Quasi-biennial and quasi-decadal variations in snow accumulation over northern Eurasia and their connections to the Atlantic and Pacific Oceans. *Journal of Climate*, *14*(24), 4573-4584.

Ye, H., & Bao, Z. (2001). Lagged teleconnections between snow depth in northern Eurasia, rainfall in Southeast Asia and sea-surface temperatures over the tropical Pacific Ocean. *International Journal of Climatology*, *21*(13), 1607-1621.

Zarfl, C., Lumsdon, A. E., Berlekamp, J., Tydecks, L., & Tockner, K. (2015). A global boom in hydropower dam construction. *Aquatic Sciences*, *77*(1), 161-170.

Zeng, X., Zeng, X., Shen, S. S., Dickingson, R. E., & Zeng, Q. C. (2005). Vegetation—soil water interaction within a dynamical ecosystem model of grassland in semi-arid areas. *Tellus B: Chemical and Physical Meteorology*, *57*(3), 189-202.

Zhang, T. (2005). Influence of the seasonal snow cover on the ground thermal regime, An overview. Reviews of Geophysics, 43(4).

Zhou, H. F., X.-J. Zheng, B. Zhou, Q. Dai, and Y. Li. (2012), Sublimation over seasonal snowpack at the southeastern edge of a desert in central Eurasia, Hydrol. Processes, doi:10.1002/hyp.8402

Appendix 1: Chapter 2 supplementary material

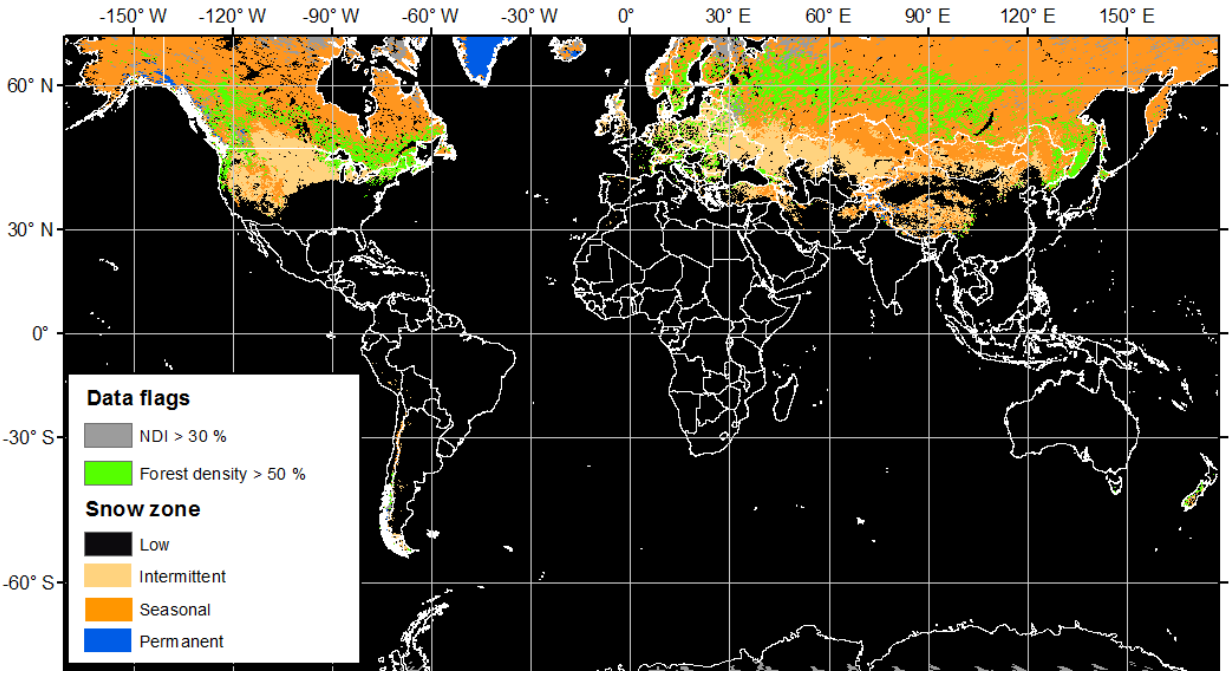

Figure 2.8. Snow zones mapped with no data index (NDI) > 30% and forest cover > 50 % for the globe. NDI is the fraction of time that cloud, sensor saturation, or other errors lead to missing data at each location. Forest cover threshold of 50 %, is a threshold above which most errors in snow presence/absence identification occur.

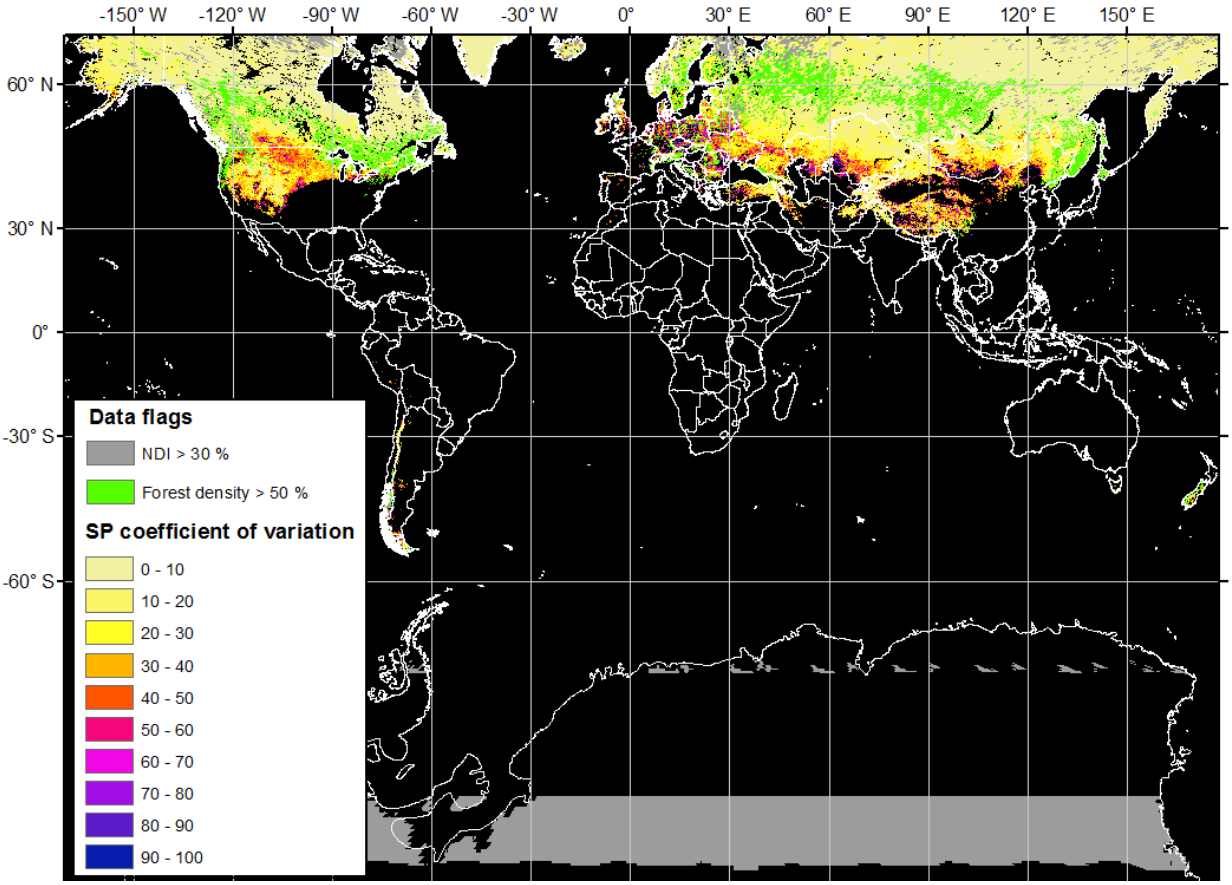

Figure 2.9. Coefficient of variation for annual 2001-2016 snow persistence mapped with no data index (NDI) > 30% and forest cover > 50 % for the globe. NDI is the fraction of time that cloud, sensor saturation, or other errors lead to missing data at each location. Forest cover threshold of 50 %, is a threshold above which most errors in snow presence/absence identification occur.

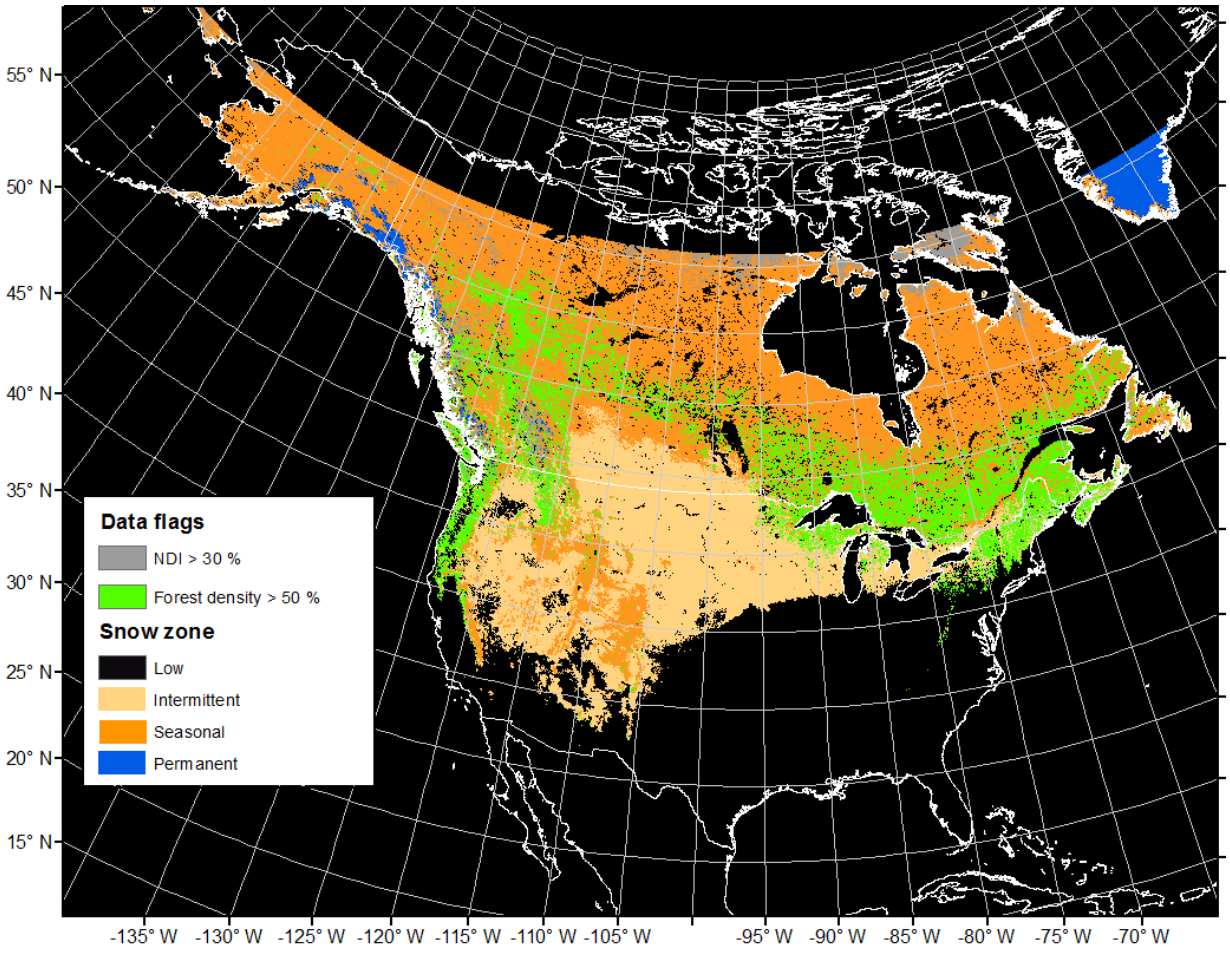

Figure 2.10. Snow zones mapped with no data index (NDI) > 30% and forest cover > 50 % for North America. NDI is the fraction of time that cloud, sensor saturation, or other errors lead to missing data at each location. Forest cover threshold of 50 %, is a threshold above which most errors in snow presence/absence identification occur.

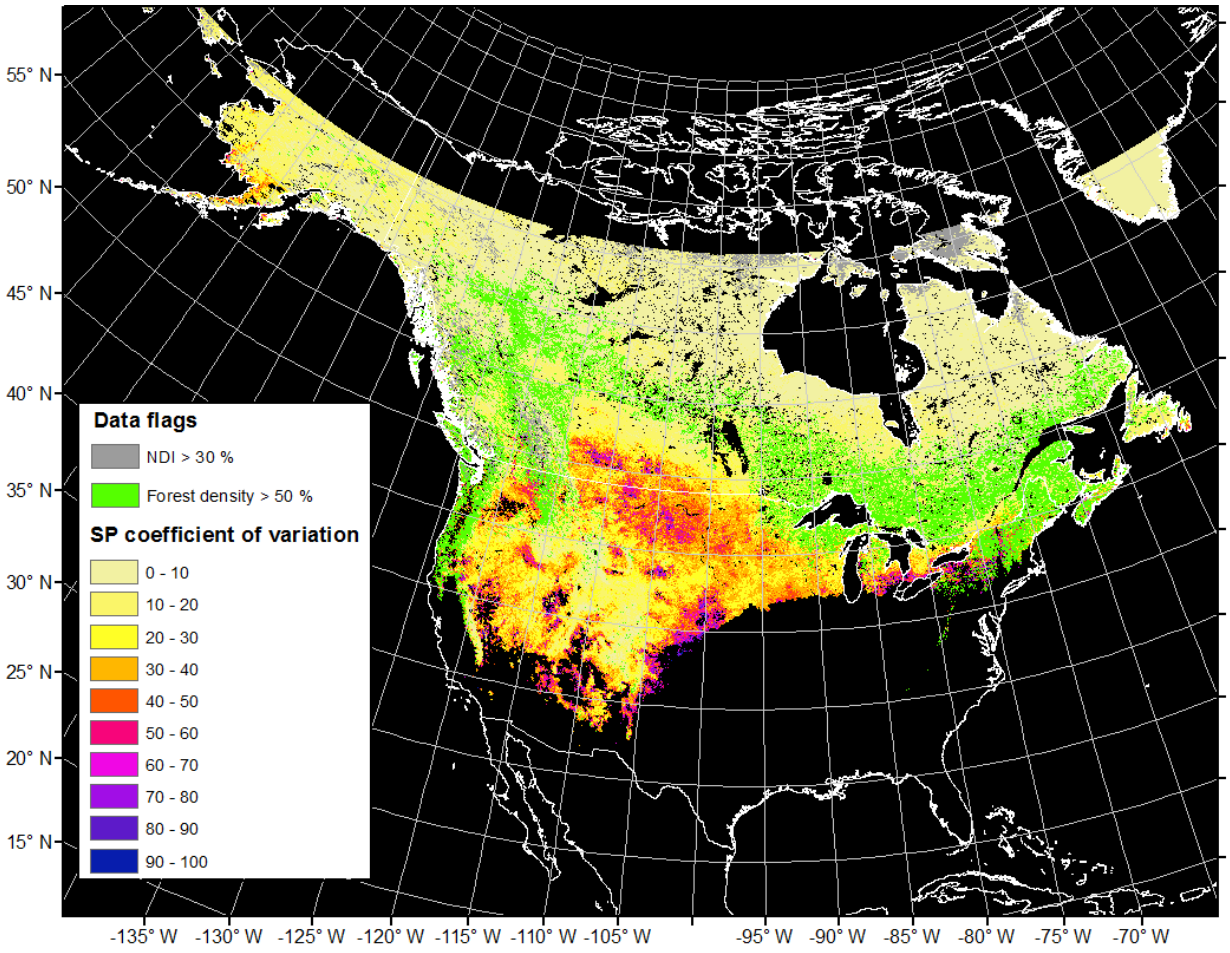

Figure 2.11. Coefficient of variation for annual 2001-2016 snow persistence mapped with no data index (NDI) > 30% and forest cover > 50 % for North America. NDI is the fraction of time that cloud, sensor saturation, or other errors lead to missing data at each location. Forest cover threshold of 50 %, is a threshold above which most errors in snow presence/absence identification occur.

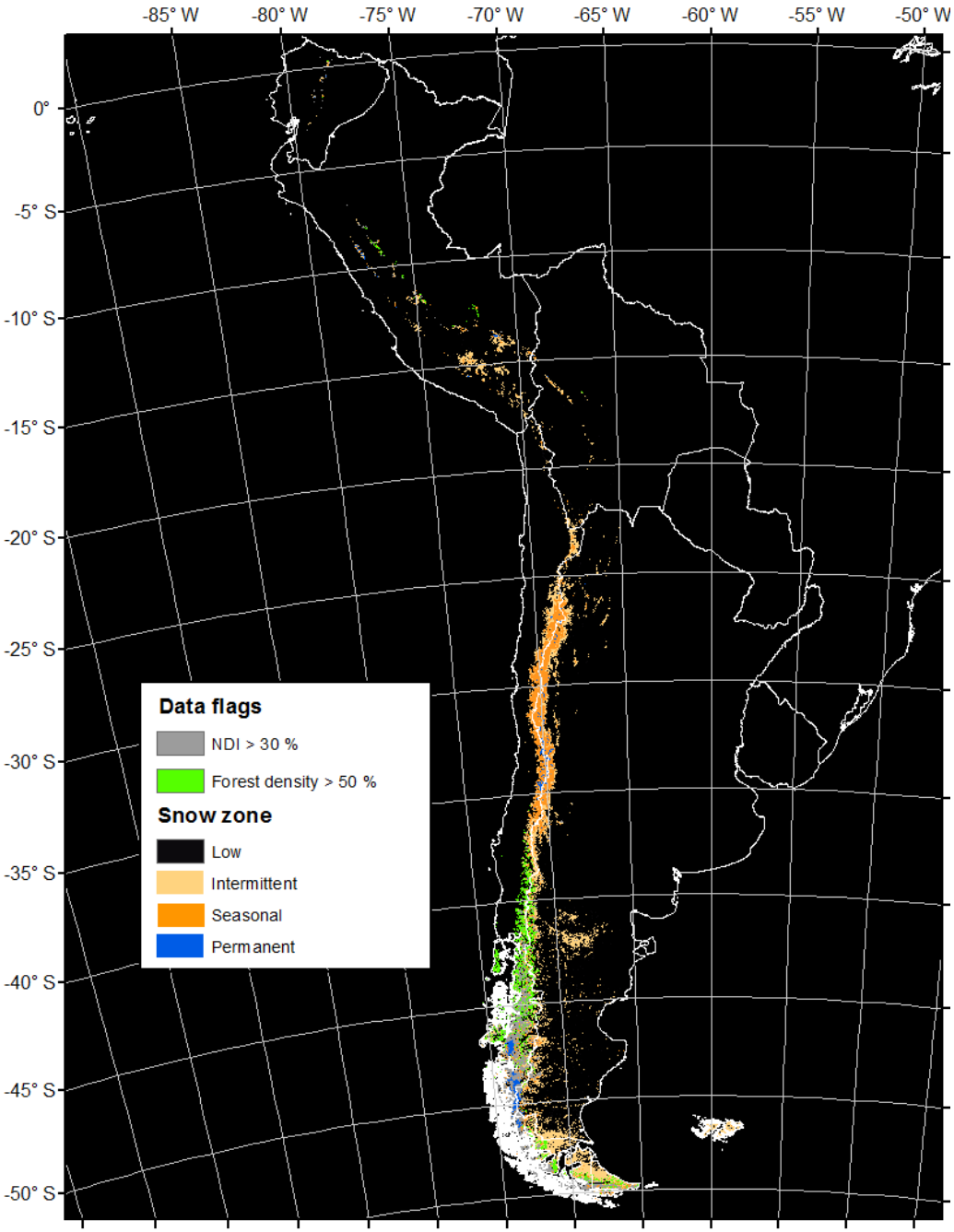

Figure 2.12. Snow zones mapped with no data index (NDI) > 30% and forest cover > 50 % for South America. NDI is the fraction of time that cloud, sensor saturation, or other errors lead to missing data at each location. Forest cover threshold of 50 %, is a threshold above which most errors in snow presence/absence identification occur.

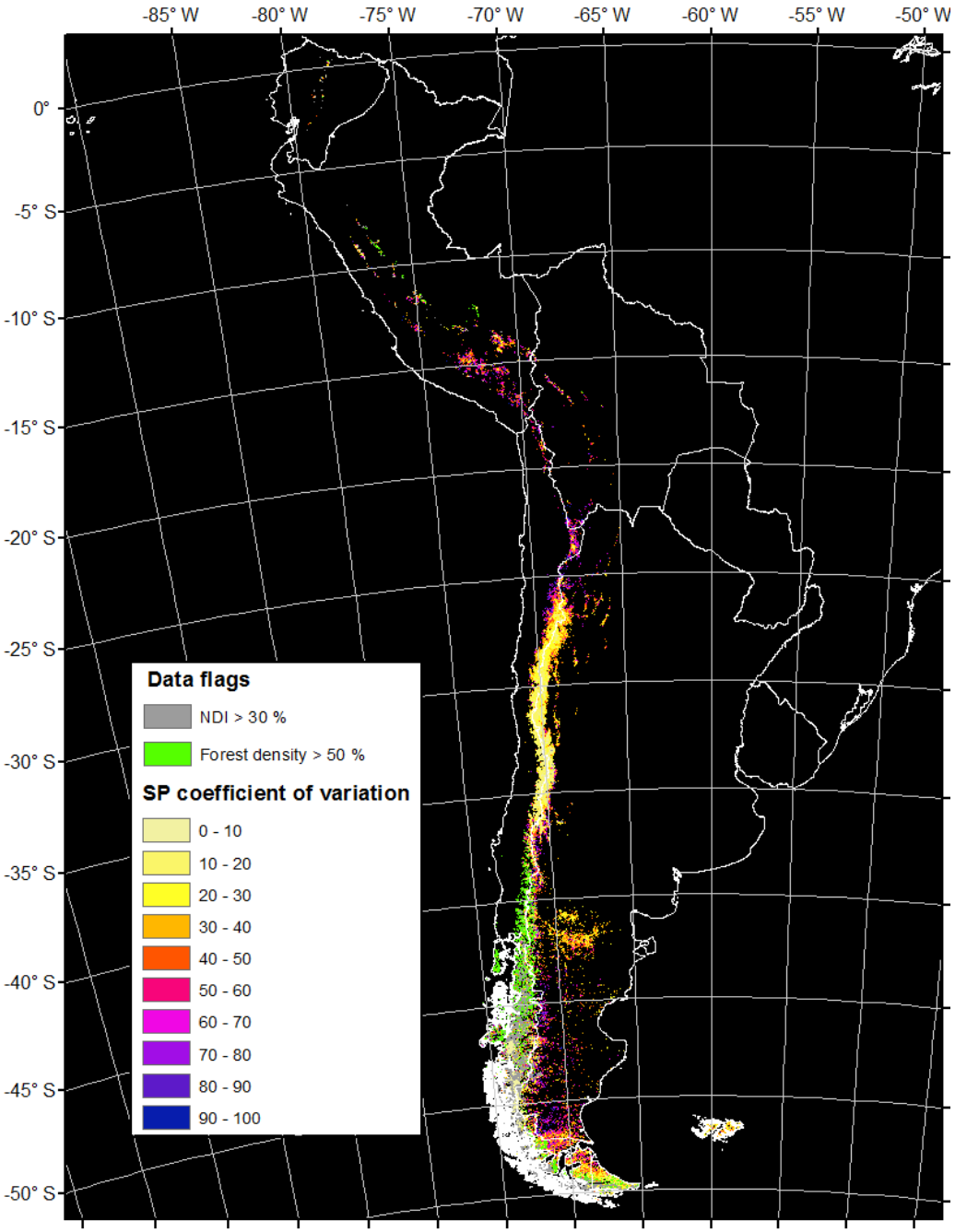

Figure 2.13. Coefficient of variation for annual 2001-2016 snow persistence mapped with no data index (NDI) > 30% and forest cover > 50 % for South America. NDI is the fraction of time that cloud, sensor saturation, or other errors lead to missing data at each location. Forest cover threshold of 50 %, is a threshold above which most errors in snow presence/absence identification occur.

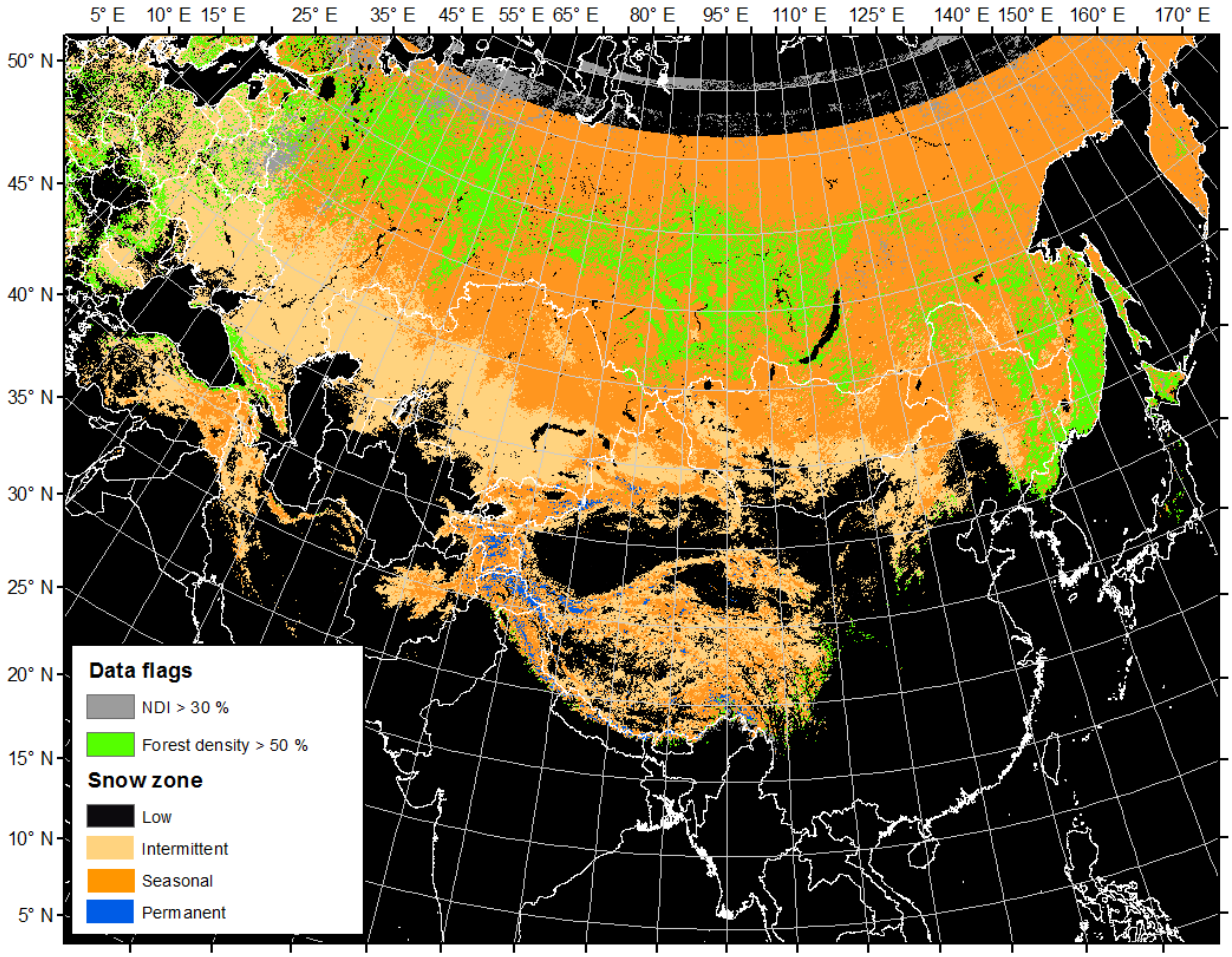

Figure 2.14. Snow zones mapped with no data index (NDI) > 30% and forest cover > 50 % for Asia. NDI is the fraction of time that cloud, sensor saturation, or other errors lead to missing data at each location. Forest cover threshold of 50 %, is a threshold above which most errors in snow presence/absence identification occur.

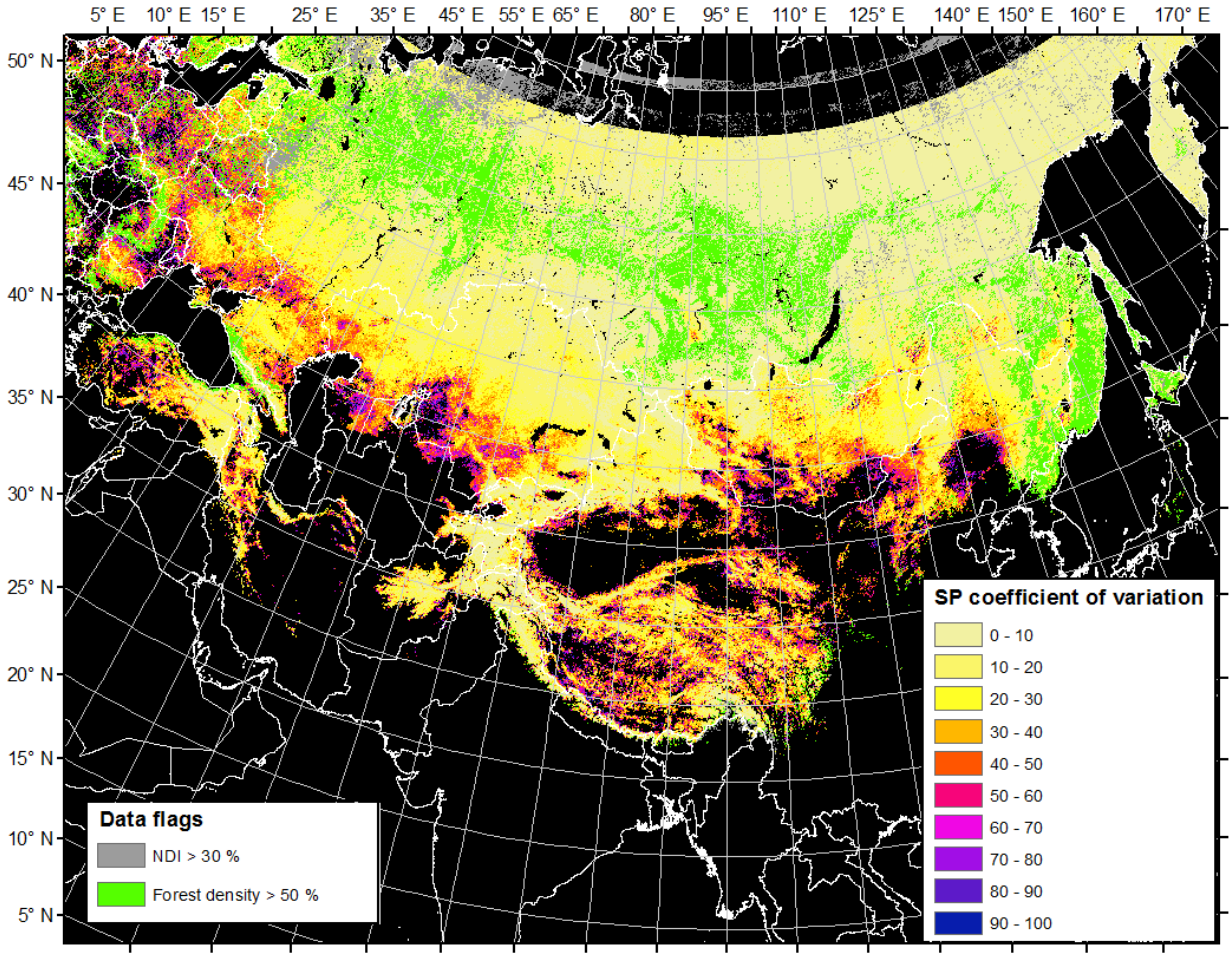

Figure 2.15. Coefficient of variation for annual 2001-2016 snow persistence mapped with no data index (NDI) > 30% and forest cover > 50 % for Asia. NDI is the fraction of time that cloud, sensor saturation, or other errors lead to missing data at each location. Forest cover threshold of 50 %, is a threshold above which most errors in snow presence/absence identification occur.

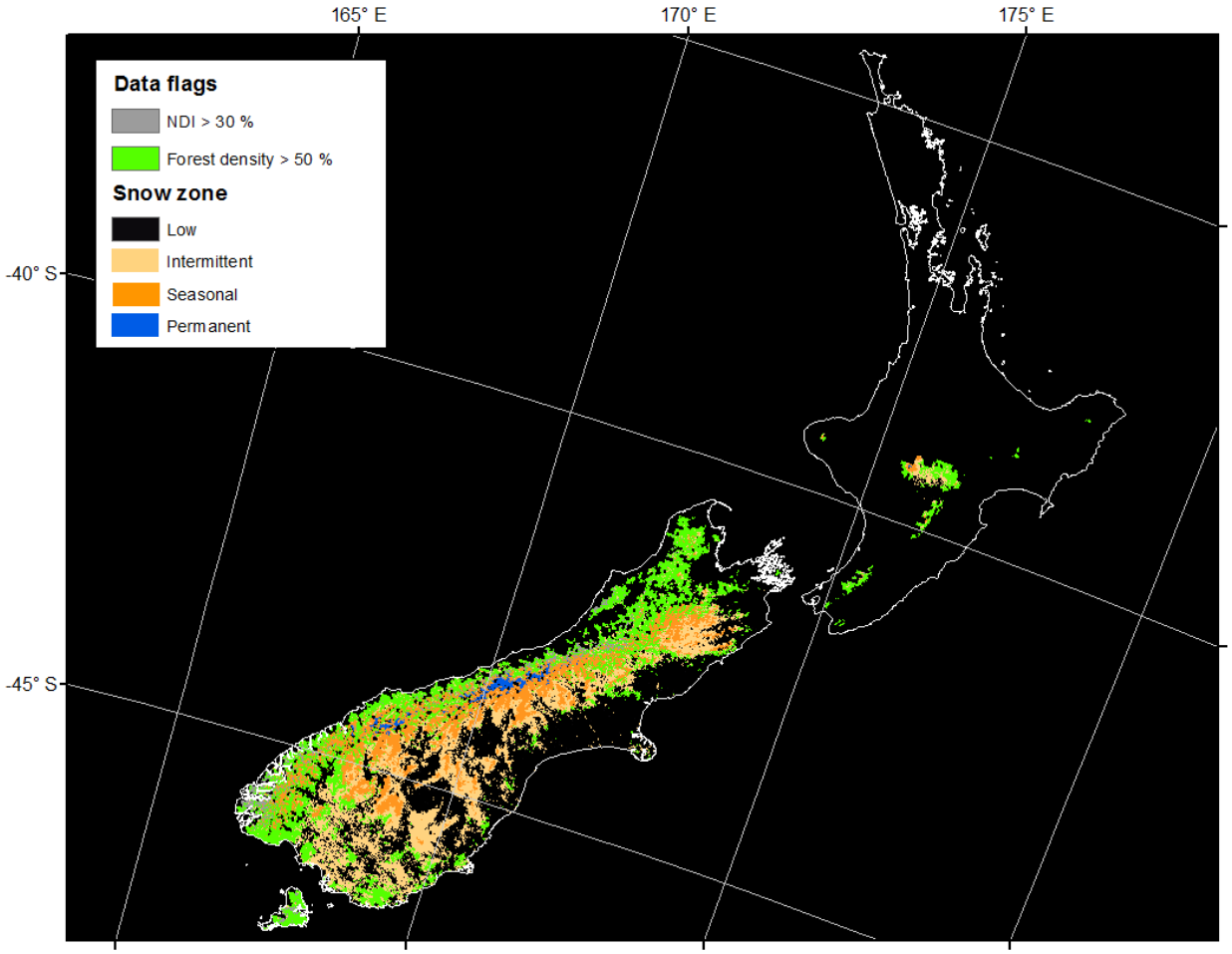

Figure 2.16. Snow zones mapped with no data index (NDI) > 30% and forest cover > 50 % for New Zealand (Oceania). NDI is the fraction of time that cloud, sensor saturation, or other errors lead to missing data at each location. Forest cover threshold of 50 %, is a threshold above which most errors in snow presence/absence identification occur.

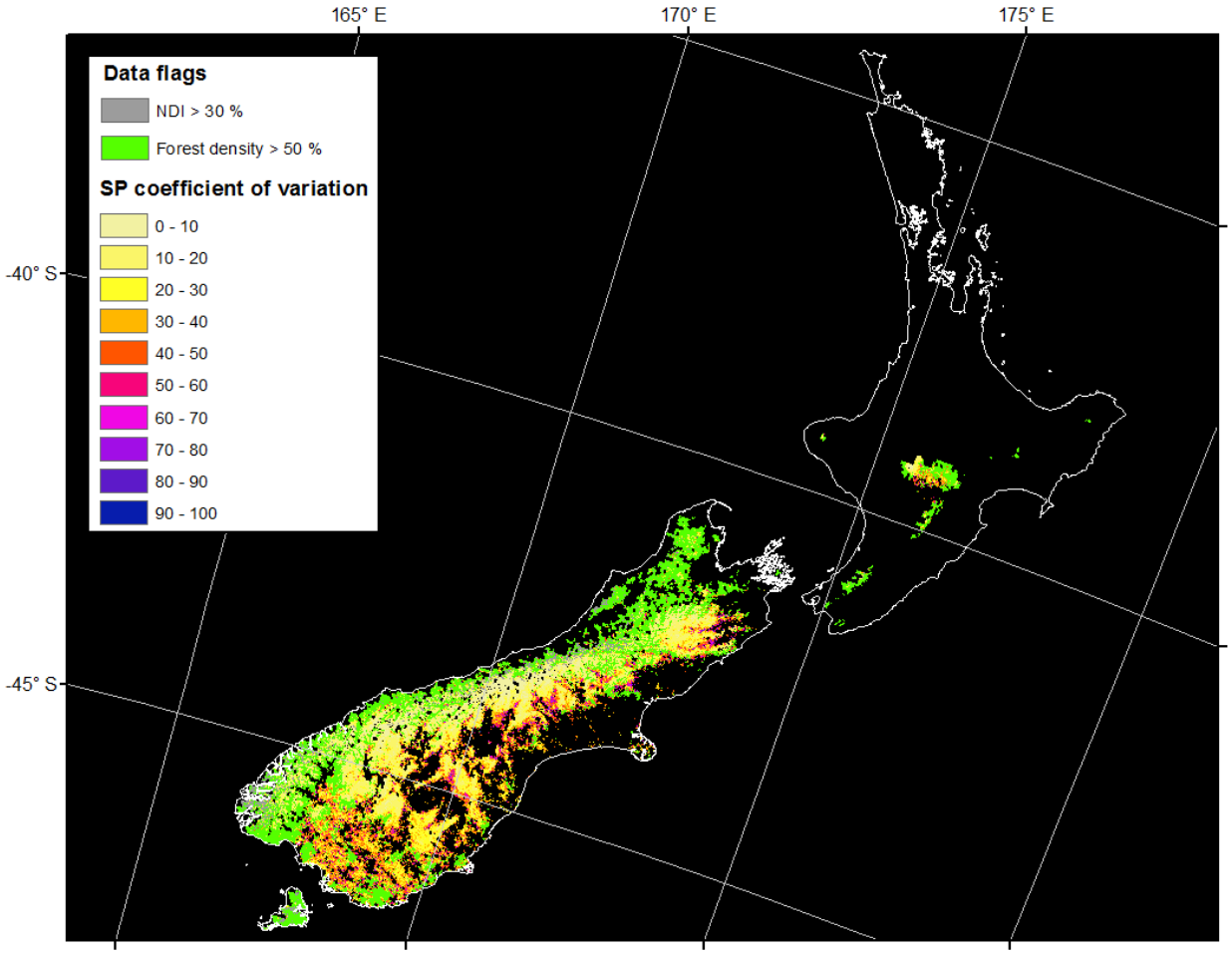

Figure 2.17. Coefficient of variation for annual 2001-2016 snow persistence mapped with no data index (NDI) > 30% and forest cover > 50 % for New Zealand (Oceania). NDI is the fraction of time that cloud, sensor saturation, or other errors lead to missing data at each location. Forest cover threshold of 50 %, is a threshold above which most errors in snow presence/absence identification occur.

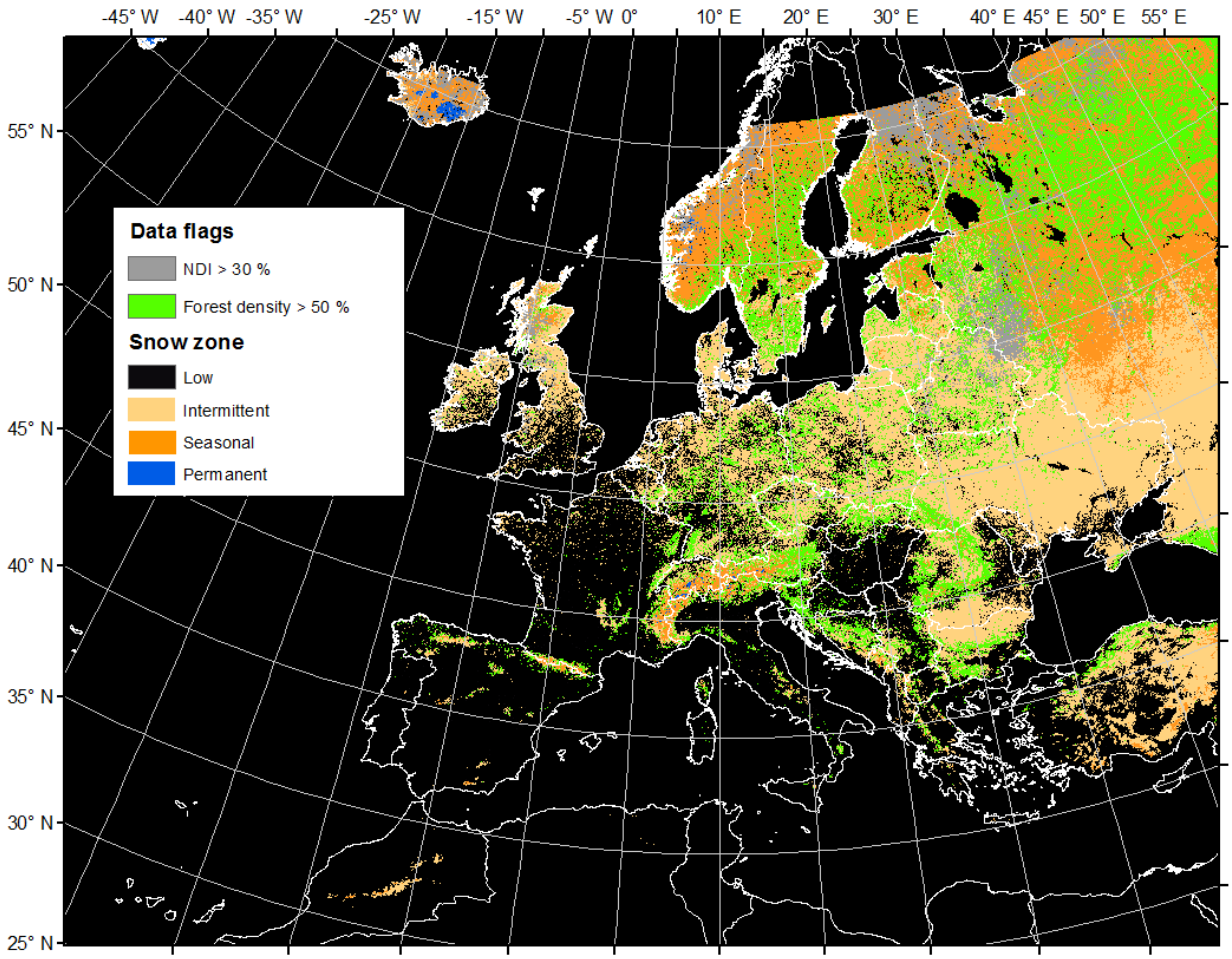

Figure 2.18. Snow zones mapped with no data index (NDI) > 30% and forest cover > 50 % for Europe and Northern Africa. NDI is the fraction of time that cloud, sensor saturation, or other errors lead to missing data at each location. Forest cover threshold of 50 %, is a threshold above which most errors in snow presence/absence identification occur.

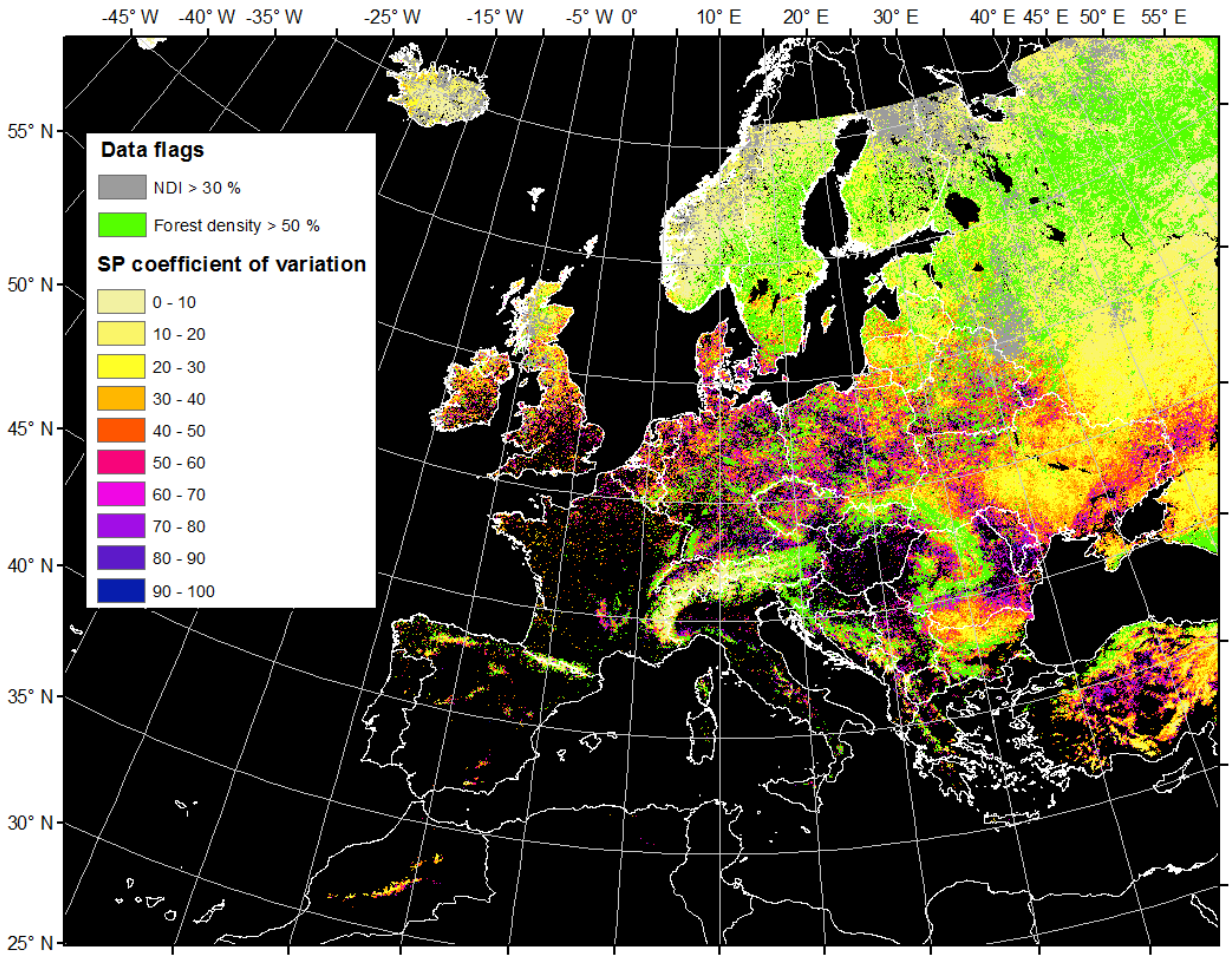

Figure 2.19. Coefficient of variation for annual 2001-2016 snow persistence mapped with no data index (NDI) > 30% and forest cover > 50 % for Europe and Northern Africa. NDI is the fraction of time that cloud, sensor saturation, or other errors lead to missing data at each location. Forest cover threshold of 50 %, is a threshold above which most errors in snow presence/absence identification occur.

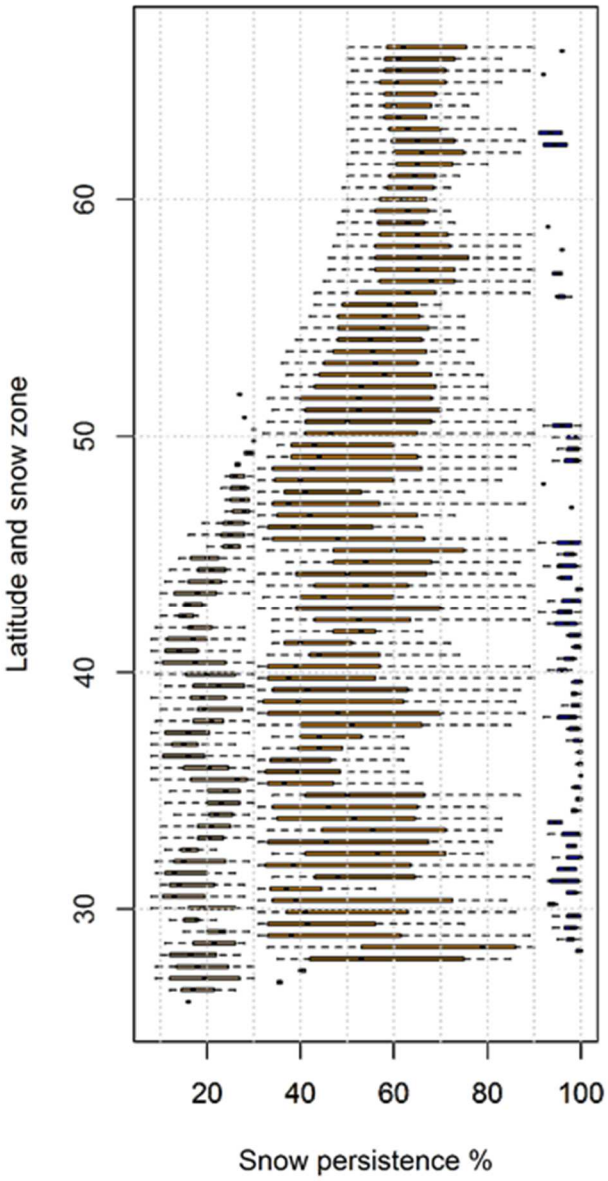

Figure 2.20. Boxplots of pixel values of mean annual snow persistence by latitude and snow zone in Asia.

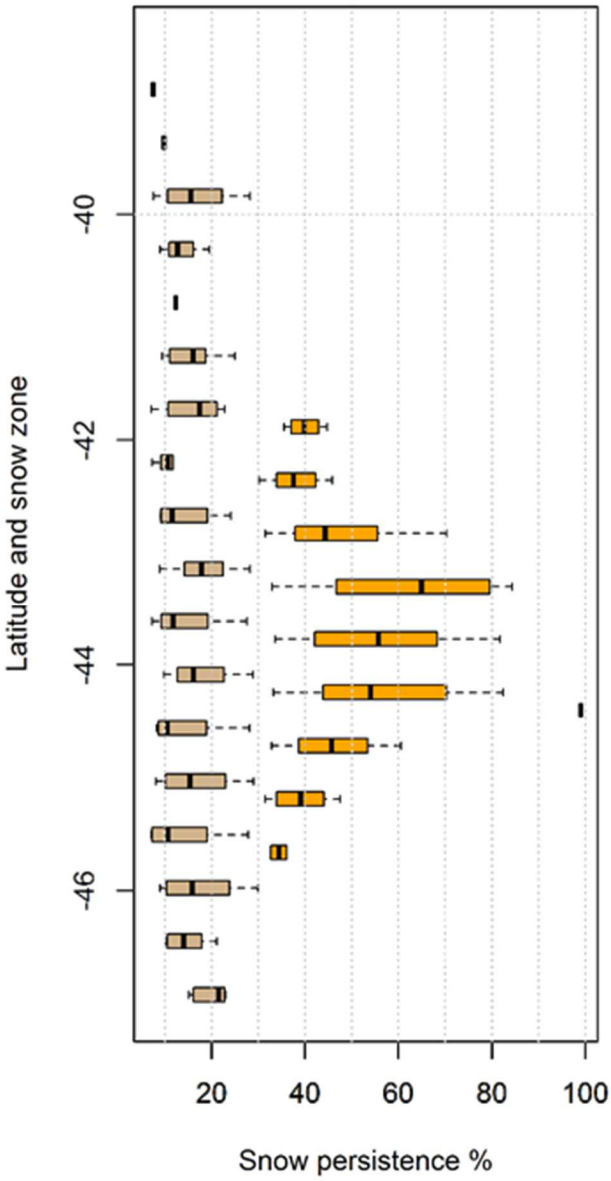

Figure 2.21. Boxplots of pixel values of mean annual snow persistence by latitude and snow zone in Oceania.

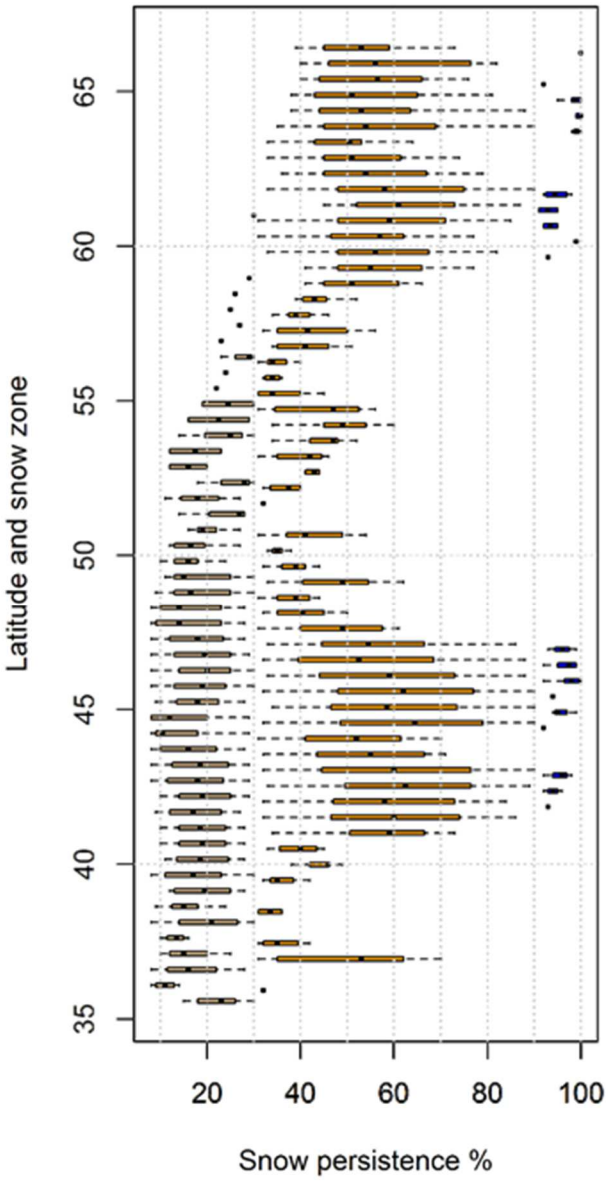

Figure 2.22. Boxplots of pixel values of mean annual snow persistence by latitude and snow zone in Europe.

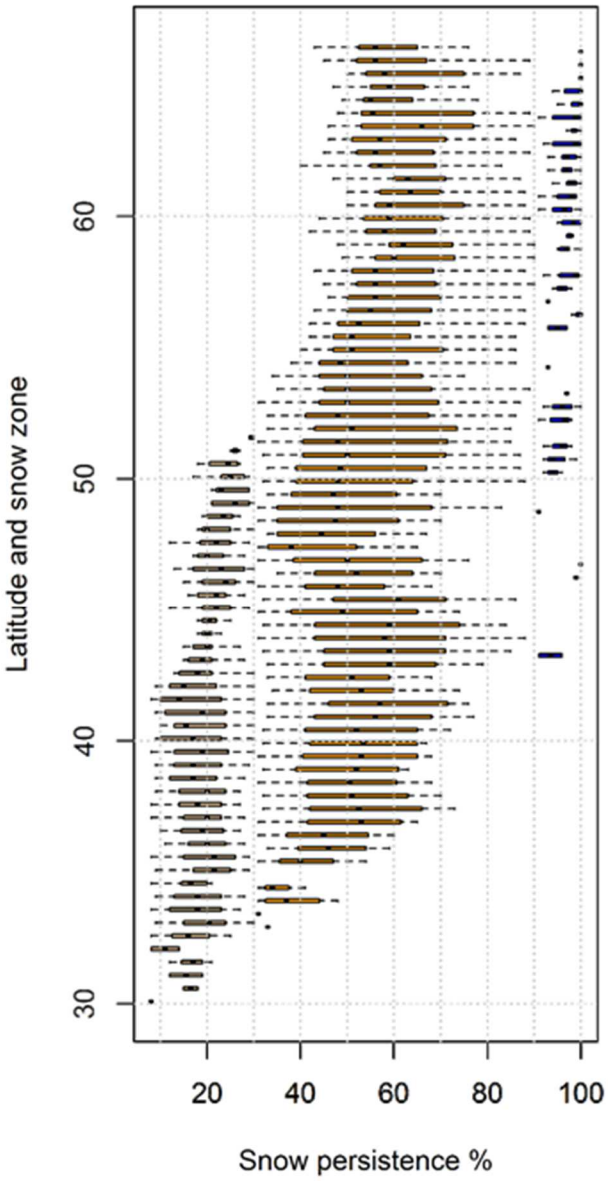

Figure 2.23. Boxplots of pixel values of mean annual snow persistence by latitude and snow zone in North America.

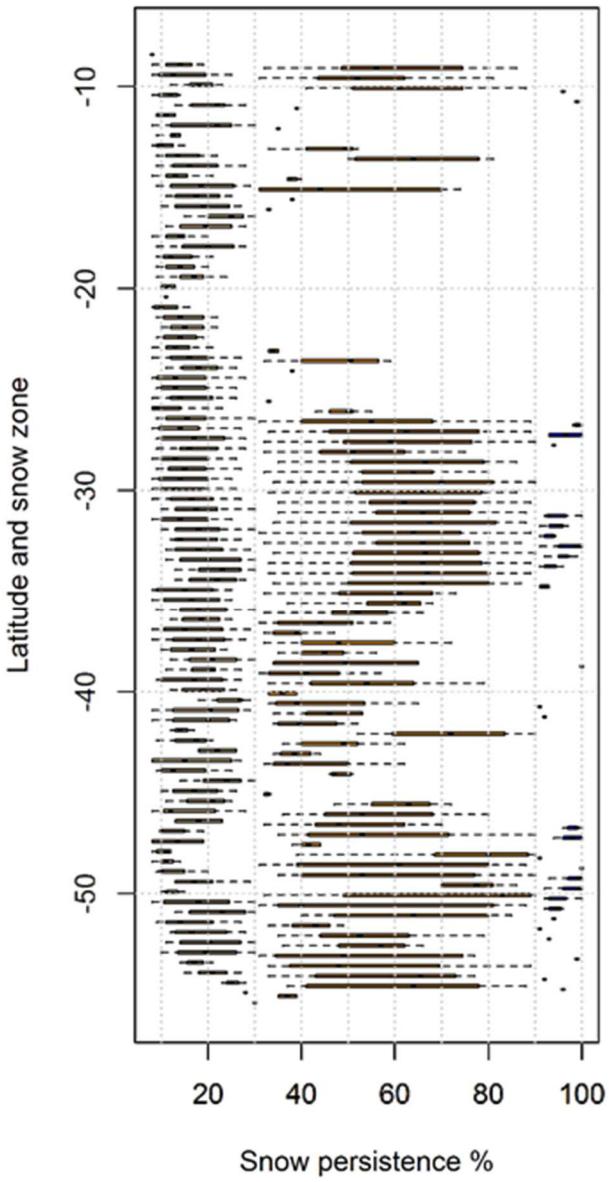

Figure 2.24. Boxplots of pixel values of mean annual snow persistence by latitude and snow zone in South America.

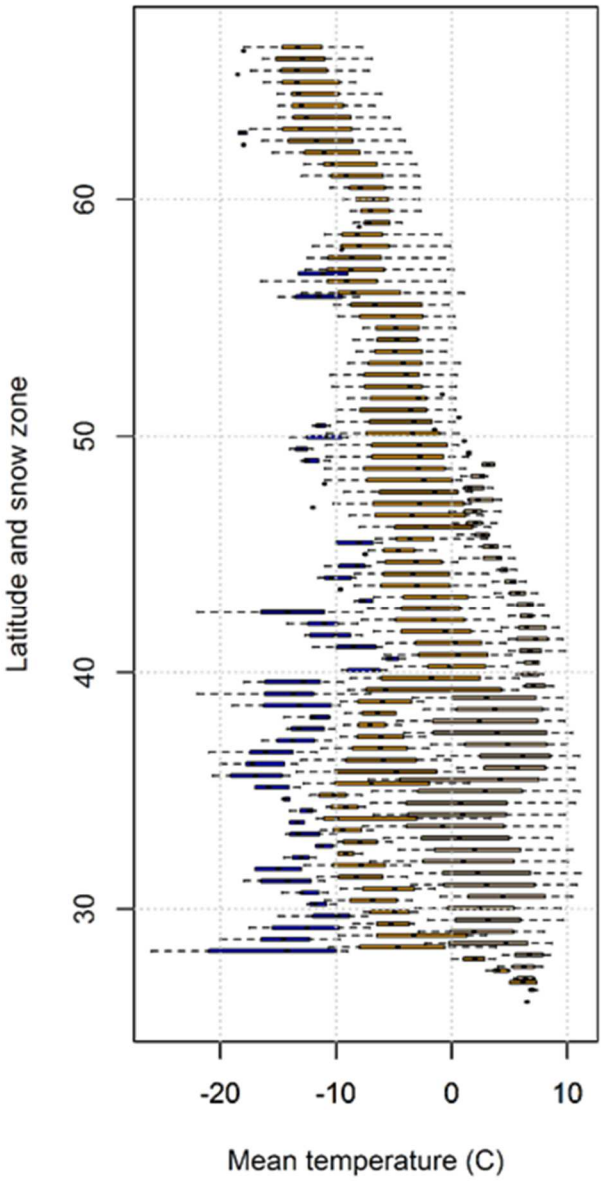

Figure 2.25. Boxplots of pixel values of mean annual mean temperature by latitude and snow zone in Asia.

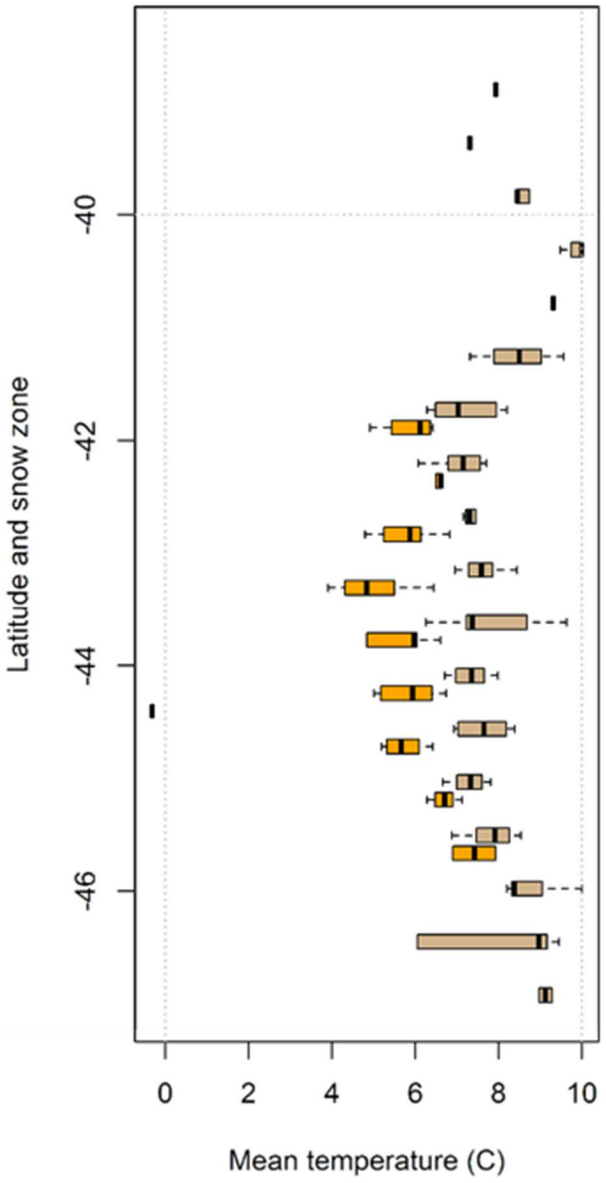

Figure 2.26. Boxplots of pixel values of mean annual mean temperature by latitude and snow zone in Oceania.

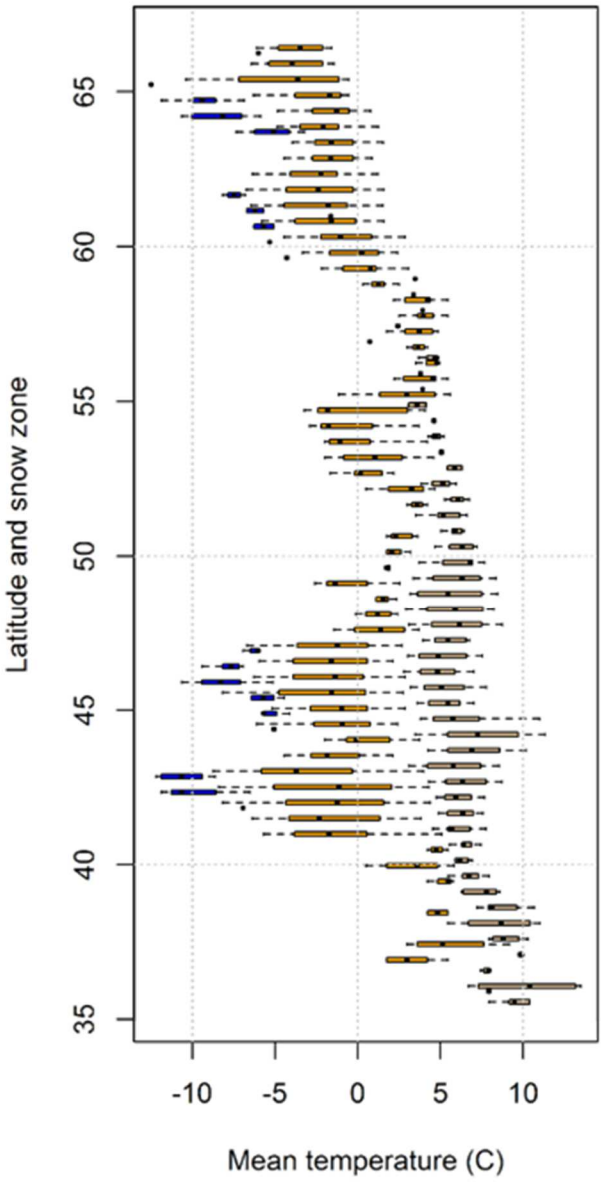

Figure 2.27. Boxplots of pixel values of mean annual mean temperature by latitude and snow zone in Europe.

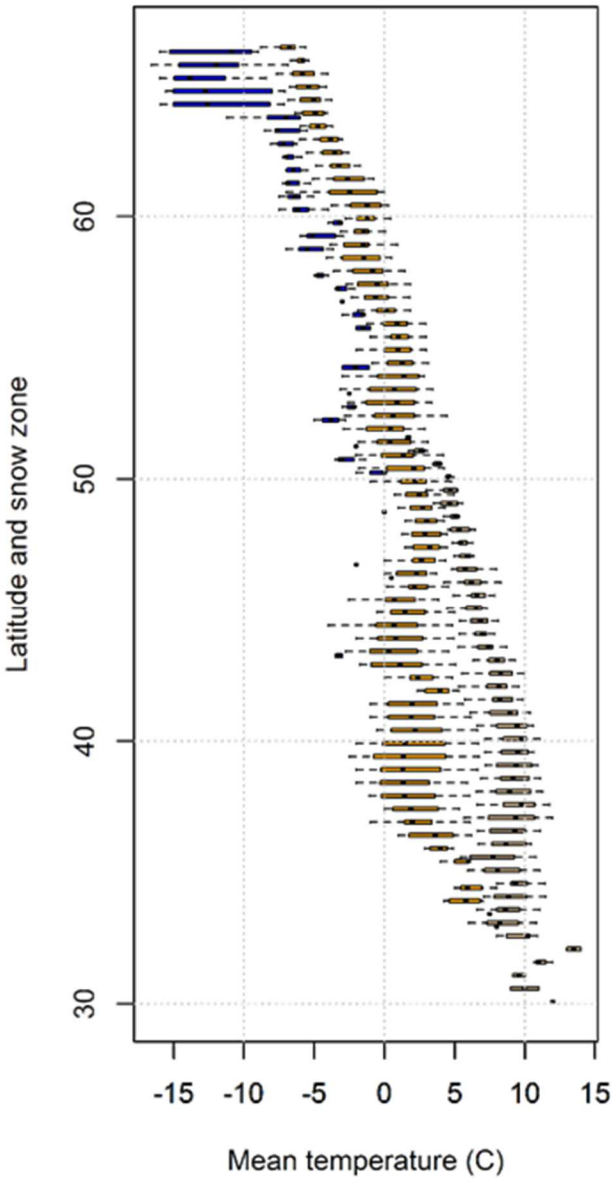

Figure 2.28. Boxplots of pixel values of mean annual mean temperature by latitude and snow zone in North America.

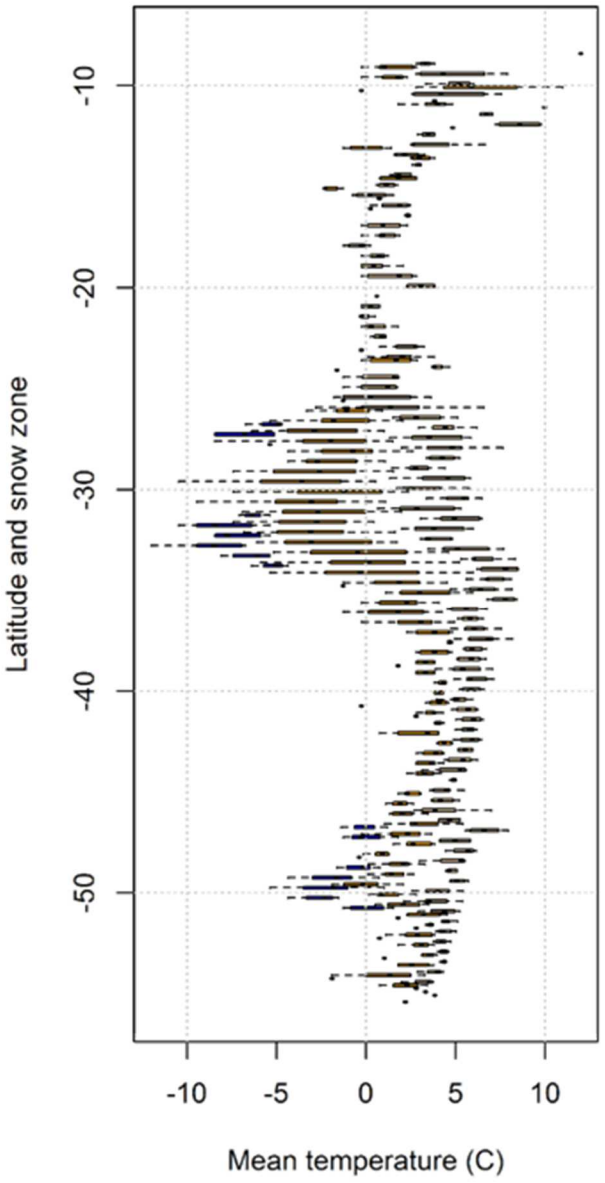

Figure 2.29. Boxplots of pixel values of mean annual mean temperature by latitude and snow zone in South America.

Table 2.5. Percent of snow covered area (SCA) in square kilometers of each continent/region with missing data (No Data Index NDI > 30%) and with potential errors from dense forest (>50% cover). Percent of SCA in each continent/region with forest cover >50% also reported.

Continent	a. NDI > 30 %	b. forest cover > 50 %	a+b	Percent SCA with forest cover >50 % and reporting positive trend	Percent SCA with forest cover >50 % and reporting negative trend
Africa	0.1	0.1	0.2	0.0	0.0
Asia	1.5	12.1	13.6	3.8	11.2
Europe	7.2	25.0	32.2	6.5	33.0
North America	3.8	17.5	21.3	14.4	12.1
Oceania	8.2	45.5	53.7	42.7	15.8
South America	20.1	16.3	36.5	16.8	7.1

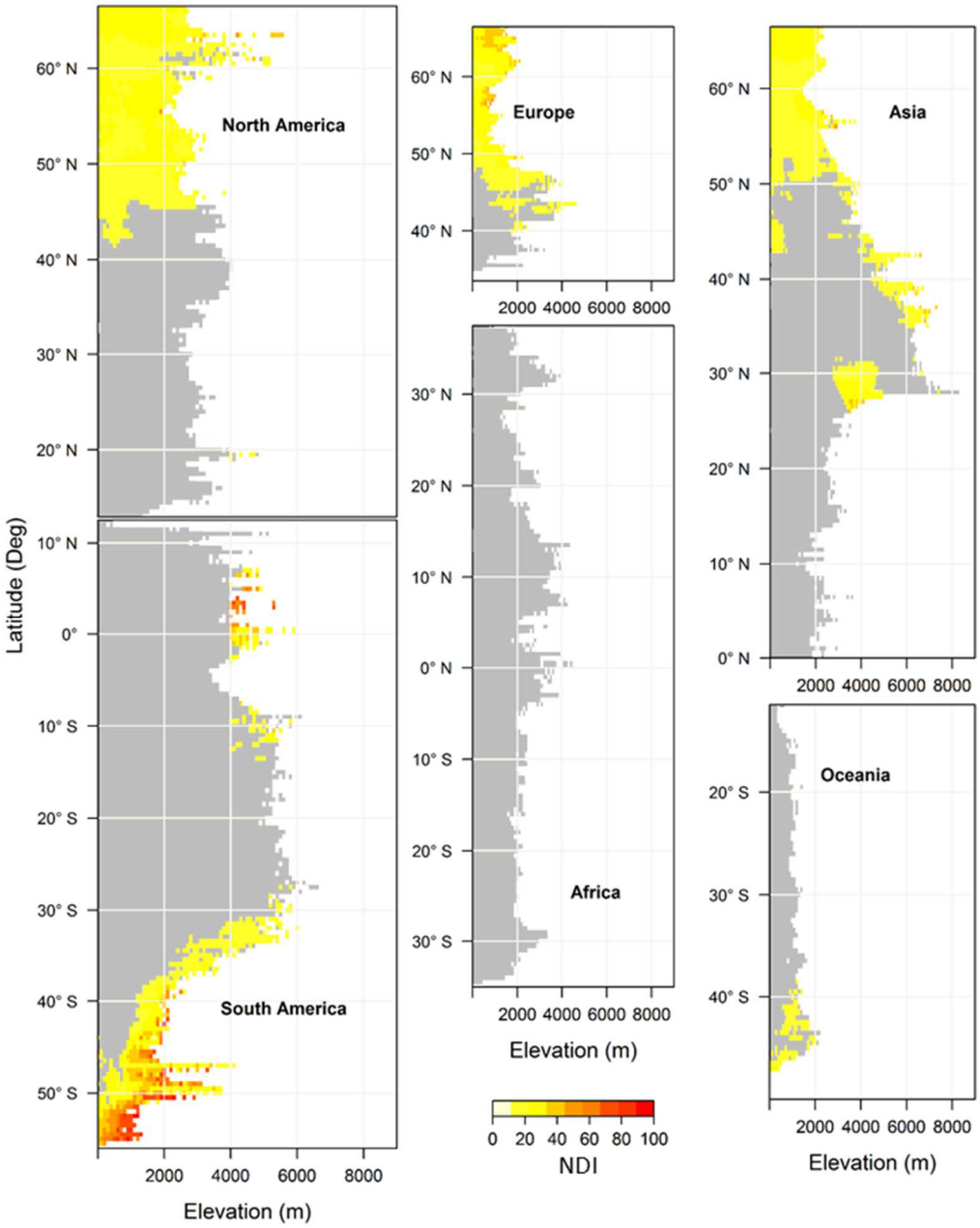

Figure 2.30. Mean annual no data index (NDI) by latitude and elevation for North America, South America, Africa, Asia, Europe and Oceania. NDI is the fraction of time that cloud, sensor saturation, or other errors lead to missing data at each location.

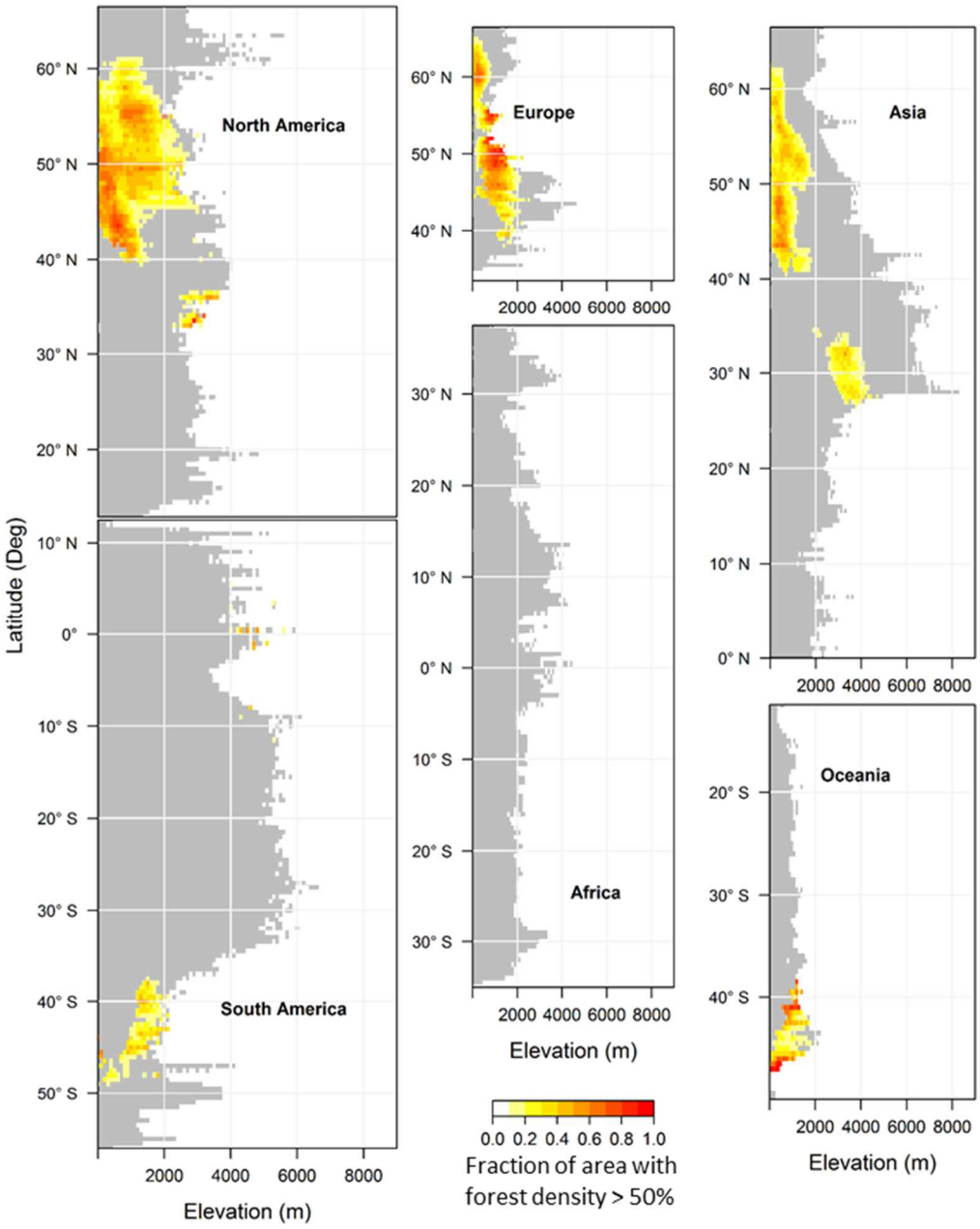

Figure 2.31. Fraction of area with forest cover > 50 % by latitude and elevation for North America, South America, Africa, Asia, Europe and Oceania. Forest cover threshold of 50 %, is a threshold above which most errors in snow presence/absence identification occur.

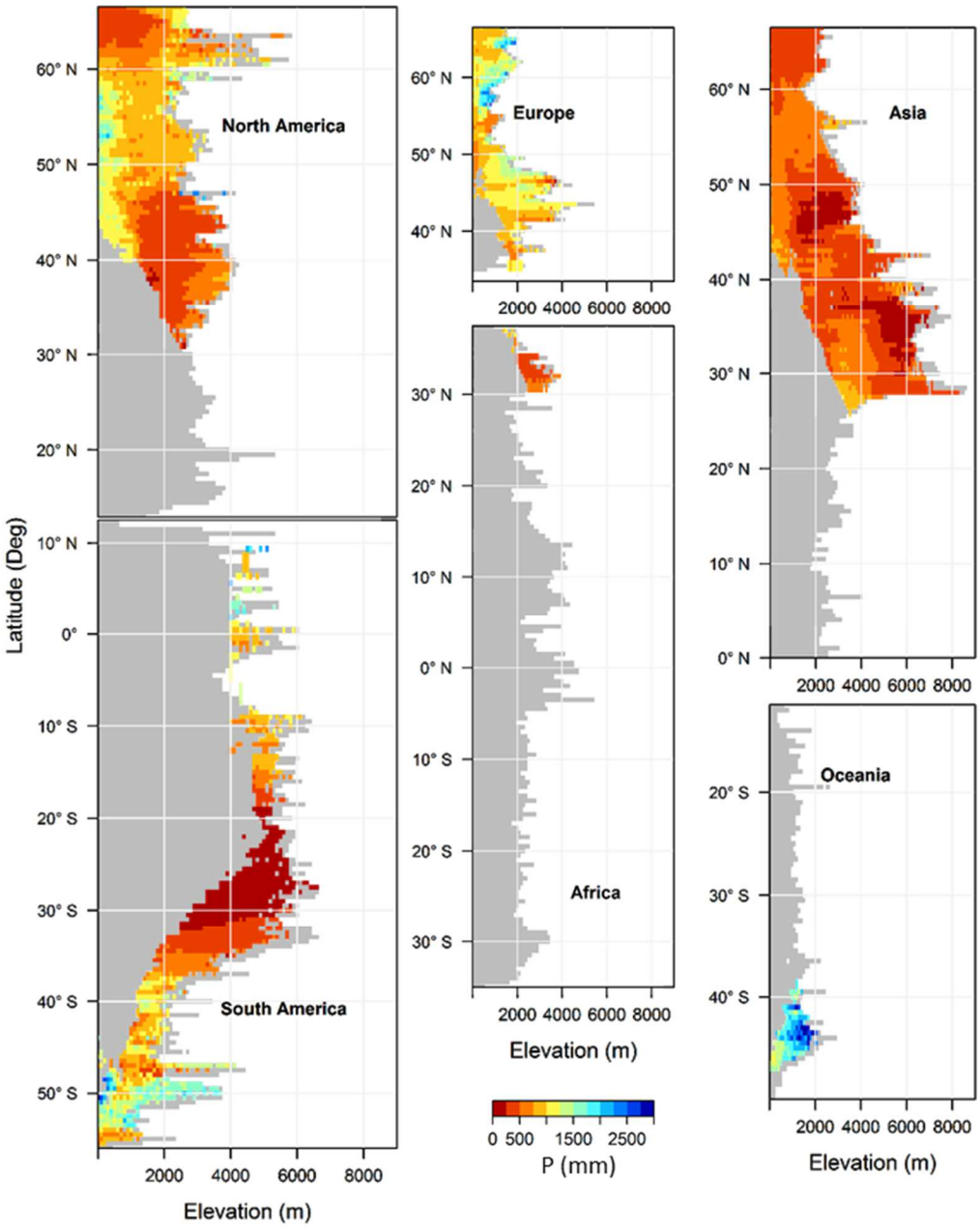

Figure 2.32. Mean annual precipitation by latitude and elevation for North America, South America, Africa, Asia, Europe and Oceania.

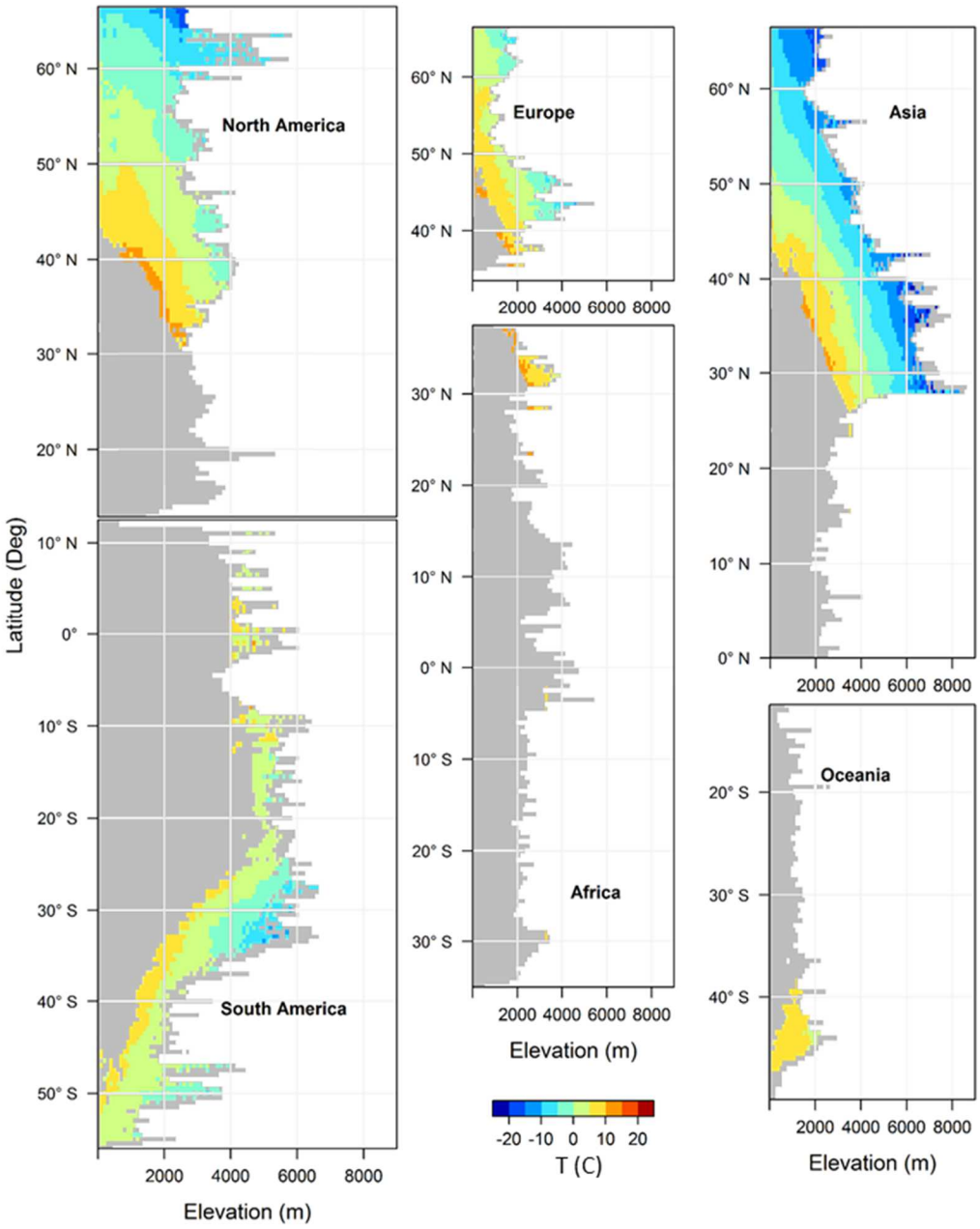

Figure 2.33. Mean annual mean temperature by latitude and elevation for North America, South America, Africa, Asia, Europe and Oceania.

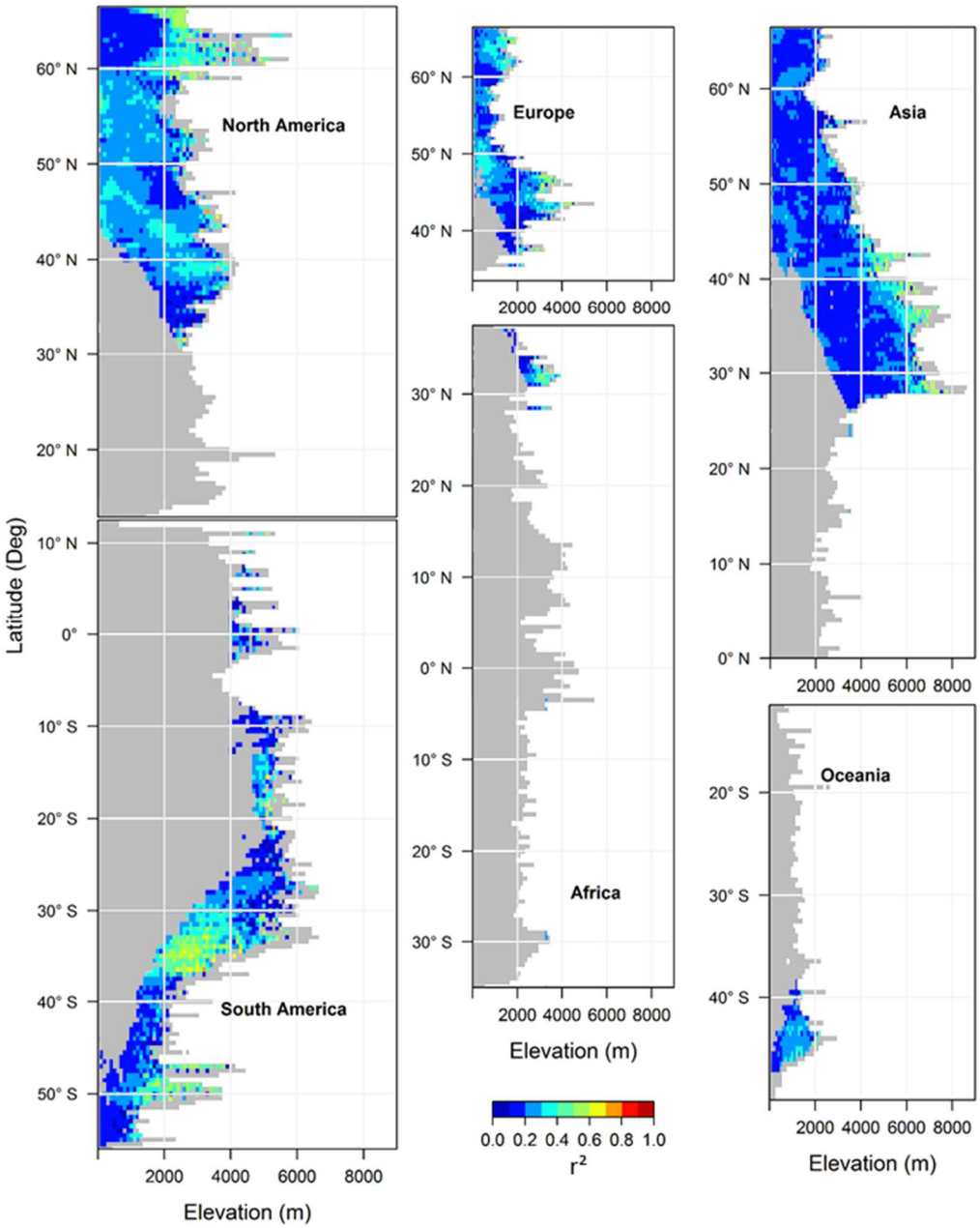

Figure 2.34. R sq. of significant relative importance fit by latitude and elevation for North America, South America, Africa, Asia, Europe and Oceania.

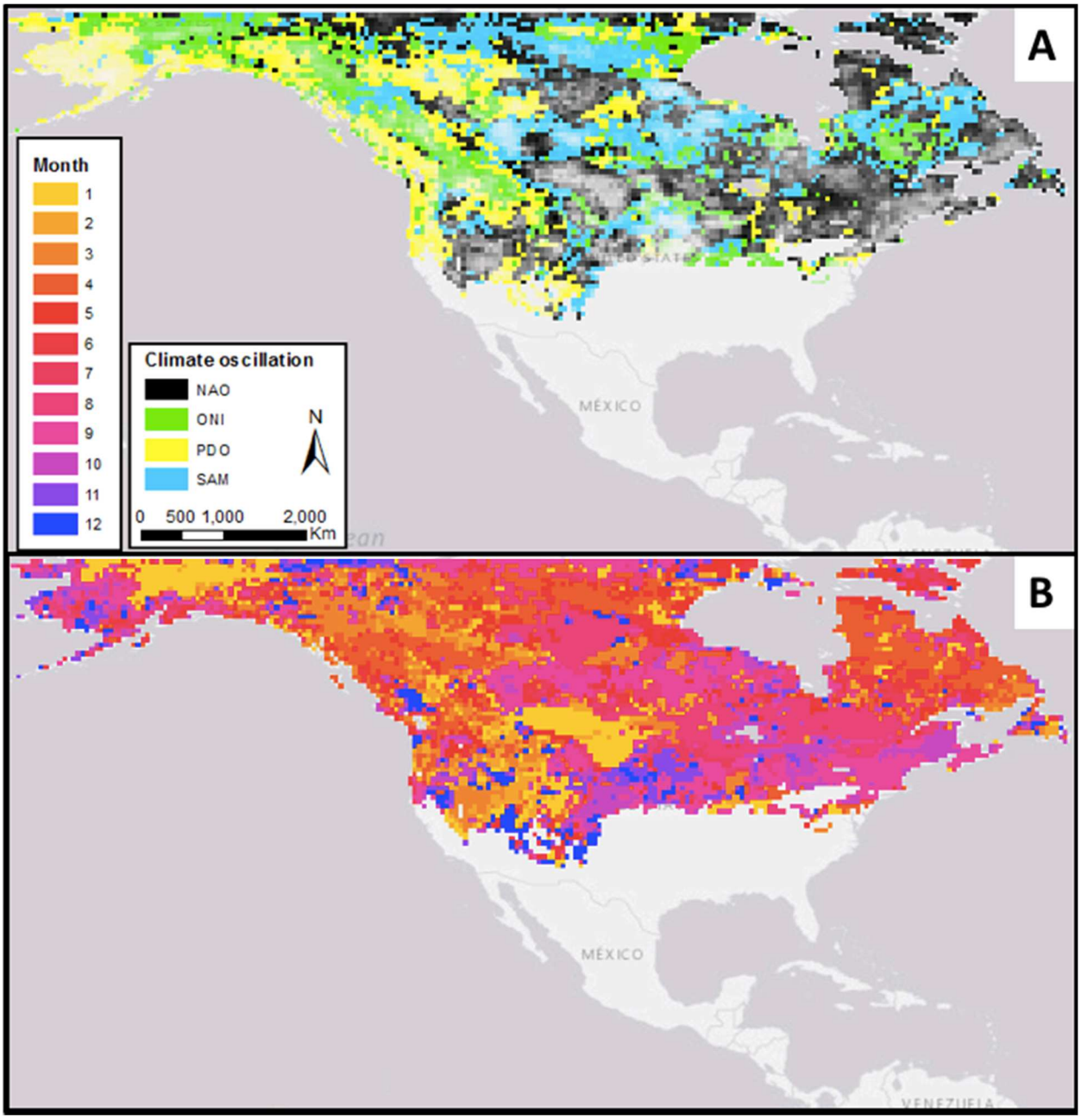

Figure 2.35. Dominant teleconnection index as determined by monthly index correlation with annual SP for half degree latitude and longitude grid cells in North America (A) and month with the strongest correlation between the dominant teleconnection index and annual snow persistence (B).Relative strength of correlation shown with transparency where weaker correlations are shown by transparent colors and stronger correlations are shown by opaque colors.

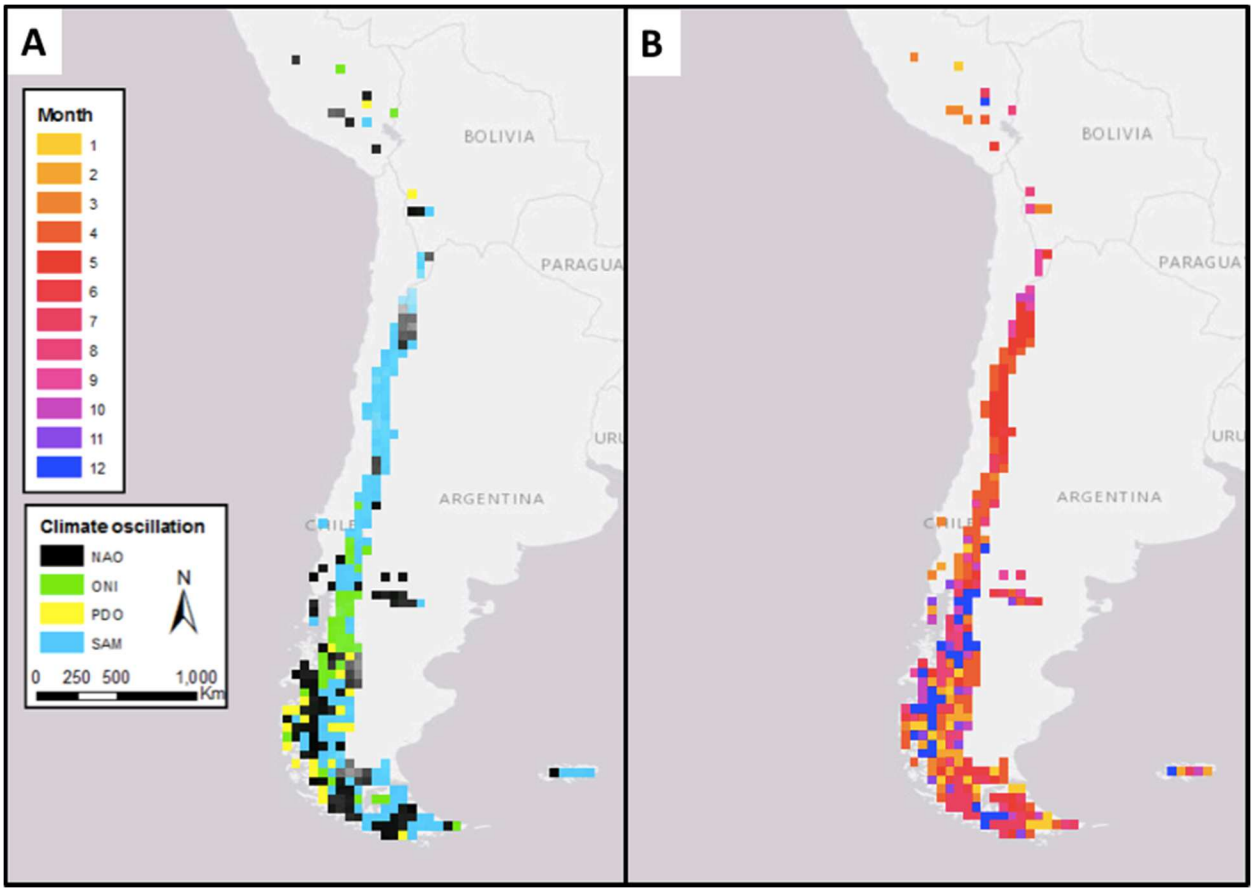

Figure 2.36. Dominant teleconnection index as determined by monthly index correlation with annual SP for half degree latitude and longitude grid cells in South America (A) and month with the strongest correlation between the dominant teleconnection index and annual snow persistence (B).Relative strength of correlation shown with transparency where weaker correlations are shown by transparent colors and stronger correlations are shown by opaque colors.

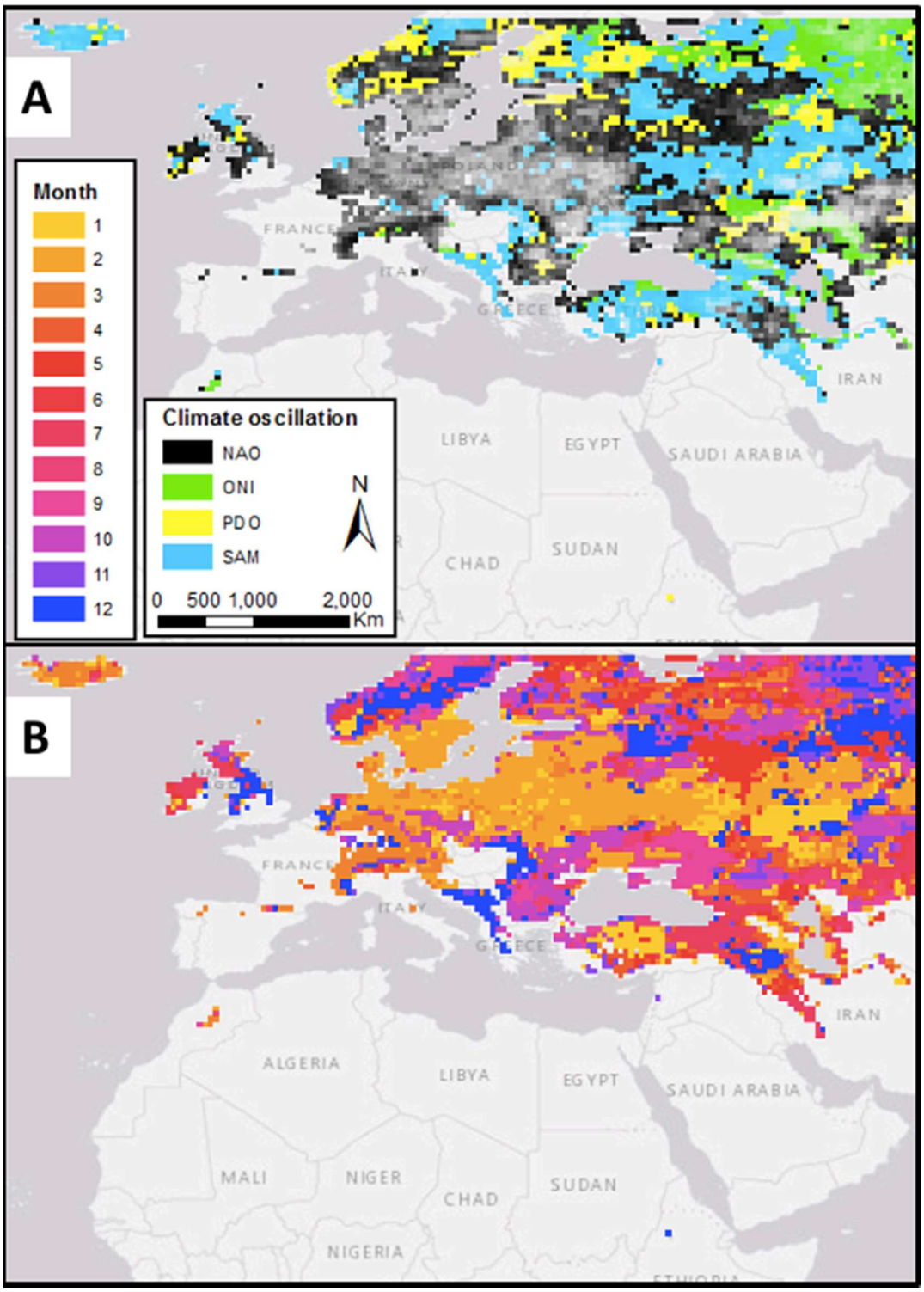

Figure 2.37. Dominant teleconnection index as determined by monthly index correlation with annual SP for half degree latitude and longitude grid cells in Europe and Northern Africa (A) and month with the strongest correlation between the dominant teleconnection index and annual snow persistence (B).Relative strength of correlation shown with transparency where weaker correlations are shown by transparent colors and stronger correlations are shown by opaque colors.

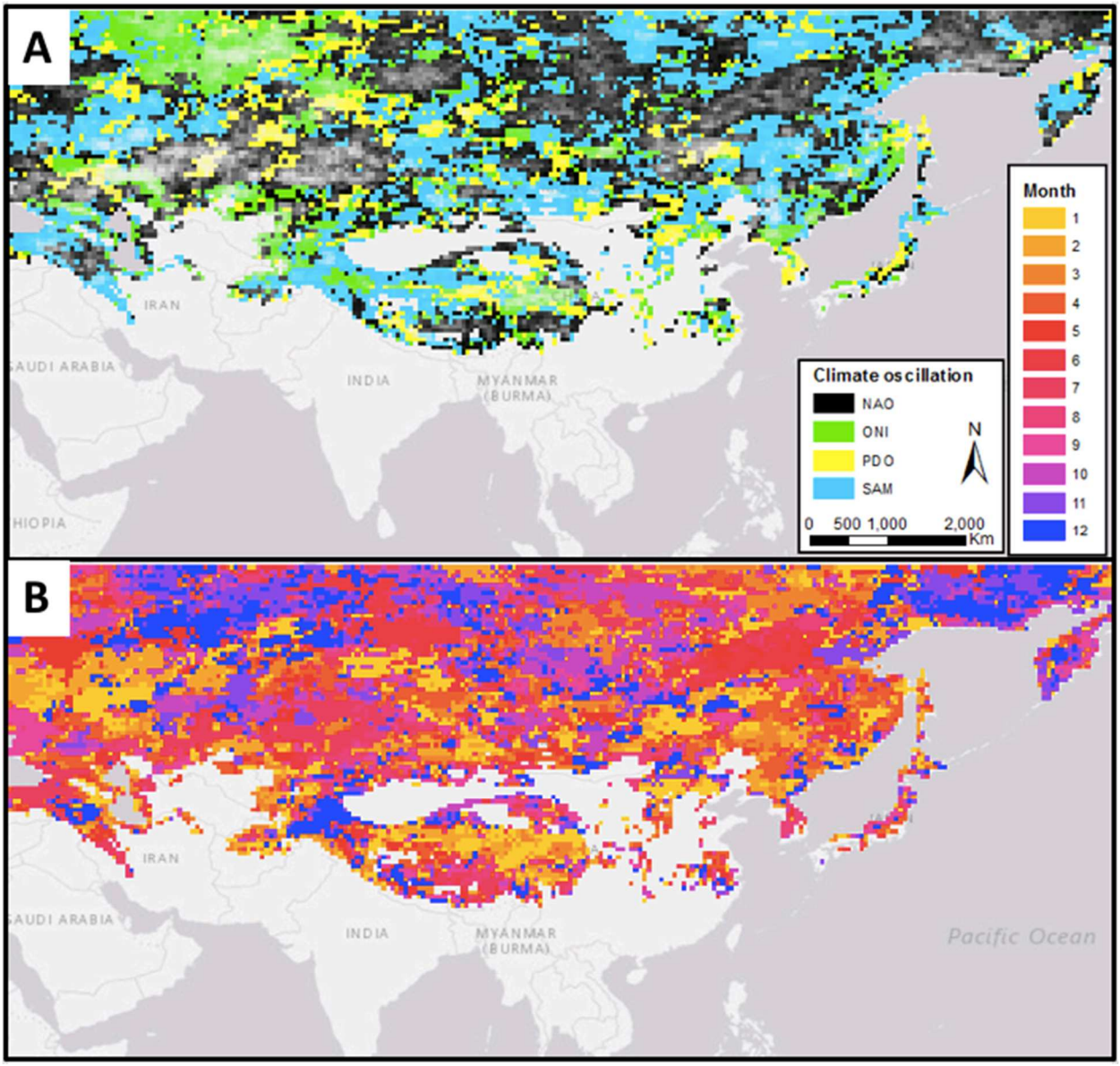

Figure 2.38. Dominant teleconnection index as determined by monthly index correlation with annual SP for half degree latitude and longitude grid cells in Asia (A) and month with the strongest correlation between the dominant teleconnection index and annual snow persistence (B).Relative strength of correlation shown with transparency where weaker correlations are shown by transparent colors and stronger correlations are shown by opaque colors.

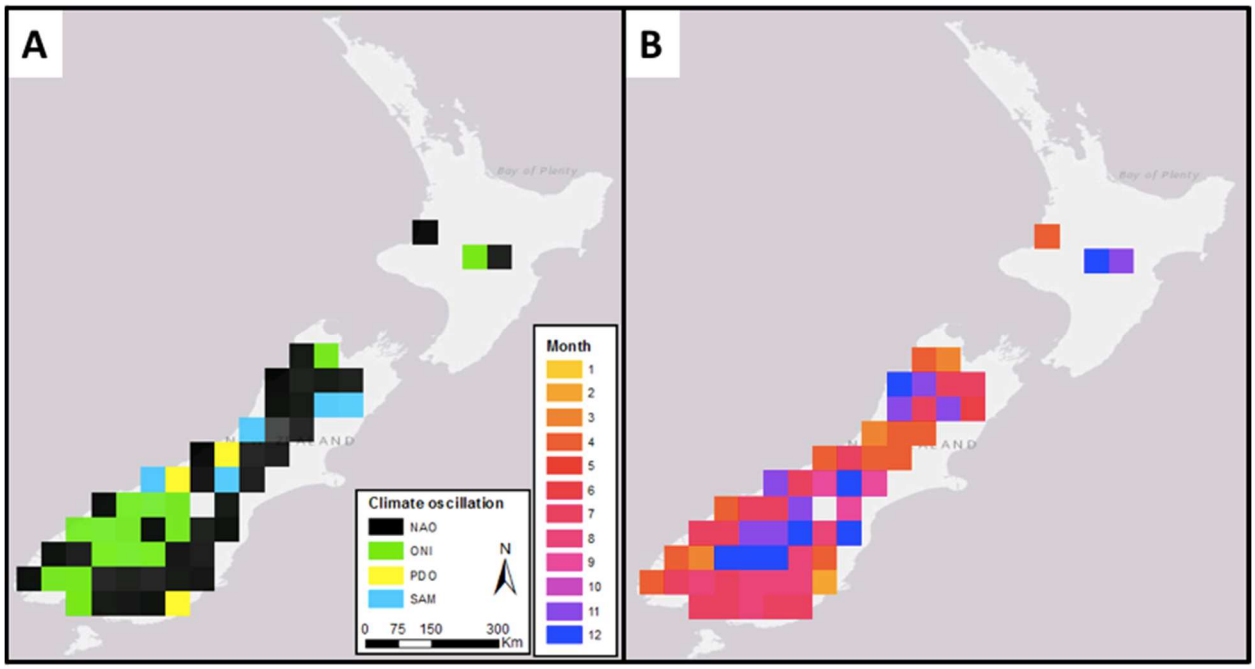

Figure 2.39. Dominant teleconnection index as determined by monthly index correlation with annual SP for half degree latitude and longitude grid cells in Oceania (A) and month with the strongest correlation between the dominant teleconnection index and annual snow persistence (B).Relative strength of correlation shown with transparency where weaker correlations are shown by transparent colors and stronger correlations are shown by opaque colors.

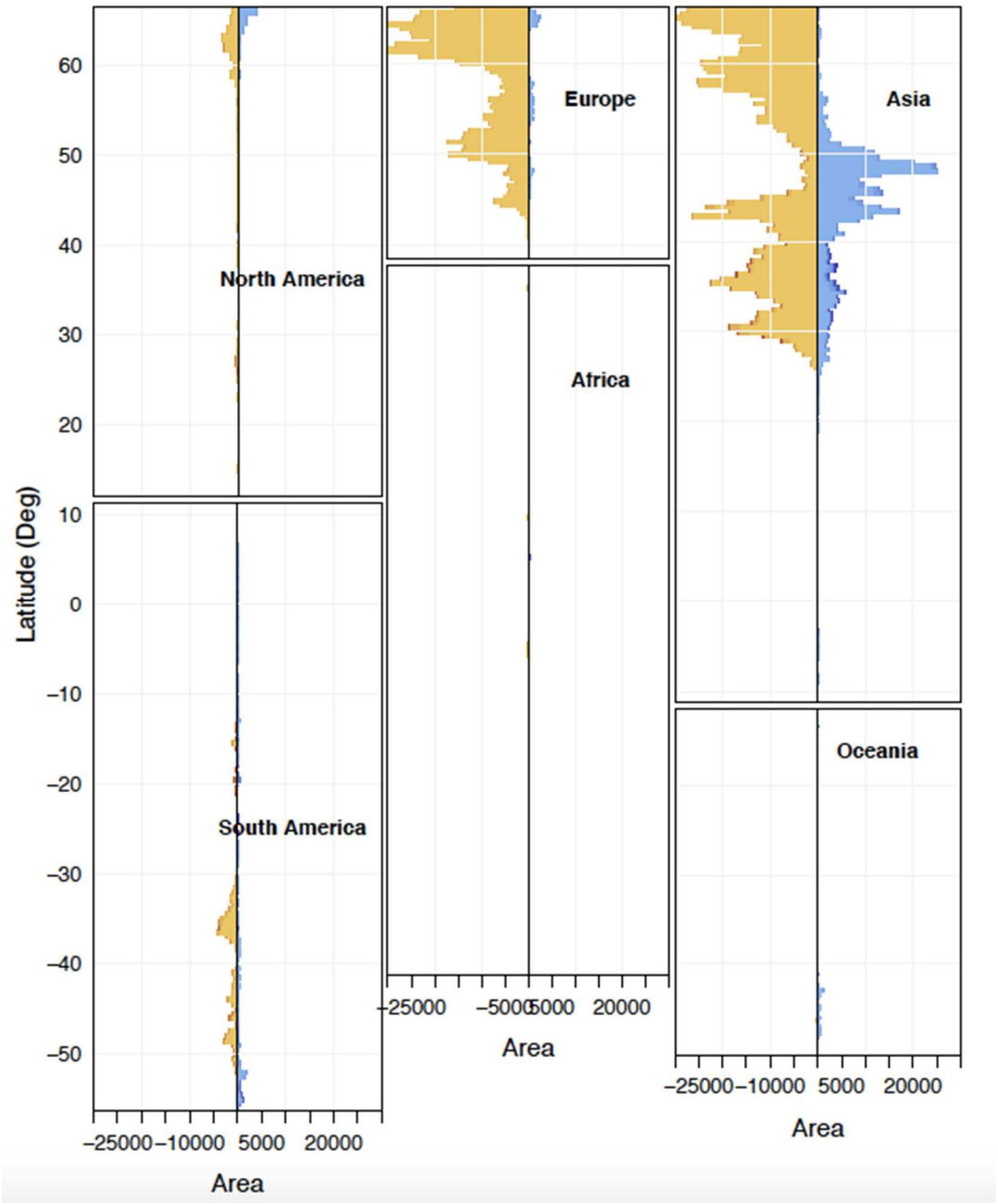

Figure 2.40. Area affected by positive and negative trends in snow persistence for each continent / region by 0.5 degree latitude band.

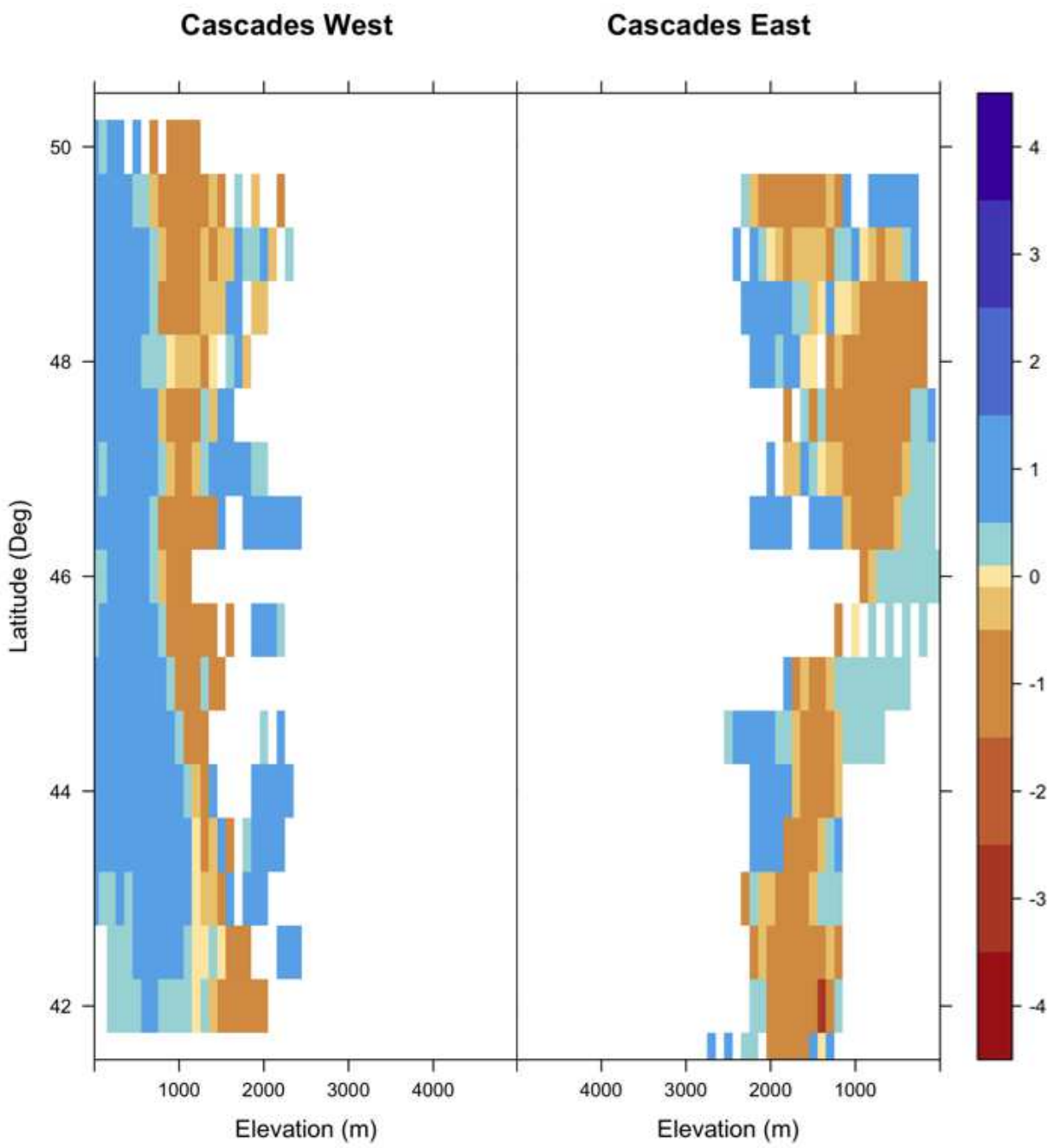

Figure 2.41. Trends in SP by 0.5 degree latitude band and 500 meter elevation band for the West and East Cascades separated by the Cascade Crest.

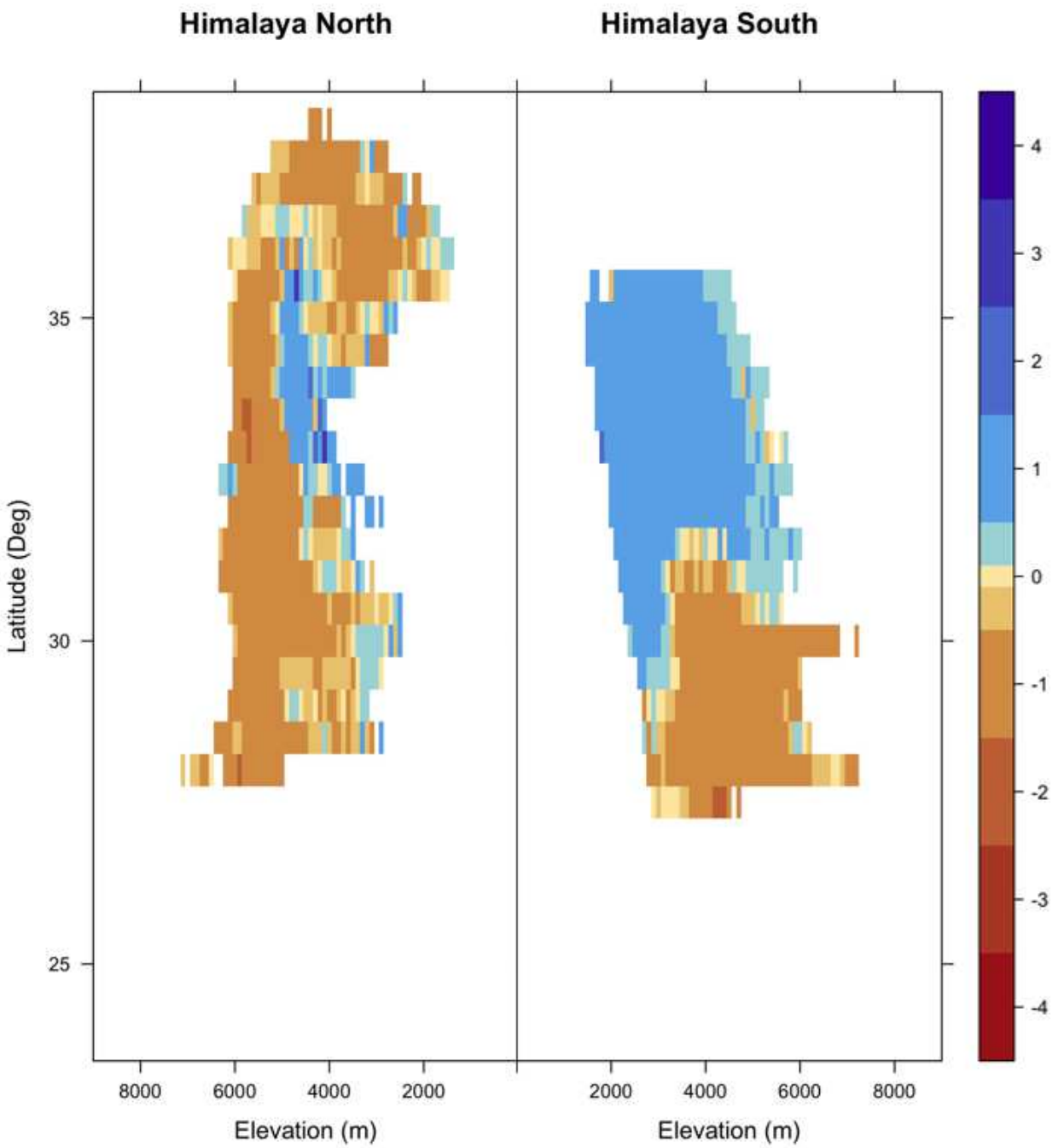

Figure 2.42. Trends in SP by 0.5 degree latitude band and 500 meter elevation band for the North and South Himalaya separated by the mountain crest.

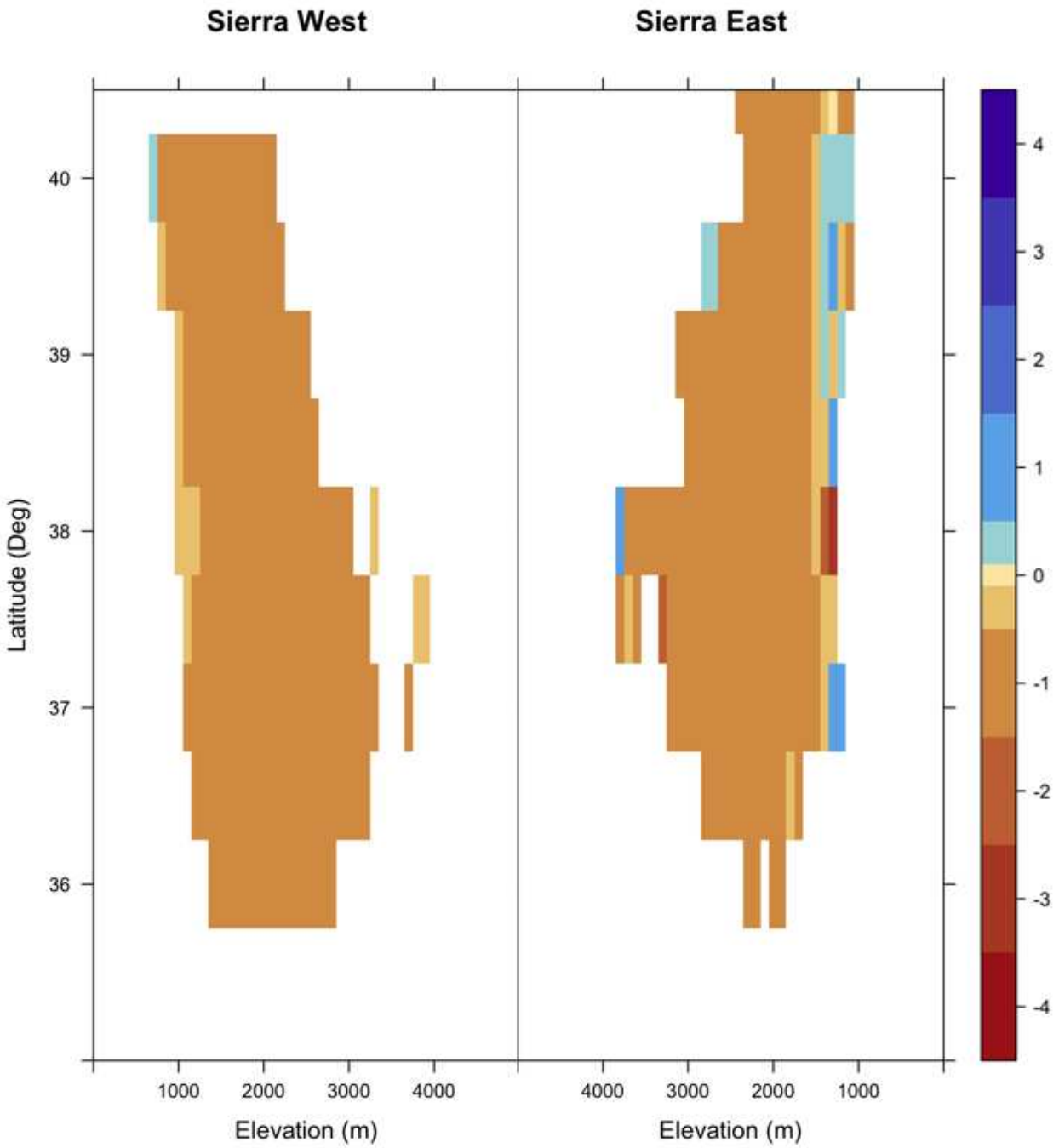

Figure 2.43. Trends in SP by 0.5 degree latitude band and 500 meter elevation band for the West and East Sierra Nevada separated by the Sierra Crest.

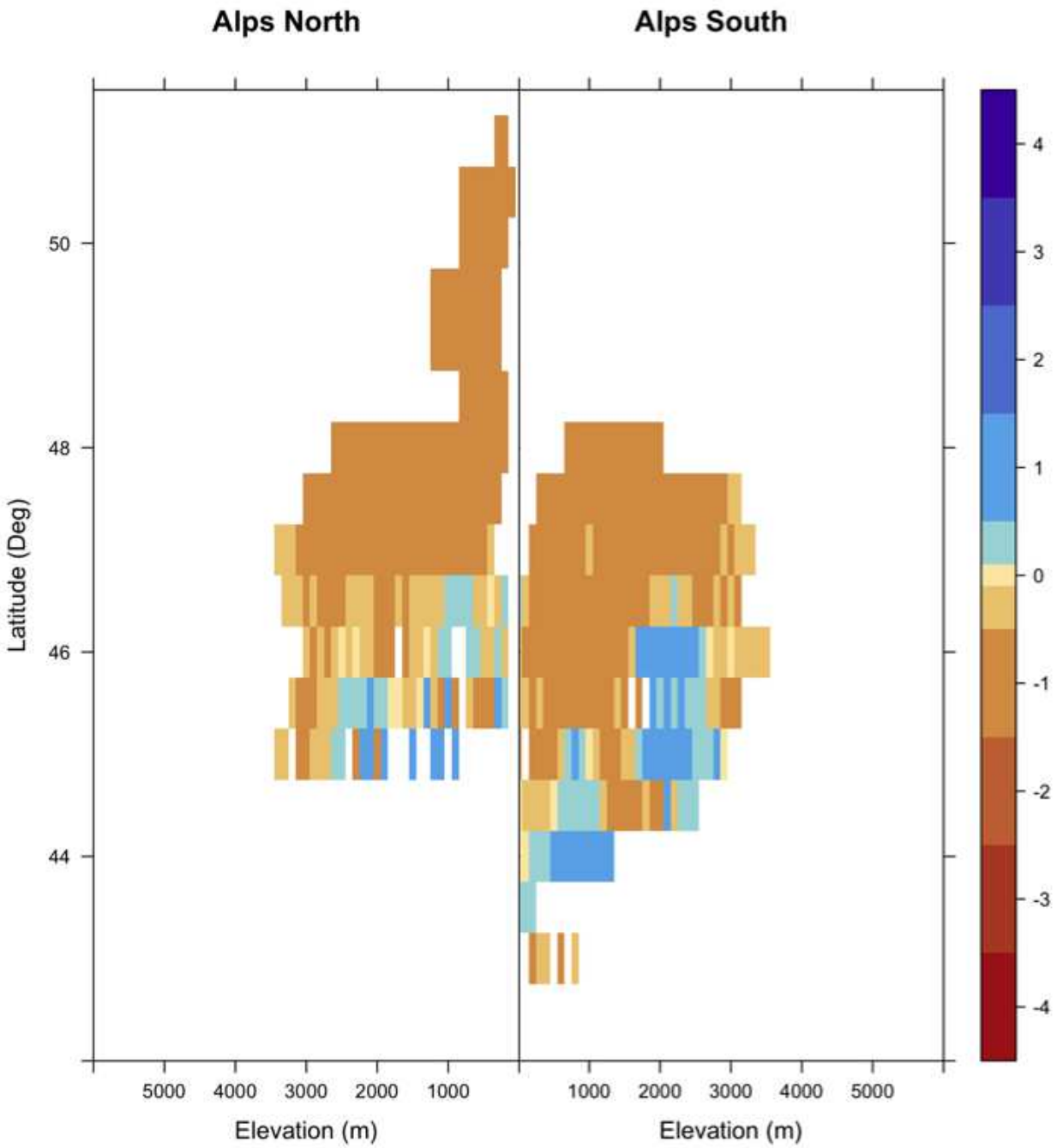

Figure 2.44. Trends in SP by 0.5 degree latitude band and 500 meter elevation band for the North and South Alps separated by the mountain crest.

Appendix 2: Chapter 3 supplementary material

Here we provide supplementary tables that display correlation coefficients between snow season length and streamflow variables (Table 3.6), and correlation results using alternate gridded climate data sets (Tables 3.7a,b,c). Tables 3.7a,b,c show similar relationships between streamflow variables and snow variables to the results presented in the main manuscript. We computed watershed-scale correlations between watershed average snow variables (SP, SNODAS peak SWE, and snow season length) and streamflow variables (Q, Q/P).

We also provide supplementary figures showing correlations between annual streamflow (Q) and precipitation (P) totaled for four different time periods (Figures 3.11, 3.12), as well as streamflow and mean temperature (T) averaged for four different time periods (Figures 3.13,3.14). Figures 3.15 and 3.16 show correlations between peak snow water equivalent (SWE) and snow persistence (SP) with climate variables P and T for the same four different time periods as shown in figures 3.11-3.14.

Table 3.6. Snow season and streamflow response correlation table. Dry (P/PET <1), Wet (P/PET ≥1). *p<0.05; **p<0.01; ***p<0.001, no asterisk = not significant at p<0.05.

Variables	All	Wet/warm	Dry/cold
SS and Q	0.22***	0.10*	0.45***
SS and Q/P	0.42***	0.19***	0.55***

Table 3.7a. Correlation coefficients for mean annual input and output variables using Livneh Hydromet data (Livneh et al., 2013) for P instead of PRISM. Dry (P/PET <1), Wet (P/PET ≥1). *p<0.05; **p<0.01; ***p<0.001, no asterisk = not significant at p<0.05.

Variables	All watersheds	Wet/warm	Dry/cold
P and Q	0.90***	0.84***	0.71***
SP and Q	0.075*	-0.13*	0.67***
SWE and Q	0.42***	0.10*	0.76***
P and Q/P	0.52***	0.21***	0.35***
SP and Q/P	0.37***	0.046	0.71***
SWE and Q/P	0.47***	0.061	0.64***

Table 3.7b. Correlation coefficients for mean annual input and output variables using Livneh Hydromet data (Livneh et al., 2013) for P instead of PRISM and Cristea PET (Cristea et al., 2013) data instead of gridMET (Abatzoglou, 2013). Dry (P/PET <1), Wet (P/PET ≥1). *p<0.05; **p<0.01; ***p<0.001, no asterisk = not significant at p<0.05.

Variables	All watersheds	Wet/warm	Dry/cold
P and Q	0.90***	0.90***	0.89***
SP and Q	0.075*	-0.082	0.27***
SWE and Q	0.42***	0.065	0.76***
P and Q/P	0.52***	0.52***	0.48***
SP and Q/P	0.37***	0.14**	0.56***
SWE and Q/P	0.47***	0.059	0.61***

Table 3.7c. Correlation coefficients for mean annual input and output variables using Cristea PET data (Cristea et al., 2013) instead of gridMET (Abatzoglou, 2013). Dry (P/PET <1), Wet (P/PET ≥1). *p<0.05; **p<0.01; ***p<0.001, no asterisk = not significant at p<0.05.

Variables	All watersheds	Wet/warm	Dry/cold
P and Q	0.96***	0.95***	0.83***
SP and Q	0.075**	- 0.12**	0.66***
SWE and Q	0.38***	0.012	0.75***
P and Q/P	0.69***	0.57***	0.58***
SP and Q/P	0.38***	-0.0074	0.73***
SWE and Q/P	0.48***	0.029	0.63***

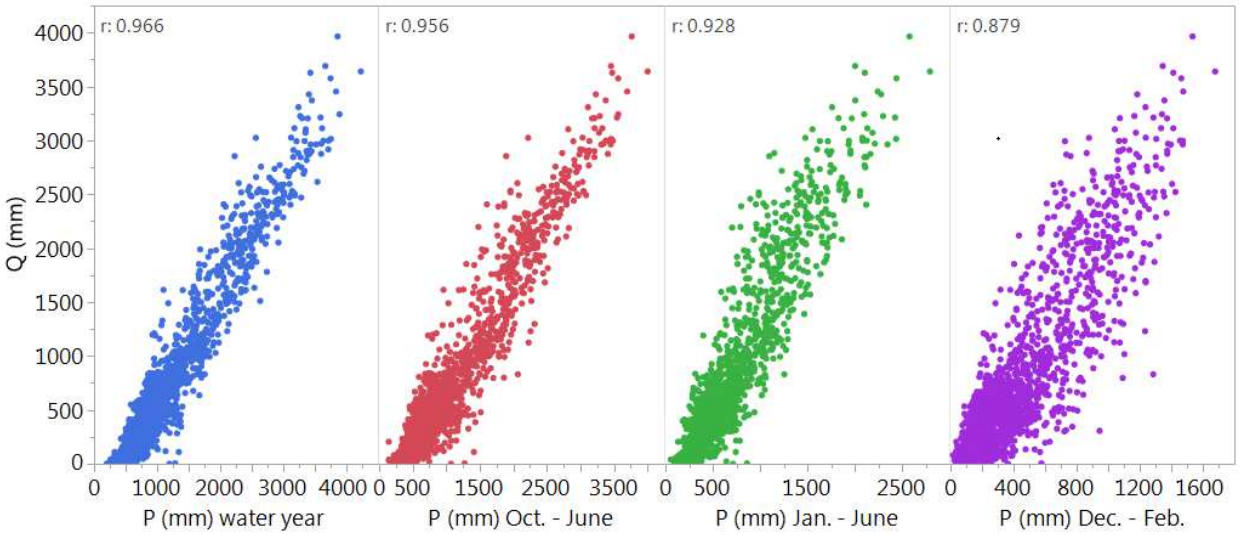

Figure 3.11. Annual streamflow (Q) vs precipitation (P) totals for the water year, October to June, January to June, and December to February.

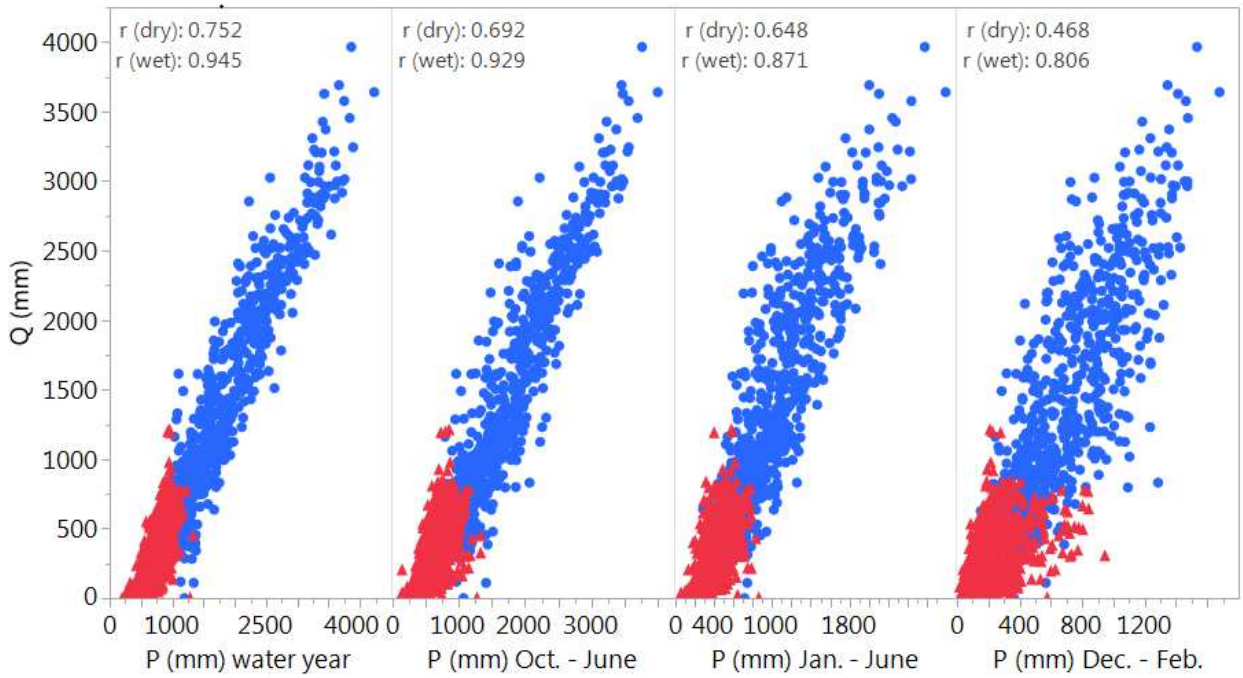

Figure 3.12. Annual streamflow (Q) vs precipitation (P) total for the water year, October to June, January to June, and December to February, with climatic separation into dry/cold and wet/warm watershed groupings.

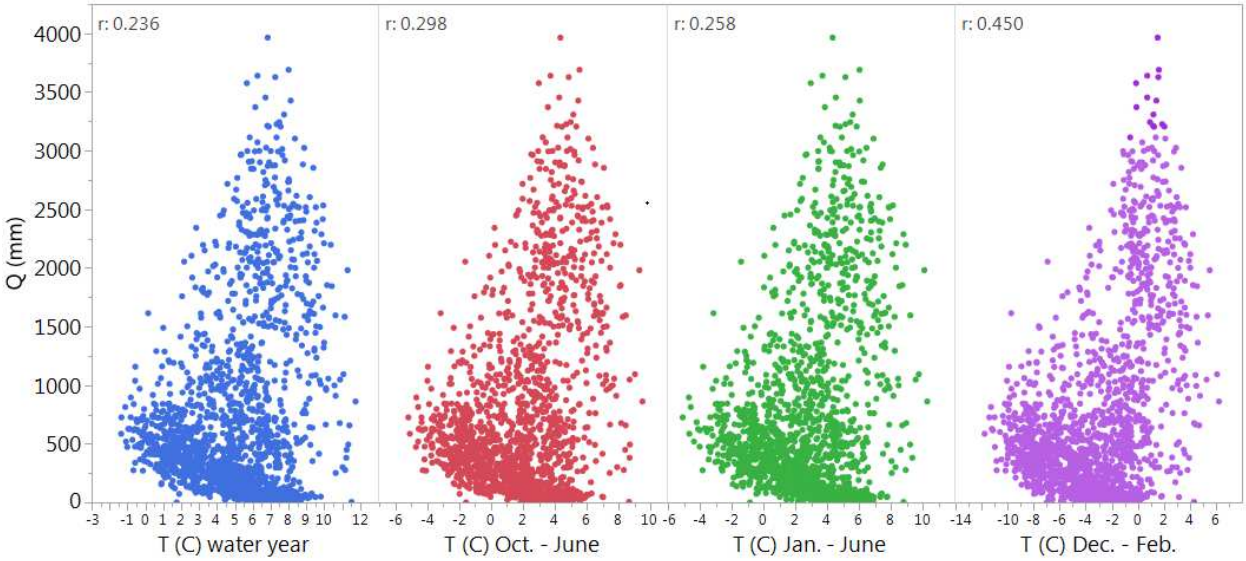

Figure 3.13. Annual streamflow (Q) vs mean temperature (T) averaged for the water year, October to June, January to June, and December to February.

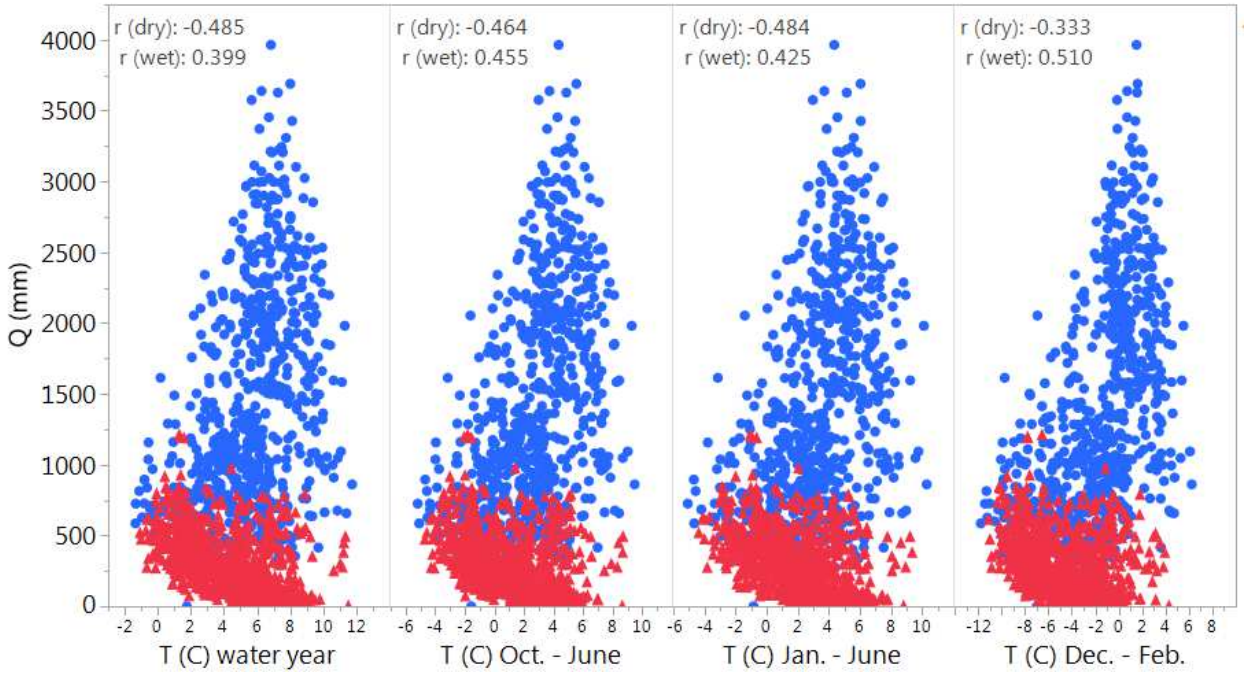

Figure 3.14. Annual streamflow (Q) vs mean temperature (T) averaged for the water year, October to June, January to June, and December to February, with climatic separation into dry/cold and wet/warm watershed groupings.

Figure 3.15. SP and peak SWE vs P total for three periods, water year, October 1 to June 30, and January 1 to June 30, with climatic separation into dry/cold and wet/warm watershed groupings.

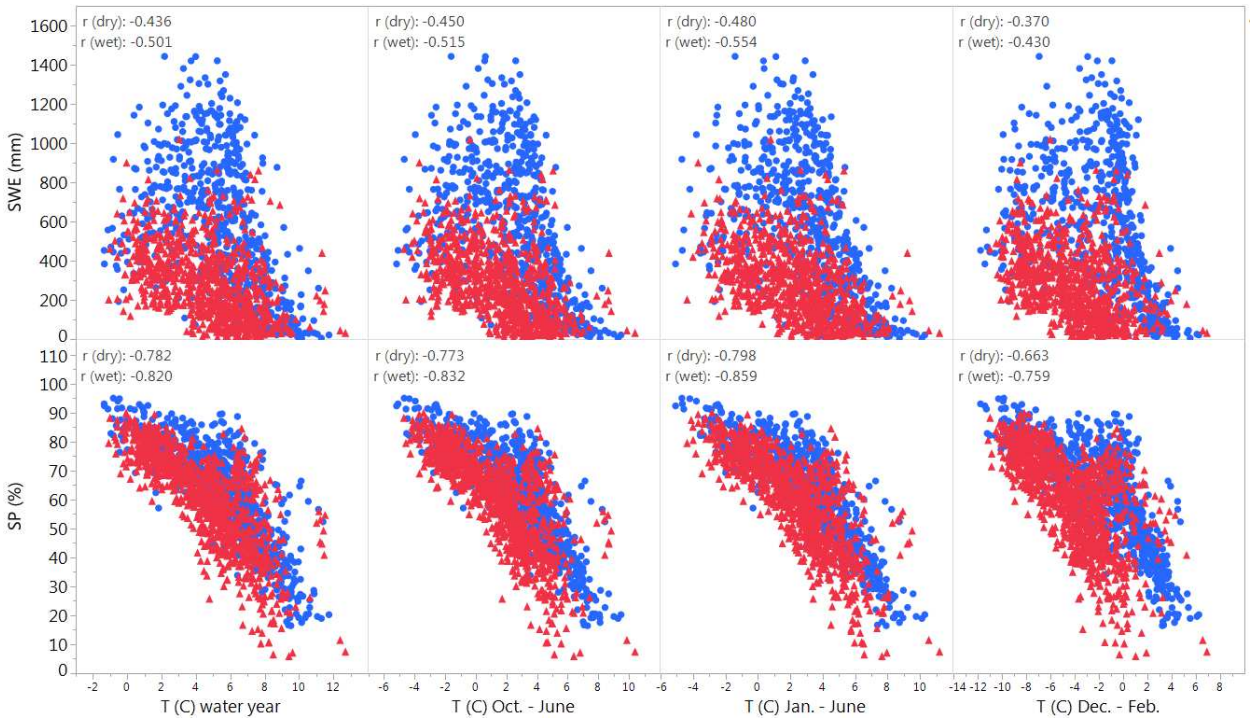

Figure 3.16. SP and peak SWE vs T averaged for three periods, water year, October 1 to June 30, and January 1 to June 30, with climatic separation into dry/cold and wet/warm watershed groupings.

Appendix 3: Chapter 4 supplementary material

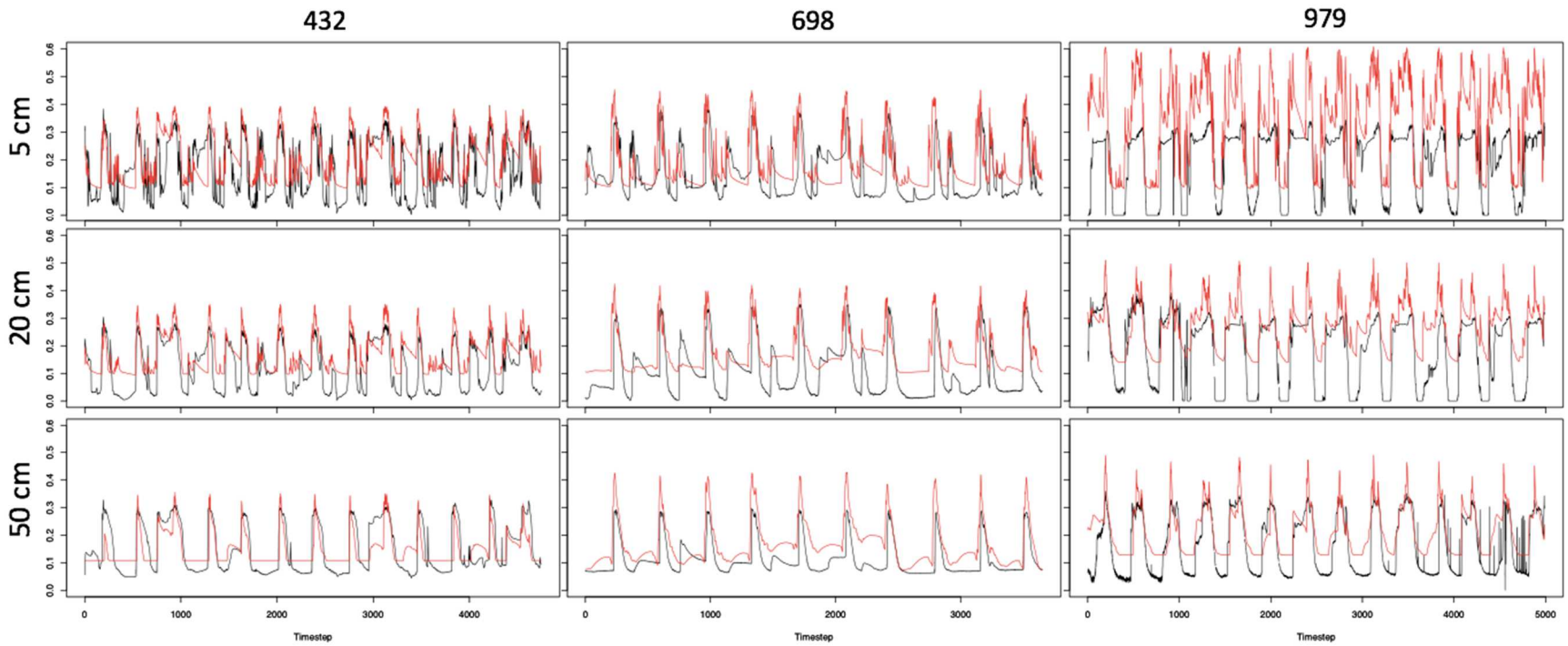

Figure 4.13. Observed (black) and simulated (red) time series of volumetric water content at 5, 20 and 50 cm for SNOTEL sites and profiles 432 Currant Creek, 698 Pole Creek R.S., and 979 Van Wyck.

Table 4.4. Table of calibration metrics NSCE, mean bias for calibration scenarios. 75 percentile VWC at 5, 20 and 50 cm depth.

	432	698	979
NSCE 5 cm	-0.33	0.15	-0.82
NSCE 20 cm	0.45	0.17	0.22
NSCE 50 cm	0.58	0.14	0.48
Mean bias 5 cm	-6.7	9.4	46.9
Mean bias 20 cm	8.5	10.4	22.4
Mean bias 50 cm	-7.4	10	19.7

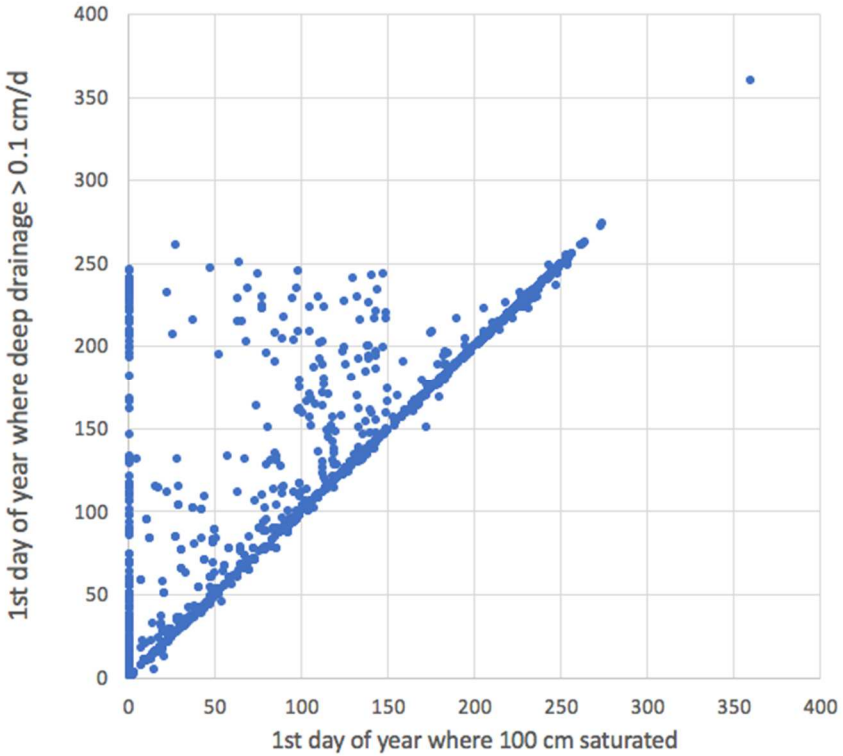

Figure 4.14. First day of measurable deep drainage vs first day of 100 cm depth saturation for all climates, historical scenarios, and loam profile.

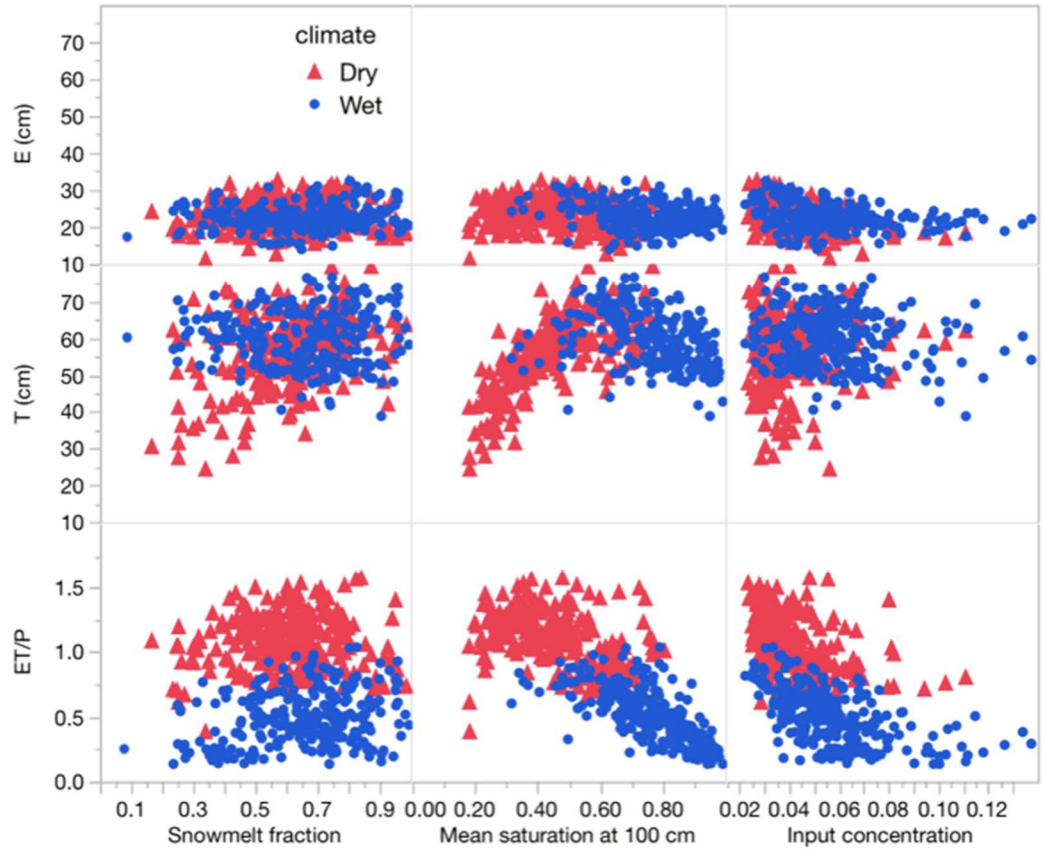

Figure 4.15. Annual evaporation (E), transpiration (T), and ET to precipitation (P) vs mean saturation at 100 cm depth for the historical scenario and loam profile. Dry P/PET <1=, Wet P/PET >1.

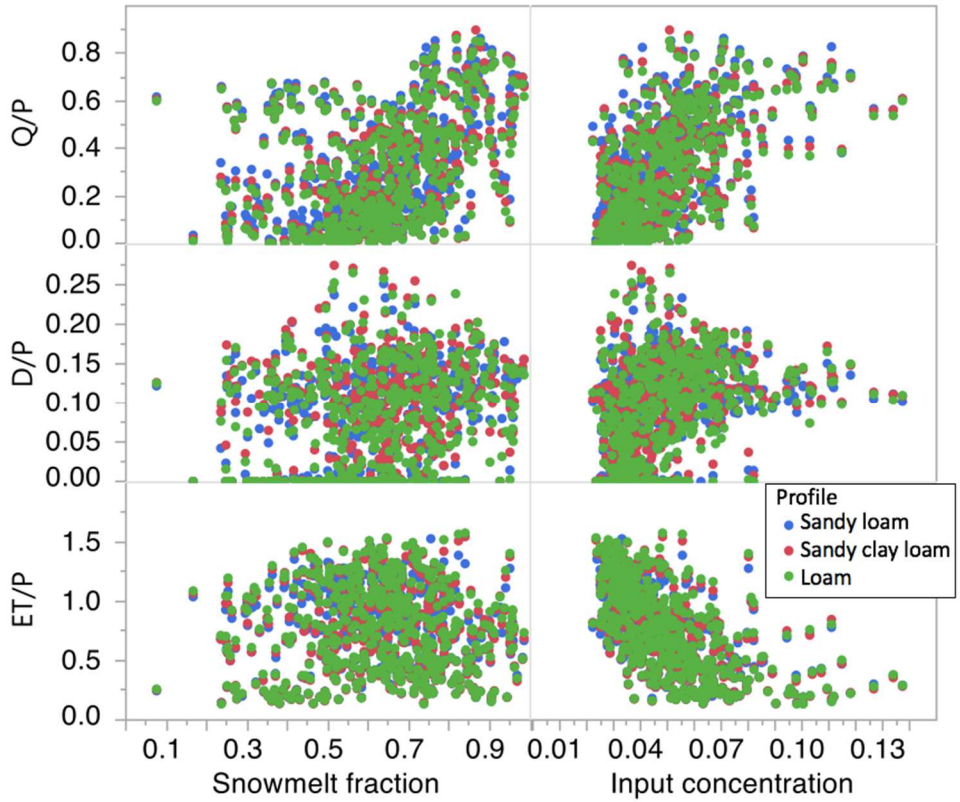

Figure 4.16. Annual ratio of runoff (Q), deep drainage (D) and evapotranspiration (ET) to input (P) vs snowmelt fraction of input by soil texture for the historical scenario and three soil profiles (515- Sandy loam, 1049- Sandy clay loam, 1056- Loam).

Table 4.5. Tabular values below plots display correlation coefficients, slopes of linear fit between explanatory and response variable, and whether slopes for different climate types are significantly different for the ratio of Q, D and ET to P vs snowmelt fraction of input and input concentration. Whether slopes were significantly different was estimated by the p-value of a pairwise difference in linear regression slope test where *<0.5, **<0.01, ***<0.001. Results from the climate scenarios in Figure 3, loam soil type. Dry P/PET <1=, Wet P/PET >1.

	All			**Dry**			**Wet**			
Variables	r		Slope	r		Slope	r		Slope	Slopes different?
Q/P vs snowmelt fraction	0.41	***	0.53	0.44	***	0.41	0.41	***	0.38	***
D/P vs snowmelt fraction	0.20	***	0.07	0.32	***	0.10	-0.02		0.00	no
ET/P vs snowmelt fraction	-0.02		0.05	0.05		0.07	0.30	***	0.33	*
Q/P vs mean saturation	0.77	***	0.87	0.60	***	0.59	0.52	***	0.65	*
D/P vs mean saturation	0.85	***	0.27	0.78	***	0.27	0.65	***	0.22	no
ET/P vs mean saturation	-0.79	***	1.41	-0.41	***	0.62	-0.62	***	0.92	**
Q/P vs input concentration	0.57	***	7.02	0.47	***	5.01	0.39	***	3.66	*
D/P vs input concentration	0.37	***	1.30	0.40	***	1.48	-0.04		0.06	no
ET/P vs input concentration	-0.60	***	11.74	-0.40	***	6.66	-0.56	***	5.93	no

Table 4.6. Tabular values below plots display correlation coefficients, slopes of linear fit between explanatory and response variable, and whether slopes for different soil textures are significantly different for the ratio of Q, D and ET to P vs snowmelt fraction of input and input concentration. Whether slopes were significantly different was estimated by the p-value of a pairwise difference in linear regression slope test where *<0.5, **<0.01, ***<0.001.

	Sandy loam			**Sandy clay loam**			**Loam**			
Variables	r		Slope	r		Slope	r		Slope	Slopes different?
Q/P vs snowmelt fraction	0.42	***	0.53	0.39	***	0.52	0.38	***	0.50	no
D/P vs snowmelt fraction	0.28	***	0.10	0.24	***	0.09	0.21	***	0.08	no
ET/P vs snowmelt fraction	0.01		0.01	0.00		0.01	0.01		0.01	no
Q/P vs mean saturation	0.75	***	0.78	0.77	***	0.93	0.80	***	0.86	***
D/P vs mean saturation	0.76	***	0.22	0.81	***	0.27	0.85	***	0.27	*
ET/P vs mean saturation	-0.81	***	1.34	-0.79	***	1.54	-0.80	***	1.43	**
Q/P vs input concentration	0.56	***	6.39	0.58	***	6.99	0.58	***	7.01	no
D/P vs input concentration	0.33	***	1.08	0.34	***	1.19	0.36	***	1.29	no
ET/P vs input concentration	-0.60	***	10.69	-0.60	***	11.54	-0.60	***	11.83	no

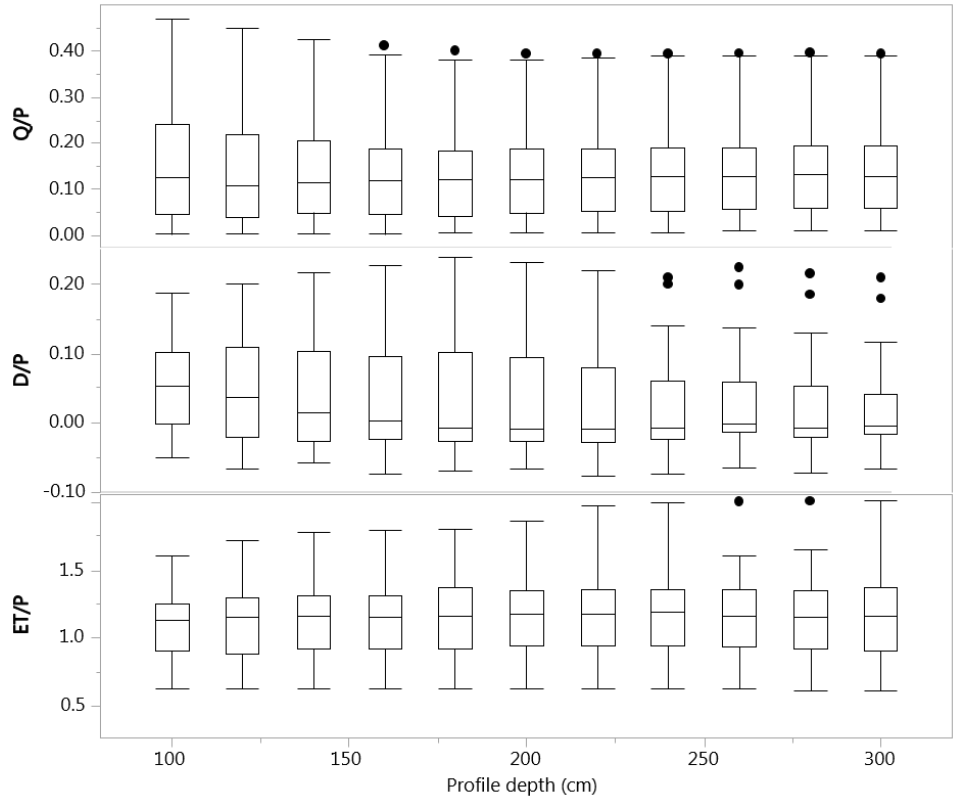

Figure 4.17. Boxplots of the annual range in historical input partitioning resulting from fine scale changes in depth for SNOTEL 396 loam profile.

Table 4.7. Correlations between annual values of climatic and water balance terms for historical input scenarios. Variables included are precipitation (P), potential evapotranspiration (PET), peak snow water equivalent (peak SWE), snow persistence (SP), average melt rate over the year (melt rate), mean saturation at 100 cm depth (Sat 100), surface runoff (Q), deep drainage (D), transpiration (T), evaporation (E), and aridity index (P/PET). P-value of correlation, *<0.5, **<0.01, ***<0.001.

	D	SP	P	PET	SWE	melt rate	Sat5	Sat20	Sat50	Sat100
SP	0.44***									
P	0.92***	0.35***								
PET	-0.55***	-0.74***	-0.43***							
SWE	0.78***	0.65***	0.74***	-0.46***						
meltrate	0.53***	0.62***	0.54***	-0.36***	0.80***					
Sat5	0.84***	0.68***	0.74***	-0.77***	0.70***	0.55***				
Sat20	0.86***	0.67***	0.75***	-0.73***	0.72***	0.56***	0.99***			
Sat50	0.88***	0.60***	0.76***	-0.65***	0.73***	0.56***	0.95***	0.97		
Sat100	0.86***	0.49***	0.73***	-0.55***	0.70***	0.50***	0.84***	0.88***	0.93***	
Q	0.91***	0.39***	0.97***	-0.42***	0.83***	0.63***	0.73***	0.75***	0.76***	0.73***
T	0.06	0.15***	0.13**	0.09*	0.08	0.20***	0.23***	0.26***	0.26***	0.30***
E	-0.18***	0.23***	-0.07	-0.07	-0.10*	0.11*	0.12**	0.06	-0.10*	-0.22***
D/P	0.77***	0.43***	0.51***	-0.52***	0.56***	0.39***	0.73***	0.77***	0.83***	0.86***
P/PET	0.93***	0.43***	0.98***	-0.55***	0.76***	0.54***	0.79***	0.79***	0.79***	0.74***
Q/P	0.81***	0.51***	0.76***	-0.38***	0.86***	0.75***	0.72***	0.76***	0.80***	0.80***
E/P	-0.82***	-0.35***	-0.77***	0.38***	-0.71***	-0.51***	-0.67***	-0.73***	-0.81***	-0.85***
T/P	-0.88***	-0.39***	-0.84***	0.46***	-0.76***	-0.55***	-0.72***	-0.75***	-0.79***	-0.78***
ET/P	-0.87***	-0.39***	-0.83***	0.44***	-0.76***	-0.54***	-0.71***	-0.75***	-0.81***	-0.82***

Table 4.7 continued. Correlations between annual values of climatic and water balance terms for historical input scenarios. Variables included are precipitation (P), potential evapotranspiration (PET), peak snow water equivalent (peak SWE), snow persistence (SP), average melt rate over the year (melt rate), mean saturation at 100 cm depth (Sat 100), surface runoff (Q), deep drainage (D), transpiration (T), evaporation (E), and aridity index (P/PET). P-value of correlation, *<0.5, **<0.01, ***<0.001.

	Q	T	E	D/P	P/PET	Q/P	E/P	T/P
SP								
P								
PET								
SWE								
meltrate								
Sat5								
Sat20								
Sat50								
Sat100								
Q								
T	0.09*							
E	-0.08	0.41***						
D/P	0.52***	0.14**	-0.32***					
P/PET	0.96***	0.03	-0.07	0.54***				
Q/P	0.84***	0.25***	-0.15**	0.70***	0.73***			
E/P	-0.74***	-0.23***	0.41***	-0.77***	-0.74***	-0.82***		
T/P	-0.81***	-0.01	0.27***	-0.71***	-0.83***	-0.82***	0.92***	
ET/P	-0.80***	-0.08	0.32***	-0.75***	-0.81***	-0.84***	0.96***	0.99***

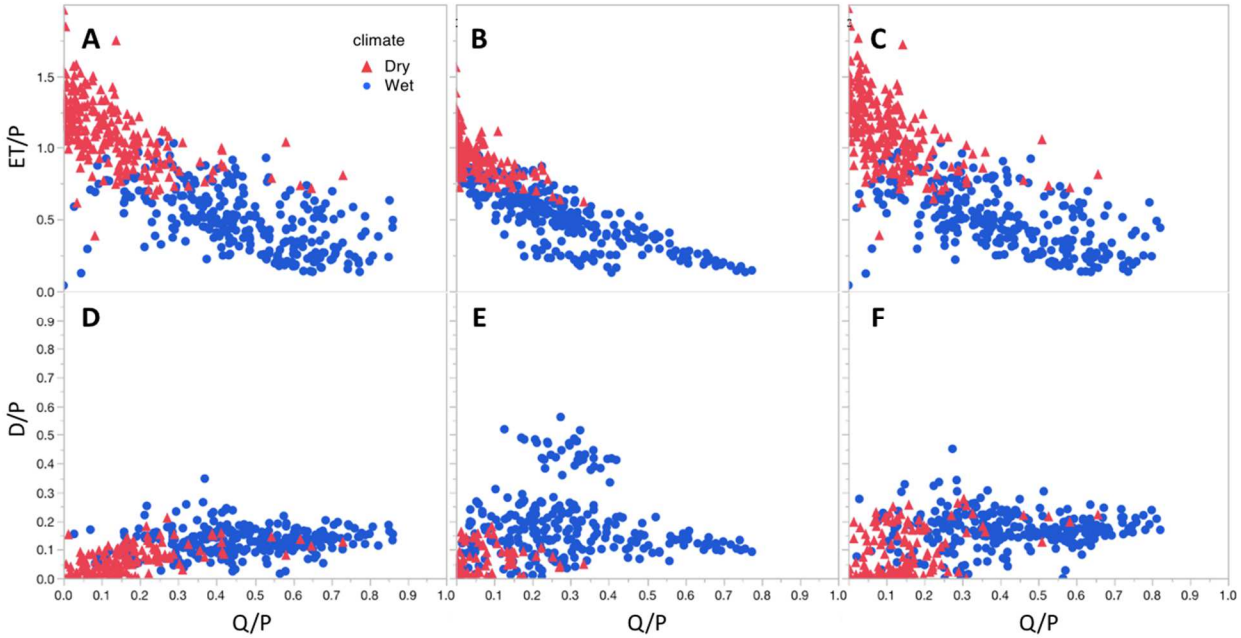

Figure 4.18. ET/P vs Q/P by climate type for historical scenarios with loam soil texture and 1x depth (A), all rain scenarios with loam soil texture and 1x depth (B), historical scenarios with loam soil texture and 2x depth (C) and D/P vs Q/P by climate type for historical scenarios with loam soil texture and 1x depth (D), all rain scenarios with loam soil texture and 1x depth (E), historical scenarios with loam soil texture and 2x depth (F). Dry P/PET <1=, Wet P/PET >1.